THE UNIVERSITY OF HULL

CXCR4 Chemokine Receptor Antagonists: New Metallodrugs

being a Thesis submitted for the Degree of Doctor of Philosophy

in the University of Hull

by

Abid Khan B.Sc. M.Sc.

December 2009

Abstract

Chemokine receptors are a target of growing interest for new therapeutic drugs, as their role in multiple disease states has been demonstrated. The CXCR4/ CXCL12 pairing has been implicated in HIV and cancer, as well as chronic inflammatory diseases, including asthma and rheumatoid arthritis. HIV uses CXCR4 or CCR5 receptors in the key binding step of the infection process, leading to the idea that drugs could be developed to block this interaction. Cancer metastasis has also been linked to cellular communication *via* the chemokine pathways and hence, receptor antagonists could potentially inhibit this important pathway of disease progression. Small synthetic CXCR4 antagonists exist including AMD3100 (Mozobil®/Plerixafor), which has been identified as a potent CXCR4 antagonist exhibiting anti-HIV, anti-inflammatory and anti-tumour activity. Configurationally restricted analogues of AMD3100 complexed to metal ions have improved binding characteristics compared to AMD3100 and its metal complexes.

Herein we report the binding of a new class of cyclen, cyclam and tris-cyclam based complexes *in vitro*. Compounds competed effectively in anti-CXCR4 competition assays with the tricyclam linear complex displaying improved binding characteristics. The difference in activity of the compounds is discussed in relation to the different possible binding interactions that are occurring. Furthermore, a monocyclam derivative conjugated to biotin competed effectively in competition with a CXCR4 mAb, however could not directly be detected via a fluorescent conjugated streptavidin molecule.

Our most potent compound to date, copper(II) cross-bridged bicyclam was found to have a significant higher relative residence time in CXCR4 compared to AMD3100 and copper(II) AMD3100 *in vitro*. Moreover, copper(II) cross-bridged bicyclam was able to totally block CXCL12 induced and partially block serum induced, invasion of CXCR4 positive cancer cells with a higher potency than AMD3100 and copper(II) AMD3100. This shows the potential of using such a drug in the clinic.

Using CXCR4 mutants, it has been shown that CXCR4 defective degradation and recycling increases invasion in breast cancer cells. Moreover the development of a multicellular tumour spheroid (MTS) is reported that could be used as a preclinical model in the evaluation of the anti-cancer activity of CXCR4 antagonists.

Table of contents

List of figures

List of tables

Acknowledgements

Many thanks to both my supervisors, Dr Stephen J. Archibald and Professor John Greenman, for their advice, discussions and encouragement throughout my PhD studies.

Special thanks go to Dr Leigh Madden for his support, advice and assistance with the work carried out at the Centre for Biomedical Research.

I am grateful to Rhonda Green for ordering all the consumables throughout the 3 years. In addition, I would like to thank Dr Graeme McRobbie, Dr Gary Nicholson and Dr Tim Hubin, for synthesising the compounds.

Further thanks go to Professor Tony Ng and Dr Gilbert Fruhwirth for fruitful discussions and support during our collaboration.

Finally I would like to thank everyone in Lab C214/5 and C120A past and present for their support and especially to my dear wife for her patience with me throughout the writing of this thesis.

Declaration

Except where specific reference is made to other sources, the work presented in this thesis is the work of the author. It has not been submitted, whole or part, for any other degree.

Abid Khan

Abbreviations and symbols

Å	Angstroms
AIDS	Acquired immunodeficiency syndrome
AIP4	Atrophin 1-interacting protein 4
AKt	serine/threonine protein kinase
Ala	Alanine
ANG II	Angiotensin II
Asn	Asparagine
Asp	Aspartic acid
B-CLL	B-cell chronic lymphocytic leukaemia
Bcl-2	B cell lymphoma cell-2 (gene)
BSA	Bovine serum albumin
ca.	Circa
cAMP	Cyclic adenosine monophosphate
CB	Cross-bridge
CCL**	CC cytokine ligand *number*
CCR**	CC cytokine receptor *number*
CD**	Cluster of differentiation *number*
CIA	Collagen II induced arthritis
Cl^-	Chloride (ion)
CNS	Central nervous system
CXCL**	CXC chemokine ligand *number*
CXCR**	CXC chemokine receptor *number*
Cy5	Cyanine 5
$\Delta G_{binding}$	Gibbs free energy (binding)
DARC	Duffy antigen receptor
DBA/1	Dilute Brown /Non-Agouti mice type 1
DC	Dendritic cell
DC*	Dendritic cell type *number*
DMF	Dimethylformamide

DMSO	Dimethylsulphoxide
DNA	Deoxyribonucleic acid
E3	Ubiquitin ligase
EC_{50}	Effective concentration (50 %)
ECL1	Extracellular loop 1
ECL2	Extracellular loop 2
ECL3	Extracellular loop 3
EGF	Epidermal growth factor
ErK	Extracellular signal regulated kinases
FAK	Focal adhesion kinase
FITC	Fluorescein isothiocyanate
FIV	Feline immunodeficiency virus
FLS	Fibroblast-like synoviocytes
FOV	Field of view
GBM	Glioblastoma multiforme
G-CSF	Granulocyte colony stimulating factor
Glu	Glutamic acid
Gp120	Glycoprotein 120
Gp41	Glycoprotein 41
GPCR	G protein coupled receptor
GRK	G-protein receptor kinase
GTP	Guanine triphosphate
hr	Hour
HIF-1	Hypoxic inducible factor -1
His	Histidine
HIV	Human immunodeficiency virus
HIV-1	Human immunodeficiency virus type 1
HIV-2	Human immunodeficiency virus type 2
HPC	Haematopoietic progenitor cell
Hu-PBL-SCID	Human peripheral blood lymphocyte-severe combined - immunodeficiency mouse model

IBD	Inflammatory bowel disease
IC_{50}	Inhibitory concentration (50 %)
IFN-α	Interferon alpha
IFN-γ	Interferon gamma
IgG-FITC	Immunoglobulin fluorescein isothiocyanate conjugate
IL-**	Interleukin *number*
JAK	Just another kinase
K	Kelvin (temperature)
K_a	Association constant
K_d	Dissociation constant
kDa	Kilodaltons
K_i	Inhibition constant
k_{off}	Off-rate constant
k_{on}	On-rate constant
LESTR	Leukocyte-derived seven transmembrane domain receptor
M	Molar (concentration)
mAb	Monoclonal antibody
MAP	Mitogen activated protein
MCP-1	Monocyte chemoattractant protein-1
MCP-3	Macrophage chemoattractant protein-3
MCP-4	Macrophage/Monocyte chemoattractant protein-4
MFI	Mean fluorescence intensity
MIF	Migration inhibitory factor
min	minute
MIP-1α	Macrophage inflammatory protein-1 alpha
MIP-2	Macrophage inflammatory protein-2
ml	Millilitre
MMP-**	Matrix metalloproteinase-*number*
μM	Micromolar (concentration)
μl	Microlitre
mRNA	Messenger ribonucleic acid

MS	Multiple sclerosis
MT-4	Metallothionein 4
MTS	((3-(4,5-dimethylthiazol-2-yl)-5-(3-carboxymethoxyphenyl)-2-(4-sulfophenyl)-2H-tetrazolium,salt)
MTS	Multicellular tumour spheroid
ng	Nanogram
NK cell	Natural killer cell
nm	Nanometre
nM	Nanomolar (concentration)
NM	Normal media
NMR	Nuclear magnetic resonance
NOD	Non-obese diabetic
NSI	Non-syncytium-inducing
OAc^-	Acetate (ion)
Obj	Objective (lens)
p38	Protein 38
p53	Protein (tumour) 53
PBL	Peripheral blood lymphocytes
PBC	Peripheral blood cells
PBMC	Peripheral blood mononuclear cell
PBS	Phosphate buffer saline
PHA	Phytohemagglutinin
PI	Propidium iodide
PI3K	Phosphoinositide-3 kinase
PKB	Protein kinase B
PLC-β	Phospholipase C-beta
PS	Phosphatidylserine
Pyk-2	Proline-rich tyrosine kinase-2
Qdot	Quantum dot
RA	Rheumatoid arthritis
RANTES	Regulated on activation normal T expressed and secreted

rhMIF	Recombinant human migration inhibitory factor
RNA	Ribonucleic acid
SB	Side-bridge
SCID	Severe combined -immunodeficiency (mouse model)
SDF-1α	Stromal cell derived factor-1 alpha
SDF-1β	Stromal cell derived factor-1 beta
SDS-PAGE	Sodium dodecyl sulphate-polyacrylamide gel electrophoresis
SF	Serum free
shRNA	Small hairpin ribonucleic acid
SI	Syncytium-inducing
siRNA	Small interfering ribonucleic acid
STAT	Signal Transducers and Activator of Transcription
τ	Residence time
$t_{1/2}^{diss}$	Dissociative half-life
Tat	Transactivator protein
TGF-β1	Transforming growth factor-beta 1
Th2	Helper T cell 2
TMIV	Transmembrane domain four
TMVI	Transmembrane domain six
TMVII	Transmembrane domain seven
TNF	Tumour necrosis factor
TNF-α	Tumour necrosis factor alpha
Trp	Tryptophan
Tyr	Tyrosine
UV	Ultraviolet
V3	Variable loop 3
VEGF	Vascular endothelial growth factor
WHIM	Warts hypogammaglobulinemia infections and myelokathexis

Chapter 1

Introduction

1.1 CHEMOKINES AND CHEMOKINE RECEPTORS

Cytokines are small proteins (with a mass of 8-30 kDa) that are used as signalling molecules to send messages to both adjacent and distant cells. They have a central role in the immune system and are involved in immunological and inflammatory responses. Chemokines are a sub-family of cytokines and are primarily involved in chemotaxis (i.e. the migration of cells or control of cell movement).[1] Chemokines recruit leukocytes to the sites of inflammation by binding and activation through specific receptors. A breakdown in the regulation of such processes can have serious consequences. Chemokines and their receptors are now known to be involved significantly in a wide spectrum of diseases, including cancer and AIDS, as well as multiple sclerosis, rheumatoid arthritis, allergic disorders, asthma, psoriasis, inflammatory bowel disease and nephritis. In some of these disease states, overexpression of the receptor is observed and, in many, the progression of the disease can be mediated by small molecule receptor antagonists. The diversity of diseases in which chemokines are involved has excited the interest of the pharmaceutical industry. The classes of antagonists for which clinical trials are most advanced are MDX-1338 (Medarex Inc) and BKT140 (Biokine Therapeutics) all targeting the CXCR4 receptor for a number of disease states including multiple myeloma, cancer and stem cell transplantation. Other small and large multinationals are also pursuing development of chemokine receptor based antagonists including Maraviroc (Pfizer), a reversible CCR5 co-receptor antagonist designed to prevent HIV infection of CD4 T-cells (approved by FDA in December 2007) and CCX168 (ChemoCentryx) an orally bioavailable antagonist of the C5a receptor for use in Crohn's disease.[2]

1.1.1 Chemokines

Chemokines are 8-12 kDa proteins that are rich in basic amino acids and contain conserved cysteine motifs forming essential disulphide bonds between the first and third, and the second and fourth cysteines. They are single polypeptide chains of 70 to 100 amino acids that share varying degrees (20%-95%) of amino acid identity. They are

divided into 2 major (CXC and CC) and 2 minor (C and CX3C) groups on the basis of the position and spacing of the first 2 conserved cysteine residues, see table (**1**).[3,4] Chemokines mediate the recruitment of effector leukocytes such as monocytes, neutrophils, T-cells, dendritic cells, NK cells, and eosinophils to sites of inflammation and secondary lymphoid organs for antigen presentation and maturation.[5] However, more recently the biological role of chemokines has been shown to go beyond trafficking of immune cells and they are now known to be involved in growth regulation, haematopoiesis (stem cell homing and proliferation), embryonic development, and angiogenesis.[6]

Chemokines initiate their biological effects by binding to cell surface receptors that belong to the G-protein coupled receptor (GPCR) super family.[7] Most chemokines and chemokine receptors are promiscuous in their interactions e.g. CXCR3 binds to CXCL9, CXCL10 and CXCL11. There are thought to be at least 46 distinct chemokines and possibly as many as 20 chemokine receptors, making it the largest cytokine family, see table (**1**).[4,8] Chemokine binding to the receptor initiates a cascade of intracellular events mediated by the receptor associated heterotrimeric G proteins. The G proteins trigger various second messenger signalling pathways, which lead to the activation, not only of chemotaxis, but also a wide range of functions in different leukocytes, such as degranulation, phagocytosis or a respiratory burst.[9] Chemokines have also been shown to bind to "atypical" chemokine receptors such as the Duffy antigen receptor (DARC) and cause no signal transduction. These atypical chemokine receptors play a role in scavenging and sequestering local chemokines. This sequestration of chemokines is an important mechanism of controlling the chemokine network.[10]

1.1.2 G-Protein Coupled Receptors (GPCR) and Chemokine Receptors

Chemokine receptors belong to the superfamily of GPCR consisting of seven transmembrane domains with three intracellular and three extracellular connecting loops that transduce signals *via* heterotrimeric G-proteins[11-13]. These loops are composed of hydrophilic amino acids which are orientated perpendicular to the plasma membrane. A

disulphide bond links highly conserved cysteines in extracellular loops 1 and 2.[14] The receptors are typically 340-370 amino acids in length with 25-80% amino acid homology. A short extracellular N-terminal domain is acidic, has an overall negative charge at physiological pH, contains tyrosine residues (some of which may be sulfonated) and is believed to be essential for ligand binding. There are also several N-glycosylation sites in the extracellular regions. An intracellular C-terminal is important for G-protein activation and this contains serine and threonine residues that act as phosphorylation sites for receptor regulation and desensitisation. Overall GPCRs constitute the targets for about 50% of therapeutic agents used at present and many are implicated in current drug development programmes.[15,16] Given the high interest in this receptor family in relation to human disease, several studies have attempted to delineate the structure of these proteins. In 2000, the first crystal structure of a mammalian GPCR (bovine rhodopsin (IF88)) was published, and for a while this formed the basis for homology models.[17] However, more recently the human β_2 - adrenergic receptor GPCR structure was solved ((2R4R, 2R4S), followed by a higher resolution version of the same structure (2RH1).[18,19]

Chemokine receptors are found to be expressed on different types of leukocytes, some restricted to certain cell types, while others are spread over a variety of cell types. They are also expressed on non-haematopoietic cells such as neurons, astrocytes and endothelial cells.[20] Chemokine receptors probably signal through the G-protein $\beta\gamma$ subunit to activate phospholipase C and phosphatidylinositol-3 kinase.[21,22] This, in turn, leads to activation of the cytoskeletal regulatory kinases FAK and Pyk-2 that mediate chemotaxis, and in some cases activation of the mitogen-activated protein (MAP) kinase proliferative pathway.[23]

Receptor name	Selective ligands	Biological function
C Receptor Subfamily		
XCR1	XCL1 & 2	Inflammation
CC Receptor Subfamily		
CCR1	CCL3, CCL3L1, CCL5, CCL9-10, CCL14-16	Anti-viral response
CCR2	CCL2, CCL7-8, CCL12-13	Macrophage recruitment
CCR3	CCL5-6, CCL11, CCL15-16, CCL23-24, CCL26	Parasite response, Th^2 recruitment
CCR4	CCL17, CCL22	Skin homing, Th^2 recruitment
CCR5	CCL3-4, CCL3L1, CCL5-6, CCL8, CCL12	Th^2 and macrophage recruitment
CCR6	CCL20	Dendritic cell homing
CCR7	CCL19, CCL21	Secondary lymphoid tissue homing of T, B, & dendritic cells NK cell recruitment
CCR8	CCL1	Th^2 recruitment
CCR9	CCL25	Intestinal homing, thymocyte migration
CCR10	CCL27-28	Skin homing of T cells
CCR11	CCL2, CCL19	Macrophage recruitment
DARC	Many CC	Does not signal-chemokine sink, malaria receptor
CXC Receptor Subfamily		
CXCR1	CXCL6-8	Neutrophil chemotaxis and deregulation
CXCR2	CXCL1-3, CXCL5-8	Neutrophil chemotaxis and deregulation
CXCR3	CXCL9-11	T cell responses
CXCR4	CXCL12	B cell responses, stem cell homing
CXCR5	CXCL13	B cell responses
CXCR6	CXCL16	Activated T cells
CXCR7	CXCL12	unknown
CX3C Receptor Subfamily		
CX3CR1	CXC3CL1	Inflammation

Table (1). Chemokine Receptors and their Major Activity. [4,15,24,25]

1.1.3 CXCR4

Over the last 10 years there has been growing interest in CXC chemokine receptor 4 (CXCR4) exemplified by a consequent increase in the number of scientific publications relating to CXCR4 every year. CXCR4 was originally cloned by Loetscher *et al.* as an orphan chemokine receptor (ligand not yet discovered) and was given the acronym

LESTR (leukocyte-derived seven transmembrane domain receptor).[26] However, it was not until the CXC chemokine CXCL12 (also known as stromal cell derived factor-1, SDF-1) was recognised as the ligand for LESTR that the receptor was reclassified as CXCR4.[27,28] CXCR4 consists of 352 amino acids with 27% of residues either being aspartate, histidine or tyrosine and has an overall electrostatic surface charge of -9, see Figure (**1**).[29,30]

CXCR4 functional receptor protein is detected in a diverse range of cells including peripheral blood lymphocytes (PBL) and monocytes, as well as pre B cells, mast cells, adult CD34+ bone marrow progenitor cells, endothelial cells, intestinal and alveolar epithelial cells, astrocytes, microglia and neurons.[31-37] A range of cytokines have been found to regulate the expression of CXCR4, for example, it can be up-regulated by TGF-β1, VEGF and IL-4 and down regulated by IL-5 and IFN-α/γ.[38,39] CXCR4 plays a fundamental role in proliferation, survival, homing and retention of primitive haematopoietic CD34+ progenitor cells (HPC) in the bone marrow.[40-44] CXCR4 positive HPC are mobilised from the bone marrow when CXCL12 levels are reduced from the usual threshold level. Cytokines such as the haematopoietic cytokine granulocytecolony stimulating factor (G-CSF) cause a reduction in CXCL12 levels in the bone marrow, mainly *via* degradation by neutrophil elastase but possibly also by downregulating the expression of CXCL12 in osteoblasts.[45-47] Mobilised HPC are then attracted to developmental sites or areas of tissue injury, where CXCL12 levels are high and have been shown to be up-regulated e.g. the liver.[48]

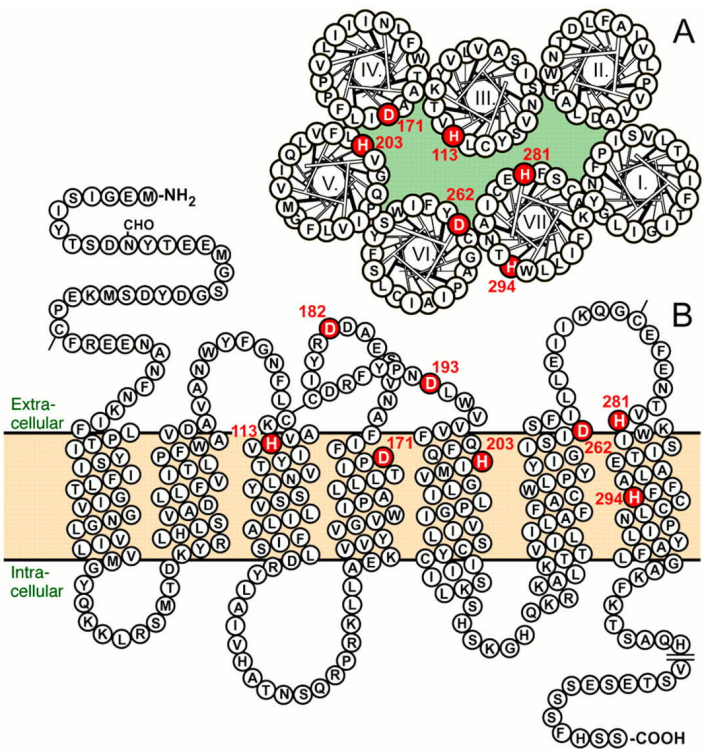

Figure (1). (**A**) Helical wheel structure of CXCR4 and (**B**) Serpentine diagram. (*Reproduced from the Journal of Biological Chemistry*)[49]

Migration and positioning of B-lymphocytes within a secondary lymphoid organ correlates with the CXCR4 response to CXCL12, and the B-cell responsiveness to CXCL12 is regulated by the differentiation state of the cell.[50] CXCR4 signalling is also involved in the migration of antibody-secreting plasma blasts from the spleen into the bone marrow during a memory immune response.[51]

Gene disruptions of CXCR4 have highlighted the importance of this receptor during embryonic development. Mice lacking the CXCR4 gene exhibit impaired B lymphopoiesis, myelopoiesis, haematopoiesis, derailed cerebellar neurone migration, defective formation of large vessels supplying the gastrointestinal tract and cardiac ventricular septal defects.[52-54] A recent study examining human foetal tissue samples confirmed the wide spread importance of CXCR4 in the bone marrow, heart, liver, kidney, brain and intestine during development.[55]

1.1.4 CXCL12 (SDF-1)

CXCL12 or SDF-1 is the only known natural ligand for CXCR4. It is a member of the CXC chemokine family and was originally described as a secreted product of stromal cells from the bone marrow.[28,56] It is generally accepted that CXCR4 and CXCL12 have a monogamous relationship, although it has recently been proposed that CXCL12 also binds to another receptor CXCR7 (RDC1).[25] Although one report suggests CXCL12 causes a cell migration response when bound to CXCR7, others have yet to determine the true nature of the effect of CXCL12 on CXCR7.[57,58]

The human CXCL12 gene is located on chromosome 10, whereas other CXC chemokines are clustered on chromosome 4. CXCL12 belongs to the CXC family, but its average amino acid sequence identity with other human CXC chemokines and to the CC chemokines is only 27% and 22%, respectively making it a distant relation. Two alternative SDF-1 are generated by differential splicing of mRNAs. SDF-1α is four amino acids shorter than SDF-1β at the carboxy terminus, but both species bind with high affinity to CXCR4.[59] However, only SDF-1α is purified from stromal cells and is generally referred to as CXCL12.

CXCL12 is a 67 residue polypeptide, the structure of which has been determined by NMR studies.[60] The NMR structure is in good agreement with individual subunits observed in the X-ray crystal structure of dimeric CXCL12.[61] CXCL12 adopts a chemokine type fold consisting of three anti-parallel β strands and an overlying α-helix Figure (**2A**). The well ordered regions include an extended loop (Arg12 to Ala19) which leads into a 3_{10} helix (Arg20 to Val23) (Figure (**2B**)). The first β strand (24 to 30) is connected by a type III turn (31 to 34) (Figure (**2C**)) to the second β strand (37 to 42) and the second and third β strands (47 to 51) are connected by a type I turn (43 to 46) (Figure (**2D**)). A type I turn (52 to 55) connects the third β strand and the C-terminal α-helix (58 to 65) (Figure (**2E**)).

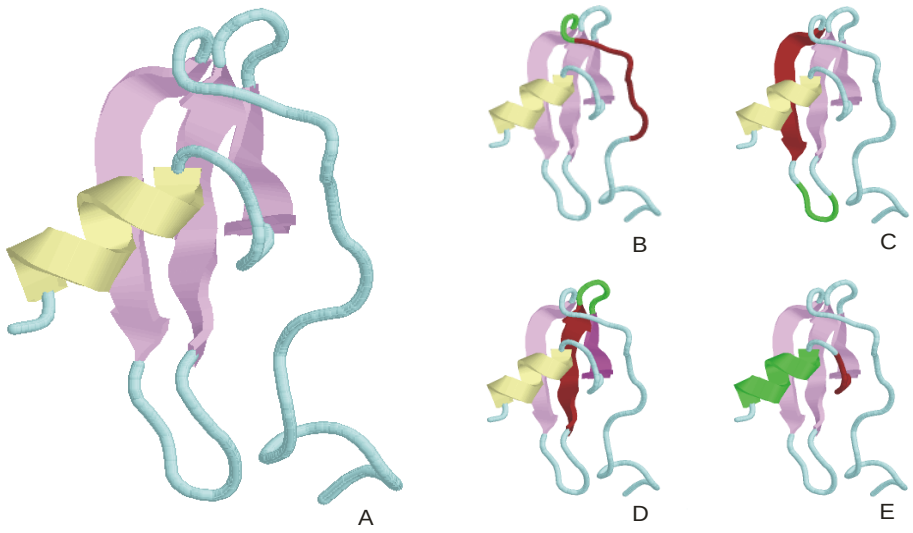

Figure (2). Representations of the NMR Solution structure of CXCL12 (PDB code: 2SDF) (**A**); (**B**) highlights the extended loop (red) and 3_{10} helix (green); (**C**) highlights the 1st ß-strand (red) and type III turn (green), (**D**) highlights the 2nd (red) and 3rd (purple) ß-strands with a type I turn (green); (**E**) highlights the type I turn (red) and c-terminal α-helix (green).

CXCL12 is a highly basic protein with 21% of the total residues being arginine, lysine or histidine. CXCL12 has positive surface charges clustered along the first and second β strands while the α-helix displays a predominantly negative surface charge.[60] These properties have important implications for the design of small molecule antagonists for CXCR4.

CXCL12 stimulates CD34+ cells, pre B cells, monocytes, neutrophils and PBL, as indicated by intracellular calcium(II) concentration variations and chemotaxis.[3,40,62,63] CXCL12 can also induce apoptosis of primary CD8+ T cells *in vitro* and is involved in the homing of haematopoietic cells such as T cells and monocytes *in vivo*.[64,65] Predominantly, the expression of most chemokines is induced by other cytokines, however, although the levels of CXCL12 can be regulated by cytokines there is also a continuous production. It is expressed and secreted by various organs including bone, lung, liver, brain, thymus and lymph nodes. CXCL12 is produced mainly by stromal cells, such as osteoblasts, fibroblasts and endothelial cells in the bone marrow.[59,66-69] The plasma concentration of the CXCL12 protein among normal healthy humans varies widely (0.28 to 106.5 ng/ml).[70]

The gene knockout of CXCL12 is lethal, as with CXCR4, leading to defects of the immune, haematopoietic, circulatory, cardiac, and central nervous systems.[53,54,71] This striking similarity between the phenotype of the two knockouts gives credence to the monogamous relationship between CXCL12 and CXCR4. Response to CXCL12 and expression of CXCR4 occurs at a very early stage of embryonic development and appears to be widely utilised wherever cell migration is required.[72]

1.2 THERAPEUTIC POTENTIAL OF TARGETING CHEMOKINE RECEPTORS

Recently, there has been an increase in our understanding of the association between chemokine receptors and certain human disease states. Chemokine-receptor activity can result in an excessive recruitment of leukocytes in tissues during inflammation and homeostasis. In addition to their role in inflammation, chemokine receptors have been found to be required by the human immunodeficiency virus (HIV) for leukocyte infection, and also tumour metastasis can be influenced significantly by activation of chemokine receptors overexpressed on tumour cells.[3,15,67,73-77]

1.2.1 The Role of Chemokines and Chemokine Receptors in Disease

The overproduction of chemokines has been associated with many inflammatory disorders. In diseases such as psoriasis vulgaris there is an elevated level of IL-8, activated neutrophils and T lymphocytes in the epidermis tissues of patients.[78] In addition, CXCR1 and CXCR2 mRNA levels have been reported to be 10 times higher in lesional psoriatic epidermis than in normal epidermis and this has led to the conclusion that overexpression of receptors CXCR1 and CXCR2 that bind to CXCL8 may be responsible for epidermal hyperplasia and leukocyte infiltration.[79] There have been reports of abundant production and expression of the chemokine, CCL2, and its receptor CCR2 in macrophage rich areas of atherosclerotic plaques, and IL-10 and IL-12 cytokines stimulating T cell infiltration in atherosclerotic lesions during atherosclerosis, suggesting that it may be appropriate to treat this disease with receptor antagonists.[80,81]

Macrophage inhibitory protein (CCL3 and CXCL1) levels have been reported to be elevated in arthritic joints, and their levels correlate with the severity of rheumatoid arthritis (RA).[82-84] Further studies have established the chemokine network to be important in the progression of rheumatoid arthritis. Chemokines CCL13, CCL18, CXCL9, CXCL12, CCL2, CXC3CL1 have been shown to be up-regulated in synovial tissue/fluid from RA patients. These chemokines were able to stimulate fibroblast-like synoviocytes (FLS) and chondrocytes to release inflammatory mediators, including cytokines and matrix metalloproteinases (MMPs), leading to cartilage degradation.[85]

Chemokines and their receptors may have a role in influencing the progression of multiple sclerosis (MS) and Alzheimer's disease.[86-89] They have also been implicated in the development of allergic airway inflammations such as allergic rhinitis and asthma.[87,90-97]

More recently, the chemokine network in particular chemokines CCL2, CXCL12 and CXC3CL1 have been implicated in chronic pain. It has been shown that neuronal and non-neuronal cells in the central nervous system (CNS) produce and release these chemokines in an up-regulated fashion. These chemokines then act as neuromodulators in neuron excitation and neurotransmitter release. However, their functional roles in the CNS still remain largely unknown.[98,99]

Many cancers express an extensive network of chemokines and chemokine receptors, often displaying a dysregulated production and abnormal signalling.[100-102] The tumour produced chemokines can be associated with the regulation of angiogenesis within the tumour, act as growth and survival factors and control the movement of tumour cells.[103,104] Chemokines such as CCL17, CCL11, CCL22 as well as CXCL10 and CXCL9 have been implicated in Hodgkin's disease and CXCL8, CXCL1, CXCL5, CXCL6 and CXCL7 increase the growth of tumours (including melanoma, ovarian carcinoma, non-small cell lung cancer and prostate cancer) by promoting angiogenesis.[104,105] In addition, CXCL1, CXCL8 and CCL20 have all been shown to stimulate growth of pancreatic tumour cell lines *in vitro*.[106,107] Furthermore, elevated levels of CXCL13 have been shown to stimulate proliferation of breast cancer cell lines *in vitro*.[108] Several excellent reviews have discussed the implication of the chemokine network in cancer.[77,109,110]

The potential role of chemokines in diabetes has been examined. In a non-obese diabetic (NOD) mouse model there was an elevated level of CCL3 and CCL4 in the pancreas and this correlated with destructive insulitis and progression to diabetes. Furthermore, a neutralising CCL3 antibody delayed the onset of diabetes in this animal model.[111] In addition, CXCR3 and its ligands CXCL10-11 are involved in the pathogenesis of type 1 diabetes.[112]

1.2.2 CXCR4 and CXCL12

Over the last few years, the CXCR4 receptor and its ligand CXCL12 have been implicated in a number of disease states. A role for CXCR4 in rheumatoid arthritis was revealed by demonstrating that receptor antagonists reduce the severity of arthritis in a collagen-induced arthritis mouse model.[76] The majority of leukocytes harvested from the inflamed joints of these mice were found to be CXCR4(+). This showed that CXCL12 plays a central role in the pathogenesis of murine collagen induced arthritis by attracting CXCR4(+) leukocytes to the inflamed joints. CXCR4 and CXCL12 have been detected in the synovium and articular cartilage of human rheumatoid arthritis patients.[113] In inflammatory liver disease, CXCL12 is up-regulated in biliary epithelial cells and plasma levels of CXCL12 are significantly higher than in normal controls (75 patient study).[114] In a murine model of airway inflammation, functional blockade of CXCR4 using an antagonist resulted not only in a therapeutic effect but a protective effect against metacholine induced airway hyperresponsiveness and inflammation in allergic mice.[5] More recently, CXCR4 has been found to be upregulated in human atrial fibrillation.[115]

Moreover, WHIM (warts, hypogammaglobulinemia, infections, and myelokathexis) syndrome, a rare immunodeficiency disease has established itself to be the result of a genetic mutation (truncation of C-tail) of the CXCR4 receptor.[116,117]

1.2.2.1 *CXCR4 and CXCL12 in Cancer*

In recent years, there have been a number of key papers published highlighting the link between tumour growth, survival and metastasis, and CXCR4/CXCL12. CXCR4

overexpression has been reported in numerous different epithelial, mesenchymal and haemopoietic cancers.[24,118-124]

Cancer is a class of disease involving abnormal and uncontrolled growth of cells. Mutagenic disruptions occur in the normal cell DNA which causes the normal group of cells to proliferate and invade surrounding tissues, forming a tumour. These tumours can invade and metastasise to other parts of the body by breaking away from the primary tumour and entering the blood or lymphatic system (intravasation) (Figure (**3**)). They then arrest in microvessels of various organs and invade through their epithelial tissues (extravasation). Once these cells have penetrated the tissues of these organs the formation of another tumour occurs and colonisation (macrometastasis).

CXCL12 stimulation of tumour growth, angiogenesis and metastasis of breast cancer cells has been described.[67,104,125] Target organs for breast metastases such as bone, liver and lung have high levels of CXCL12, resulting in the specific migration of CXCR4 +ve breast tumour cells to these sites.[122,126] Moreover, CXCR4 is highly expressed and is critically involved in lung, cervical, colorectal, pancreatic, prostate and gastric cancer.[119,120,127-136] Tissue samples of pancreatic cancer were found to constitutively express CXCL12 and this chemokine significantly increased cancer cell migration in a separate series of pancreatic cancer cell lines. The addition of a CXCR4 antagonist inhibited cell migration and hence may potentially act against growth and spread of the tumour.[132] In another study, seven pancreatic tumour surgical samples displayed up to 46,000 fold higher CXCR4 expression compared with normal pancreatic duct samples and cell lines originating from metastatic lesions displayed between 80 and 1,000 fold higher CXCR4 expression than normal cells. This was associated with CXCL12 exerting an increased anti-apoptotic, proliferative, survival and invasive effect.[137] In colorectal cancer, CXCR4 is abundantly expressed in various colorectal carcinoma cells and elevated CXCR4 expression is associated with disease progression and reduced survival in patients.[130,138,139]

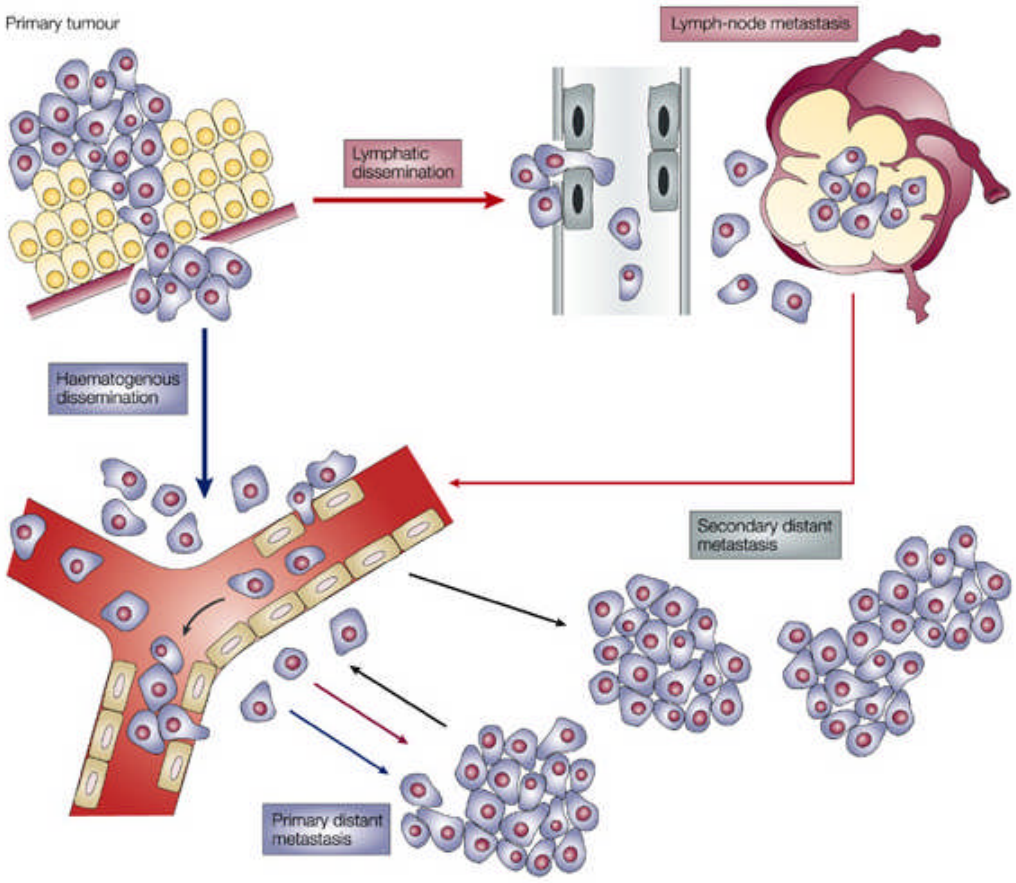

Figure (3). The invasion-metastasis cascade (*reproduced from Nature Reviews Cancer).*[140]

There are a number of cancers that respond to the CXCR4/CXCL12 signalling pair. Multiple actions of CXCL12 on CXCR4 expressing ovarian cancer cells have been shown. CXCL12 induces the production of matrix metalloproteinase (MMP) 1 mRNA and tumour necrosis factor (TNF), increases integrin expression, attracts and modulates type 2 dendritic cells (DC) into the tumour environment, and induces tumour cell migration and invasion in ovarian cancer.[141] Prostate cancer cells (SCID), where CXCR4 has been downregulated, grew smaller tumours with decreased blood vessel density and muscle invasion, compared with parental cells.[142]

More surprisingly, CXCR4 has been linked to brain tumours of both neuronal and astrocytic lineage.[143,144] Compared with normal neuronal cells, CXCR4 is found to be highly overexpressed on malignancies. CXCL12 has been found to exert a proliferative, anti-apoptotic, and invasive effect on both glioblastoma multiforme (GBM) and medulloblastoma cell lines. Systematic blocking of CXCR4 *in vivo* decreased growth of

GBM and medulloblastoma xenografts. Direct anti-tumour effects of neutralising CXCR4 were evident in reduced activation of extracellular signal regulated kinases 1 and 2 (Erk 1/2) and Akt, and increased rates of apoptosis in both tumour types.[145] Similarly, CXCR4 neutralisation has also shown potential as a novel therapeutic strategy for the treatment of non-Hodgkin's lymphoma.[146]

Until recently, genetically mutated CXCR4 receptor was only found in WHIM syndrome, however Ierano et al. has reported that an investigation of the genetic sequence of the CXCR4 receptor in a number of human melanoma and colon cancer cell lines revealed one colon cancer and one melanoma cell line to have a point mutation in the fourth transmembrane. These cancer cell lines with the CXCR4 mutants migrated to a CXCL12 stimulus.[147] This is the first report of CXCR4 mutant expression in active human cancer cells.

The growing elucidation of the involvement of the CXCR4 and CXCL12 in a number of diseases coupled with the positive response from receptor blocking suggests an immense therapeutic potential in targeting the CXCR4-CXCL12 axis.

1.2.2.1.1 *Manipulation of the signalling process*

The ability of cancer cells to evade and resist death is by the manipulation of the intracellular signalling machinery. One of the most important methods by which cancer cells survive is by inactivating the apoptotic machinery by activation of the Akt/PKB pathway, increasing the levels of anti-apoptotic Bcl-2 related proteins and inactivation of p53 controlling the tumour suppressor gene.[148,149] However more recently, the chemokine network has been implicated in further roles, such as enhancing growth, promoting angiogenesis and increasing the survival of many types of cancer. It has been suggested that this is primarily due to the dysregulation of the chemokine receptor signalling (section 1.2.1).

1.2.2.1.2 *CXCR4 signalling and regulation*

As discussed earlier (section 1.1.4), CXCL12 has been proposed to interact with CXCR4. Glycosaminoglycans such as heparin sulfate can interact with CXCL12 and induce oligomerisation (dimerisation) resulting in an enhanced function.[150,151] After activation of CXCR4 by CXCL12 binding, a whole spectrum of complexed intracellular signalling cascades are activated leading to a variety of biological responses (Figure (**4**)).

CXCL12 activation of CXCR4 leads to several G-protein dependent signalling pathways.[152,153] These heterotrimeric G-proteins are composed of α, β and γ subunits. Inactive Gαβγ complex is associated with a GDP molecule with the α subunit. Once activated by CXCL12 binding, a conformational change occurs in the receptor which allows the release of GDP and the binding of GTP instead. The α-GTP subunit then dissociates from the βγ complexed subunit. The splitting of the Gα and Gβγ subunits allows them to act as effector molecules for downstream signalling. The Gα subunit is able to inhibit adenylyl cyclase (decrease cAMP levels) and activate the Src kinase pathway. Furthermore the Gβγ subunit is able to activate the phospholipase C-β (PLC-β) and phosphoinositide-3 kinase (PI3K) pathways which ultimately lead to gene regulation, cell migration and adhesion.[152] The effect of Gα and Gβγ is regulated by the hydrolysis of GTP back to GDP, which allows the reassociation of the Gα and Gβγ subunits to the inactive Gαβγ protein.[154] It is important to note that a number of isoforms of G-protein subunits exist and have been proposed to exert varying downstream signalling.[153]

Although the majority of CXCR4 signalling is believed to occur via G-proteins, other G-protein independent signalling pathways have been described. CXCR4 has been proposed to activate the JAK/STAT pathway. CXCL12 activation of CXCR4 leads to association of several JAK enzymes (JAK2/3). These JAK enzymes are able to phosphorylate tyrosine residues on the cytoplasmic tails of the dimerised receptor molecule. Such phosphotyrosines are able to attract STAT transcription factors which eventually dimerise upon interaction with the receptors. STAT dimers then migrate to the nucleus and target a number of genes that are important for cell proliferation and apoptosis.[155]

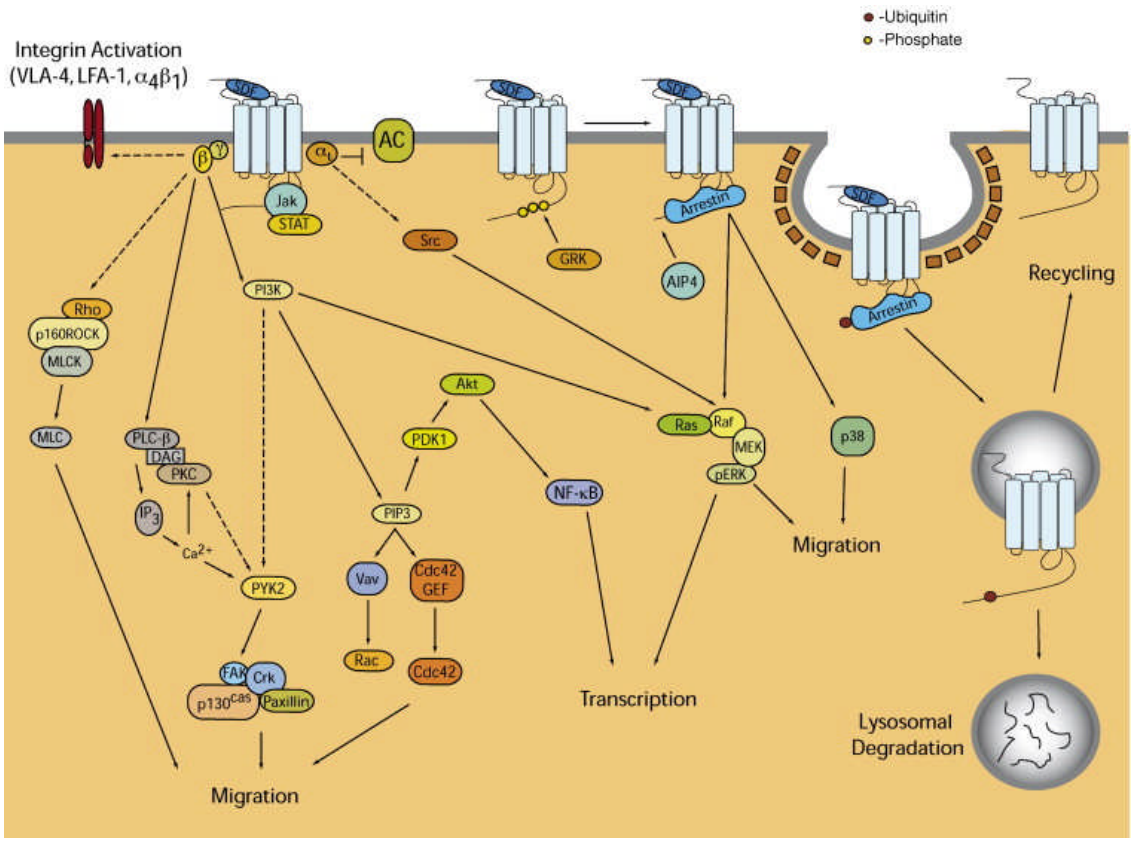

Figure (4). CXCR4 downstream signalling pathways (*reproduced from Biochimica et Biophysica Acta).*[152]

Upon CXCL12 activation, serine and tyrosine residues in the C-tail of CXCR4 can become phosphorylated by G-protein coupled receptor kinases (GRK). GRK phosphorylation specifically prepares the activated receptor for arrestin binding and this blocks further G-protein mediated signalling (desensitisation). This reduces the effect of the CXCL12 induced Gα subunit and hence inhibition of adenylyl cyclase and cAMP. CXCR4-arrestin complex binds to the monomeric GTPase Raf and activates the Erk1/2 MAP kinase pathways. In addition the CXCR4-arrestin complex is able to activate the p38 pathway and both this and the Erk1/2 MAP kinase pathway are important in chemotaxis and metastasis.[152,153]

Binding of arrestin can redirect CXCR4 and become ubiquitinated, a process mediated by E3 AIP4 a ubiquitin ligase, forming part of its internalisation and degradation mechanism. This process directs the CXCR4 receptor to lysosomes for degredation. However, depending on the specific residues phosphorylated on the C-tail, the receptor could alternatively be recycled back to the surface.[152]

1.2.2.1.3 *Cancer signalling and dysregulation*

CXCR4 has been shown to be highly expressed in cancer cells and this in part is related to the aggressive nature of the cancer. Work on the EGF-receptor in cancer suggests overexpressed receptors are capable of dimerisation without their respective ligands, resulting in ligand-independent signalling.[154] This could allow excessive signalling of CXCR4 in low CXCL12 environments. However, excessive activation of CXCR4 is able to be counter regulated and increased receptor activation alone may not be enough to drive cancer growth. Alterations in the normal regulation of CXCR4/CXCL12 signalling may well play a part in allowing cancer cells to grow and survive. Medulloblastoma and glioblastoma cells have been reported to show abnormal cAMP suppression as the basis for CXCL12-induced growth.[156] Furthermore, breast cancer cells expressing CXCR4 have been found to display inhibition of ubiquitination and abnormal tumour associated integrin activation has been linked to CXCR4/CXCL12 signalling.[157] The C-terminal tail of CXCR4 is critical for CXCR4 regulation and signalling. Although several *in vitro* studies have shown genetically modified truncation of the C-tail of CXCR4 giving rise to higher levels of proliferation and invasion (due to an amplification of the downstream signalling), C-tail truncated CXCR4 receptor to date has only been found in WHIM syndrome.[117]

A detailed basic understanding of receptor regulation is still not available. Understanding the precise signalling mechanisms of CXCR4 and how these are altered in disease will allow the development of drugs targeting such pathways.

1.2.2.2 *HIV Infection: Utilisation of CXCR4*

In the 1990s it was discovered that the CD4 receptor alone was not sufficient to allow HIV-1 infection and that chemokine receptors CCR5 and CXCR4 acted as co-receptors for HIV-1 cell entry.[158-163]

The process of viral entry involves fusion of the viral envelope with the host cell membrane and requires the interaction of the envelope with specific cell surface receptors. The two viral envelope glycoproteins, gp120 and gp41, are conformationally

associated to form a trimeric functional unit consisting of three molecules of gp120 exposed on the virion surface that are associated with three molecules of gp41 inserted into the viral lipid membrane Figure (**5A**) Trimeric gp120 on the surface of the virion binds to the CD4 receptor, which is expressed mainly on T-cells and monocytes/macrophages.

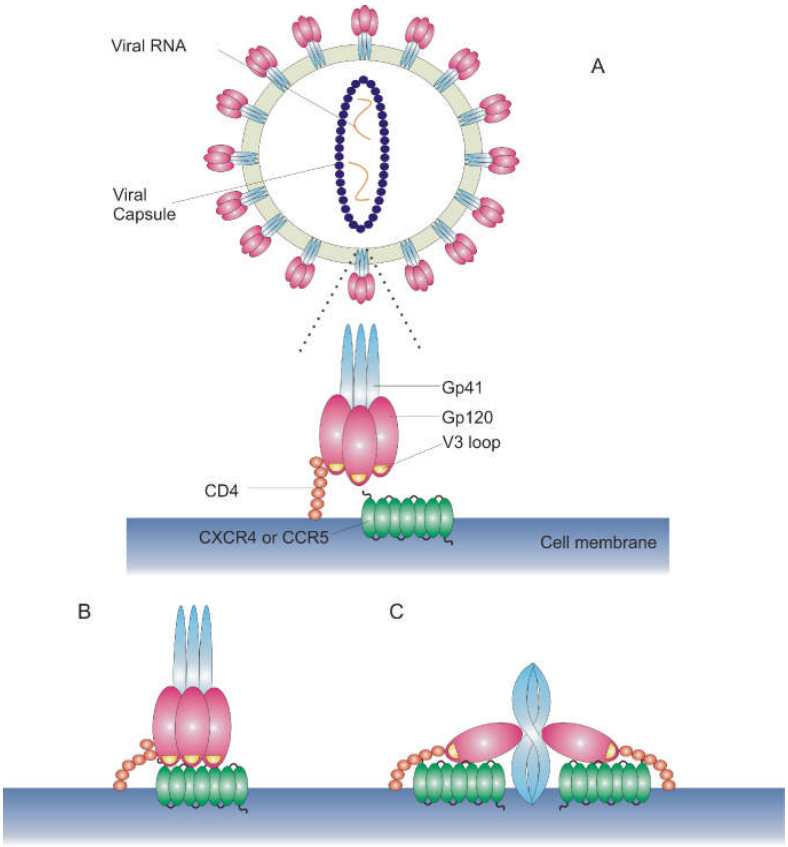

Figure (5). HIV Cell Entry involving (**A**) interaction of gp120 with CD4 followed by (**B**) interaction of gp120 with co-receptor CXCR4 or CCR5 and (**C**) conformational change in gp41 (coiling) followed by fusion.

This induces a conformational change in the envelope proteins that, in turn, allows binding of gp120, or more specifically its V3 loop, to either CCR5 (in R5 strains) or CXCR4 (in X4 strains), Figure (**5B**).[159,164,165] The binding of gp120, CD4 and CXCR4 or CCR5 produces a radical conformational change in gp41, see Figure (**5C**). Gp41 assembled as a trimeric coil, springs open, projecting itself into the lipid bilayer of the target cell. Gp41 proteins then form hairpin like structures that draw the virion and cell

membranes together to promote fusion, leading to the release of the viral core into the cell and hence infection.[159,166,167]

1.3 CXCR4 ANTAGONISTS (NON-BICYCLAM)

The therapeutic potential of targeting CXCR4 in many disease states has led to the development of a number of receptor antagonists. The initial interest was in their potential as anti-HIV drugs but the field of research has quickly expanded as other disease states have been shown to involve CXCR4.

1.3.1 HIV Cell Entry Inhibition

The widespread use of current anti-HIV drugs, reverse transcriptase and protease inhibitors has resulted in a significant decrease in mortality of HIV-infected persons in the developed world. However, the efficacy of these drugs has become limited by the emergence of drug-resistant HIV strains.[94,168-172] This has resulted in the development of anti-HIV agents that target other stages in the HIV life cycle. Since the discovery that CXCR4 acts as a co-receptor for HIV-entry, there has been intense research which has resulted in the development of several agents which target CXCR4 and act as "HIV entry inhibitors".

Several molecules that specifically interact with CXCR4 have been described as anti-HIV agents, see Figure (**6**). One of the first of these was the peptide T22, a cationic 18 residue peptide which inhibits both laboratory strains and primary isolates of HIV-1 (200 nM) by specific binding to the N-terminus and two extracellular loops of CXCR4.[173] An analogue of T22, the 14-residue peptide called T140 has shown stronger inhibitory activity against HIV-1 entry compared to T22.[174] The binding of T140 is thought to be the result of electrostatic and hydrophobic interactions of Arg2, Nal3 (napthylamine), Tyr5, and Arg14 pharmacophore of T140.[175,176]

Several T140 analogues have been synthesised to reduce the cytotoxicity of T140 by replacing some of the basic arginine and lysine residues with non basic polar residues such as L-citrulline and glutamine.[177,178] Some of these analogues displayed similar anti-

HIV activity to T140 (IC_{50} values in the range of 8 to 50 nM).[178] To further increase the biostability of these T140 analogues, a 4-fluoro-benzoyl group has been added by N-terminal acylation. Surprisingly, this addition resulted in an increase of anti-HIV activity (EC_{50} of 0.2 nM (4F-benzoyl-TE14011)) compared with T140 (120 nM).[179] Developments of these T140 analogues and their therapeutic potential have been discussed in several recent reviews.[180-182]

ALX40-4C a polypeptide of nine arginine residues designed to mimic the TAT domain of HIV displayed a high anti-HIV activity against X4 strains in the nanomolar range (IC_{50} of 3 nM) in the MT4 assay.[162,183] However, in human clinical trials no significant reduction in viral load was noted and trials were abandoned.[184] Another peptide CGP64222 a basic oligomer of nine residues has also been shown to inhibit a wide range of HIV strains albeit with a reduced potency (IC_{50} of 3-9 μM (MT-4 assay)).[185] Other peptide based CXCR4 antagonists such as cyclopentapeptides [cyclo(Nal-Gly-D-Tyr-Arg-Arg)] based on the pharmacophore of T140 have also been reported and display a high anti-HIV activity (3.2 nM (MT-4 assay)).[177,186,187] ALX40-4C and AMD3100 (see Figure (**7**)) are the only drugs of this type to have been administered to humans against HIV.

Another peptide CTCE-9908 (Chemokine Therapeutics Corp, Canada) an analogue of CXCL12, has been in development for a number of years and has displayed activity against a number of cancers.[188] A disadvantage of the peptidic drugs is that their relatively complex synthesis increases the overall cost of the drug. In addition, they are not orally bioavailable and must be administered by injection.

Several other small molecule CXCR4 antagonists have been developed. One of these is KRH-1636 (Kureha Chemical Industry Co. Ltd., Nishiki, Japan) a small molecule which has potent anti-HIV activity. KRH-1636 selectively inhibits X4 strains in a variety of cells (EC_{50} of 19.3 nM (MT-4 assay)) and, moreover, showed potent antiviral activity in the human peripheral blood lymphocytes/severe combined immunodeficiency (hu-PBL-SCID) mouse model.[189] KRH 3955 and KRH 3140 are orally bioavailable forms of KRH-1636 and are reported to be in development.[190] These two compounds have demonstrated efficacy in protecting hu-PBL-SCID mice from HIV infection.[191]

AMD070 (Genzyme, Cambridge, USA) is a potent small molecule antagonist of CXCR4, displays high anti-HIV activity (1-20 nM) in a range of T cells and more importantly is reported to be orally bioavailable.[192] AMD070 progressed to Phase II clinical trials. This group has also reported the development of AMD3465 (Figure (**6**)), an N-pyridinylmethylene xylyl monocyclam based CXCR4 antagonist. AMD3465 inhibits the binding of CXCL12 in the nanomolar range.[193]

In addition to these CXCR4 specific antagonists, AMD3451 (*N*-pyridinylmethyl cyclam) (Figure (**6**)) a dual CCR5/CXCR4 antagonist has been reported. Although AMD3451 inhibited the binding of several types of HIV in a variety of cells, a relatively high concentration was required to achieve an effect (1.2-26.5 μM) and thus AMD3451 is regarded as a low potency antagonist.[194]

Several other new agents are in advanced clinical trials targeting the CXCR4 receptor such as MDX-1338 (Medarex Inc) and BKT140 (Biokine Therapeutics).[2]

It should be considered that all co-receptor antagonists applied to HIV can elicit mutational escape, although the timescale can vary considerably. AMD3100 required 60 passages (300 days) in MT-4 cells for the virus to become resistant, whilst other HIV drugs such as T-20 (Fuzeon) have been reported to more rapidly produce resistant strains (45 days).[195,196] In contrast to using co-receptor antagonists, HIV gene therapy has also been investigated.[197] Down regulation of CXCR4 and CCR5 using gene splicing (siRNA/shRNA) confers viral resistance to both X4 and R5-tropic strains of the virus.

This research demonstrates the considerable interest in developing drug candidates targeting CXCR4 and CCR5 for anti-HIV therapies. Greater emphasis is now being placed on targeting both receptors simultaneously and developing orally bioavailable drug formulations for improved ease of dosing.

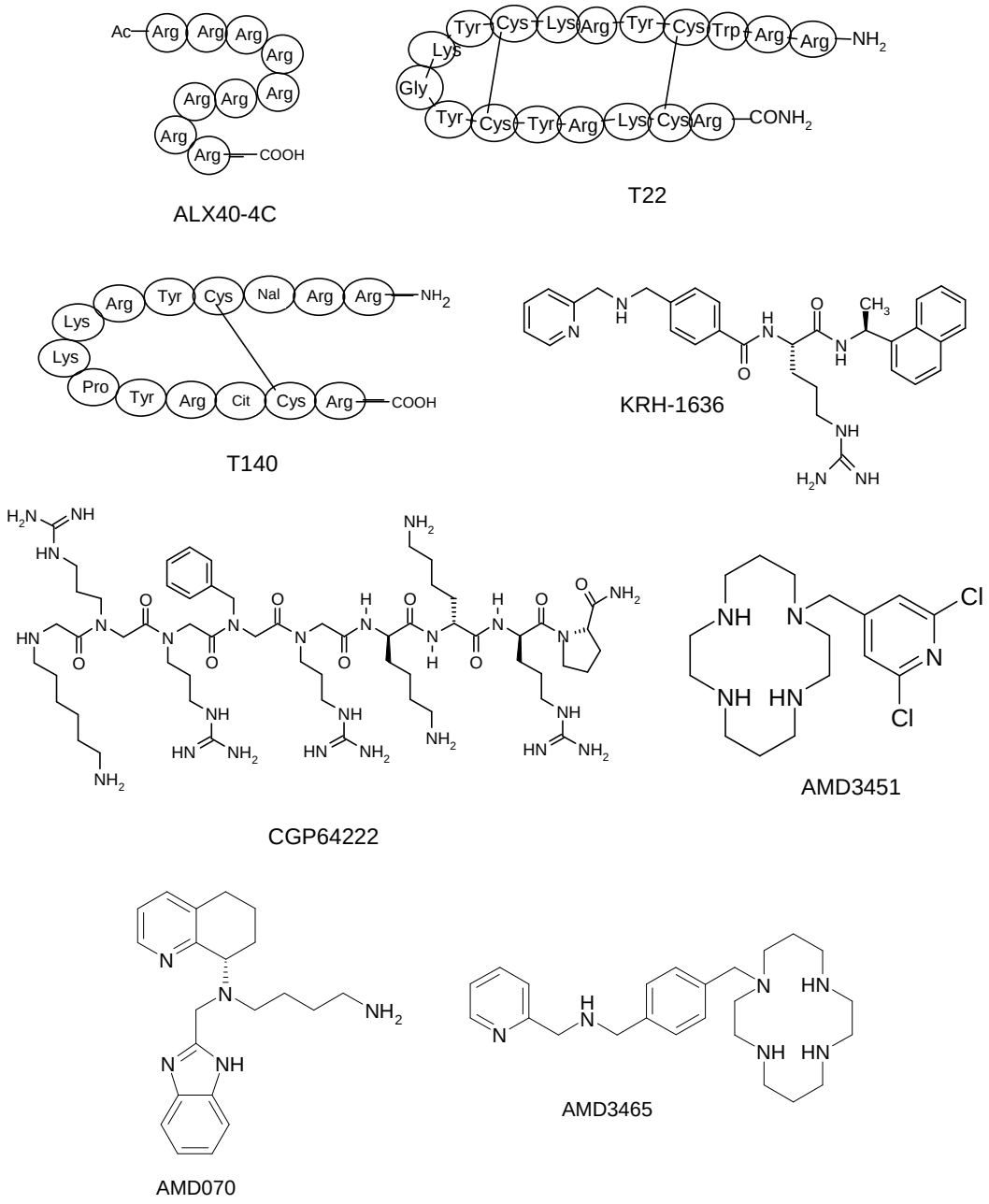

Figure (6). Molecular structures of some CXCR4 antagonists.

1.4 CXCR4 ANTAGONISTS (BICYCLAM)

Bicyclam compounds, composed of two cyclam (1,4,8,11- tetraazacyclotetradecane) units linked by an aliphatic or aromatic linker, represent the most thoroughly investigated class of CXCR4 antagonists to date. Bicyclams have been identified as potent inhibitors of

HIV type 1 and 2 replication that act by binding to the CXCR4 receptor.[198-200] The initial compound of the bicyclam series was discovered as an impurity that was responsible for an unusually potent antiviral effect observed for a sample of cyclam.[167] The bicyclam, AMD3100, Figure (**7**), in which two macrocyclic rings are connected by an aromatic linker, shows remarkable potency against HIV-1 and HIV-2 infection at concentrations of 1-10 nM and has been in clinical trials, which were abandoned in 2001 due to possible cardiac toxicity and limited efficacy.[167,198,200,201] However, it was not understood that AMD3100 was a specific CXCR4 antagonist when trials commenced, hence it was not tested against an appropriate patient population. It has since been approved by the FDA as a stem cell mobilizing agent.

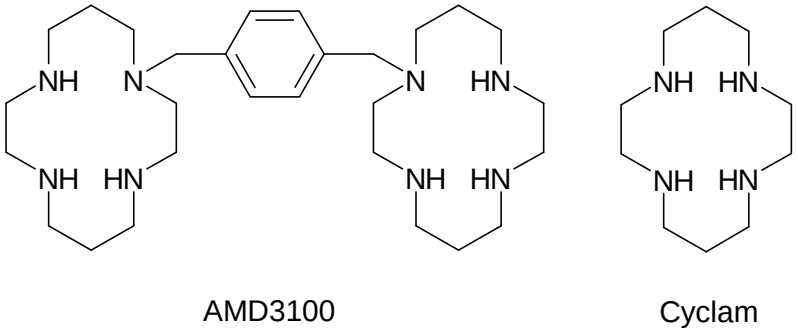

Figure (7). Cyclam (1,4,8,11-tetraazacyclotetradecane) and 1,1'-[1,4-phenylenebis(methylene)]-bis-[1,4,8,11 tetraazacyclotetradecane] (AMD3100).

1.4.1 Binding to CXCR4

As discussed above, the inhibitory action of the bicyclams against HIV infection stems from a binding interaction with the CXCR4 receptor that blocks viral entry. AMD3100 has also been shown to inhibit binding and signalling of the natural ligand CXCL12 by blocking the CXCR4 receptor. In this section, the binding efficacy of AMD3100 and data on molecular interactions of cyclam and bicyclams with specific amino acids on CXCR4 are reviewed. A measure of the potential activity of an antagonist or more precisely, its strength of binding to a receptor can be analysed by competition of the antagonist with an agonist for receptor binding or by competition of monoclonal

antibodies (mAb) that have been raised to specifically bind to the receptor in question. Other assays can probe the downstream effects of receptor binding, such as intracellular calcium flux.

1.4.1.1 *Inhibition of CXCL12 Binding by AMD3100*

A number of bicyclams, including AMD3100, have been shown to inhibit CXCL12 mediated cell migration and calcium mobilisation. AMD3100 dose dependently inhibited calcium signalling in SupT1 cells, see Figure (**8**). Calcium flux occurs after the initial cascade mechanism by way of activating other regulatory intracellular kinases.

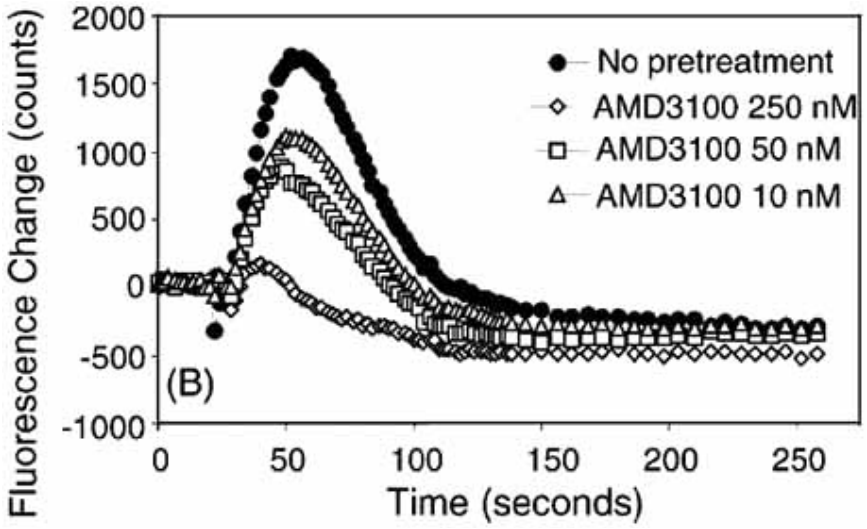

Figure (8). Inhibitory effect of AMD3100 on CXCL12-induced intracellular calcium signalling in SupT1 cells (*Reproduced from Biochemical Pharmacology*).[202]

CXCL12 binding to CXCR4 initiates an easily detectable calcium flux (intracellular) and it was of interest to determine whether AMD3100 is capable of causing a similar response. AMD3100 did not cause a calcium flux in T-lymphoid SupT1 cells and primary human monocytes, even at a concentration level (ca. 40 μM) that is 500 fold greater than that required for CXCL12. This suggests that AMD3100 does not have a functional effect on the CXCR4 receptor.[203] In another study, AMD3100 at 2 μM totally abrogated the calcium response in transfected cells in response to 2 ng/ml

CXCL12.[204] AMD3100 has also dose dependently inhibited CXCL12 induced migration of human peripheral blood mononuclear cells (PBMC), see Figure (**9**).

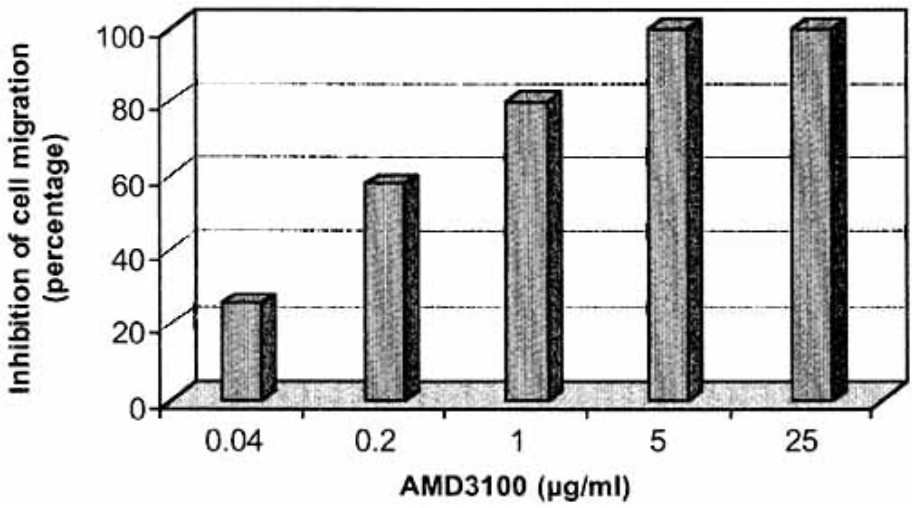

Figure (9). Dose dependent inhibition of CXCL12 (200 ng/ml) induced chemotaxis of human PBMC by AMD3100 (*Reproduced from FEBS Letters*).[203]

However, Gupta *et al.* reported inconsistent AMD3100 IC_{50} values in competitive binding assays with CXCL12.[205] In two functional assays, AMD3100 had inhibited cell migration and GTP binding, with similar IC_{50} values of ca. 4 nM and 6 nM, respectively, when stimulated with 25 nM CXCL12. However, in a competitive binding assay with CXCL12, AMD3100 had a much higher IC_{50} value of ca. 10 µM. In fact, up to a 3000-fold higher concentration was required to inhibit binding of CXCL12 to CXCR4 as opposed to blocking the signalling process. In support of this study, Banisadr *et al.* have also reported rather weak antagonism of CXCL12 binding by AMD3100 (only 30% inhibition at 1 µM).[206]

These results suggest a CXCR4 antagonist like AMD3100 may be a potent functional antagonist by virtue of perturbing ligand interaction at one site, but without a concomitant effect on ligand displacement in binding assays. This supports the two-site binding model for CXCL12 reported by Crump *et al.* see Figure (**10**).[60] The possibility of multiple binding sites for CXCL12 should be taken into account when designing competitive assays and comparing antagonist activity using data obtained from other model systems.

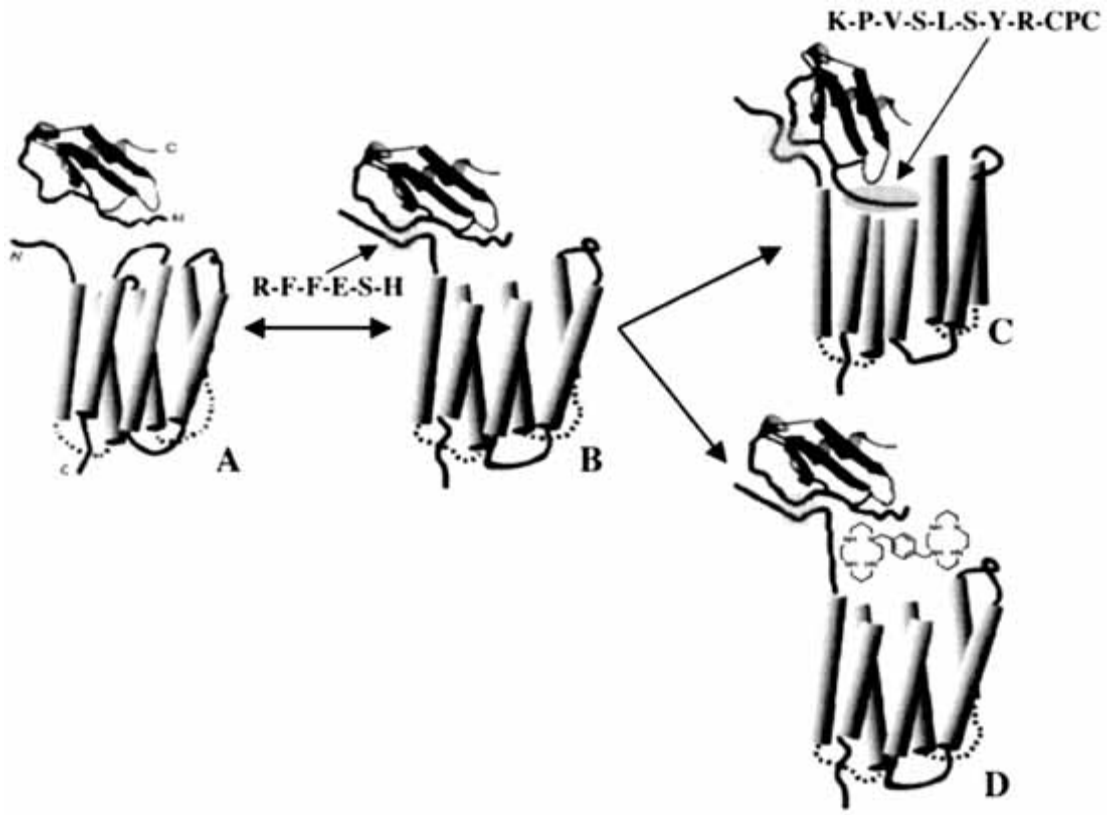

Figure (10). (**A**) and (**B**) The initial docking step between the N-terminal residues of CXCR4 and the R-F-F-E S-H motif of CXCL12. (**C**) Conformational changes lead to interaction of the extracellular loops of CXCR4 with aa 1–11 of CXCL12. (**D**) Interaction of AMD3100 inhibits functional signal transduction without displacement of radiolabeled CXCL12 (*Reproduced from Immunology Letters*).[205]

1.4.1.2 *Inhibition of Anti-CXCR4 Antibody Binding by AMD3100*

A number of studies have been undertaken to evaluate the efficacy of AMD3100 in blocking the binding of CXCR4 specific antibodies and a wide range of values are reported. AMD3100 dose dependently inhibits the binding of mAb 12G5 to CXCR4. AMD3100 at 2 μM completely inhibited the binding of mAb 12G5 and at concentrations of 0.2 and 0.02 μM still inhibited up to 79%. AMD3100 was found to inhibit the binding of mAb 12G5 efficiently even when the cells were washed to remove excess AMD3100 and regardless of whether added 1 min or 15 min before mAb. This data demonstrates strong direct binding of AMD3100 to CXCR4 and indicates that this compound did not cause inhibition by interfering with the mAb.[173,185,199] The specificity of AMD3100

towards CXCR4 is further demonstrated by its inability to inhibit CCL3 (MIP-1α) binding to CCR5 even at concentrations up to ca. 40 μM.[199] In other studies, AMD3100 showed an affinity of 0.5-1 μM in competition with ^{125}I-12G5 in COS-7 cells.[49,207]

AMD3100 has also been reported to stay bound to CXCR4 for relatively long periods of time. Immediately after preincubation of SUP-T1 cells with AMD3100 (10 μM), the binding of mAb 12G5 was inhibited by 85%. This inhibitory effect remained the same after 24 h and after 48 h had declined to only 60%, pointing to a high-affinity interaction between AMD3100 and CXCR4.[203] Moreover, AMD3100 at 2 μM completely blocked the binding of another CXCR4 mAb (44717) on feline thymocytes and had an IC_{50} of ca. 0.03 μM.[208]

1.4.2 Cyclam *vs.* AMD3100 Binding

The CXCR4 binding properties of the bis-macrocyclic AMD3100 can be compared with the single ring component, cyclam, see Figure (**7**). Cyclam competes for ^{125}I-Met-CXCL12 binding in COS-7 cells transfected with CXCR4 with an affinity of ca. 10 μM, however, it is unable to displace the mAb ^{125}I-12G5 from CXCR4 even at high millimolar concentrations. Whereas AMD3100 showed an affinity of ca. 50 nM in competition with ^{125}I-Met-CXCL12, a 200 fold higher affinity than observed for cyclam, and was able to compete against ^{125}I-12G5 binding as illustrated in Figure (**11**).[49]

1.4.3 Effect of Asp and His Mutations on Cyclam and AMD3100 Binding

Receptor mutagenesis studies of histidine (His) and aspartate (Asp) residues in CXCR4 have been used to characterise the main binding site for AMD3100 and its metal complexes. His and Asp residues were chosen on the basis of the fact that they could form potentially important interactions such as coordinate and hydrogen bonds.[209] Therefore all histidine residues located in the extracellular loops or in the transmembrane domains (TM) of CXCR4 (i.e. His113, His203, His281, and His294) were mutated to alanine (Ala) and four Asp residues (Asp171 located in TM-IV, Asp182 and Asp193 in extracellular loop 2, and Asp262 in TM-VI) to Asn residues.[49]

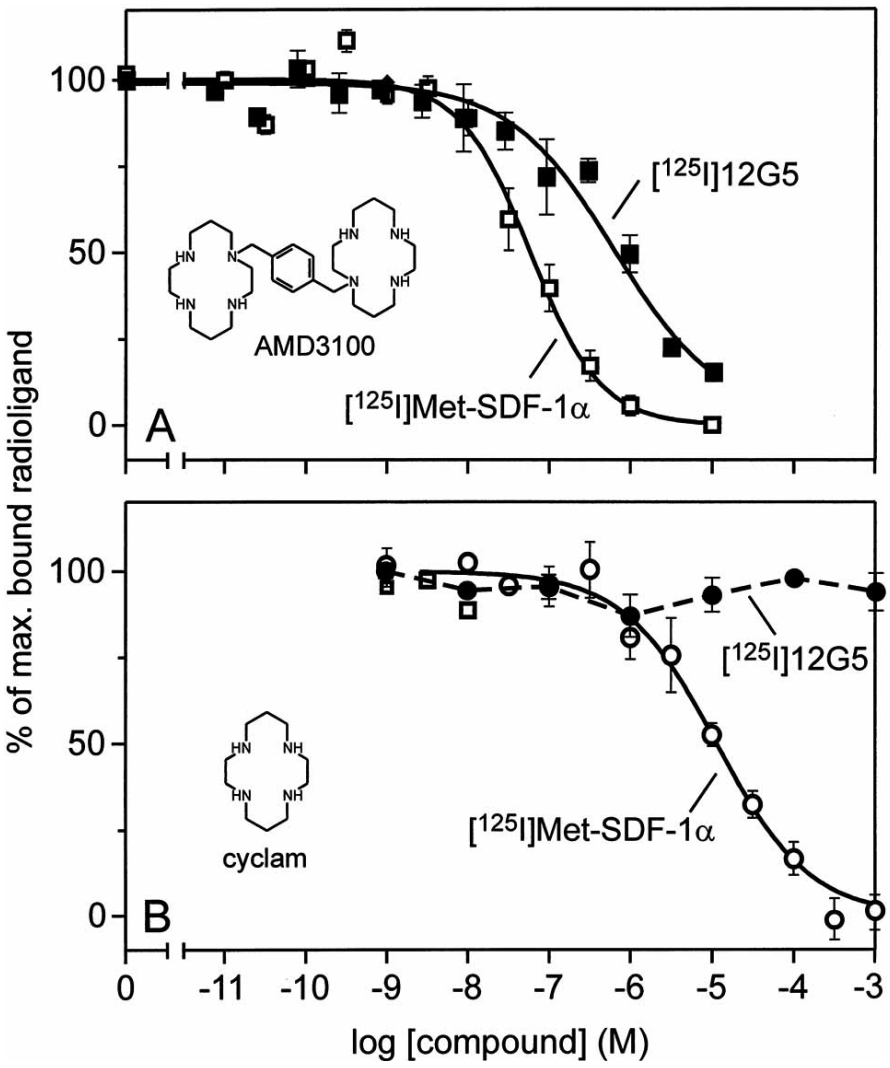

Figure (11). Competition binding experiments using AMD3100 (a) or cyclam (b). (*Reproduced from the Journal of Biological Chemistry*).[49]

The affinity of cyclam, determined in competition with radiolabelled ^{125}I-Met CXCL12, was unaffected by each mutation except in the case of Asp171, located in TM-IV. This mutation led to a 30-fold decrease in the binding affinity of cyclam, see Figure (**12b**) and table (**2**). AMD3100 binding was only affected by mutations Asp171 and Asp262, located in TM-IV and VI, respectively, Figure (**12a**) and table (**2**).

With these two mutations, AMD3100 was unable to compete with mAb ^{125}I-12G5 for binding to CXCR4 and displayed a reduced affinity (up to 180 fold) for the receptor, see table (**3**).

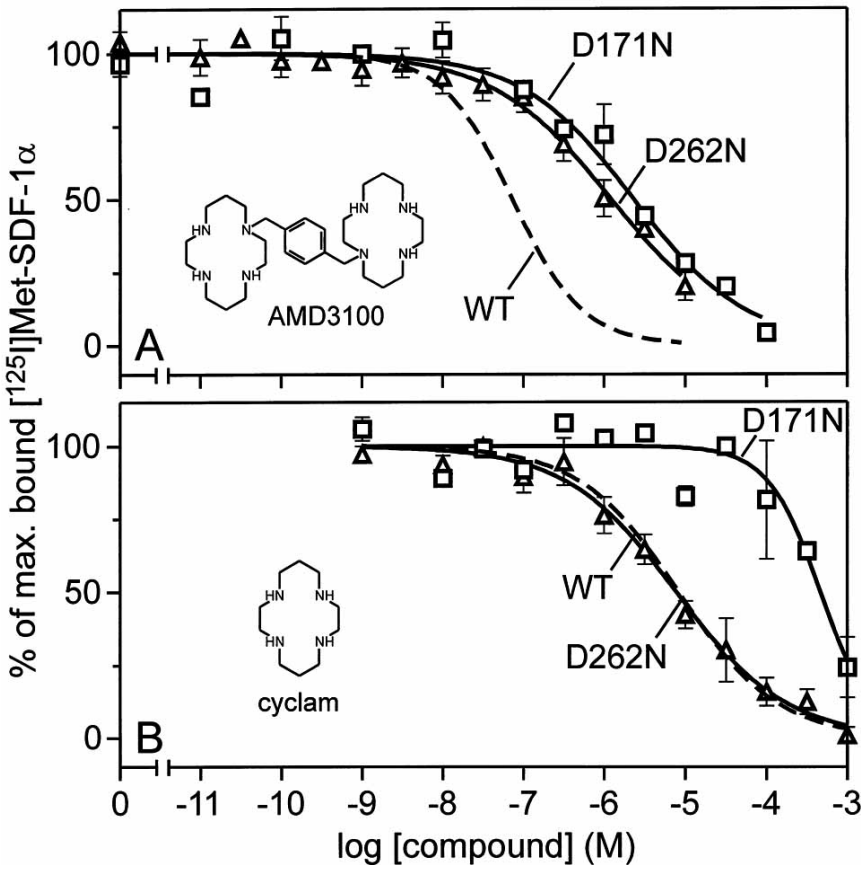

Figure (12). Effect of Asp to Asn substitution at positions 171 and 262 in CXCR4 on AMD3100 (a) and cyclam (b) competition binding for CXCL12 (SDF-1α) binding. (*Reproduced from the Journal of Biological Chemistry*).[49]

In support of the importance of Asp171 and Asp262 in the binding of AMD3100 to CXCR4, these mutations also affected the capability of AMD3100 to block the calcium response initiated by CXCL12. In the CXCR4 wild type, 2 μM AMD3100 totally abrogated a calcium response, however, with the Asp171 and Asp262 mutations, AMD3100 failed to block the calcium response.[204] AMD3100 (2 μM) inhibited the binding of 12G5 mAb to a lower degree in the Asp171 and Asp262 mutations compared with the wild type CXCR4 (Figure (**13**)). However, unexpectedly the His281 mutation had a positive effect and appeared to increase the binding potential of AMD3100 (from 88% inhibition to 98%). Of course, as this is a competition study, effects may also be observed if a residue change decreases the binding affinity of the competing 12G5 mAb, and this may be the case for the His281 mutant.

	B_{max} ± S.E.	Met-CXCL12		AMD3100		Cyclam	
		Log K_d ± S.E.	K_d (n)	Log K_i ± S.E.	K_i (n)	Log K_i ± S.E.	K_i (n)
	fmol / 100,000 cells	nM		nM		µM	
Human WT CXCR4	34 ± 5.2	-9.30 ± 0.09	0.49(15)	-7.13 ± 0.10	74(11)	-4.90 ± 0.11	13(6)
H113A	9.2 ±2.5	-9.55 ± 0.15	0.28(8)	-6.89 ± 0.01	130(3)	-5.07 ± 0.25	8.5(6)
D171N	10.0 ± 3.4	-9.24 ± 0.30	0.58(7)	-5.56 ± 0.31	**2800(3)**	-3.43 ± 0.11	**370(3)**
D182N	20 ± 7.8	-9.36 ± 0.12	0.43(5)	-6.89 ± 0.10	130(3)	-4.93 ± 0.09	12(3)
D193N	24 ± 10.0	-9.36 ± 0.26	0.44(3)	-7.09 ± 0.13	81(3)	-5.04 ± 0.11	9.2(3)
H203A	7.8 ± 2.6	-9.27 ± 0.23	0.53(5)	-7.17 ± 0.16	68(3)	-4.79 ± 0.16	16(3)
D262N	20. ± 7.0	-8.92 ± 0.21	1.2(7)	-5.95 ± 0.10	**1100(5)**	-5.02 ± 0.22	9.6(4)
H281A	7.2 ± 1.5	-9.55 ± 0.06	0.28(7)	-7.62 ± 0.17	24(5)	-4.49 ± 0.15	33(4)
H294A	73 ± 14	-9.06 ± 0.20	0.88(3)	-6.86 ± 0.05	140(3)	-4.59 ± 0.13	26(3)
H113A/ H281A	9.2 ± 5.4	-9.54 ± 0.13	0.29(4)	-7.22 ± 0.07	61(3)	-5.11 ± 0.08	7.8(3)
D171N/ D262N		Low expression		ND		ND	

Table (2). Affinity of Met-CXCL12, AMD3100 and cyclam for the wild-type CXCR4 receptor and His and Asp substituted CXCR4 receptor mutants.[49]

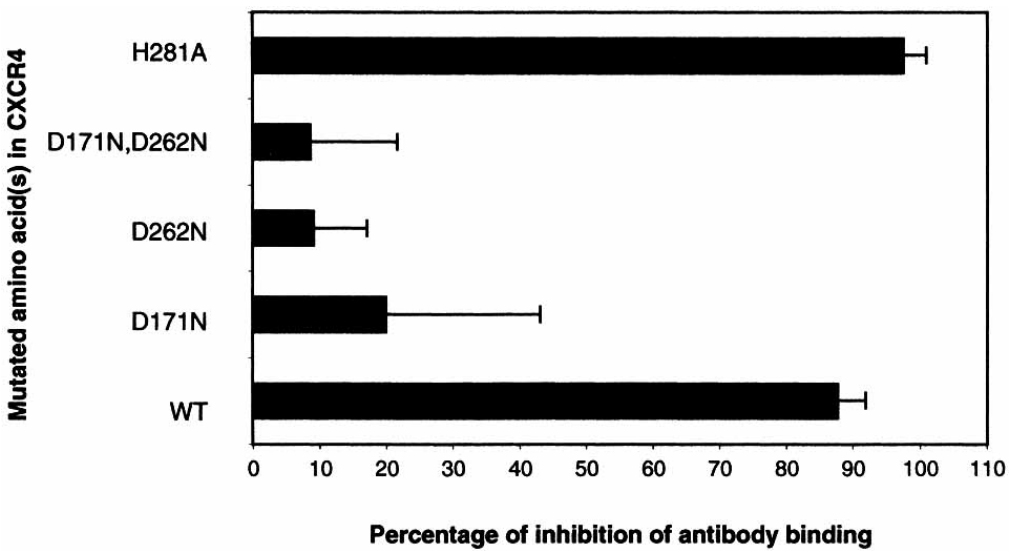

Figure (13). Inhibition of 12G5 mAb binding to the different CXCR4 mutants by AMD3100 (*Reproduced from Molecular Pharmacology*).[204]

1.4.4 Binding Model for AMD3100

It is believed that each cyclam macrocyclic ring component (protonated at physiological pH) of AMD3100 forms hydrogen bonds with the carboxylate groups of Asp171 and Asp262 of CXCR4. This was confirmed by preparation of a series of AMD3100 derivatives and testing them on Asp171 and Asp262 mutants. The mono-macrocyclic compound, cyclam (Figure (**7**)), may also bind to Asp262, but with very low affinity, relative to Asp171. In the Asp171 mutant the affinity of cyclam for CXCR4 decreased to 400 μM, which could represent the affinity of cyclam to the Asp262 site, however this can only be confirmed by a double Asp171 and Asp262 mutation, which could not be studied due to low expression.[49]

	B_{max} ± S.E.	**12G5**		**AMD3100**	
		Log K_d ± S.E.	**K_d (n)**	**Log K_i ± S.E.**	**K_i (n)**
	fmol / 100,000 cells	**nM**		**nM**	
Human WT CXCR4	39 ± 10	-9.17 ± 0.12	0.678(10)	-6.27 ± 0.14	550(3)
H113A	25 ± 7.4	-8.70 ± 0.19	2.0(5)	-5.84 ± 0.46	1500(3)
D171N	28 ± 7.9	-8.80 ± 0.17	1.6(9)	> -4	**> 100,000(6)**
D182N	79 ± 46	-8.14 ± 0.12	7.2(4)	-5.51 ± 0.09	3100(2)
D193N	91 ± 24	-8.15 ± 0.11	7.1(3)	-5.50 ± 0.16	3200(2)
H203A	88 ± 71	-8.35 ± 0.23	4.5(2)	-5.69 ± 0.22	2100(2)
D262N	77 ± 33	-8.71 ± 0.19	1.9(4)	> -4	**> 100,000(4)**
H281A	5.8 ± 1.6	-9.33 ± 0.17	0.48(2)	-7.58 ± 0.01	26(2)
H294A	133 ± 59	-8.08 ± 0.08	8.3(3)	-6.03 ± 0.16	930(2)
H113A/ H281A	6.0 ± 1.4	-9.44 ± 0.04	0.36(2)	-6.29 ± 0.29	510(2)

Table (3). Affinity of 12G5 and AMD3100 for the Wild-Type CXCR4 Receptor and His and Asp Substituted CXCR4 Receptor Mutants.[49]

1.4.5 AMD3100 as a Prodrug

As already mentioned, AMD3100 is protonated at physiological pH and therefore each cyclam ring would reasonably be expected to bind to CXCR4 by double hydrogen bonding with the two oxygens of the carboxylate groups of Asp171 and Asp262. However, transition metal ions, such as zinc(II), strongly bind to cyclam and the concentration of zinc(II) in blood plasma is approximately 20 μM. Therefore, it is reasonable to assume that when AMD3100 is injected into the body it may rapidly form a zinc(II) complex *in vivo*.[210] Taking this into consideration, AMD3100 could be regarded as a prodrug and, in the majority of cases *in vivo*, it may be the metal complex of AMD3100, which binds to CXCR4. Therefore, it is highly appropriate to characterise the metal complexes of AMD3100 and determine their mode of CXCR4 binding, which may occur *via* a direct coordination of the metal centres to carboxylates.

1.4.6 Characteristics of Cyclam and Bicyclams

Macrocyclic polyamines such as cyclam, see Figure (**7**), are known to bind to metal ions and form highly stable metal complexes.[210-216] Metal complexes of AMD3100 have shown improved anti-HIV activity in relation to the free chelator. This has been attributed to the enhanced interaction of the metal *via* coordinate bonds with Asp171 and Asp262 of CXCR4. In addition, when a metal complex is formed the cyclam rings in AMD3100 can adopt a number of different configurations and this may influence the interaction between the CXCR4 receptor and the metal macrocycle complex. The following section introduces some of the general properties and characteristics of metal-cyclam and metal-bicyclam complexes, with a particular focus on zinc(II) complexes due to the high anti-HIV activity of $[Zn_2AMD3100]^{4+}$.[217]

1.4.7 Metallo-Cyclams and Bicyclams: General Properties

Cyclam is a well characterised chelator and can form stable complexes with transition metal ions, such as Zn^{2+}, Cu^{2+}, Ni^{2+}, Co^{2+} and Pd^{2+}. For example, the Ni^{2+} cyclam

complex has been estimated to have a demetallation half-life of about 30 years in 1 M $HClO_4$ at 25°C.[218] Small metal ions offer the best fit, in terms of M-N bond distances, to be accommodated in the macrocyclic cavity.[219,220] They are mainly from the first row of the transition series, exhibiting ionic radii of less than <0.75 Å. Taking into account the flexibility of the cyclam ring, a metal complex is formed with the configuration which is most thermodynamically stable on matching the coordination requirements of the metal ion. Once the metal is bound, each nitrogen atom becomes chiral giving rise to six possible configurations that the macrocycle can adopt, see Figure (**14**).[221]

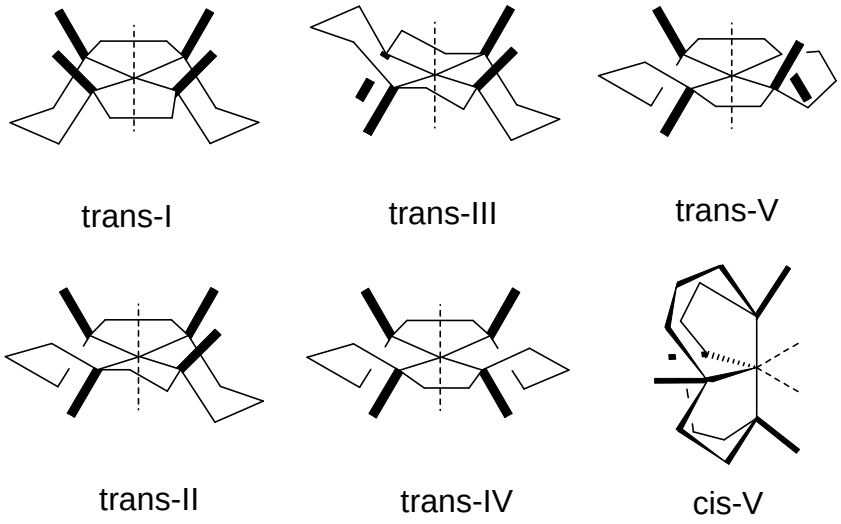

Figure (14). Conceivable configurations of metal-cyclam complexes. One *cis* and five *trans* configurations are possible.[221]

The six-membered chelate rings adopt either chair or twist-boat conformations and the five-membered rings are either gauche or eclipsed. *Trans*-IV and *trans*-V are generally less stable due to the higher energy (twist boat conformation) of the six-membered rings. *Trans*-V can be transformed into an alternative configuration by folding along the diagonal N-N of the macrocycle to give the *cis*-V configuration, where the six-membered rings are in the chair conformation. For Ni^{2+} complexes the *trans*-III conformation has the lowest energy and is the most stable, however *trans*-I becomes more favourable as the metal coordination number decreases from 6 to 5 to 4, respectively.[222] The coordination number, donor preference and availability of additional

donor atoms will have major effect on the observed configuration. It has also been demonstrated that these complexes can give a configurational equilibrium in solution.[223]

1.4.7.1 *Zinc(II) Cyclam and Bicyclam Complexes*

To further understand the configurational preferences of cyclam complexes and the way this may influence binding to CXCR4, Sadler and co-workers have studied the solid state (X-ray) and NMR solution behaviour of the metal complexes shown in Figure (**15**).[224,225]

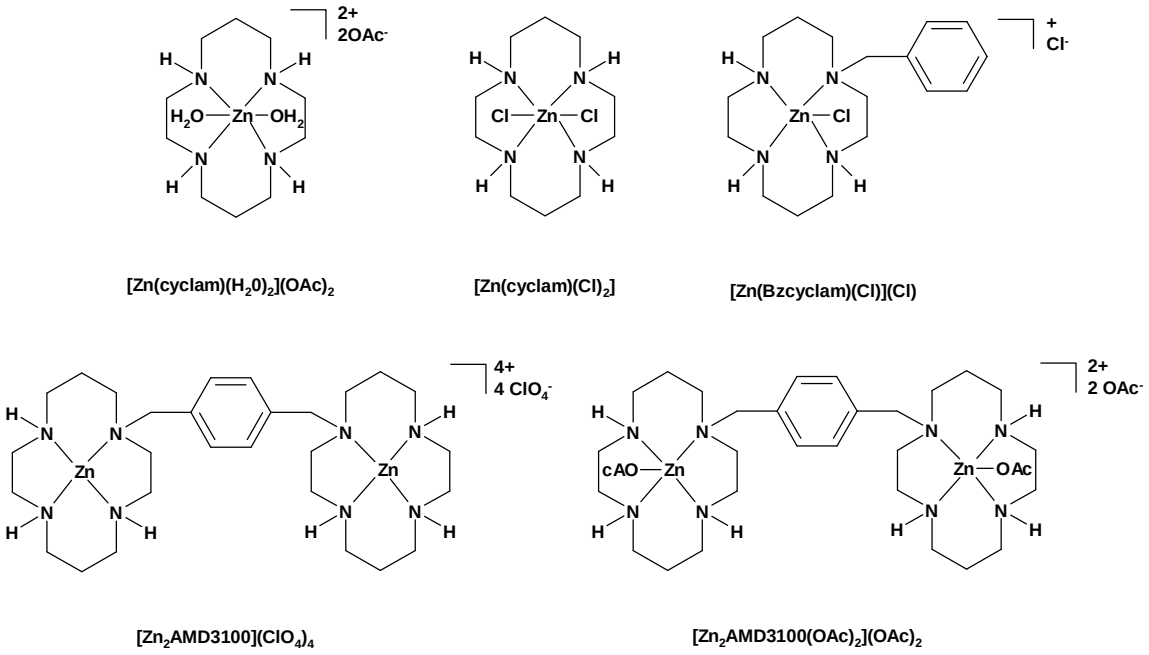

Figure (15). Structures of zinc(II) cyclam complexes studied by Sadler and co-workers.

In the solid state structure of $[Zn(cyclam)(H_2O)_2](OAc)_2$, the macrocycle adopts the *trans*-III configuration.[225] However, in solution the equilibrium mixture consists of *trans*-I, *trans*-III and *cis*-V. The proton NMR spectrum of $[Zn(cyclam)(H_2O)_2](OAc)_2$ is highly time dependent; initially only *trans*-III is detected, however, ten hours after dissolution, the combination of *cis*-V and *trans*-I increases slightly at the expense of *trans*-III. $[Zn(cyclam)(H_2O)_2](OAc)_2$ in solution at equilibrium consists of 43% *trans*-III, 42% *cis*-V and 15% *trans*-I. Altering the pH of the solution also affects the proton NMR

spectrum of complex Zn(cyclam)$(OAc)_2$, see Figure (**16**). Increasing the pH leads to an increase in *trans*-I and a reduction in *cis*-V. The amount of *trans*-III remains unchanged and is therefore not affected by pH.

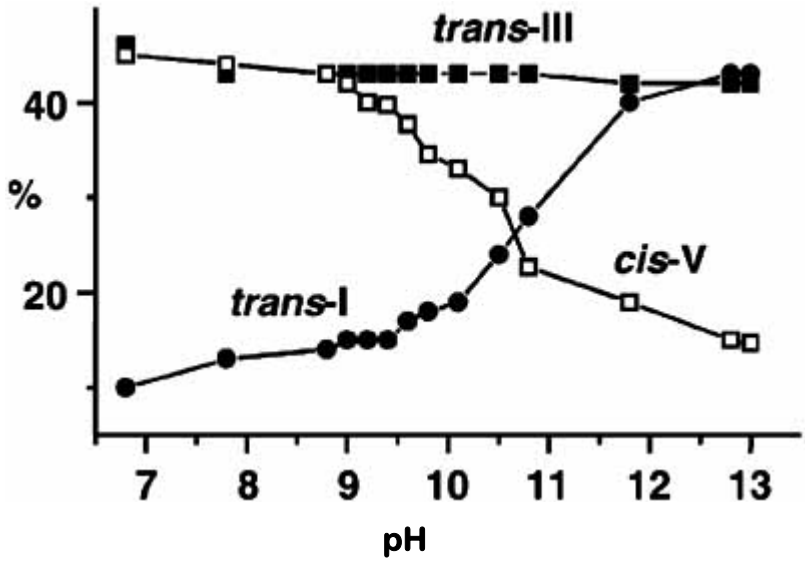

Figure (16). pH dependence of the configuration of complex [Zn(cyclam)$(H_2O)_2$]$(OAc)_2$ (*Reproduced from Chemistry-a European Journal*).[225]

The zinc(II) chloride benzyl-cyclam complex, [Zn(Bzcyclam)(Cl)](Cl), see Figure (**17**), also shows the macrocycle in the *trans*-III configuration in the solid state. After dissolution in water, the equilibrium mixture splits into three configurations; 43% *trans*-III, 42% *trans*-I and *cis*-V 15%.[224]

The solid state X-ray structure of [Zn_2AMD3100]$(ClO_4)_4$ has not been determined but it is most likely that it would be in the *trans*-III configuration. In solution, the equilibrium mixture of complex [Zn_2AMD3100]$(ClO_4)_4$ is 34% *trans*-III, 45% *trans*-I and 21% *cis*-V. The proton NMR spectra of complexes [Zn(Bzcyclam)(Cl)](Cl) and [Zn_2AMD3100]$(ClO_4)_4$ are almost identical, which suggests that the two macrocyclic rings have little influence on each other, although other complexes may exhibit cooperative effects between the two rings.

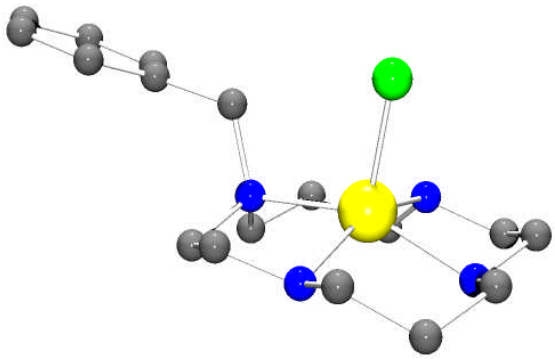

Figure (17). Ball and stick representation of the X-ray crystal structure of [Zn(Bzcyclam)(Cl)]Cl.[224]

Receptor mutagenesis studies have revealed that CXCR4 binding or blocking is dependent on the carboxylate groups of Asp171 and Asp262 (section **1.4.3**). Therefore carboxylate ligands such as acetate have been used to model the aspartate carboxylate residue interaction with the metal centres and determine the consequent configurational distribution. Aqueous solutions of complex [Zn(Bzcyclam)(Cl)](Cl) have an equilibrium mixture of 11.2% *trans*-I, 79.6% *trans*-III and 9.2% *cis*-V. On addition of acetate, the amount of *trans*-III decreases and *cis*-V increases but *trans*-I stays constant as shown in Figure (**18**).

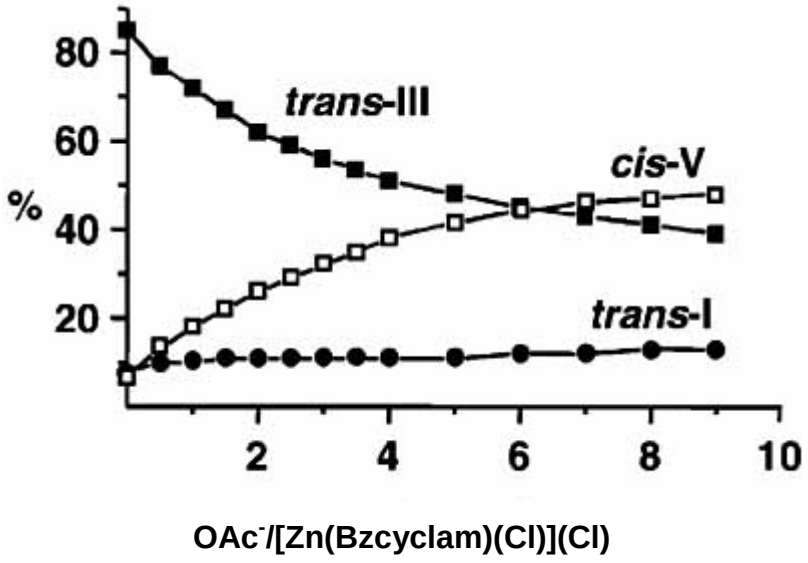

Figure (18). Effect of acetate on the configuration of [Zn(Bzcyclam)(Cl)](Cl) as determined by integration of the proton NMR resonances (*Reproduced from Chemistry-a European Journal*).[225]

Addition of acetate to complex $[Zn_2AMD3100](ClO_4)_4$ also changes the proton NMR spectrum. The effect of adding acetate is shown in Figure (**19**). The proportion of the *cis*-V/*cis*-V configuration increased from 0% to almost 19% on addition of four molar equivalents of acetate. The proportion of the *cis*-V/*trans*-I configuration increased from 26% to 38%. These are important results as they demonstrate that there may be an ideal configuration for binding to the CXCR4 receptor.

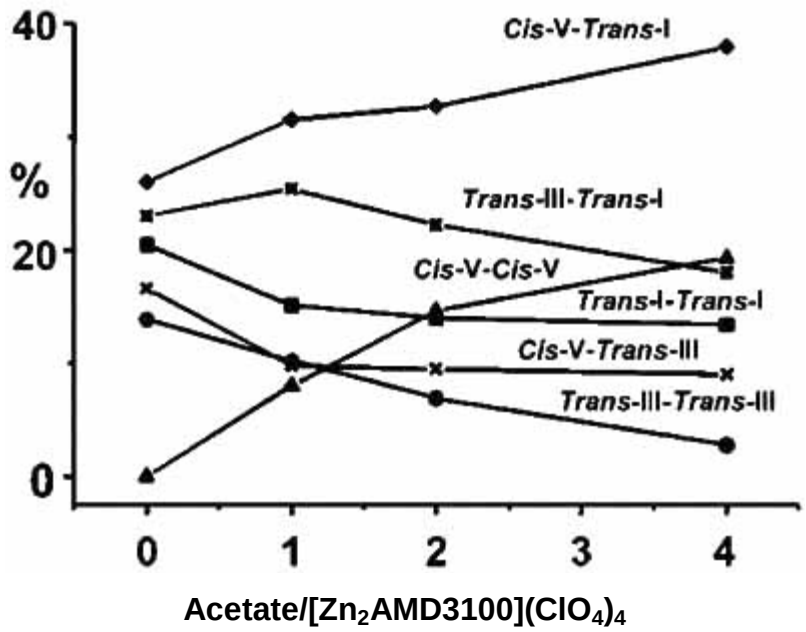

Figure (19). Effect of acetate on the distribution of cyclam configurations of $[Zn_2AMD3100](ClO_4)_4$ as determined by integration of the proton NMR resonances for the aromatic linker. (*Reproduced from the Journal of the American Chemical Society*).[224]

The zinc(II) acetate complex of AMD3100, $[Zn_2AMD3100(OAc)_2](OAc)_2$, Figure (**20**), was prepared and the solid state structure was determined to further characterise the acetate interaction. The macrocyclic rings are crystallographically equivalent in the X-ray structure and both adopt the *cis*-V configuration, with the zinc ion in a distorted octahedral geometry. The *cis*-V configuration results in two cyclam nitrogens occupying axial coordination sites and two occupying equatorial positions. A bidentate acetate coordinates in the remaining two equatorial coordination sites. Although not shown in Figure (**20**), a further equivalent of acetate forms a double hydrogen bond to the two equatorial amine ring nitrogens.

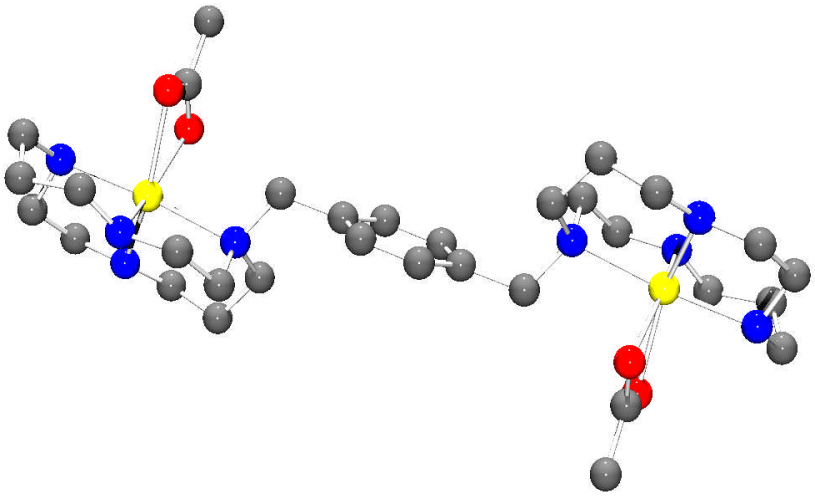

Figure (20). X-ray crystal structure of $[Zn_2AMD3100(OAc)_2](OAc)_2$.[224]

On dissolution of $[Zn_2AMD3100(OAc)_2](OAc)_2$ in aqueous solution (10% D_2O/90% H_2O), the configurational equilibrium was rapidly reached (<20 min), with the mixed configuration *cis*-V/*trans*-I predominating (44%) and 29% of the original *cis*-V/*cis*-*V* configuration present. This distribution is similar to that observed after the addition of acetate to $[Zn_2AMD3100](ClO_4)_4$.

This data shows that carboxylates influence the configurational equilibrium and increase the amount of *cis*-V configuration present. It is suggested that a bidentate coordination interaction could be occurring between AMD3100 bound zinc ions and the carboxylates of Asp171 and Asp262 resulting in the high anti-HIV activity of zinc metallo-bicyclams. Taking into account the configurational distribution of zinc(II) cyclam and bicyclam complexes, it is difficult to determine the actual configuration of the molecule when binding to CXCR4 and it is not clear what influence the configuration of the cyclam rings will have on the binding interactions such as the metal coordination and the hydrogen bonding that can occur. Our recent studies at Hull have demonstrated that further enhancement of the binding can be engineered by synthesising novel compounds that are configurationally restricted to give a single optimized configuration.[226]

1.4.7.2 *CXCR4 Binding Studies of Metal Complexes of AMD3100*

Bridger and co-workers reported that the incorporation of a metal ion into the macrocyclic rings of AMD3100 increased binding affinity to CXCR4 in the order:

$$Zn^{2+} \sim Ni^{2+} > Cu^{2+} > AMD3100 > Co^{3+} > Pd^{2+}$$

However, other studies report the free ligand AMD3100 as having a higher binding affinity than its copper(II) complex.[49,224,227] Nevertheless, the zinc(II) complex of AMD3100 increases the binding affinity to CXCR4 by 6 to 36 fold in competition binding assays with ^{125}I-Met-CXCL12 and ^{125}I-12G5 mAb respectively, see Figure (**21**).[207]

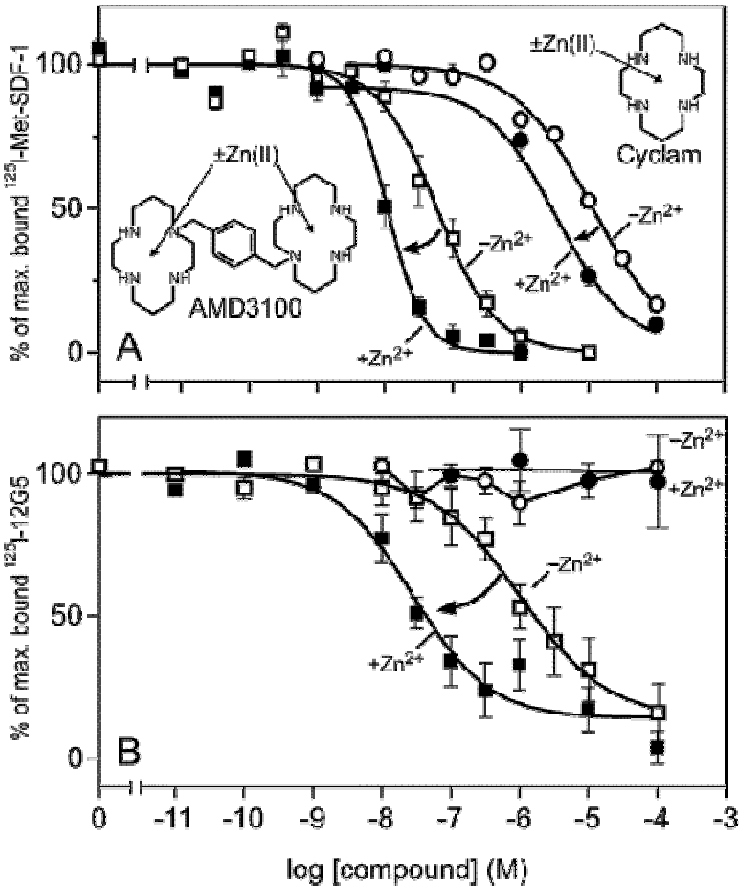

Figure (21). Increased binding affinity of Zn_2AMD3100 and Zn(cyclam) compared to their respective free ligands, in competition with ^{125}I-CXCL12 and ^{125}I-12G5. AMD3100 (□), Zn_2AMD3100 (■), cyclam (○) and Zn(cyclam) (●). (*Reproduced from Biochemistry*).[207]

It has been suggested that the increased binding affinity observed for zinc(II) AMD3100 and other transition metal complexes could be due to a bonding (coordination) interaction from only one of the metal cyclam rings with the residue Asp262. This theory of single metal coordination to Asp262 has been tested using AMD3100 metal complexes and studying their binding interaction with CXCR4. Figure (**22**) shows that only one metal ion in either of the cyclam rings of AMD3100 is required to increase the ligand binding affinity for the nickel(II) and copper(II) complexes. This is supported by the data presented in Figure (**23**) showing that the metal enhancement effect can be eliminated by Asp262 mutation.

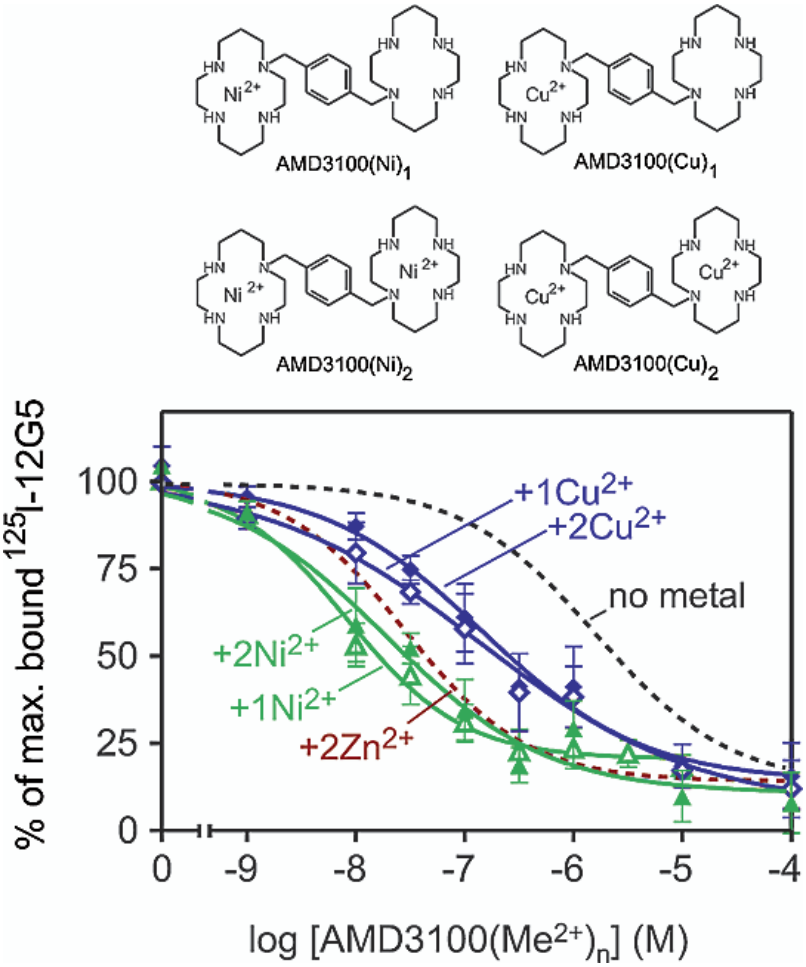

Figure (22). Effect of incorporation of one (open symbols) or two (closed symbols) nickel(II) or copper(II) ions in AMD3100 on wild-type CXCR4. (*Reproduced from Biochemistry*).[207]

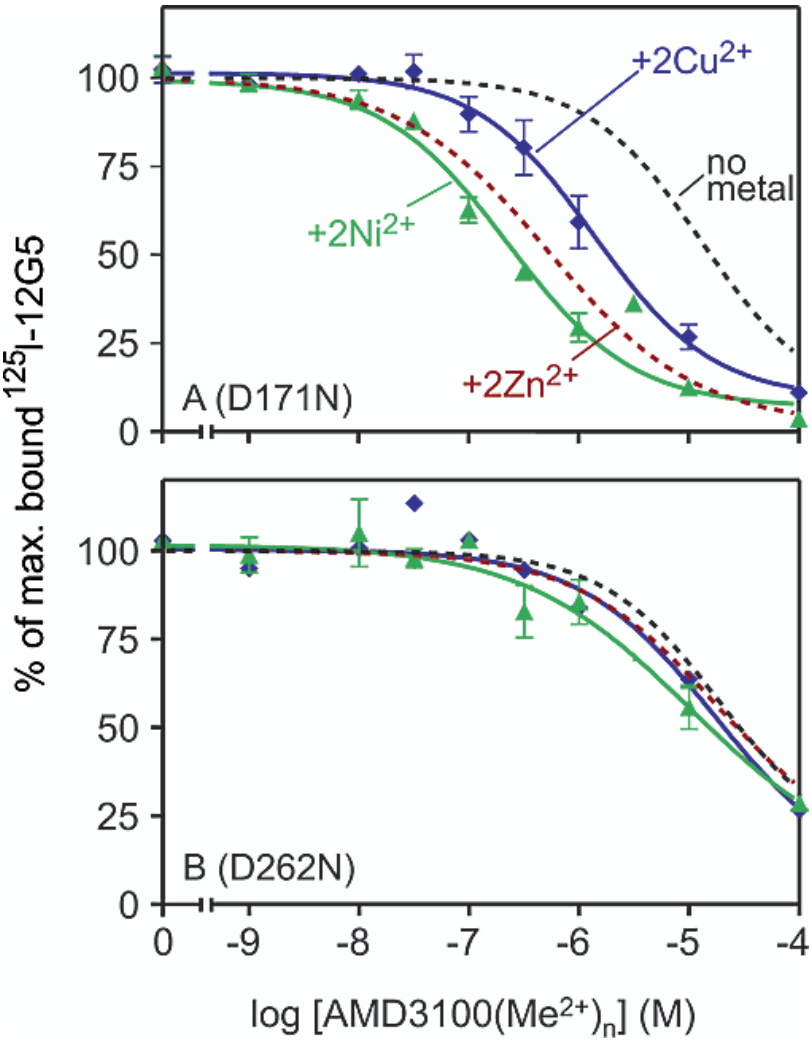

Figure (23). Effect of incorporation of two zinc(II), nickel(II) or copper(II) ions in AMD3100 in competition with ^{125}I-12G5 mAb in mutants (**A**) Asp171 and (**B**) Asp262 CXCR4 receptor. (*Reproduced from Biochemistry*).[207]

Other studies by this group have shown that the binding potency of the zinc(II) complex of cyclam increases for the Asp262 mutant CXCR4. Cyclam binding inhibition towards ^{125}I-CXCL12 had previously been reported to be dependent on Asp171.[49] This appears contradictory in relation to AMD3100, however, the AMD3100 metal complexes will have spatial and configurational restrictions of the two rings relative to one another. From the data, shown in Figures (**22**) and (**23**), it is clear that Asp262 is essential to the binding interaction but the nature of the interaction with the second residue, Asp171, is less well defined. It is certainly possible that a coordination interaction could form with both aspartate residues but the binding pocket may only allow optimisation of one of

these bonds. Hydrogen bonding interactions with the secondary amine nitrogens of the metal complexes may also be important, for example a *trans*-III ring configuration can potentially form up to three separate hydrogen bonds with carboxylate oxygens.[228]

Further studies are required to more accurately characterise the interaction of the metal ion in each of the cyclam rings of AMD3100 with Asp171 and Asp262 of CXCR4. Computational modelling techniques have been used to simulate the binding and gain further insight into the key interactions of the drug with the receptor *via* docking studies.

1.4.7.3 *Computational Binding Model for the Zinc(II) Complex of AMD3100*

A calculated representation of the zinc(II) complex of AMD3100 binding to CXCR4 has been generated using a homology model of human CXCR4 based on the X-ray structure of bovine rhodopsin. Such docking studies have been carried out independently by both Sadler and co-workers, see Figure (**24**), and Gerlach *et al.* see Figure (**25**).[224,229] It was assumed that the key interactions would occur with Asp171 and Asp262, but Glu288 has more recently been proposed as a further possible interaction site for AMD3100. Mutation of Glu288 in TM-VII, impairs co-receptor activity and it may be involved in HIV gp120 binding.[230] The X-ray structure of a zinc(II) AMD3100 complex has shown that a further equivalent of acetate can double hydrogen bond with the two amines on the opposite face of the macrocyclic ring (Figure (**20**)). This hydrogen bonding position could be occupied by the Glu288 residue in the binding cavity.

The *cis*-V/*trans*-I configuration, which is found to be predominant under physiological conditions, was docked into a CXCR4 model by Sadler and co-workers.[224] In this model, the *cis*-V cyclam ring has the zinc(II) ion coordinated by the oxygens of the carboxylate group from Asp262 (bond lengths of 2.27 Å) and the two hydrogens on the opposite face of the cyclam ring double hydrogen bonding with the oxygens of Glu288 (O···H-N = 2.01 Å). The *trans*-I cyclam ring contains a Zn^{2+} with a distorted octahedral geometry, coordinating to the oxygens of Asp171 (Zn-O 2.28 Å) Figure (**24**).

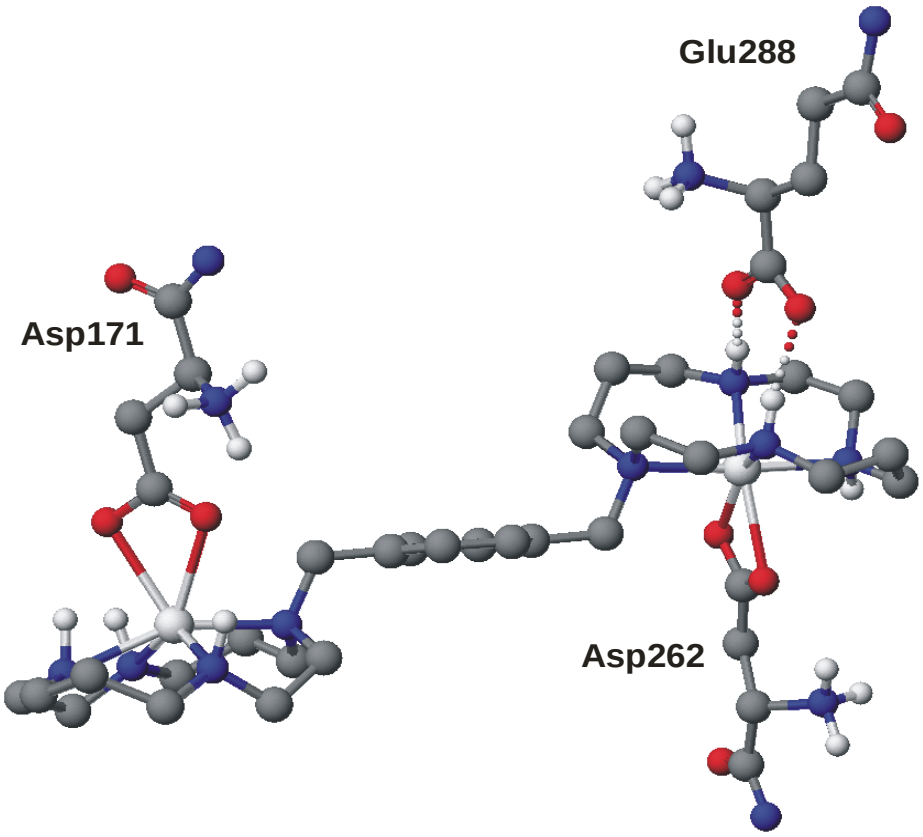

Figure (24). Ball and stick representation of the interactions of zinc(II) AMD3100 (Zn_2 Xylyl-bicyclam) with amino acid residues Asp171, Asp262 and Glu288 of CXCR4.[224]

The docking model developed by Gerlach *et al.* Figure (**25**) for binding of the Zn_2AMD3100 to the receptor has both cyclam rings in the *trans*-III configuration.[229] This model again has a coordination interaction to both metal centres (Asp171 and Asp262) although in this case the coordinate bond is monodentate. A stronger and more geometrically optimised interaction is observed with the Asp262 residue. As in Sadler's model, one macrocycle has additional H-bonding to Glu288 in the binding pocket *via* the secondary amines. Hydrogen bonding between the cyclam rings and aspartate residues was further confirmed by structural X-ray binding studies in lysozyme (HEWL) by sadler's group.[231] However the resolution was insufficient and the binding environment was not identical to CXCR4.

Therefore, studies from both these groups and our work strongly suggest metal coordination is an important interaction for both cyclam rings.[232-235] Metal bicyclam

complexes show increased binding potency to CXCR4 and configuration of the metal based drug (Zn_2AMD3100) is highly likely to be of key importance. There could potentially be further improvement to the binding and inhibitory effects by "locking" the drug in the optimal configuration.

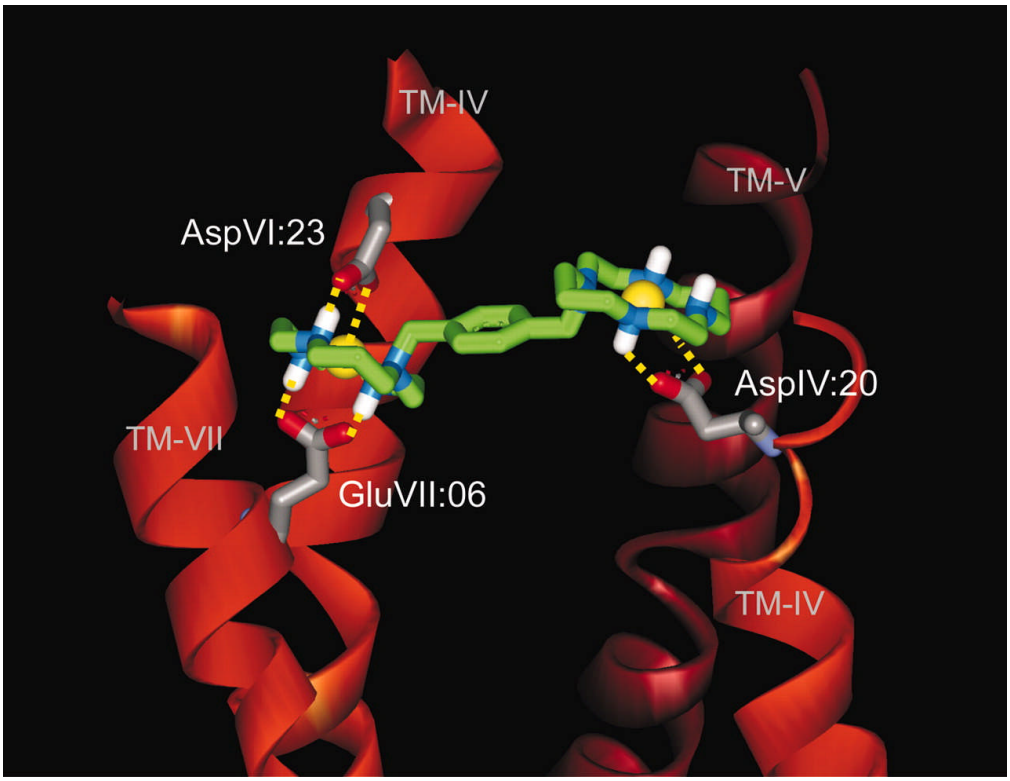

Figure (25). Molecular model of the presumed binding mode of Zn_2AMD3100 to CXCR4. The receptor homology model is based on the X-ray crystal structure of rhodopsin and shows the interaction of one of the cyclam rings of Zn_2AMD3100 with AspIV:20 (Asp171 in CXCR4), whereas the other cyclam ring is "sandwiched" between AspVI:23 (Asp262 in CXCR4) and Glu- VII:06 (Glu288 in CXCR4). (*Reproduced from the Journal of Biological Chemistry*).[229]

1.4.8 Configurationally Restricted Macrocycles

Both the docking studies of zinc(II) AMD3100 complexes and the NMR solution studies reported by Sadler and co-workers (sections **1.4.7.1** and **1.4.7.3**) highlight the importance of the configuration of the macrocyclic rings to the binding interactions and suggest that metal complexes of configurationally restricted bicyclams could potentially be more potent antagonists of CXCR4 than AMD3100 metal complexes.

1.4.8.1 *Configurational Restriction of Cyclam*

The first challenge is how to restrict the configuration with minimal changes to the overall structure of the drug molecule. The extensive literature on macrocyclic complexes reveals that the influence of short alkyl chains between nitrogen atoms may be sufficient to fix configuration. "Reinforced" macrocycles have previously been synthesised in which two amine groups are linked by an ethylene bridge. This ethylene bridge can be inserted between adjacent or non-adjacent nitrogen atoms, leading to the 'side-bridged' and 'cross-bridged' analogues of cyclam, see Figure (**26**).[236-238]

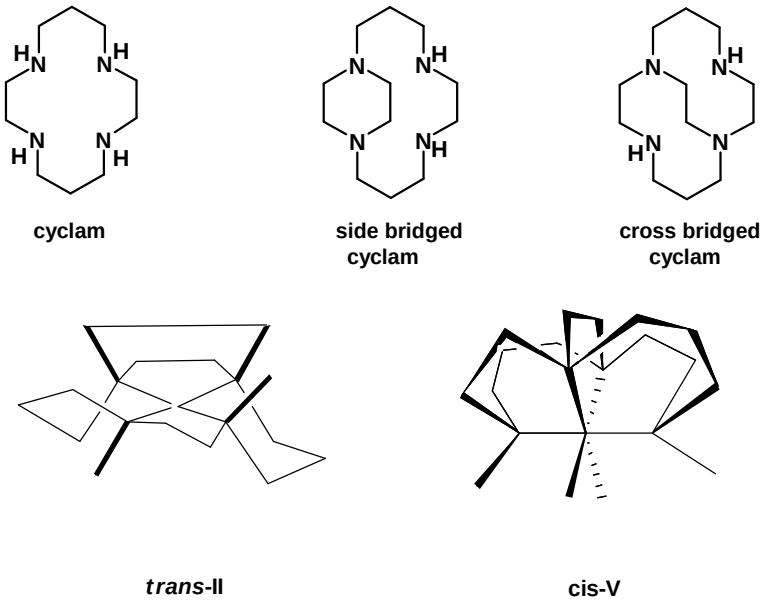

Figure (26). Configuration of cyclam with the addition of an ethylene bridge between adjacent (*trans*-II) and non-adjacent (*cis*-V) nitrogen atoms.

Through the synthesis of novel compounds and the analysis of previously published data, we have shown that metal complexes of these reinforced macrocycles exhibit restricted configuration of the macrocyclic rings.[239] The cross bridged macrocycle is topologically constrained to adopt only the cis-V configuration, see Figure (**26**).[240-243] Steric factors result in two possible configurations for the side bridged macrocycle dependent on the alkylation pattern.[226,244] We have shown that the mono-N

alkylated derivatives only adopt the *trans*-II configuration on complexation with zinc(II) and copper(II).[226,233,245]

The configurations described have been observed in a series of X-ray crystal structures and solution NMR studies show a single configuration in solution for the zinc complex of both side and cross bridged cyclam. This is in contrast with the work of Sadler and co-workers, who revealed the presence of multiple configurations for zinc AMD3100 in solution, (section 1.4.7.1). It is expected that both the *trans*-II and *cis*-V fixed configurations will have improved binding interactions with the aspartate residues on the CXCR4 receptor compared to the *trans*-III configuration that is most common for metal cyclam complexes. This is due to the availability of two *cis* sites on the metal centre that can better accommodate bidentate coordination of the aspartate residues. We have carried out studies to investigate the effectiveness of this strategy in producing CXCR4 antagonists with optimised binding characteristics.

1.4.8.2 *Configurationally Restricted CXCR4 Antagonists*

The syntheses of both *trans*-II and *cis*-V configurationally fixed bicyclam compounds have been investigated by our group alone and in collaboration with Hubin and co workers.[246] The metal complexes of the 'side bridged' bis-macrocyclic compound, $\mathbf{L^1}$**,** see Figure (**27**), adopt solely the *trans*-II configuration. In the single crystal X-ray structure of the zinc(II) acetate complex of $\mathbf{L^1}$, see Figure (**27**), the zinc(II) ion occupies the macrocyclic cavity with a distorted octahedral geometry and an acetate anion coordinated in an anisobidendate fashion. As before, the acetate interaction can be related to the binding mode with the CXCR4 receptor. The presence of a sole configuration in solution was confirmed using high field NMR (800 MHz). Flow cell cytometry displacement studies with anti-CXCR4 monoclonal antibodies confirmed binding to the CXCR4 receptor with characteristics at least as good as the zinc(II) complex of AMD3100. The results of *in vitro* infection assays are discussed in section 1.5.1.

There may be other useful properties related to configurational restriction. Metal complexes of cross bridged teraazamacrocycles show a remarkable increase in the kinetic

stability relative to cyclam complexes. This is attributed to the topological constraint within the cyclam ring decreasing the likelihood of the dissociation process occurring. The increased stability could be a useful property to be exploited further, especially if the metal complexes are to be used *in vivo*.[240,243] The configurational restriction may also influence the bonding interactions of the non-macrocyclic ligands that complete the coordination sphere of the bound metal ion, including coordination to aspartate side chains in the protein.

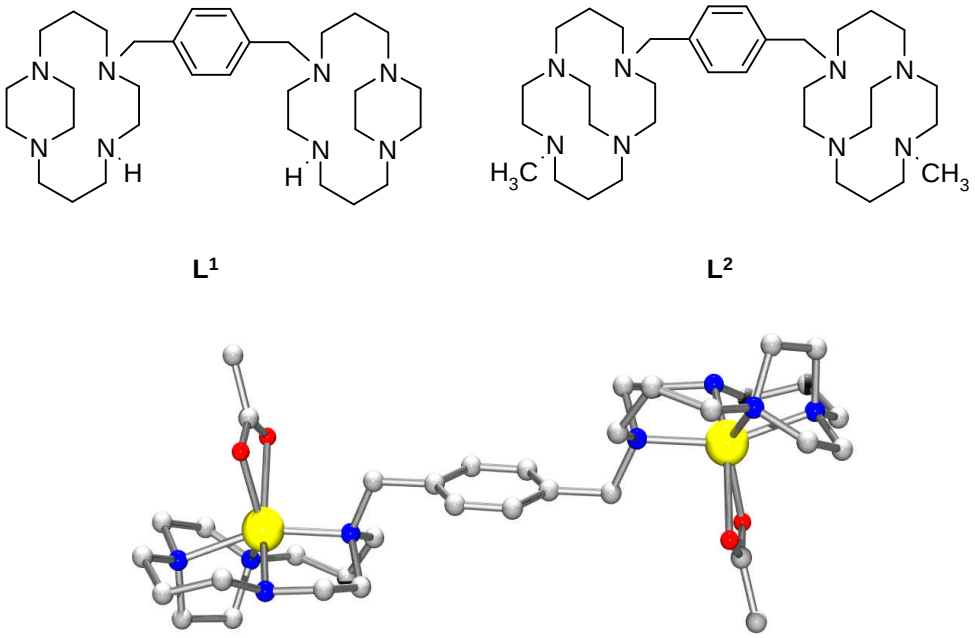

Figure (27). Structures of configurationally restricted bis-macrocyclic compounds ($\mathbf{L^1}$ and $\mathbf{L^2}$) and a ball and stick representation of the X-ray crystal structure of $[Zn_2\mathbf{L^1}(OAc)_2](OAc)_2$ with the unbound carboxylates omitted for clarity.

We have also synthesised a fluorescently tagged metal complex of a configurationally restricted cyclam for use in cellular imaging or applications in CXCR4 drug candidate screening.[235] This mono-macrocyclic compound shows metal activated binding to the receptor and can compete against anti-CXCR4 antibodies. The current compounds are not sufficiently selective due to the effects of the dye molecule on the cellular uptake properties. New compounds are being developed where cellular uptake and binding will not be influenced by the dye component. This strategy of binding

enhancement may open up new applications in medical imaging for macrocyclic chemokine receptor antagonists.

1.5 THERAPEUTIC POTENTIAL OF AMD3100

As discussed in section 1.2, the chemokine receptor CXCR4 and its ligand CXCL12 have a critical role in the establishment and progression of a number of disease states including HIV and many cancers. Therefore AMD3100 has been evaluated for its therapeutic effect against some of these disease states, and also as a stem cell mobiliser, to produce stem cells for transplantation as haematopoietic rescue for patients undergoing high-dose chemoradiotherapy.

1.5.1 HIV

"Time of addition" experiments, where antiviral drugs are added at different times after infection have been used to determine which stage of the virus replicative cycle is affected by the bicyclams.[185] A stage between virus adsorption and reverse transcriptase was found to be affected by the bicyclams (i.e. virus-cell fusion or uncoating).[247] Studies with AMD3100 resistant viruses have pointed to the importance of gp120 of HIV as the target of the bicyclams. This was confirmed by the repeated passages of the virus in the presence of AMD3100. It took more than 60 passages (300 days) in MT-4 cells for the virus to become 400-fold resistant to AMD3100 whilst only 10-20 passages were required to achieve the same resistance to several reverse transcriptase inhibitors e.g. TIBOL.[195] Analysis of the resistant virus showed several mutations over the whole of the gp120 glycoprotein, especially in the V3 loop. In addition, substitutions of amino acids in close proximity to the V3 loop have shown that the gp120 glycoprotein is responsible for resistance and sensitivity of HIV strains to AMD3100 and the bicyclams.[248]

The bicyclams were described several years ago as potent and selective inhibitors of HIV-1 and HIV-2 but not simian immunodeficiency virus replication. AMD3100 exhibits anti-HIV potency at concentrations of 1-10 nM, with a selectivity index >100,000 in an MT-4 assay. AMD3100 did not prove toxic to host cells at

concentrations up to 500 μM.[198,201,249] AMD3100 has shown activity against a wide variety of X4 and even R5/X4 strains in PBMC but not against R5 strains.[200,248,250,251]

AMD3100 has been shown to be active in phytohemagglutin (PHA) stimulated blasts against X4 virus strains such as IIIB and also against HIV-2 ROD strain but was totally ineffective against R5 strains, table (**4**). This shows the specificity of AMD3100 to CXCR4. AMD3100 has also been shown to reduce syncytia formation by 50% in HeLa cells infected with feline immunodeficiency virus at a concentration of 0.1 μM and displayed an IC_{50} of 0.02 μM against HIV-IIIB strain.[208]

		IC_{50} nM	
HIV strain	**Co-receptor used**	**AMD3100**	**SDF-1α**
HIV-1 IIIB	CXCR4	4	3
HIV-1 RF	CXCR4	10	6
HIV-1 NL4-3	CXCR4	6	13
HIV-2 ROD	CXCR4	14	7
HIV-1 Bal	CCR5	>49723	>125
HIV-1 SF-162	CCR5	>49723	>125
HIV-1 ADA	CCR5 (CCR2b, CCR3)	>49723	>125
HIV-1 JR-FL	CCR5 (CCR2b, CCR3)	>49723	>125

Table (4). AMD3100 Inhibition of Various HIV Strains.[200]

In another report AMD3100 blocked both syncytium formation and single-cell killing by apoptosis in a dose dependent manner in four different cell lines. The IC_{50} values ranged from 0.018 to 0.477 μM (table (**5**)).

	IC_{50} (μM)	
Cell line	**CXCL12**	**AMD3100**
CEM	>1.25	0.438 ± 0.06
SUP-T1	>0.125	0.477 ± 0.04
MT-4	0.008 ± 0.004	0.026 ± 0.018
PBMC	0.015 ± 0.088	0.018 ± 0.008

Table (5). The Inhibition of HIV-Envelope-Induced Apoptosis by CXCR4 Ligands.[252]

Furthermore, the zinc(II) complex of AMD3100 has been reported to have an increased potency of 6-fold as an anti-HIV agent compared with AMD3100 alone (MTT assay).[217] In another study the zinc(II) and nickel(II) complexes of AMD3100 reduced syncytia formation in FIV infected cells with an IC_{50} of 0.007 μg/ml and 0.03 μg/ml, respectively, whereas AMD3100 alone had an IC_{50} of 0.055 μg/ml.[208] Thus Zn_2AMD3100 was up to 8-fold more potent than AMD3100 alone. We have recently reported a configurationally restricted analogue, the zinc(II) complex of $\mathbf{L^1}$, see table (**6**), which displayed anti-HIV activity 3-fold higher than zinc(II) AMD3100 and 4-fold higher than AMD3100 (MT-4 assay).

Compound	HIV strain	Av EC_{50}(μM)[a]	SD[b]	Av CC_{50}(μM)[c]	SD[b]	SI[d]
$\mathbf{L^1}$	HIV-1 (IIIB)	6.98	1.84	>225	-	>32
$Zn_2(OAc)_4\mathbf{L^1}$	HIV-1 (IIIB)	0.0025	0.0010	60.56	4.73	24225
AMD3100[182]	HIV-1 (IIIB)	0.011	-	>225	-	>20455
Zn_2AMD3100[182]	HIV-1 (IIIB)	0.008	-	>225	-	>28125

[a] average effective concentration to reduce the HIV-induced cytopathic effect by 50% in MT-4 cells. [b] standard deviation over three assays. [c] Concentration required to have a cytotoxic effect reducing MT-4 cell viability by 50%. [d] Selectivity index based on μM conversion.

Table (6). Anti-HIV Activities, Cytotoxicity and Selectivity Index in MT-4 Cells.[226]

1.5.1.1 *Clinical Studies (HIV)*

The first human study of AMD3100 evaluated the safety, bioavailability, and single dose pharmacokinetics of AMD3100 from 10-160 μg/kg in healthy individuals.[253] AMD3100 was well tolerated in all patients with 50% of patients having mild side effects, primarily of a gastrointestinal nature. Absorption following subcutaneous injection was very good with 87% bioavailability; however no drug was detectable in the blood following oral

dosing. Pharmacokinetic profiles were dose proportional with an estimated half-life of 3.6 hours. A surprising, and ultimately exciting, observation was that most patients experienced transient, dose dependent increase in white blood cell count 1.5 – 3 times baseline values within 6 h of the infusion, which returned to baseline within 24 h of dosing. It was later confirmed that AMD3100 dose-dependently mobilised stem cells from the bone marrow (see section 1.5.4).[4]

Phase II clinical trials against HIV were carried out to evaluate AMD3100 for its safety, pharmacokinetic and antiviral activity.[254] Forty patients with a high viral load (>5000 copies/ml of HIV RNA) were enrolled, with the following HIV-phenotypes: SI (30%), NSI (45%) and not tested (25%). AMD3100 was administered for 10 days by continuous intravenous infusion, dose escalation from 2.5 up to 160 μg/kg/h. Most patients in the 80 160 μg/kg/h cohorts had paresthesias. One patient (5 μg/kg/h) had serious and possibly drug related thrombocytopenia. Two patients (40 and 160 μ/kg/h) had unexpected, though not serious, premature ventricular contractions; however, it was later determined these patients had previous cardiac complications.

Overall only one patient receiving the highest dose (160 μg/kg/h) had a significant 0.9 $\log^{10}$ copies/mL HIV RNA drop at day 11. It was later confirmed that this patient had only the CXCR4 utilising X4 strain and was many years into his HIV infection. This showed that in future studies more stringent examination of patients past medical records, virus strain and time into infection would need to be carried out at the time of clinical study to correctly ascertain the efficacy and effectiveness of an anti-HIV drug. At the time of the clinical trials an understanding of the mode of action of AMD3100 was not well developed. Further testing of AMD3100 as an anti- HIV drug was discontinued in favour of orally available CXCR4 antagonists such as AMD070.

1.5.2 Cancer

In addition to its anti-HIV effect, AMD3100 has been evaluated in its inhibitory effects towards a number of other diseases. Mice treated with AMD3100 (1.25 mg/kg) displayed delayed growth of experimental lung metastases.[255] Treatment of ovarian cancer cells with AMD3100 (2 μM) abrogated the increase in cell number after CXCL12

stimulation (100 ng mL-1).[256] AMD3100 (4 μM) also abolished approximately 80% of actin polymerisation in BCLL cells thus inhibiting chemotaxis.[257] In a high CXCR4 expressing pancreatic cancer cell line (Hs766T), originating from metastatic lesions, AMD3100 (2 μM) significantly reduced cell migration, in response to 300 ng mL^{-1} CXCL12, and proliferation in serum.[137] Moreover, AMD3100 (500 ng/ml) totally blocked the increase in invasion of two osteosarcoma cell lines stimulated by CXCL12 (100 ng/ml).[258]

More recently AMD3100 has been shown to function as a proapoptotic and antiproliferative agent for brain tumours growing intracranially, leading to a decrease in tumour size.[145] *In vitro*, proliferation and survival of medullablastoma and GBM cell lines by CXCL12 was blocked by AMD3100. *In vivo* studies showed that AMD3100 at 0.24–0.36 mg/day inhibited tumour growth compared to negative controls. In another study, AMD3100 (10 μM) inhibited SDF-1 (500 ng/ml) and VEGF (500 ng/ml) induced glioma cell invasion *in vitro*.[144] This data demonstrates that AMD3100 has a direct antitumour effect on GBMs and medullablastoma, and provides the scientific rationale for clinical evaluation of this or other CXCR4 antagonists in treating malignant brain tumours.

1.5.3 Inflammation

AMD3100 has also been evaluated for its anti-inflammatory effects to experimental fungal asthma. AMD3100 (1mg/kg) administered daily in *A. fumigatus* sensitised mice significantly ($P < 0.05$) reduced airway hyperresponsiveness and continued to do so at a concentration of 10 μg/kg/day after 15 days. Thus, AMD3100 exerted a therapeutic and protective effect during experimental fungal asthma and was suggested to do this by inhibiting the peribronchial distribution of eosinophils and T lymphocytes.[5]

AMD3100 has further shown its anti-inflammatory effect against rheumatoid arthritis. AMD3100 (180 μg/day) in a collagen II-induced arthritis (CIA) DBA/1 mouse model reduced leukocyte infiltration into inflamed joints and the clinical scores of arthritis were substantially lower in AMD3100 treated mice (<1) compared with control

(>4).[76] These studies suggest the potential of treating such inflammatory disorders with AMD3100 and warrant further clinical investigation.

1.5.4 Stem Cell Mobilisation

As mentioned earlier the CXCL12/CXCR4 pair has been found to play an important role in the homing and retention of HPC within the bone marrow.[40-44] These HPC can be used in stem cell transplantation in immuno-compromised patients, such as those receiving radiotherapy, and more recently it has been suggested HPC could repair damaged tissue in myocardial infarction.[259] Commonly, G-CSF is used alone as a HPC mobiliser but some complications with the process suggest a need to produce alternative mobilisation agents.

In healthy humans, AMD3100 dose dependently (80-240 µg kg-1) and rapidly (3-9 h) mobilised CD34+ HPC into peripheral blood. AMD3100 (80 µg/kg) induced 20.7 ± 3.5/µl of HPC and the highest dose of AMD3100 (240 µg/kg) induced 40.4 ± 3.4/µl of CD34+ HPCs into peripheral blood.[260] An increase in circulating CD34+ HPC of more then 20/µl is generally regarded as sufficient for stem cell transplantation.[261] Similar dose dependent rapid mobilisation of CD34+ HPC by subcutaneous administration of AMD3100 was reported in multiple myeloma and non-Hodgkin's lymphoma patients.[262] Following on from this initial study, a phase I clinical trial of the stem cell mobilisation capability of AMD3100 in combination with G-CSF was initiated in healthy patients. A single dose of AMD3100 (160 µg/kg) increased (3.8 fold) the number of mobilised CD34+ HPC compared with GCSF alone.[263] Subsequent Phase II studies have shown AMD3100 to efficiently mobilise CD34+ HPC from the bone marrow into peripheral blood, not only in healthy patients but in patients with cancer, multiple myeloma and non-Hodgkin's lymphoma and it is superior to G-CSF, especially in those patients who fail to mobilise enough HPC with G-CSF alone.[264,265]

AMD3100 has been given the generic name Mozobil® and brand name Plerixafor and has completed Phase III clinical trials in 2008. It is proving to be a successful drug for both HPC mobilisation, engraftment and transplantation of these cells in immuno-

compromised patients and has been approved by the FDA in December 2008 (NDA 02311) for use in non-Hodgkin's lymphoma and multiple myeloma patients.

1.6 PURPOSE OF THIS WORK

The aim of the first part of the project was to develop some new macrocyclic based metal complexes and to evaluate their binding capability and potency *in vitro* using anti-CXCR4 mAb competition assays. These new molecules were designed taking into account our previous work into configurationally restricted derivatives. This new group of compounds which included cyclen, cyclam and tris-cyclam derivatives, were probed in order to possibly improve the potency by fine tuning the binding interactions such as the metal ion coordination and additional cyclam moiety interaction via stereospecific hydrogen bonding. This had the potential of producing much more potent CXCR4 antagonists than previous compounds and providing a further understanding into the most important interactions that lead to a high affinity CXCR4 antagonist.

The second part of the project was to further characterise our most potent compound to date, copper(II) cross-bridged bicyclam, as a potential future drug candidate by evaluating its residence time with the CXCR4 receptor. It is thought that drugs with long residence times tend to have a high therapeutic activity due to their prolonged interaction with their specific protein targets.

Finally AMD3100 has been evaluated in its therapeutic effects by antagonism of CXCR4 with positive results. Therefore the anti-cancer effect of our configurationally restricted derivatives was probed, in particular anti-proliferative, apoptotic and anti-metastatic properties *in vitro*. This may allow a correlation of the therapeutic effect an antagonist has in relation to its binding affinity and residence time. Furthermore, in collaboration with Prof. Tony Ng's group at King's College London, the effects of CXCR4 dysregulation and its role in cancer progression were probed. In particular, the effect on cancer cell invasion was investigated. This will allow us to determine the key signalling pathways that are involved in cancer progression and may lead to the development of drugs targeting such pathways.

Chapter 2

Binding of configurationally restricted cyclam and cyclen based complexes

2.1 INTRODUCTION

The binding of an antagonist to a receptor can be investigated in a competition reaction with a natural ligand or with monoclonal antibodies (mAb) that have been raised to specifically bind to the receptor in question. Other assays can probe the downstream effects of receptor binding, such as intracellular calcium flux. As discussed earlier (sections 1.4.1 and 1.4.3), the binding epitopes within CXCR4 for CXCL12, anti-CXCR4 mAbs and AMD3100 have been reported to overlap and hence AMD3100 is able to block the binding of both CXCL12 and anti-CXCR4 mAbs. Furthermore, the blocking effects of AMD3100 on CXCL12, anti-CXCR4 mAb and HIV binding, and the abrogation of CXCL12 induced Ca^{2+} flux are reported to have a close correlation.[167]

These mAbs, in particular mAb 12G5 which is specific in its binding to the CXCR4 receptor; compete with the synthetic compound for receptor binding. The potency of compound is reported as a concentration required to inhibit a specified amount (%) of the mAb. Several studies have been carried out using this model and have reported a wide range of affinities and IC_{50} values for AMD3100 (sections 1.4.1 and 1.4.2). The use of IC_{50} as a value for affinity is widely accepted and has been discussed in detail by Goodrich and Kugel.[266]

Two main methods for analysing binding have been employed in reported studies; radiolabelling and flow cytometry. Radiolabelling includes the use of a radioactive isotope such as iodine-125 (^{125}I) attached to mAbs and this unit acts as a radioactive tracer. Other possible radioisotopes include positron emitters such as fluorine-18 or copper-64. Flow cytometry involves the automated analysis of cells or subcellular components by detection of the fluorescence or light-scattering of sample fractions passing as droplets in a narrow-stream droplet through a laser beam. In this case, secondary mAbs are conjugated to a fluorescent molecule such as fluorescein isothiocyanate (FITC) which can be exclusively detected at a relevant wavelength. Such binding studies have been reported for numerous cell lines including CXCR4 transfected cells, and cells that constitutively express CXCR4 on their cell surface such as SUP-T1 and Jurkat of T-lymphocytic origin.[198,200,201,203,267,268]

Here, we have employed the same flow cytometry strategy using Jurkat cells, that constitutively express CXCR4, which have previously been used in related studies.[175,194,203,205,269]

A range of our ethylene bridged compounds and their respective metal complexes have been analysed in their blocking efficacy towards an anti-CXCR4 mAb. We have previously reported an extensive study into the binding of a wide range of bicyclam and monocyclam based complexes to understand the important structural features and interactions that may be occurring.[233]

Here, we have employed the same method and analysed the binding affinity of a range of new monocyclam complexes, bicyclam, bicyclen and tris-cyclam complexes. The bicyclam complexes were not included in the previous study and are substituted at the 1,3 position (meta-xylyl) on the benzyl ring rather than the 1,4 position (para-xylyl) of the compounds previously studied. In addition, the bicyclen complexes were included in this study to analyse the effect of reducing the size of the tetra-aza ring (12 membered) compared to the cyclam ring (14 membered). Tris-cyclam compounds were investigated using the rationale that an extra cyclam moiety may provide an additional interaction on binding to CXCR4.

2.2 CYCLAM AND CYCLEN BASED COMPLEXES

Stock solutions of all compounds were prepared in phosphate buffer solution (PBS). The range of compounds included ethylene side bridged zinc(II) and copper(II) complexes of the monocylam with a benzyl NH_2 arm ($\mathbf{L^3}$) with two different counter ions (Cl^- and ClO_4^-) ($\mathbf{L^{3a-d}}$).

The bis-macrocyclic group of compounds studied were:

- $[Zn_2\mathbf{L}^4(OAc)_2](PF_6)_2$ and $[Cu_2\mathbf{L}^4(OAc)_2](PF_6)_2$ complexes of the meta-xylyl cross bridged bicyclam.
- $[Zn_2\mathbf{L}^{5\text{-}6}(OAc)_2](PF_6)_2$ and $[Cu_2\mathbf{L}^{5\text{-}6}(OAc)_2](PF_6)_2$ complexes of para-xylyl ($\mathbf{L^5}$) and meta-xylyl ($\mathbf{L^6}$) cross bridged bicyclens.
- $[Zn_2\mathbf{L}^7(OAc)_2](PF_6)_2$ and $[Cu_2\mathbf{L}^7(OAc)_2](PF_6)_2$ complexes of para-xylyl side bridged bicyclen.

Tris-cyclam based compounds included side bridged (**L**^{8}) zinc(II), copper(II) and nickel(II) complexes, the cross bridged (**L**^{9}) copper(II) complex and the linear side bridged (**L**^{10}) copper(II) complex.

These metal ions were selected for the following reasons:

1. The cyclam and cyclen rings have an appropriate cavity size to fit the first row transition metals (section 1.4.7)
2. Zinc(II) and copper(II) are represented in most of the published literature in terms of binding to CXCR4 and studies of the solution behaviour of zinc(II) relating to binding have been reported (section 1.4.7.1). Although other metals such as manganese(II) have been used in previous binding studies, due to time restrictions other metals were not included in these studies.
3. Our previous studies have shown that zinc(II) and copper(II) complexes have the highest binding affinities.

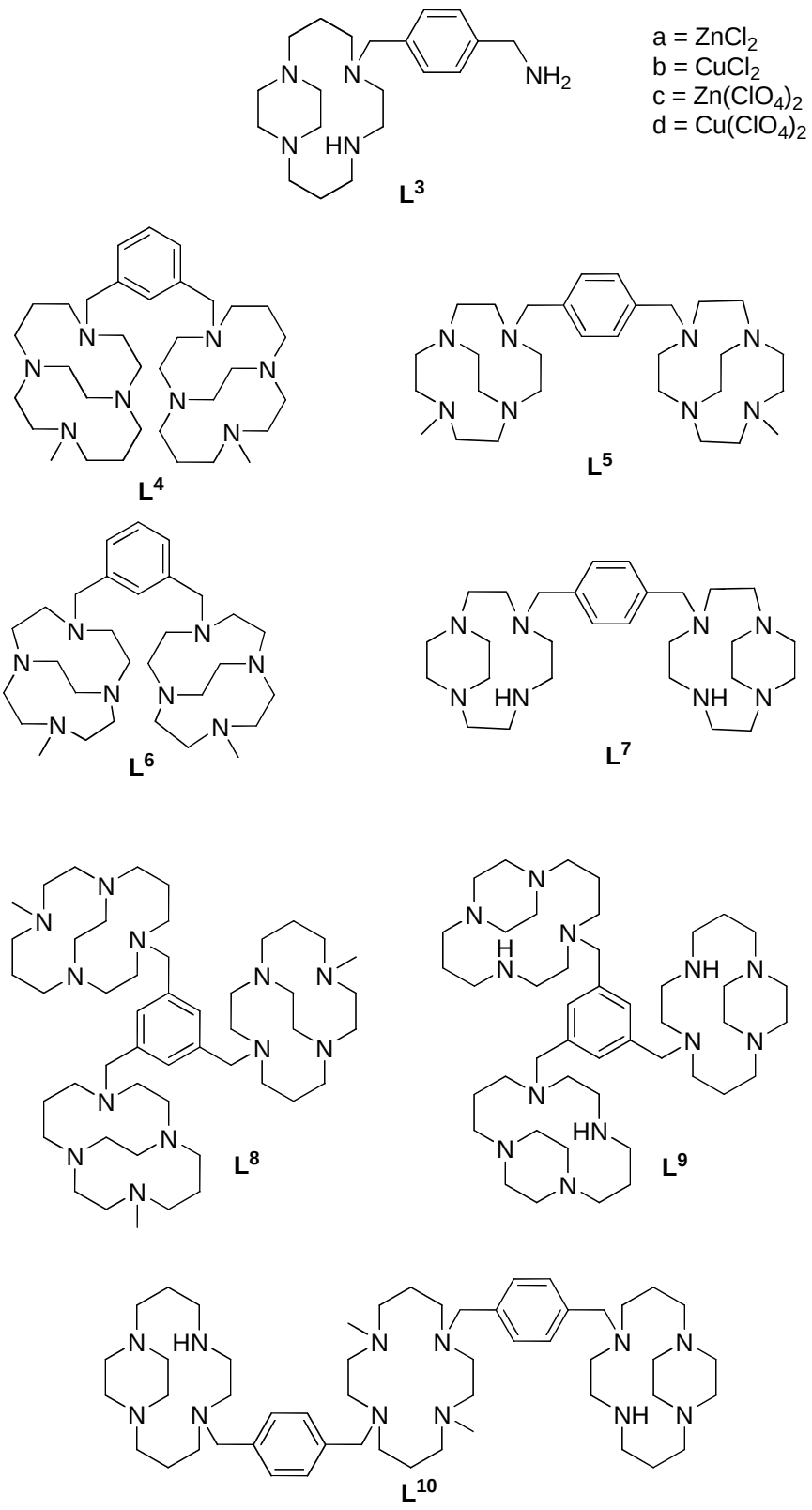

Figure (28). Configurationally restricted mono, bis and tris-macrocyclic componds

2.3 ANTI-CXCR4 MAB COMPETITION BINDING (BLOCKING) ASSAY

2.3.1 Monocyclam compounds

Varying concentrations of $\mathbf{L}^{\mathbf{3a-d}}$ were preincubated with Jurkat cells for 30 min to allow the compound to bind. Thereafter cells were washed to remove the excess compound and then incubated with the CXCR4 specific mAb 44716 (10 µg/ml) for 1 hour to allow the antibody to displace the antagonist and bind. Cells were washed again to remove excess antibody and were incubated with a secondary fluorescein isothiocyanate conjugated anti-mouse antibody (IgG-FITC) for 30 minutes and binding analysed by flow cytometry.

Blocking activities of $\mathbf{L}^{\mathbf{3a-d}}$ are shown as flow cytometric plots (Figures (**29-33**)). Fluorescent peaks of $\mathbf{L}^{\mathbf{3a-d}}$ are superimposable on the positive control and therefore show no inhibition towards the antibody at µM concentrations. This suggests monocyclam based derivatives were completely displaced by the mAb and are at best weak CXCR4 antagonists.

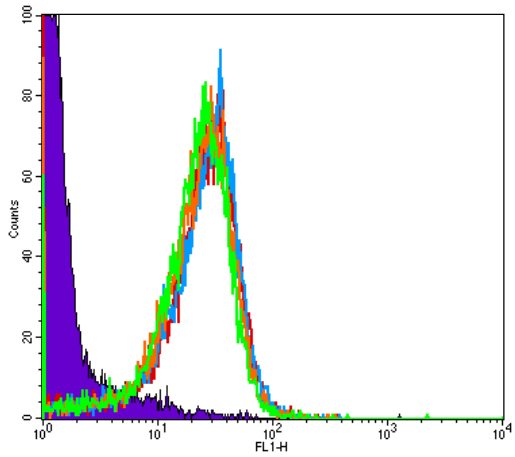

Figure (29). Flow cytometric plots of the inhibition of CXCR4 mAb 44716 by varying concentrations of $\mathbf{L}^{\mathbf{3a}}$ (85.695, 8.5695, 0.85695 µM). (-) control (purple) and (+) control (green) are shown. Plot represents one replicate.

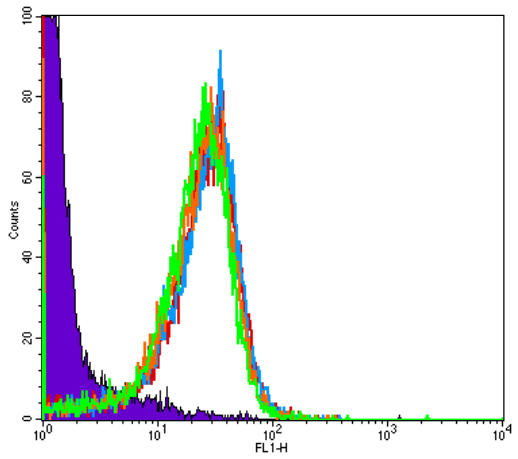

Figure (30). Flow cytometric plots of the inhibition of CXCR4 mAb 44716 by varying concentrations of **L**^{3b} (86.03, 8.603, 0.8603 µM). (-) control (purple) and (+) control (green) are shown. Plot represents one replicate.

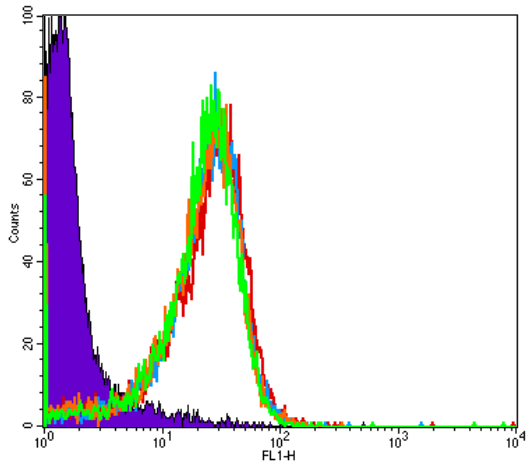

Figure (31). Flow cytometric plots of the inhibition of CXCR4 mAb 44716 by varying concentrations of **L**^{3c} (53.8, 5.38, 0.538 µM). (-) control (purple) and (+) control (green) are shown. Plot represents one replicate

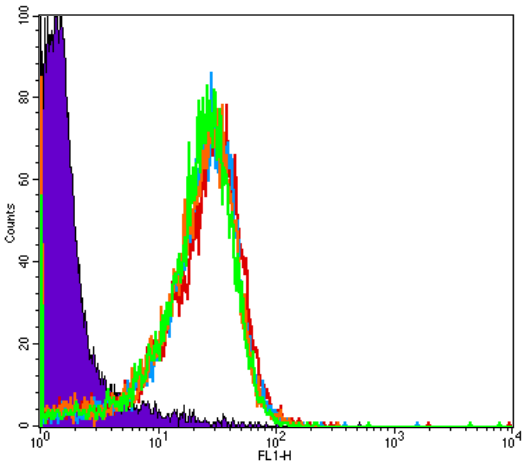

Figure (32). Flow cytometric plots of the inhibition of CXCR4 mAb 44716 by varying concentrations of **L**^{3d} (80.95, 8.95, 0.895 µM). (-) control (purple) and (+) control (green) are shown. Plot represents one replicate

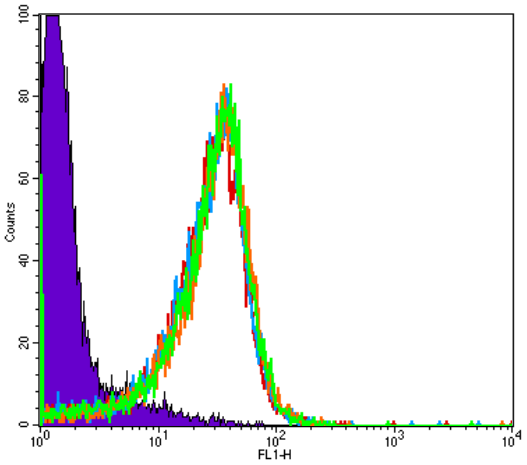

Figure (33). Flow cytometric plots of the inhibition of CXCR4 mAb 44716 by varying concentrations of **L**^{3} (78.43, 7.843, 0.7843 µM). (-) control (purple) and (+) control (green) are shown. Plot represents one replicate

2.3.2 Bicyclam and bicyclen compounds

2.3.2.1 *Displacement assay*

In contrast, the bicyclam and bicyclen complexes did inhibit the CXCR4 mAb binding (table (**7** and **8**)). Initially, metal complexes of $\mathbf{L^6}$ and $\mathbf{L^7}$ in excess were pre-incubated with CXCR4 expressing Jurkat cells for 1 hr. Unbound compound was removed by washing and cells were then exposed to a CXCR4 specific mAb. The binding of the CXCR4 mAb was detected using a secondary fluorescein isothiocyanate conjugated antibody (IgG-FITC) in a flow cytometer.

Several previous studies have reported the use of the mean fluorescent intensity (MFI) as a measure of binding and a quantitative way of calculating the percentage inhibition of the mAb (Equation (**1**)).[194,200,208,270,271] Here we have employed the same strategy. Flow cytometric plots for table (**7**) can be found in appendix (A2).

Equation 1:

$$100 - \frac{(\text{MFI of cells with compound - MFI of negative control})}{(\text{MFI of positive control - MFI of negative control})} \text{X100} = \% \text{ mAb inhibition}$$

Antagonist	Inhibition of CXCR4 mAb (%)
$[Zn_2\mathbf{L^6}(OAc)_2](PF_6)_2$	96.2 ± 0.3
$[Cu_2\mathbf{L^6}(OAc)_2](PF_6)_2$	98.2 ± 2.4
$[Zn_2\mathbf{L^7}(OAc)_2](PF_6)_2$	39.9 ± 3.0
$[Cu_2\mathbf{L^7}(OAc)_2](PF_6)_2$	90.8 ± 0.5

Table (7). CXCR4 antibody blocking activities of bicyclen based compounds (20 μM). Percentages are based on the mean of duplicates.

Table (**7**) shows zinc(II) and copper(II) complexes of $\mathbf{L^6}$ were highly potent in blocking the binding of the CXCR4 mAb. In contrast, the zinc(II) complex of $\mathbf{L^7}$ displayed a significant lower inhibition of CXCR4 mAb binding (~ 43% lower than $[Cu_2\mathbf{L^7}(OAc)_2](PF_6)_2$).

2.3.2.2 *Concentration dependent assay (competition)*

In accordance with current literature and our previous work, the potency of $\mathbf{L^4}$ and $\mathbf{L^5}$ compounds was assessed by the concentration required to inhibit 50% of the antibody binding (IC_{50}). Cells were incubated with varying concentrations of compound and anti-CXCR4 mAb simultaneously. Binding of anti-CXCR4 mAb was then detected as described before. Percent inhibition was calculated by using the mean fluorescent intensity of the peaks (MFI) (Equation (**1**)). Mean percentage inhibition at each concentration interval was plotted and IC_{50} extrapolated.

Antagonist	**IC_{50} (μM)**
$[Zn_2\mathbf{L^4}(OAc)_2](PF_6)_2$	13.425 ± 2.498
$[Cu_2\mathbf{L^4}(OAc)_2](PF_6)_2$	1.364 ± 0.340
$[Zn_2\mathbf{L^5}(OAc)_2](PF_6)_2$	0.938 ± 0.873
$[Cu_2\mathbf{L^5}(OAc)_2](PF_6)_2$	0.236 ± 0.003

Table (8). IC_{50} concentrations of CXCR4 antagonists ($\mathbf{L^4}$-$\mathbf{L^5}$) towards the inhibition of mAb 44716 in Jurkat cells.

Table **(8)** shows that the metal complexes of bicyclen ($\mathbf{L^5}$) have the lowest IC_{50} values (<1μM) of the four compounds and therefore in this assay are more potent than the metal bicyclam complexes ($\mathbf{L^4}$) (>1μM). In addition the plot of the mean percentage inhibition at each concentration interval is also shown (Figure (**34**))

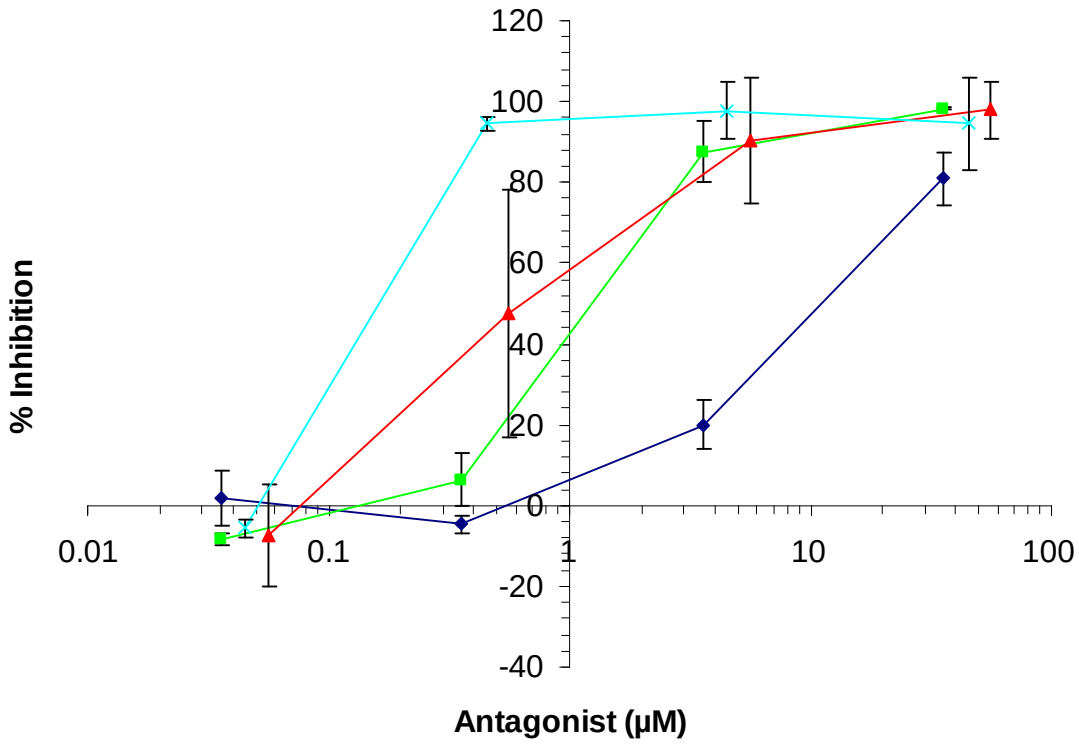

Figure (34). MAb (44716) binding inhibition by CXCR4 antagonists, $[Zn_2\mathbf{L}^4(OAc)_2](PF_6)_2$, $[Cu_2\mathbf{L}^4(OAc)_2](PF6)_2$, $[Zn_2\mathbf{L}^5(OAc)_2](PF_6)_2$, $[Cu_2\mathbf{L}^5(OAc)_2](PF_6)_2$ in Jurkat cells.

2.3.3 Tris-cyclam compounds

A similar displacement assay (section 2.3.2.1) was used to investigate the blocking capability of the tris-cyclam based complexes ($\mathbf{L}^{8\text{-}10}$) *in vitro* and this data is summarised in table (**9**).

Antagonist	Inhibition of CXCR4 mAb (%)
$\mathbf{L}^8$	15.9 ± 3.4
$[Zn_3\mathbf{L}^8Cl_3](PF_6)_3$	84.3 ± 4.6
$[Cu_3\mathbf{L}^8(OAc)_3](OAc)_3$	65.1 ± 7.4
$[Ni_3\mathbf{L}^8](ClO_4)_6$	53.3 ± 3.6
$[Cu_3\mathbf{L}^9(OAc)_3](OAc)_3$	75.1 ± 2.5
$[Cu_3\mathbf{L}^{10}Cl_3]Cl_3$	97.9 ± 0.4

Table (9). CXCR4 antibody blocking activities of tris-cyclam based compounds. Percentages are based on the mean of duplicates.

The tris (side-bridged) ($\mathbf{L^8}$) group of compounds showed varied activity. As expected the free ligand ($\mathbf{L^8}$) displayed the lowest inhibition. The formation of the $[Zn_3\mathbf{L^8}Cl_3](PF_6)_3$, $[Cu_3\mathbf{L^8}(OAc)_3](OAc)_3$ and $[Ni_3\mathbf{L^8}](ClO_4)_6$ metal complexes increased the activity by at least 3-fold with the $[Zn_3\mathbf{L^8}Cl_3](PF_6)_3$ complex displaying the highest inhibition in this group (84.3 ± 4.6%). The complex $[Cu_3\mathbf{L^9}(OAc)_3](OAc)_3$ also showed a considerable inhibition towards antibody binding, this inhibition was slightly higher (75.1 ± 2.5%) than the related side bridge complex (65.1 ± 7.4%). However, the linear $[Cu_3\mathbf{L^{10}}Cl_3]Cl_3$ complex displayed the highest inhibition of all the tris-macrocyclic complexes suggesting that the linear three ring motif has improved binding compatibility (see table (**9**)).

2.4 DISCUSSION

It has been proposed that the bicyclam type drugs interact with the amino acid residues Asp171, Asp262 and possibly Glu288 of the CXCR4 receptor. The suggested interaction is with the carboxylate groups of each of the residues, forming stereospecific hydrogen bonds between the amines on the rings of cyclam and cyclen and the carboxylate groups of the amino acids. However, for metal complexes, co-ordination of the carboxylate oxygens to the metal centre can occur, which is a much stronger interaction than hydrogen bonding. This co-ordination interaction is believed to be the dominant interaction for the metal complexes.

The activity of the compounds in relation to their molecular structure will be discussed in terms of their key structural features.

2.4.1 Cavity size

As mentioned earlier we have previously reported an extensive study into the binding of a range of bicyclam type compounds in relation to their blocking efficacy towards CXCR4 specific antibodies.[233] They displayed a high binding affinity to CXCR4 with low IC_{50} values.

In this study, the displacement assay revealed that the zinc(II) side bridged bicyclen compound ($\mathbf{L}^7$) which is in the previously studied para 1,4 arrangement displayed a very low mAb blocking percentage (39.9%). We have previously reported that the related zinc(II) side bridged bicyclam compound displays a very high blocking capability (98.3%) towards this antibody. The only significant difference is the change in ring cavity size between cyclen and cyclam. However, upon further analyses of the results it can be seen that the copper(II) complex of $\mathbf{L}^7$ displayed a high blocking capability (90.8%). Furthermore the copper(II) complex of $\mathbf{L}^7$ displayed very similar results to its sister compound the side bridged bicyclam compound (85.4%). Therefore it can be said the effect of the cavity size is very much metal ion dependent. The difference between the activity of the zinc(II) and copper(II) complexes has been discussed previously.[233]

Assuming the metal ions are co-ordinating to the carboxylate groups on the aspartate residues, then it would be reasonable to expect the zinc(II) complex to be more potent due to a stronger interaction with the oxygens than copper(II) and hence not be readily displaced by the antibody. The Irving Williams series would suggest that the copper(II) ion forms more thermodynamically stable complexes than zinc(II) due to the additional ligand field stabilisation energy. However, Irving Williams's series is based on all six bonds for the complete octahedral metal complex. In co-ordinating with CXCR4, only 1 or 2 restricted metal coordination sites (metal co-ordination with oxygens) are important in the binding of the molecule. Zinc(II) being a d^{10} metal has no co-ordination preference and therefore its co-ordination number will vary. Copper(II) has a preference for five co-ordinate square-based pyramidal or Jahn-Teller distorted six co-ordinate complexes.[272] The other key factor is the kinetic stability of the co-ordination interaction between the metal complex and the protein. Both the stability of the interaction of the metal ion with amino acids oxygens and the co-ordination number when bound to the receptor must be taken into consideration when rationalising the binding.

2.4.2 Meta *vs* para substitution

The position of the macrocycle ring on the phenyl ring significantly influences the binding interaction. The metal cross bridged bicyclam compounds (para-xylyl) have been investigated by us previously and displayed very high activity (the zinc(II) complex displayed an IC_{50} of 0.230 μM).[233] However the zinc(II) complex of **L**^{4} displayed a high IC_{50} value (13.425 μM). This is 50 times higher than the equivalent para complex clearly showing the lower binding affinity of this compound. Although the copper(II) complex of **L**^{4} displayed a higher activity (IC_{50}: 1.364 μM) than the zinc(II) complex (13.425 μM), it nevertheless confirmed a lower affinity of the meta derivatives when compared to the copper(II) para-xylyl cross bridged bicyclam (IC_{50}: 0.160 μM) from our previous study.[233]

It is important to consider the structural differences of the bicyclam complexes employed in this study; they have the cyclam rings substituted in the 1,3 (meta) position on the central phenyl ring and not in the 1,4 (para) position used previously. The metal ion-metal ion distance will be shorter and therefore it is reasonable to assume whilst one cyclam ring positions itself to interact with one of the aspartate residues the other cyclam ring may well be out of position relative to the second aspartate residue. However, if this is the case, the second ring, which cannot interact with the other aspartate residue, could form weaker interactions in the cavity of the receptor such as hydrogen bonding, or electrostatic interactions.

2.4.3 Tris-cyclam compounds

Tris-cyclam compounds were investigated to potentially increase the binding affinity to CXCR4 by providing an additional binding interaction site with the inclusion of an extra cyclam moiety. Two different motifs were studied which included a central unit (benzene) with three cyclam rings around it or three cyclam rings linked in a linear arrangement (see Figure (**35**)).

Inclusion of metal ions increased the binding affinity by at least 3-fold (see table (**9**)) and confirmed our previous results of providing a dominant metal ion co-ordination

interaction with CXCR4. Although the zinc(II) and copper(II) complexes of **L**^{8} displayed high activity (table (**9**)), this was slightly lower than the side bridged bicyclam compounds reported previously (zinc(II) side bridge bicyclam: 98.3%, copper(II) side bridge bicyclam: 85.4%). This can be explained by examining the structure of the tris-cyclam molecule in more detail. We have already discussed (above) the effect of the meta-xylyl (1,3) position on the phenyl ring in reducing the activity and potentially the strong interaction within CXCR4. Here on the tris-cyclam ring molecule, the side bridged cyclam rings are substituted at the 1,3,5-positions on the phenyl ring. The first two cyclam rings are substituted on similar positions compared to the meta (1,3) bicyclam molecule. Therefore we can assume the interaction of two of the cyclam rings would behave as if they were in the meta-xylyl position on a bis-macrocyclic structure. The third cyclam ring may well be forming an additional interaction within CXCR4. However, due to the lower % inhibition values it is reasonable to suggest that in this class of molecule as a whole, the interaction may incorporate hydrogen bonding or electrostatic interactions rather than two or three strong metal ion co-ordination bonds.

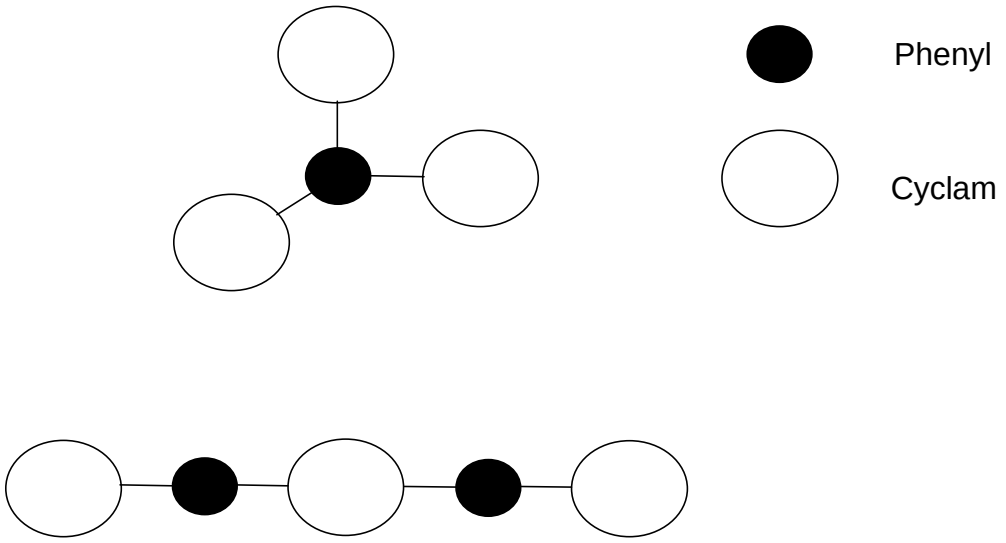

Figure (35). Ring and linear arrangement of tris-cyclam compounds

This concept is further supported when examining the activity of the linear (**L**^{10}) tris-cyclam complex. The $[Cu_3\mathbf{L}^{10}Cl_3]Cl_3$ which displayed the highest (97.9 ± 0.4%)

inhibition in this class of compounds. Furthermore this is higher than the related copper(II) side bridged bicyclam based complex reported previously by us (85.4%).[233] Using this design of a linear tris-cyclam molecule we have successfully increased the activity with an additional cyclam moiety and therefore we can presume at least two strong metal ion co-ordination interactions are occurring with a possible third or multiple weaker hydrogen bonds forming with the additional cyclam moiety and other amino acid groups in close proximity. To establish the exact nature of the interactions of the linear based tris cyclam molecules within the CXCR4 receptor would require computational docking studies coupled with site directed mutagenesis of the receptor.

2.4.4 Monocylam binding

We have previously reported the weak antagonistic activity of a range of monocyclam derivatives.[233] Here we evaluated the antagonistic activity of a range of monocyclam aniline derivatives (**L**$^{\mathbf{3a\text{-}d}}$) with the possibility of the amine group (NH_2) being protonated (NH_3^+) and electrostatically interacting with an aspartate residue or other residues within the binding cavity. The low activity is similar to what has been reported previously and would suggest that the amine group had no significant influence. A likely explanation for this could be the protonated amine group was not close enough to any of the residues within the binding cavity to interact. To address this, an alkyl chain could be added to act as a spacer between the cyclam ring and the NH_2 group.

2.5 CONCLUSION

This investigation into the structure-binding affinity relationship of a range of macrocyclic based complexes has shown and confirmed a number of key structural features that are important in trying to design a high affinity CXCR4 antagonist. In general, reduction in the cavity size of the macrocyclic ring and substitution or position of this ring in the meta (1,3) position reduces the affinity of the complex in binding to the CXCR4 protein. In support of our previous study, inclusion of a metal ion is crucial in increasing the affinity of the complex. Furthermore, the type of metal ion used

strongly influences the affinity and this can be attributed to the kinetics and thermodynamics of metal ion coordination. In addition, the design of the tris-cyclam linear complex has shown promise as a potential high activity CXCR4 antagonist and warrants further development.

Chapter 3

Residence time of macrocyclic based complexes

3.1 RESIDENCE TIME

The majority of biochemical activity in cell physiology is controlled and mediated by distinct macromolecule-receptor interactions and the macromolecule-receptor complex formation. The duration of the effect of the biological macromolecule can be related to the lifetime of the macromolecule-receptor complex itself. Thus the longer the macromolecule is in "residence" with its receptor, the longer the biological effect. This can be especially important in for example, controlling enzyme activity. Most substrates are bound to enzymes for less than 50 ms^{-1}, however, enzyme inhibitors can stay complexed for days and months, which translates to a sustained inhibition of enzyme activity.[273]

In terms of pharmaceutical drug development, programs rely heavily on the thermodynamic dissociation constant, K_d (or K_i), as the primary measure of drug target potency. An alternative parameter in drug optimisation is to consider the drug-target residence time. It has been proposed that one of the most crucial factors for sustained drug efficacy *in vivo* is not the apparent affinity of the drug for its target but rather the residence time of the drug with its molecular target.[273-275]

3.2 KINETIC ASPECTS OF MACROMOLECULE-RECEPTOR COMPLEX

The binding of a macromolecule to its receptor has been commonly assessed by quantitatively measuring the binding affinity using a number of parameters such as IC_{50} and K_d (equilibrium constant). However the affinity of a macromolecule to its receptor does not define the efficacy and extent of the biological effect. It is instead the residence time that dictates the effectiveness of the biological macromolecule.[274,275]

Thermodynamic constants (K_a, K_d, $\Delta G_{binding}$) serve well in defining complex affinity, however Copeland *et al*, argue that the dissociation rate of the macromolecule-receptor complex is the critical factor in biological function.[275] The dissociation rate can be defined by the term off-rate and is represented by k_{off}.

Our macrocyclic molecules are believed to bind in a one step binding mechanism, and therefore the association and dissociation can be represented by Equation (**2**).

Equation 2:

$$R + M \underset{k_2}{\overset{k_1}{\rightleftharpoons}} RM$$

Here the receptor (R) and macromolecule (M) combine to form a complex (RM) with the association rate constant k_{on} (k_1) and k_{off} (k_2). The equilibrium dissociation constant (K_d) is defined by the ratio (k_2/k_1). The residence time (τ) can be defined by the reciprocal of the off-rate ($1/k_{off}$). In pharmacology the concept of half-life is usually used and therefore Copeland *et al*, have devised the term dissociative half-life ($t_{1/2}^{diss}$) to represent the half-life of the receptor-macromolecule complex.[275] $t_{1/2}^{diss}$ is given by $0.693/k_{off}$. Examples of $t_{1/2}^{diss}$ of some current drugs are represented in table (**10**).

Drug	**Target**	**$t_{1/2}^{diss}$**
Compactin	HMG-CoA reductase	15 min
Candesartan	Angiotensin-II type 1 receptor	1-3 hrs
Deoxyconformycin	Adenosine deaminase	40 hrs
Oseltamivir (Tamiflu®)	Viral neuroaminidase	47 min

Table (10). $t_{1/2}^{diss}$ of some current drugs.[275]

An investigation of the relative residence times was carried out on a group of bicyclam based compounds complexed to the CXCR4 receptor *in vitro*. Ideally, the amount of compound bound to the receptor should be measured directly by the concentration of compound bound, either by radiolabelling or fluorescent tagging. However in this case we have indirectly measured the amount of bound compound to the CXCR4 receptor by competition with anti-CXCR4 antibodies. As these compounds are antagonists of CXCR4 and have been demonstrated to inhibit anti-CXCR4 antibody binding, we have measured the amount of antibody binding to indicate inversely the amount of compound bound.

3.3 BICYCLAM ANTAGONISTS

Stock solutions of all compounds were prepared in distilled phosphate buffer solution (PBS) at 40 μM. Compounds were chosen on the basis of the data collected in the previous study investigating the structure-activity relationship of configurationally restricted bicyclam-based antagonists.[233] The range of compounds consisted of:

- AMD3100 ($\mathbf{L^{11}}$) and its $[Zn_2\mathbf{L^{11}}Cl_2]^{2+}$ and $[Cu_2\mathbf{L^{11}}Cl_2]^{2+}$ complexes
- $[Zn_2\mathbf{L^1}]^{4+}$ and $[Cu_2\mathbf{L^1}]^{4+}$ (complexes of the side bridged bicyclam)
- $[Zn_2\mathbf{L^2}Cl_2]^{2+}$ and $[Cu_2\mathbf{L^2}Cl_2]^{2+}$ (complexes of the cross-bridged bicyclam)

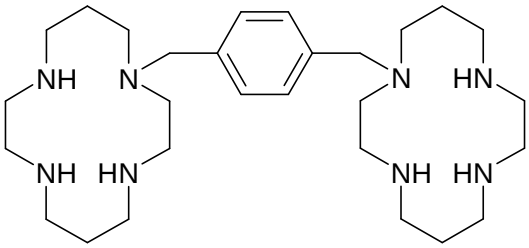

AMD3100 ($\mathbf{L^{11}}$)

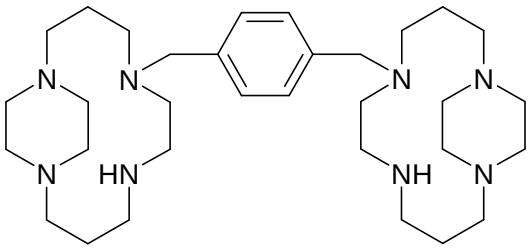

$\mathbf{L^1}$

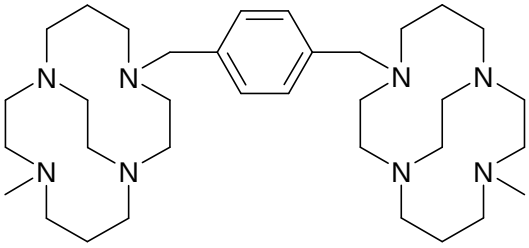

$\mathbf{L^2}$

Figure (36). Structures of bicyclam-based compounds

3.4 RESIDENCE TIMES OF BICYCLAM ANTAGONISTS

Metal complexes with ligands $\mathbf{L}^{1\text{-}2,11}$ were added in excess (40 µM) to a specific number of CXCR4 expressing Jurkat lymphoma cells and incubated for 1 hour to allow the compound to bind. Thereafter cells were washed to remove excess compound and incubated for a 96 hr period. At 24 hr intervals an anti-CXCR4 antibody was added to bind to any available CXCR4 sites and bound antibody was detected by flow cytometry. The MFI was used as previously described (section 2.3.2.1) to calculate amount of antibody inhibited and this was used as the percentage compound bound. The percentage compound bound was then plotted as a function of time, see Figure (**37**). This shows the amount of compound complexed to the available receptors, which varies with each type of compound. After a 24 hr period most of the compounds are still bound to the receptor (80 – 90%). However, after a 48 hr period some of the compounds started to dissociate with $[Zn_2\mathbf{L}^{1}]^{4+}$ dissociating most rapidly, dropping by ~ 60%. After 72 hrs, it was found that AMD3100 and its metal complexes dissociated by 40% or more, followed by a steady dissociation of $[Cu_2\mathbf{L}^{1}]^{4+}$. Finally after the total 96 hr period, most of the compounds had shown significant dissociation with the exception of the metal cross-bridged compounds. $[Zn_2\mathbf{L}^{2}Cl_2]^{2+}$ and $[Cu_2\mathbf{L}^{2}Cl_2]^{2+}$ did not display any significant dissociation throughout the 96 hr incubation period with the cells.

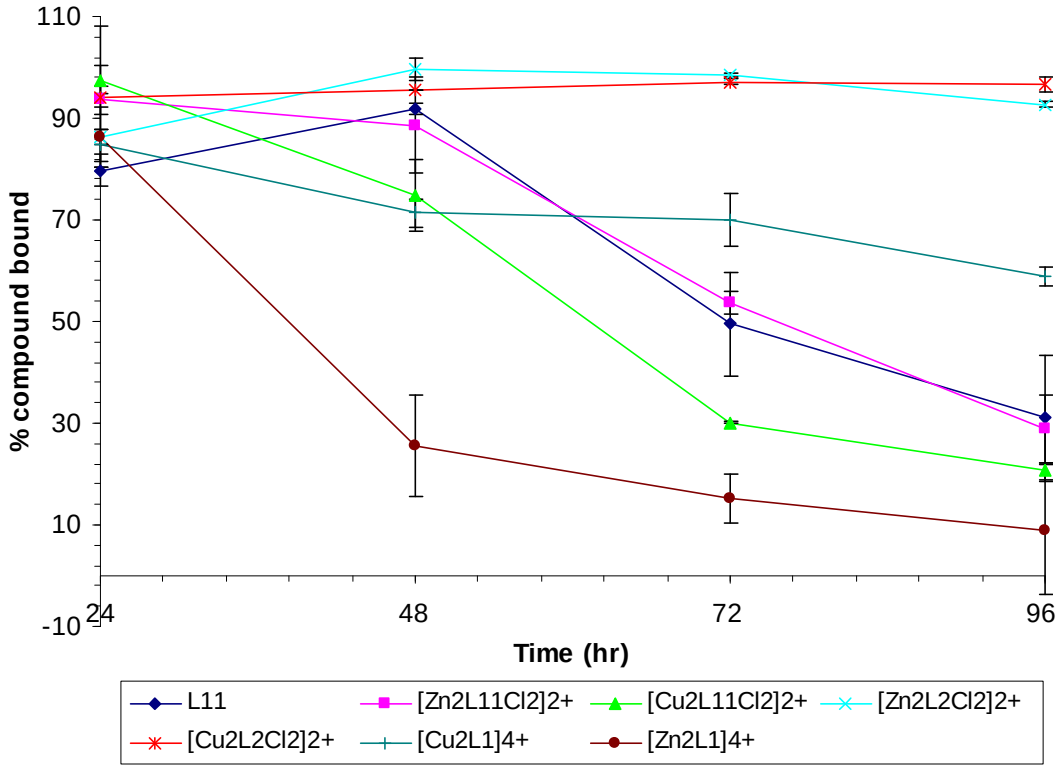

Figure (37). Dissociation of macrocyclic based complexes (40 µM) in Jurkat cells. Each interval plotted as mean of duplicates.

It must be noted that whilst the cells were incubated with the compounds over the 96 hr period, cell proliferation must be occurring. This would have increased the cell population over time and hence also increased the number of available CXCR4 binding sites. Any compound not washed away, which is likely due to the large amount of excess used (40 µM) would be able to bind to the new CXCR4 sites or exchange with the old compound. However, cell proliferation is a factor that will be involved in all the cell samples at the same rate (due to the use of the same Jurkat cell line) and thus any dissociation seen over time must be due to differing residence times of each type of compound. Therefore residence times are in relative terms to this particular experiment.

All of these compounds have been reported by us previously to be highly potent CXCR4 antagonists, demonstrated using anti-CXCR4 antibodies.[233] From Figure (**37**) it is clear that metal cross-bridged compounds have a higher residence time than the other compounds analysed in this study. Therefore a more detailed analysis of the dissociation process of the cross-bridged compounds was carried out.

3.4.1 Residence time of cross-bridge bicyclam antagonists

To more accurately determine relative residence times, modifications were required in the experimental model used above. With the use of excess compound it was noted that kinetics of ligand exchange would play an important part in the overall potency of the compound. The amount of CXCR4 receptors expressed on Jurkat cells have been reported to be ~140,000 receptors per cell.[276] Based on this figure, in the previous study 1.78×10^4 molecules of compound were added per receptor i.e. 17800 in excess per receptor (see A5). Washing of the compound to remove excess is quite efficient in removing most of the compound, however some compound will always remain. With such a large excess of compound per receptor, even reasonably efficient removal of the compound would still leave a significant residual number of molecules. This could be enough to allow exchange of bound compound with new compound. Thus to reduce this effect a considerable reduction in starting concentration was required. However, this would need to be balanced by having sufficient compound to bind to every available CXCR4 site (initial binding saturation).

$[Cu_2\mathbf{L}^{\mathbf{2}}Cl_2]^{2+}$ was chosen as it was the most potent compound in our previous study (IC_{50} = 0.160 µM), and for comparison AMD3100 ($\mathbf{L}^{\mathbf{11}}$) and its copper(II) complex $[Cu_2\mathbf{L}^{\mathbf{11}}Cl_2]^{2+}$ were also included in this study.[233]

As a preliminary study into the effect on binding potency with a reduced initial concentration, Jurkat cells were incubated with AMD3100 ($\mathbf{L}^{\mathbf{11}}$) and $[Cu_2\mathbf{L}^{\mathbf{2}}Cl_2]^{2+}$ in a lower concentration range of (0.08 – 16 nM) over a 24 hr period.

Table (**11**) shows that AMD3100 ($\mathbf{L}^{\mathbf{11}}$), which is known to be less potent than $[Cu_2\mathbf{L}^{\mathbf{2}}Cl_2]^{2+}$, rapidly dissociated at all concentrations. $[Cu_2\mathbf{L}^{\mathbf{2}}Cl_2]^{2+}$ displayed a slower dissociation rate at higher concentrations (8.0-16.0 nM) (table (**11**)).

Compound (nM)	% Compound bound (after incubation period (hr))	
AMD3100 (L^{11})	**1**	**24**
0.08	62.0	5.1
0.4	62.7	7.5
0.8	82.3	14.1
4.0	84.5	9.9
8.0	88.9	1.3
16.0	89.4	12.7
$[Cu_2\mathbf{L}^{2}(Cl_4)]$		
0.08	93.1	6.7
0.4	69.1	14.9
0.8	89.5	13.6
4.0	98.5	34.2
8.0	95.8	82.2
16.0	97.2	62.1

Table (11). Amount of compound (% of total) bound to CXCR4 after incubation (1 and 24 hr) with Jurkat cells.

Therefore it was concluded that 16 and 32 nM would be used as starting concentrations. This equated to ~ 7 fold (16 nM) and ~ 14 fold (32 nM) excess molecules of compound per CXCR4 receptor binding site (see appendix (A5) for full calculation). After washing, it was hoped that the amount of compound remaining would be negligible.

3.4.1.1 *Kinetics of binding (residence time constants)*

As discussed in the previous section, Jurkat cells were incubated with compounds AMD3100 ($\mathbf{L}^{11}$), $[Cu_2\mathbf{L}^{11}Cl_2]^{2+}$ and $[Cu_2\mathbf{L}^{2}Cl_2]^{2+}$ (16 and 32 nM) for 1 hr. The cells were washed and the binding analysis carried out as in section 3.4. Figures (**38**) and (**39**) show the dissociation of compound over the 96 hr period.[234]

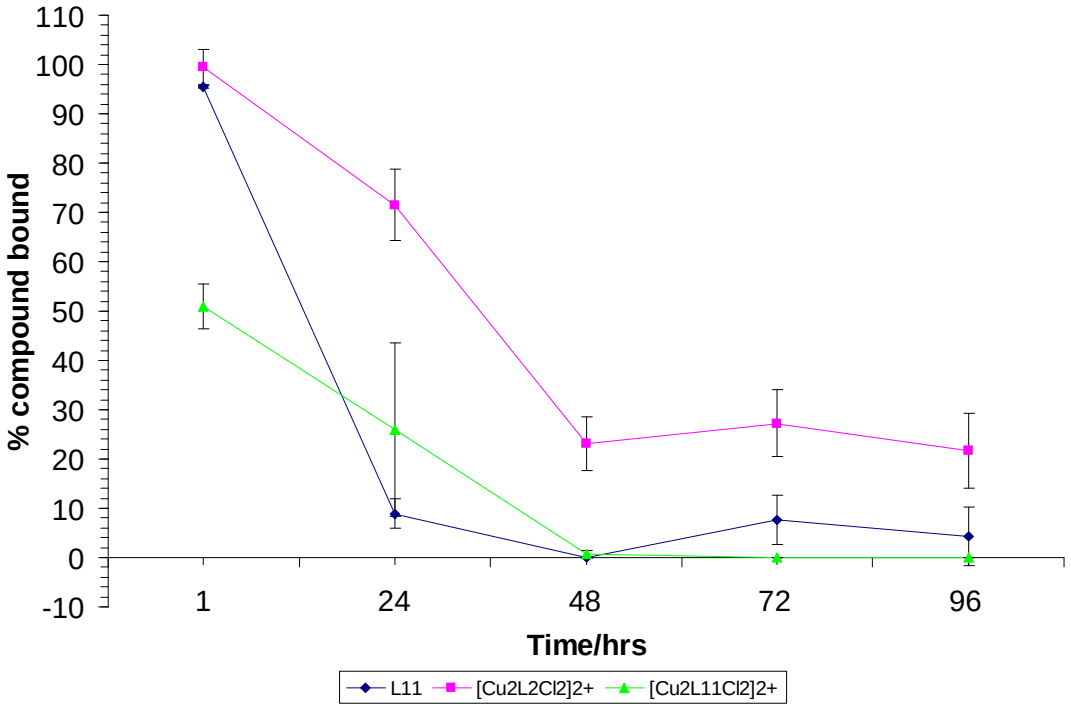

Figure (38). Dissociation of AMD3100 ($\mathbf{L^{11}}$), $[Cu_2\mathbf{L^{11}}Cl_2]^{2+}$ and $[Cu_2\mathbf{L^{2}}Cl_2]^{2+}$ (16 nM) in Jurkat cells. Negative values have been zeroed. Each interval plotted as mean of duplicates.

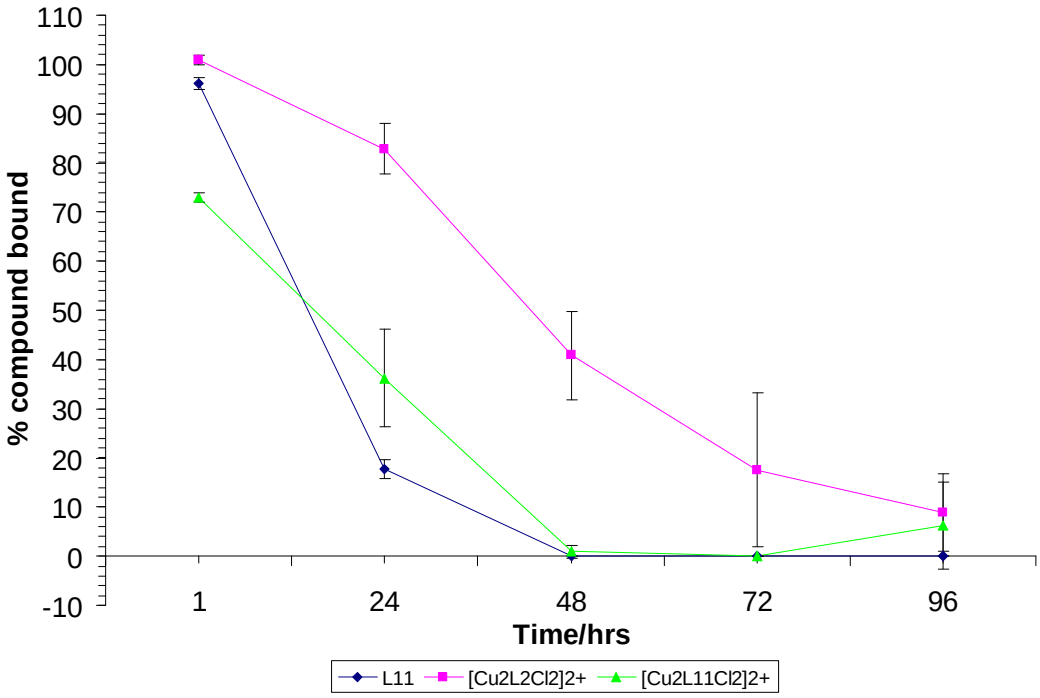

Figure (39). Dissociation of AMD3100 ($\mathbf{L^{11}}$), $[Cu_2\mathbf{L^{11}}Cl_2]^{2+}$ and $[Cu_2\mathbf{L^{2}}Cl_2]^{2+}$ (32 nM) in Jurkat cells. Negative values have been zeroed. Each interval plotted as mean of duplicates.

Both concentrations of compound (16 and 32 nM) display similar rates of dissociation. After a 24 hr period, AMD3100 ($\mathbf{L^{11}}$) displayed a considerable dissociation (<20% bound) from the receptor followed closely by $[Cu_2\mathbf{L^{11}}Cl_2]^{2+}$. At 48 hr most (<10% bound) of the AMD3100 ($\mathbf{L^{11}}$) and $[Cu_2\mathbf{L^{11}}Cl_2]^{2+}$ have dissociated. However the dissociation rate observed for $[Cu_2\mathbf{L^{2}}Cl_2]^{2+}$ was much slower compared to the other two compounds over the whole incubation period (Figures (**38**) and (**39**)). After an initial 24 hr period, >70% of $[Cu_2\mathbf{L^{2}}Cl_2]^{2+}$ was still bound to the receptor with significant dissociation observed only after the 48 hr incubation interval.

3.4.1.2 *Determination of the relative residence time (τ) and $t_{1/2}^{diss}$*

The data from Figures (**38**) and (**39**) were used to calculate the relative residence time (τ) and $t_{1/2}^{diss}$ constants for each of the three compounds. These are not corrected for cell growth and so are not true $t_{1/2}^{diss}$ or τ but do allow a limited comparison of these compounds. Firstly, the mean (%) of compound bound was plotted as a function of time (hr) and "fitted" using the one phase exponential decay model and subjected to non linear regression analysis. The one phase exponential decay model uses the graphical method of calculating the k_{off} rate and hence calculates $t_{1/2}^{diss}$. Full analyses can be found in appendix (A6), including the 95% confidence intervals for the relative residence time. Table (**12**) shows the relative (τ) and $t_{1/2}^{diss}$ constants for each of the compounds.

Compound	**Concentration (16 nM)**		**Concentration (32 nM)**	
	(τ) (hr)	**$t_{1/2}^{diss}$ (hr)**	**(τ) (hr)**	**$t_{1/2}^{diss}$ (hr)**
($\mathbf{L^{11}}$)	9.7	6.7	13.2	9.1
$[Cu_2\mathbf{L^{11}}Cl_2]^{2+}$	23.5	16.3	23.6	16.4
$[Cu_2\mathbf{L^{2}}Cl_2]^{2+}$	49.0	33.9	48.9	33.9

Table (12). Relative (τ) and $t_{1/2}^{diss}$ constants for compounds binding to CXCR4 receptor in Jurkat cells. Constants for both starting concentrations are shown.

It can be seen from table (**12**), that the relative (τ) and $t_{1/2}^{diss}$ values correlate well for both concentrations. AMD3100 (L^{11}) displayed the lowest relative residence time and

$t_{1/2}^{diss}$ of all three compounds. $[Cu_2\mathbf{L}^{11}Cl_2]^{2+}$ had up to 2.5 fold higher relative residence time than AMD3100 (L^{11}). However, the cross bridged $[Cu_2\mathbf{L}^{2}Cl_2]^{2+}$ compound displayed the longest relative residence time and $t_{1/2}^{diss}$ (see table (**12**)).

3.5 CYTOTOXICITY

To analyse the cytotoxic effect of the compounds, all compounds were subjected to a cell viability study. Jurkat cells were incubated with excess compound (40 µM) and cell viability over a 96 hr period was analysed using the tryphan blue exclusion test under a light microscope. Cell samples with compounds all displayed nominal growth profiles and therefore have no cytotoxicity at these concentrations (Figure (**40**)).

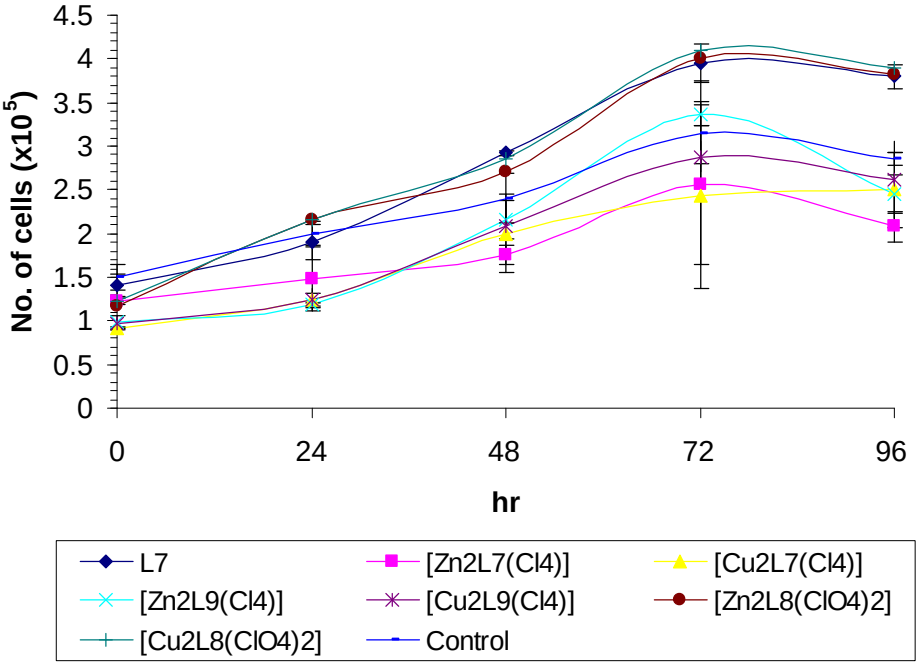

Figure (40). Viable growth profile of Jurkat cells with compound (40 µM) over a 96 hr incubation period. Each data point represents the mean of duplicates.

3.6 DISCUSSION

Binding affinity is an important parameter which can be used to investigate the interaction between a protein and its biological target. However, other factors such as the

residence time of a macromolecule with its protein target need to be taken into consideration, especially in optimisation of pre-clinical drugs. Here we have investigated the relative residence times of a number of configurationally restricted bicyclam based antagonists on binding to the CXCR4 protein. All the compounds used in the initial study using excess concentration (Figure (**37**)), have previously shown a very similar high binding affinity to the CXCR4 receptor (~100% anti-CXCR4 mAb inhibition).[233] However from Figure (**37**), it is clear that this group of compounds have different relative receptor residence times. It is interesting to note that anti-HIV data collected on these particular compounds (unpublished) also reveal marked differences. The anti-HIV assay is carried out over a 5 day period and hence the difference in activity could be due to the residence times of these compounds. Compounds with similar binding affinity and varied residence times have been reported previously.[273]

Furthermore the calculated relative (τ) and $t_{1/2}^{diss}$ values were interesting results. Data from our previous study shows the binding affinity of AMD3100 (**L**^{11}) is high, however it can be further improved by the inclusion of a metal ion and the resulting co-ordinative interactions. Our configurationally restricted metal based bicyclam compounds have been demonstrated to have improved binding characteristics due to the dominant interaction of the metal ion and optimization of this co-ordination interaction by restricting the geometry of the macrocycle (see section 2.4 for discussion).[233-235] This contributes to the increased relative residence time parameters observed for copper based complexes (table (**11**)). The $[Cu_2\mathbf{L}^{2}Cl_2]^{2+}$ complex had a relative (τ) of 49.0 and 48.9 hr, which was up to 5-fold higher than for AMD3100 (**L**^{11}) and the relative $t_{1/2}^{diss}$ half-life was again up to 5-fold higher (table (**12**)).

$[Cu_2\mathbf{L}^{2}Cl_2]^{2+}$ is now established as the most potent compound binding to CXCR4 (IC_{50} = 0.160 μM).[233] Furthermore $[Cu_2\mathbf{L}^{2}Cl_2]^{2+}$ (EC_{50} = 4.3 nM) is significantly more effective as a anti-HIV inhibitor than AMD3100 (**L**^{11}) (EC_{50} = 11 nM) and $[Cu_2\mathbf{L}^{11}Cl_2]^{2+}$ (EC_{50} = 47 nM).[234] This higher activity may stem from its higher residence times (table (**12**)).

It is likely that a coordinate bond will form with an aspartate side chain when the complex interacts with the chemokine receptor. X-ray crystallography can be used to study models of the bonding interaction and gain precise geometric parameters. X-ray

crystal structures of monocyclam compounds similar to $[Cu_2\mathbf{L}^{2}Cl_2]^{2+}$ and $[Cu_2\mathbf{L}^{11}Cl_2]^{2+}$ have been used to characterise the binding mode of the fifth ligand position. Examination of the X-ray crystal structures revealed that in the folded configuration of the cross-bridged monocyclam copper(II) compound, the chelator occupied 3 of the equatorial sites and the axial site, which is in contrast to copper monocyclam which occupied all four equatorial sites (Figure (**41**)). The formation of a shorter, stronger equatorial bond with the chloride (or aspartate when bound to CXCR4) will offer a more favourable interaction in comparison to the axial interaction with the copper(II) AMD3100 complex.

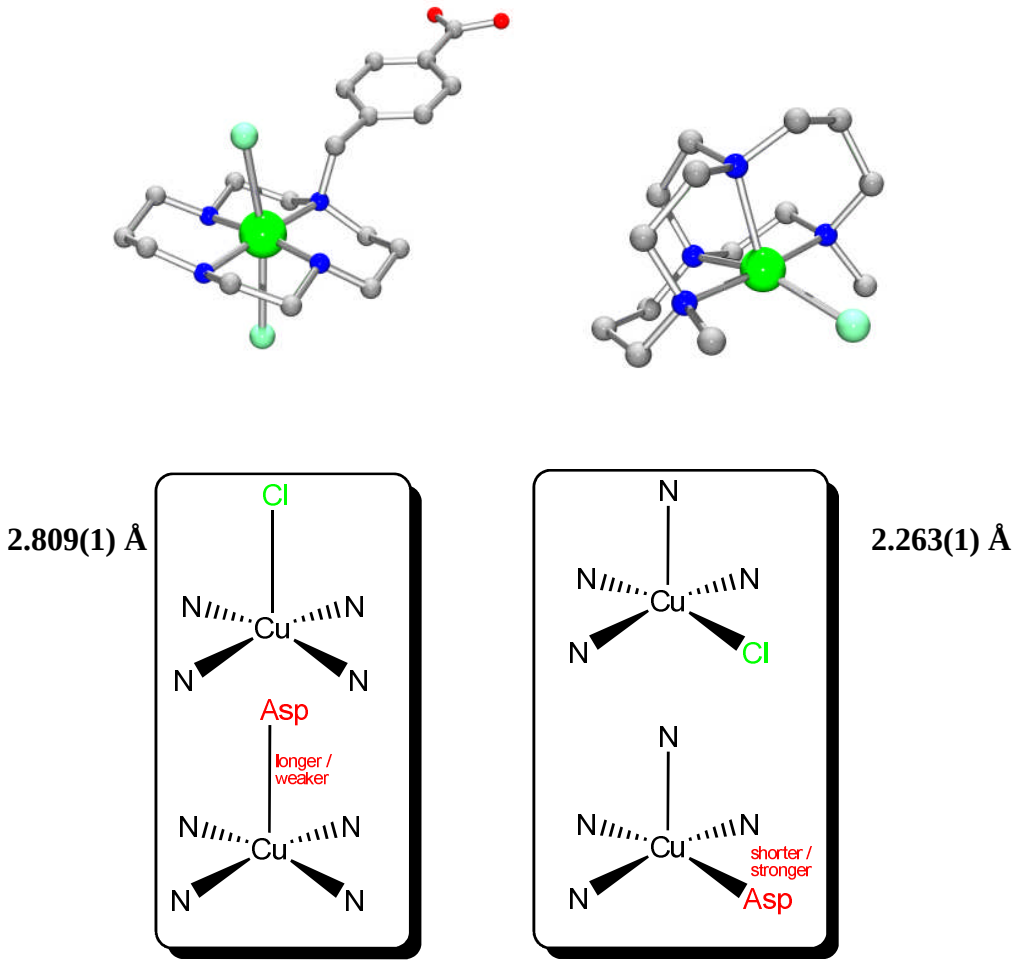

Figure (41). X-ray crystal structures of copper(II) cyclam (left) and cross-bridge (right). Below are copper(II) bonds. Bond lengths shown are Cu-Cl.[277,278]

3.7 CONCLUSION

The importance of residence time in relation to coordination interactions of bicyclam based antagonists has been established. The result of this investigation further supports the theory that a highly active pharmaceutical compound needs not only to have a high binding affinity but also a long residence time. The copper(II) cross-bridged compound $[Cu_2\mathbf{L^2}Cl_2]^{2+}$ has been shown to fulfil these two requirements. Furthermore cross-bridged macrocyclic complexes with copper(II) have been reported to be "ultrastable" in their kinetic stability dissociation (regarding the metal ion binding to the chelator). With these characteristics this compound has the potential to become a lead CXCR4 antagonist in therapeutic applications.

Chapter 4

Fluorescent cyclam derivatives

4.1 INTRODUCTION

An under-represented area is the analytical and diagnostic potential of targeting chemokine receptors such as CXCR4 for imaging applications. Such methodology could be of use in drug discovery for rapid screening of novel antagonist candidates. We have previously reported a rhodamine conjugated small molecule that selectively binds to CXCR4.[235] Direct analysis of the binding of this fluorescent molecule could not be determined due to the non-specific cellular uptake of the rhodamine dye. Here we present an alternative strategy using quantum dots (Qdot). Quantum dots are semiconductor nanocrystals with a metallic core made up of cadmium selenide. A quantum dot has a discrete quantum energy spectrum and will emit light of varying wavelengths. The type of wavelength emitted depends on the size of the core. Qdots have many advantages over standard organic dyes such as long term photostability, water solubility, a large range of absorbance (UV-500 nm), narrow emission bands and essentially no cellular uptake. These quantum dots can be coated with a polymer and biomolecules such as proteins or antibodies can be conjugated to the quantum dot. These biomolecules coated Qdots can be used for cellular and tissue staining, cell tracing and *in vivo* imaging.[279,280]

Qdots have been conjugated to CD5, CD19 and CD45 antibodies and bound successfully to specific cell markers on lymphocytes.[281] Furthermore, a Qdot-antibody conjugate has been used to detect tumour associated carbohydrates (Tn) in breast tumours *in vivo* (Figure (**42**)).[282]

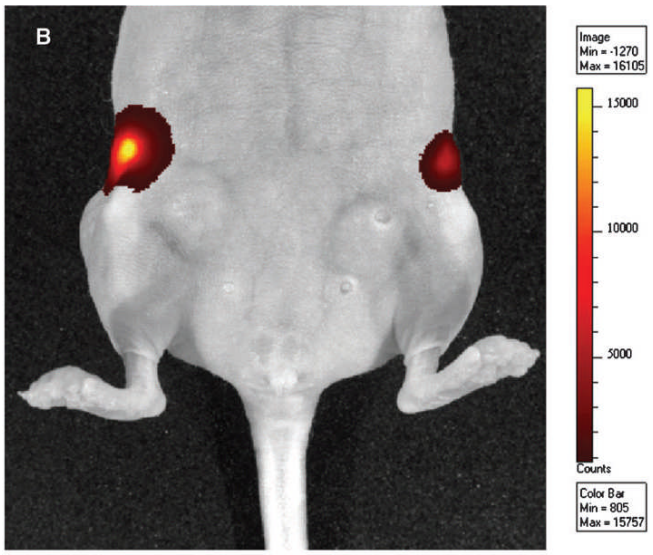

Figure (42). *In vivo* imaging of MCF7 tumor bearing mice. Fluorescent signal captured by IVIS Lumina Imaging System in tumor bearing mice after injection with anti-Tn QDot800-conjugated mAb 2154F12A4. *(Reproduced from Glycobiology)*[282]

4.2 BIOTIN TAGGED CYCLAM DERIVATIVE

A solution of an ethylene bridged zinc(II) cyclam biotin conjugate $[ZnL^{12}]^{2+}$ was prepared in distilled 95% H_2O and 5% DMSO.

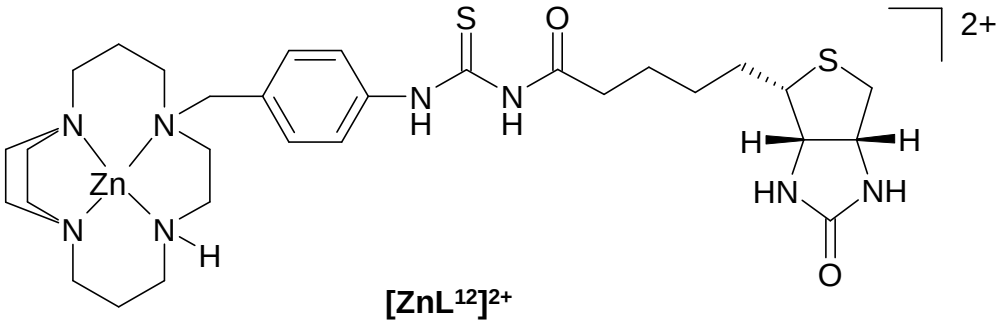

$[ZnL^{12}]^{2+}$

Detection of various biomolecules in tissue can be assayed using the biotin-streptavidin model. Streptavidin a tetramer (52.8 kDa) has a strong affinity (K_d ~10^{-15} M) for biotin and is able to bind four biotin molecules. This can result in an amplification of the signal being detected and is said to be another advantage of using such a model. Furthermore, streptavidin is said to have a neutral ioselectric point and a non-

glycosylated structure (unlike avidin), giving it a lower tendency to bind non-specifically.[283,284]

The strong nature of the interaction of biotin and streptavidin has been used to conjugate fluorescent probes, proteins, antibodies and this model is widely used in biochemical research.[285,286]

A Qdot-streptavidin conjugate has successfully been used to detect glycine receptors on neuron cells using a glycine-biotinylated monoclonal antibody.[287] Moreover, a biotinylated agonist (Bombesin) for the ANG II GPCR was labeled with a Qdot-streptavidin conjugate to detect this receptor in a variety of cancer and epithelial cells.[288]

4.3 CONFOCAL IMAGING

Initially Jurkat cells which are well known to express CXCR4 (A7), were incubated with $[Zn\mathbf{L}^{12}]^{2+}$ (77.6 µM) for 1 hr. Thereafter cells were washed to remove excess $[Zn\mathbf{L}^{12}]^{2+}$ and incubated with Qdot conjugated to streptavidin (655 nm) (1 µM) (Invitrogen, UK) for 30 min. Cells were then washed and analysed by confocal microscopy for binding. The sample was excited at 488 nm and emission was analysed at >600 nm. The images revealed no labeling by Qdot-streptavidin (655 nm) either outside on the membrane or inside the cell.

The results from this initial study suggested either the Qdot-streptavidin molecule was not binding to the biotin, or $[Zn\mathbf{L}^{12}]^{2+}$ was not binding to CXCR4. To answer these fundamental questions further experimental work was carried out.

4.4 BIOTIN-STREPTAVIDIN MODEL

To analyse whether the biotin-streptavidin model worked under these conditions, a two step experiment was devised whereby Jurkat cells were incubated with a CD8 mAb (Jurkat cells known to express the CD8 antigen) for 30 min. Cells were washed and then incubated with a generic biotinylated IgG antibody (30 min) which would bind to the CD8 mAb. The cells were then further incubated with Qdot-streptavidin (565, 585, 605,

655 & 705nm) and Cy5-streptavidin (cyanine dye) (positive control). The binding of both sets of these fluorescent molecules was analysed by flow cytometry (488 nm) (Figures (**43**) and (**44**)). Detection of Qdot-streptavidin 705 nm was attempted at FL-4, 605 and 655 nm at FL-3 and 565 and 585 at both FL-2 and FL-3 channels.

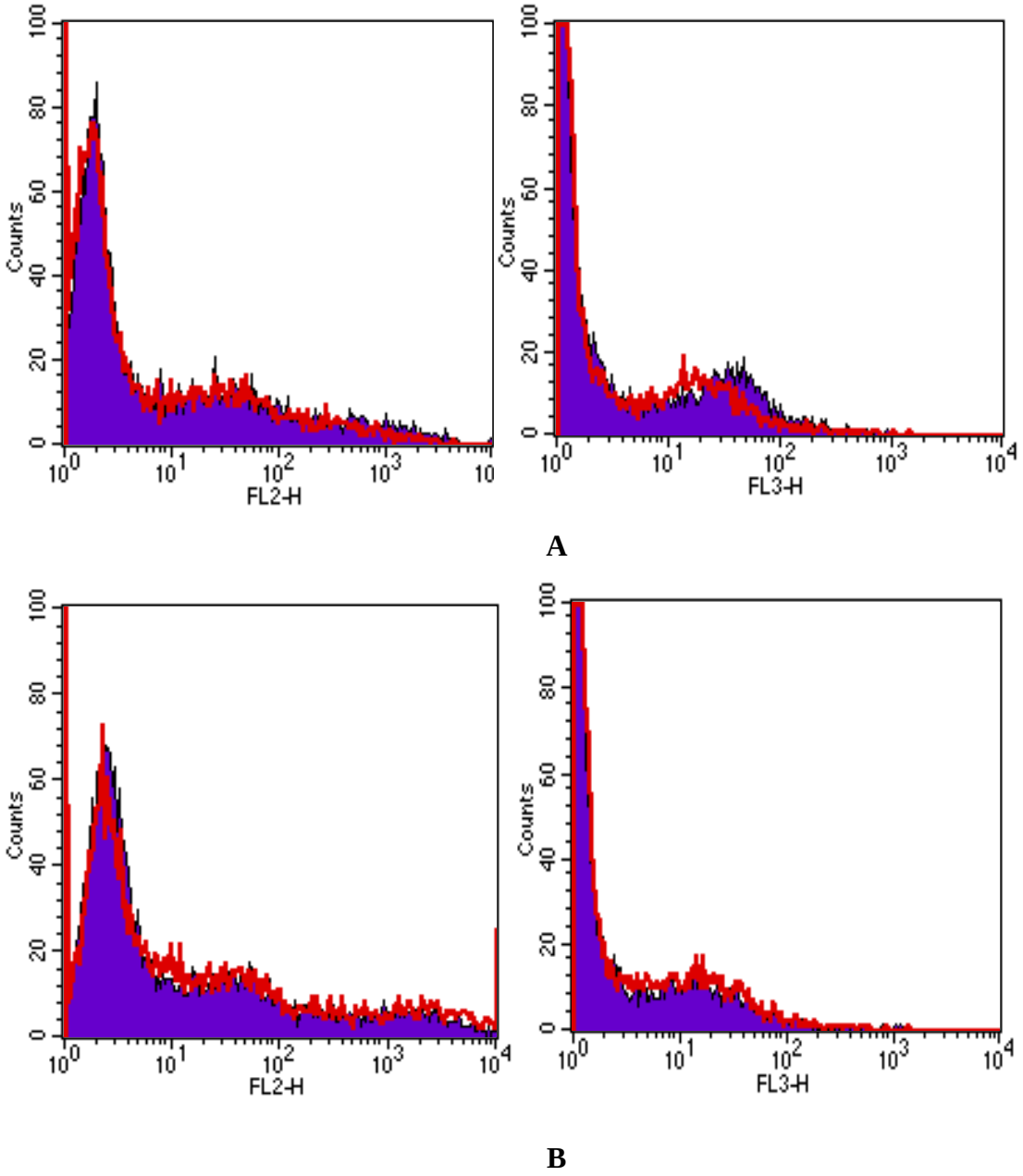

Figure (43). Flow cytometric plots of the binding of Qdot-streptavidin conjugate (A) 565 nm and (B) 585 nm in jurkat cells (red). Purple represents negative control (Plots represent FL-2 and FL-3 channels).

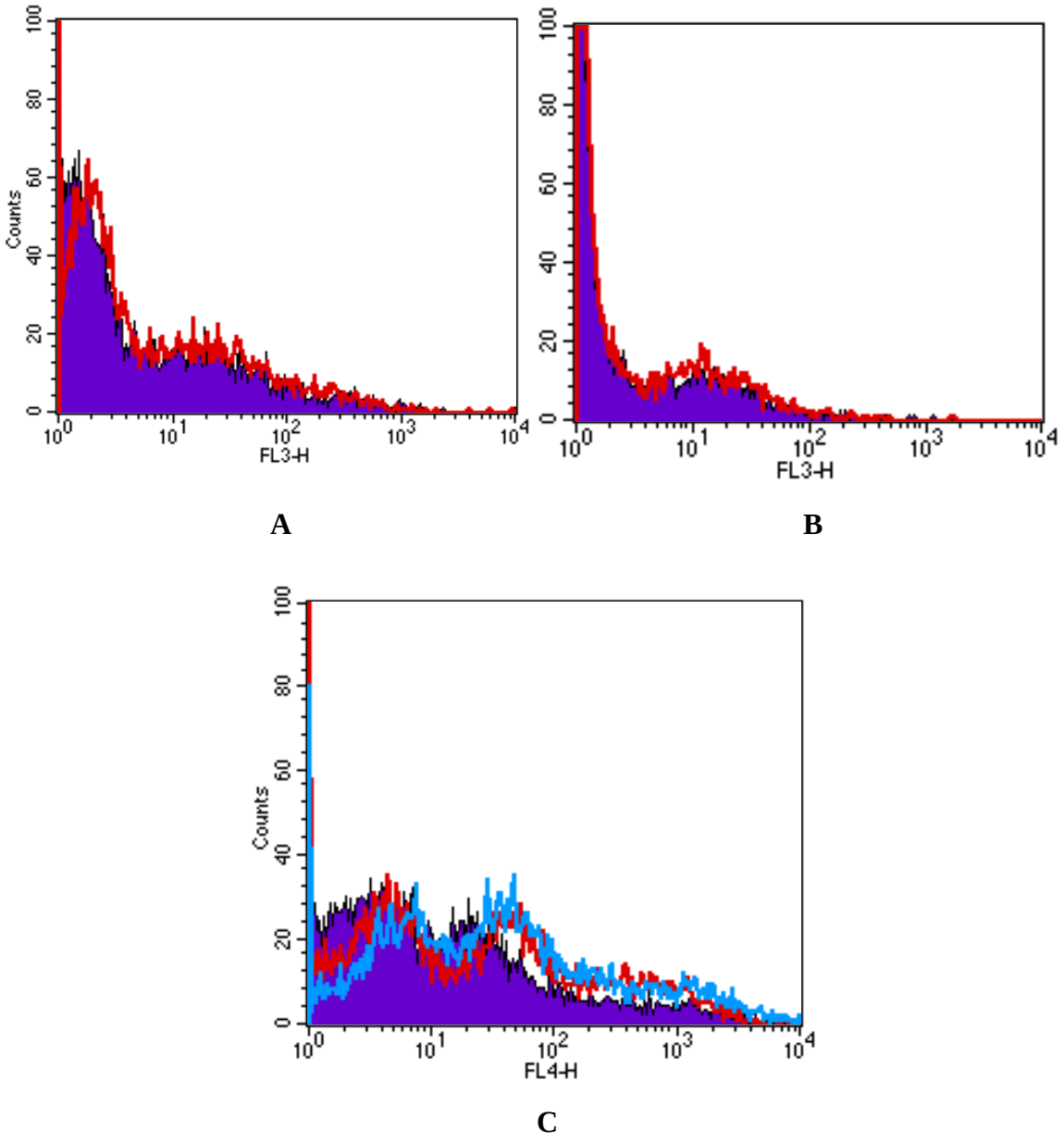

Figure (44). Flow cytometric plots of the binding of Qdot-streptavidin conjugate (A) 605 nm, (B) 655 nm and (C) 705 nm in jurkat cells (red) (blue represents duplicate). Purple (full) represents negative control.

Figures (**43**) and (**44**) show none of the Qdot-streptavidin conjugates were detected. However a 2 log fluorescent shift was detected of the cy5-streptavidin conjugate showing binding (Figure (**45**)).

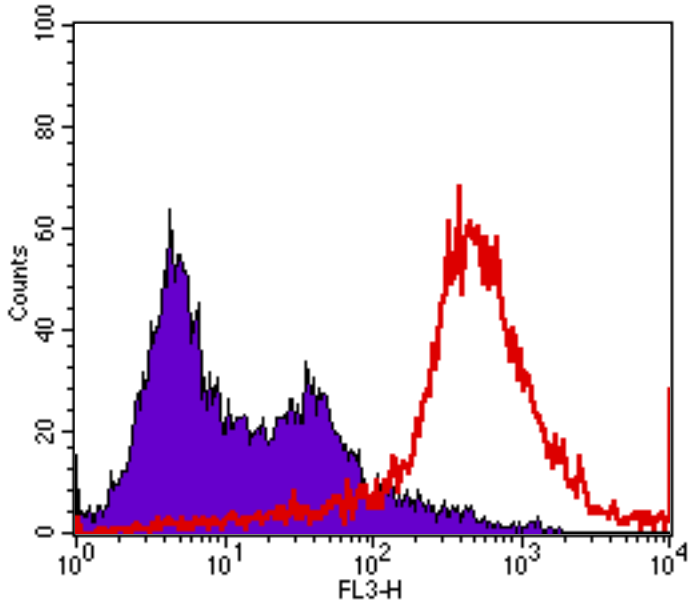

Figure (45). Flow cytometric plot of the binding of cy5-streptavidin conjugate in jurkat cells (red). Purple represents negative control.

The detection of the cy5-streptavidin conjugate suggested the biotin-streptavidin model was successful under these conditions. Although no fluorescence was detected for the Qdots, this did not necessarily suggest they did not interact and bind to the biotin. Another possibility was that the batch of Qdots were not emitting light at the wavelengths expected.

To probe this possibility, the emission spectra of some of the commercial Qdot-streptavidin conjugates were analysed.

4.4.1 Emission spectra of Qdot-streptavidin conjugates

Qdot-streptavidin conjugates 605, 655 and 705 (3.3 nM) were analysed by recording their emission (488-900 nm) spectra, excitation at 488 nm in a fluorescent spectrophotometer set at high sensitivity. Rhodamine B (3.5 nM) was used as a positive control and distilled water as a negative control (Figure (**46**)).

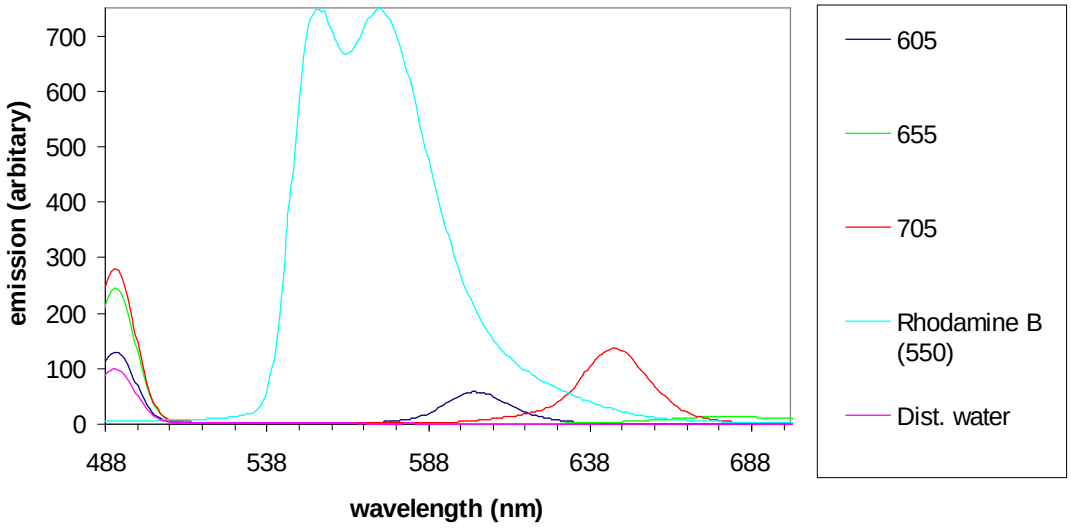

Figure (46). Emission spectra of Qdot-streptavidin conjugate 605, 655 and 705 (3.3 nM) in distilled water (excitation at 488 nm). Rhodamine B (excitation at 550 nm, 3.5 nM) and distilled water used as controls.

The intensity of the emission peak of the Qdots analysed was much lower than expected. All of the Qdots emitted after excitation at 488 nm. The emission of Qdot 605 and 655 near its expected emission band was much lower than would be expected. Furthermore none of the Qdot-streptavidin conjugates had a comparable emission intensity to rhodamine B (Figure (**46**)).

In conclusion, these Qdots-streptavidin conjugates were not emitting with sufficient intensity in their expected narrow emission bands. The Qdots could have degraded on storage prior to being supplied by the manufacturer.

4.5 $[ZnL^{12}]^{2+}$ AND CY5

Taking into account the cy5-streptavidin conjugate had bound and was detected in the previous experiment (Figure (**45**)). $[Zn\mathbf{L}^{12}]^{2+}$ (77.6 µM) was incubated with Jurkat cells for 1 hr. Thereafter cells were washed and incubated with the cy5-streptavidin conjugate for 1 hr. Binding of the cy5 was then analysed by flow cytometry (Figure (**47**)).

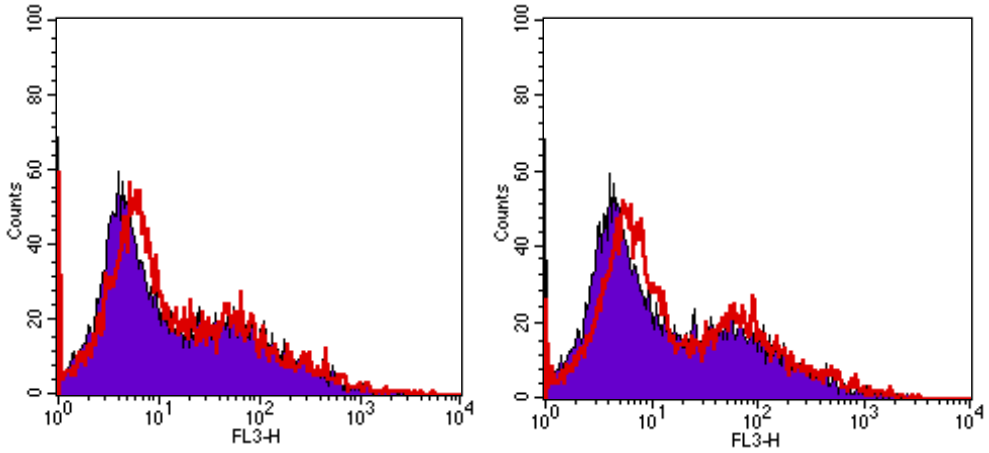

Figure (47). Flow cytometric plot of the binding of cy5-streptavidin and $\mathbf{L}^{3}$ conjugates in jurkat cells (red). Purple represents negative control. (Both plots represent replicates)

Both replicates showed no binding or detection of the cy5 dye. This suggested the possibility that the $[Zn\mathbf{L}^{12}]^{2+}$ cyclam-biotin conjugate was not binding to CXCR4 and thus cy5-streptavidin did not have a site to bind and hence was not detected.

As previously reported, we showed the binding of a fluorescent cyclam CXCR4 antagonist by competing it with CXCR4 specific mAbs.[235] Here we employed the same method to detect the binding of $[Zn\mathbf{L}^{12}]^{2+}$. The only difference in the experiment was the compound contains a zinc(II) ion rather than a copper(II) ion.

4.6 COMPETITION WITH A CXCR4 MAB

Jurkat cells were preincubated with $[Zn\mathbf{L}^{12}]^{2+}$ (77.6 µM) for 30 min. Thereafter the cells were washed and incubated with the anti-CXCR4 specific mAb 44716 at a concentration of 10 µg/ml for 1 hr. Thereafter cells were washed and incubated with an IgG FITC mAb to detect the CXCR4 mAb. Finally the cells were washed and binding of the anti-CXCR4 mAb analysed by flow cytomtery (Figure (**48**)).

In parallel the cy5-streptavidin conjugate was incubated with the anti-CXCR4 specific mAb as in section 4.4 (Figure (**49**)).

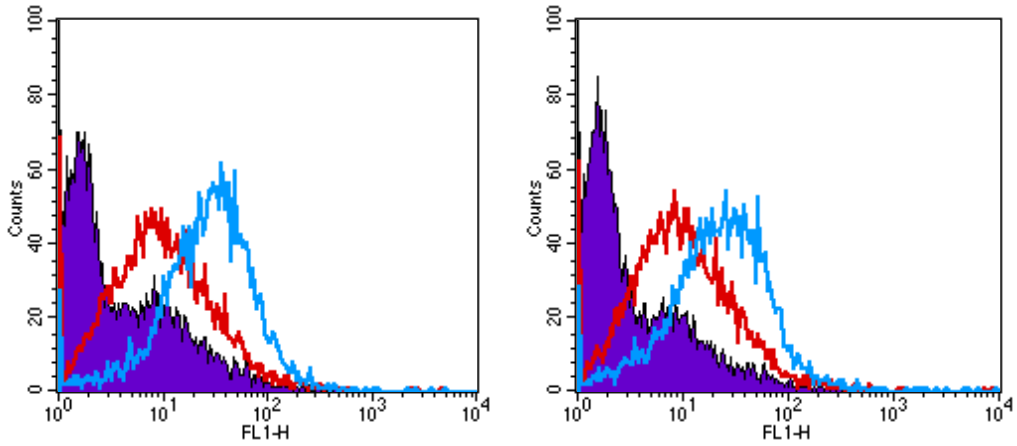

Figure (48). Flow cytometric plots for the binding of CXCR4 mAb 44716 (red, 10 µg/ml) in competition with $[Zn\mathbf{L}^{12}]^{2+}$ (77.6 µM). (-) control (purple) and (+) control 44716 (blue) are shown. Both plots are replicates.

The results show CXCR4 mAb binding to CXCR4 was inhibited to some degree by $[Zn\mathbf{L}^{12}]^{2+}$ (red histogram has shifted towards the negative control) in both replicates. This showed as expected that the CXCR4 specific molecule $[Zn\mathbf{L}^{12}]^{2+}$ was binding to CXCR4. As expected the cy5-streptavidin dye was also detected using the anti-CXCR4 mAb 44716 (Figure (**49**)).

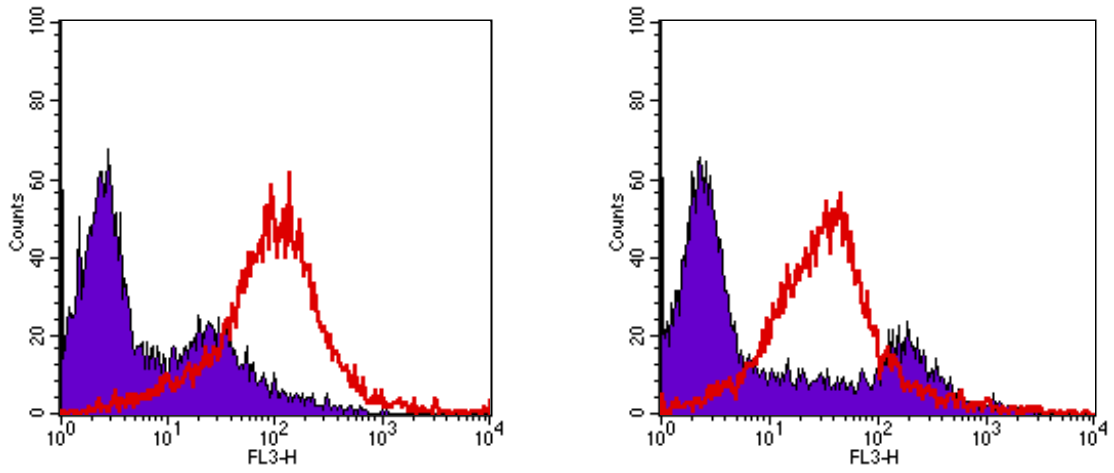

Figure (49). Flow cytometric plot of the binding of cy5-streptavidin conjugate in Jurkat cells (red) using CXCR4 specific mAb 44716 (10 µg/ml). (-) control (purple).

4.7 CONCLUSION

The use of the cy5-streptavidin dye in this study showed a) the biotin-streptavidin model was valid in this system and b) this was a reasonable fluorescent molecule to use instead of the Qdots as no non-specific binding was detected (Figure (**47**)). Qdots are well known to exhibit the desired fluorescent properties (section 4.1) and therefore degradation of the product prior to supply was likely to be the cause for their low activity.

$[Zn\mathbf{L}^{\mathbf{12}}]^{2+}$ was shown to bind to CXCR4 as anticipated, however when $[Zn\mathbf{L}^{\mathbf{12}}]^{2+}$ was incubated with the cy5-streptavidin conjugate, there was no detection of the dye even though other experiments in this study detected the cy5-streptavidin conjugate. The most likely explanation is that although $[Zn\mathbf{L}^{\mathbf{12}}]^{2+}$ binds to CXCR4, $[Zn\mathbf{L}^{\mathbf{12}}]^{2+}$ is deep inside the receptor cavity with the biotin molecule close by. Due to steric hindrance, the much larger streptavidin molecule cannot access the biotin deep inside the cavity of the receptor to bind. This could be addressed by adding a longer linking spacer between the biotin molecule and the metal cyclam complex.

Chapter 5

Migration inhibitory factor

5.1 INTRODUCTION

MIF belongs to the group of proteins known as cytokines. MIF was originally identified as a controlling molecule in the migration of macrophages. However further studies have revealed MIF to be an important regulator of the immune and inflammatory systems.[289] MIF has been described to activate proliferation of T-cells and enhance an immune response by suppressing the activity of steroids which regulate production of cytokines (interleukins).[289,290]

More recently the activity of MIF has been attributed to a number of disease states including arthritis and tumour growth.[289,291] MIF has been shown to increase carcinoma cell proliferation, angiogenesis and may be an autocrine regulator of tumour growth stimuli. However, the regulatory mechanisms and receptor/protein interactions of MIF is not well established. Bernhagen and co-workers have tried to identify the possible receptor interaction of MIF. Their investigation revealed the interaction of MIF with receptors CXCR2 and to a lesser extent CXCR4.[290] This provides the potential for therapeutic targeting of MIF interactions in disease by antagonism of these receptors.

Here we describe an investigation into the binding of MIF to the CXCR4 receptor *in vitro*, with the aim of blocking this interaction with our CXCR4 specific small molecule configurationally restricted bicyclam antagonists.

5.2 MIF AND CXCR4

To investigate MIF binding to CXCR4, recombinant human MIF (rhMIF) was incubated (20-60 mins) with Jurkat lymphoma cells which endogenously express CXCR4. Thereafter an anti-MIF antibody was added which would bind to the rhMIF protein bound to the CXCR4 receptor. Finally a specific IgG-FITC that would bind to the anti-MIF antibody was added and fluorescence was analysed in a flow cytometer.

The histogram plots (Figure (**50**) showed that no additional fluorescence was detected beyond the background cell fluorescence. Therefore bound MIF was not detected in Jurkat cells.

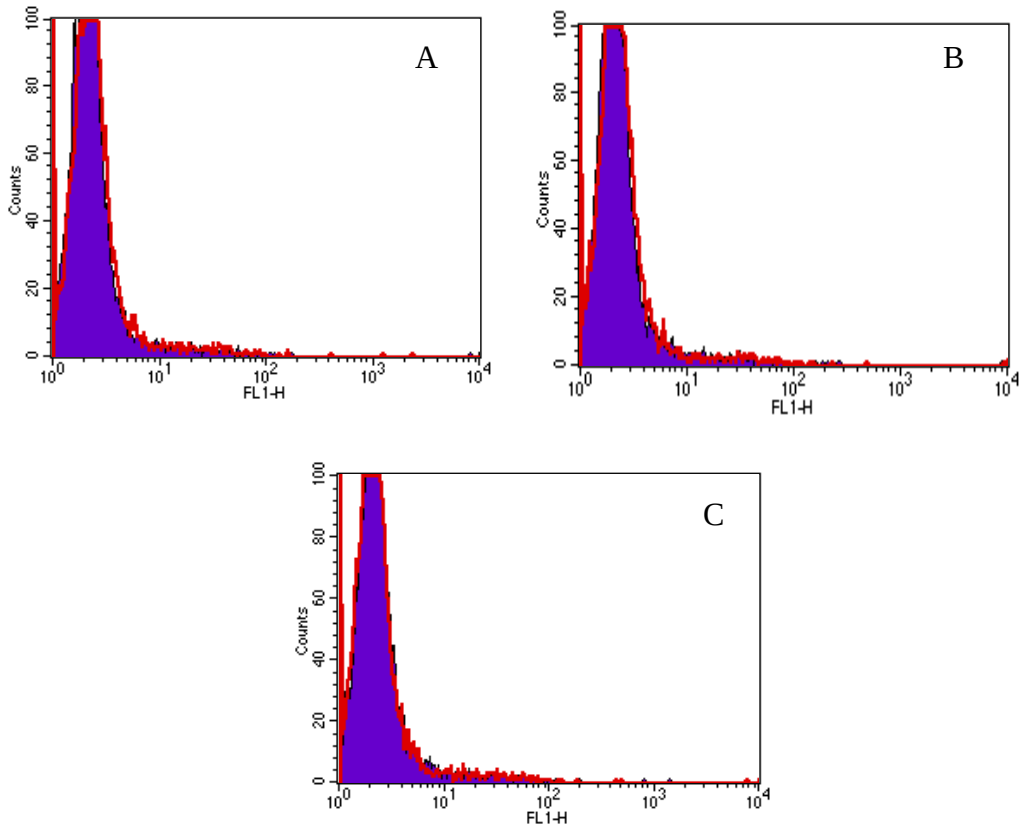

Figure (50). Flow cytometric plots of the binding of rhMIF in Jurkat cells. A) 20 min, B) 40 min, C) 60 min incubation period with rhMIF. (-) control (purple) (cells only) and rhMIF and cells (red) are shown. Plots represent one replicate.

5.2.1 Internalisation of CXCR4 with MIF

Internalisation of chemokine receptors is a common phenomenon with regards to their ligand interaction and signalling pathways.[292] To investigate whether MIF was not being detected directly because of an internalisation reaction with CXCR4, Jurkat cells were incubated with rhMIF for periods of 10-30 mins and 2-4 hrs. Thereafter a CXCR4 specific mAb was added to bind to CXCR4. Bound CXCR4 mAb was then detected using an IgG-FITC molecule and analysed in a flow cytometer. It was assumed that internalisation of CXCR4 would reduce the number of CXCR4 receptors on the cell surface for the CXCR4 mAb to bind to and hence a reduction of fluorescence would be observed.

However the histogram plots (Figure (**51**)) revealed that the fluorescence peaks recorded for all the time periods were the same as the positive control and thus no reduction in fluorescence was observed.

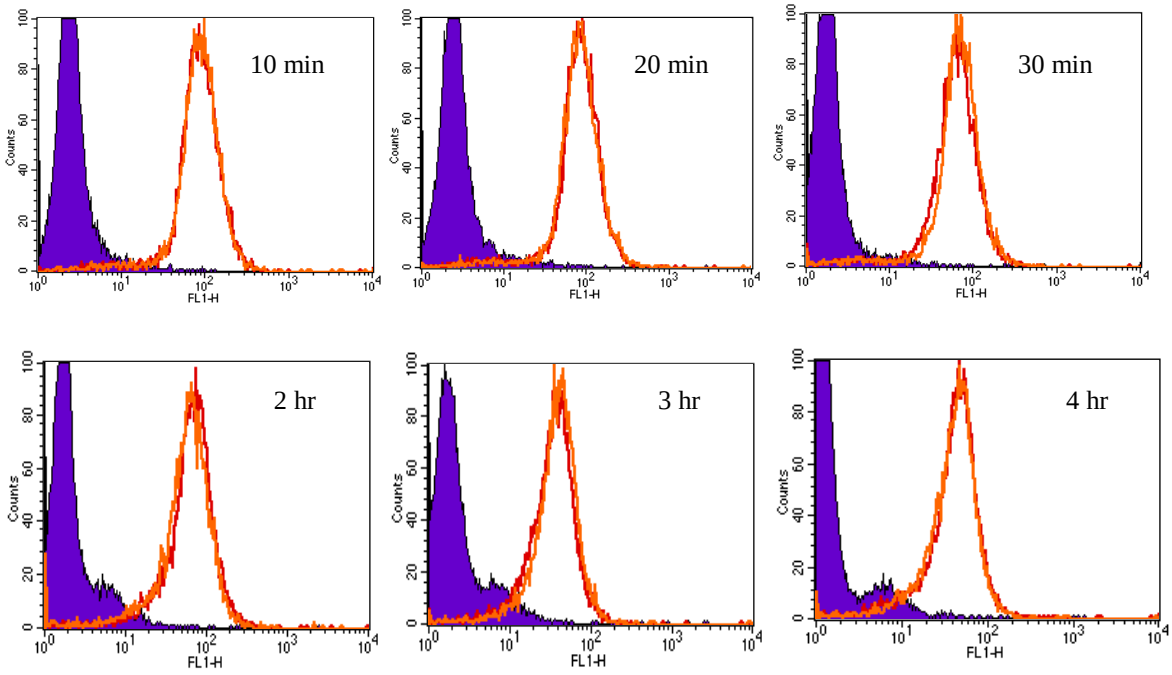

Figure (51). Flow cytometric plots of the binding of CXCR4 mAb (44717) in Jurkat cells after incubation with rhMIF (10-30 min, 2-4 hr). (-) control (purple) (cells only), CXCR4 mAb after rhMIF interval (red) and (+) control (orange, CXCR4 mAb only) are shown. Plots represent one replicate.

5.3 CONCLUSION

The binding of MIF to CXCR4 *in vitro* was investigated. It was found that MIF did not bind to CXCR4 expressed on Jurkat cells and did not appear to interact with any other cell membrane protein present on these cells (Figure. (**50**)). Furthermore a CXCR4 internalisation effect was not observed for MIF (Figure. (**51**)). It was surprising to find that our results contradicted the published work by Benhagen and co-workers even though the same cell line was used and experimental work was carried out in a similar fashion. It should be noted that this is the only published report of MIF binding to chemokine receptors. My work has shown that it is imperative that further research on a

variety of cell lines be carried out to confirm the interaction of MIF with chemokine receptors.

Chapter 6

Cancer therapeutics

6.1 CANCER CELL PROLIFERATION AND APOPTOSIS

Uncontrolled cell proliferation is the primary characteristic of cancer and leads to the invasion of the surrounding tissue forming tumours (tumourigenesis). These tumours can spread to other parts of the body via the lymph or blood circulatory system (metastasis). Arrest of tumour cell proliferation tends to be the ultimate objective of anticancer therapy. While traditional treatments such as chemotherapy, radiotherapy and surgery are available, these have high toxicity, side effects and the long term success of removing the cancer is sometimes questionable. Moreover, once the tumours have metastasised to other parts of the body, it is difficult to control and treat them with traditional treatments described above and this is reflected in the high mortality rate. Thus new approaches are required to complement these existing treatments.[154]

As discussed earlier, CXCR4 has been identified in many cancers and CXCL12 has been found to increase the proliferation of these cancers. Blocking the interaction of CXCL12 has been carried out previously in animal models and *in vitro*, with positive effects.

Here, we have tried to analyse the proliferative activity of CXCL12 in cancer with the potential of inhibiting this with our configurationally restricted bicyclam CXCR4 antagonists *in vitro.* In addition, these antagonists will be investigated to establish any anti-invasion/metastatic effect.

6.1.1 MTS assay

Cell proliferation can be determined by using the standard MTS ((3-(4,5-dimethylthiazol-2-yl)-5-(3-carboxymethoxyphenyl)-2-(4-sulfophenyl)-2H-tetrazolium-salt) method as described previously.[293,294] This method relies on the bioreduction of the MTS into a formazan product by the NADH and NADPH dehydrogenase enzymes in metabolically active cells. The amount of formazan product in solution can be determined by absorbance in the visible region (~490 nm) and is directly proportional to the number of living cells.

Here we employed the same strategy in determining the effect on proliferation after CXCL12 stimulation.

6.1.1.1 *CXCR4 screening*

Using CXCR4 specific antibodies, CXCR4 expression was determined in a range of cancer cell lines available at the Centre for Biomedical Research. This list included colorectal cancer cell lines (HT29, Colo320, CaCo-2), breast cancer cell line (T47-D, MCF-7), ovarian cancer cell line (A2780), lung cancer lines (Corl105, Corl23), melanoma line (A2058) and an osteosarcoma cell line (SJSA). However, only the osteosarcoma SJSA cell line was found to express CXCR4 (Figure (**52**)) in line with published literature.[295]

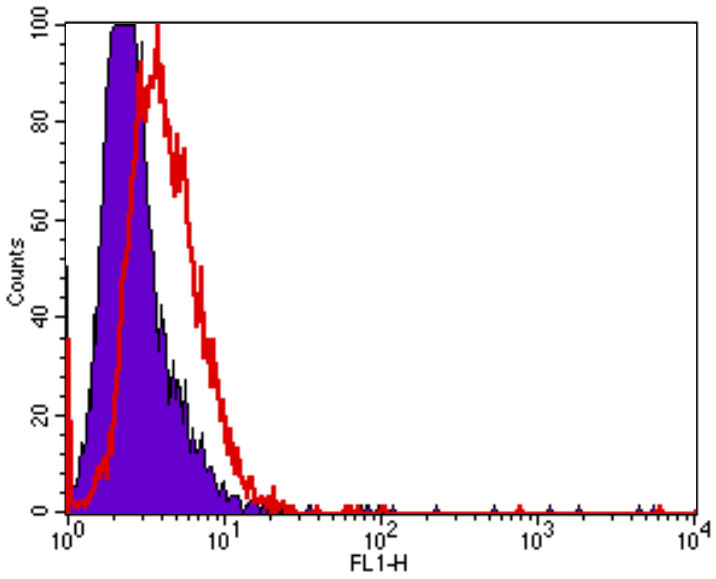

Figure (52). SJSA osteosarcoma cell surface expression of CXCR4 (red). Background fluorescence is also shown (- control).

6.1.1.2 *MTS assay development*

To determine the correct parameters i.e. amount of media, concentration of cells and rate of growth, several preliminary assays were carried out using MTS.

6.1.1.2.1 *Growth in normal media*

Initially two concentrations (1 x 10^4 & 2 x 10^4) of SJSA cells were grown in a 96 well plate over 48 hr in 200 µl of media (Figure (**53**)). The results from Figure (**53**) suggested the cells were stable and displayed proliferation at 48 hr.

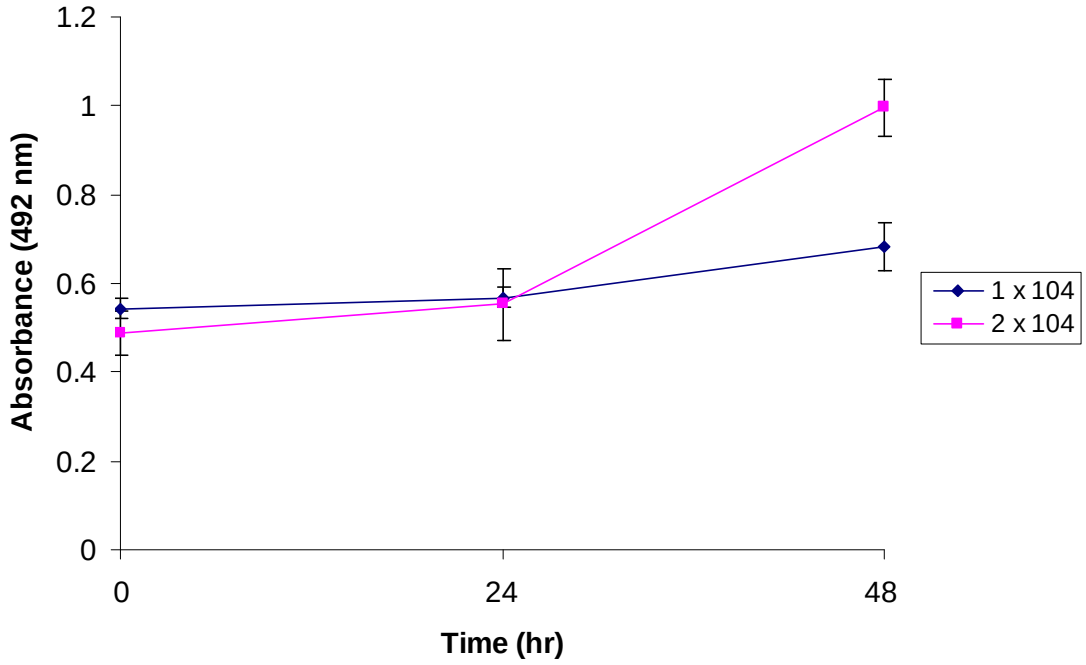

Figure (53). SJSA cell proliferation (MTS assay) using two concentrations of cells (1 x 10^4 & 2 x 10^4) over a 48 hr period. (Error bars represent triplicates)

This was followed by two more cell proliferation assays over a period of 5 days or more (Figure (**54**)).

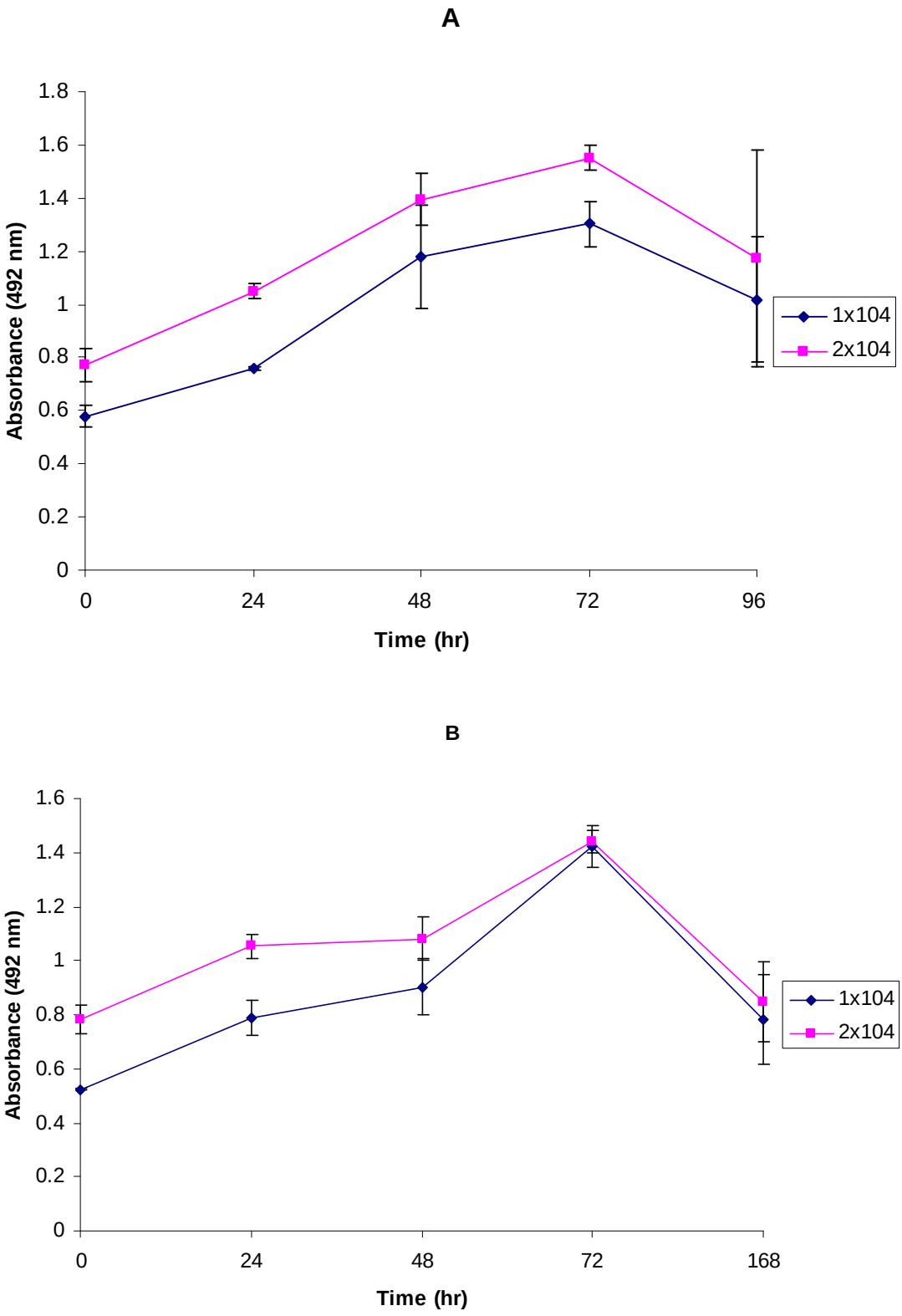

Figure (54). SJSA cell proliferation (MTS assay) using two concentrations of cells (1×10^4 & 2×10^4) over **A)** 96 hr period **B)** 168 hr period. (Error bars represent triplicates)

The results showed the cells were viable under the parameters chosen and the decline of growth occurred after 72 hr. Furthermore both cell concentrations displayed growth over an extended period of time.

6.1.1.2.2 *Growth in serum free media*

Serum deprivation causes cell stress and has been reported to induce cell death in a number of cell types including cancer cells.[132,296] To evaluate the effect on growth of serum deprivation in SJSA cells, the MTS assay was employed using the parameters established above. SJSA cell proliferation was determined in two assays, firstly over 2 days and then secondly over 5 days (Figure (**55a**) & (**55b**)) using 1 x 10^4 cells/well only. Figure (**55a**) and (**55b**) show growth in normal media, however in serum free media rather than a decline in growth there is a stationary phase (0 – 72 hr) with a small increase in viability after 72 hr of incubation (Figure (**55b**)).

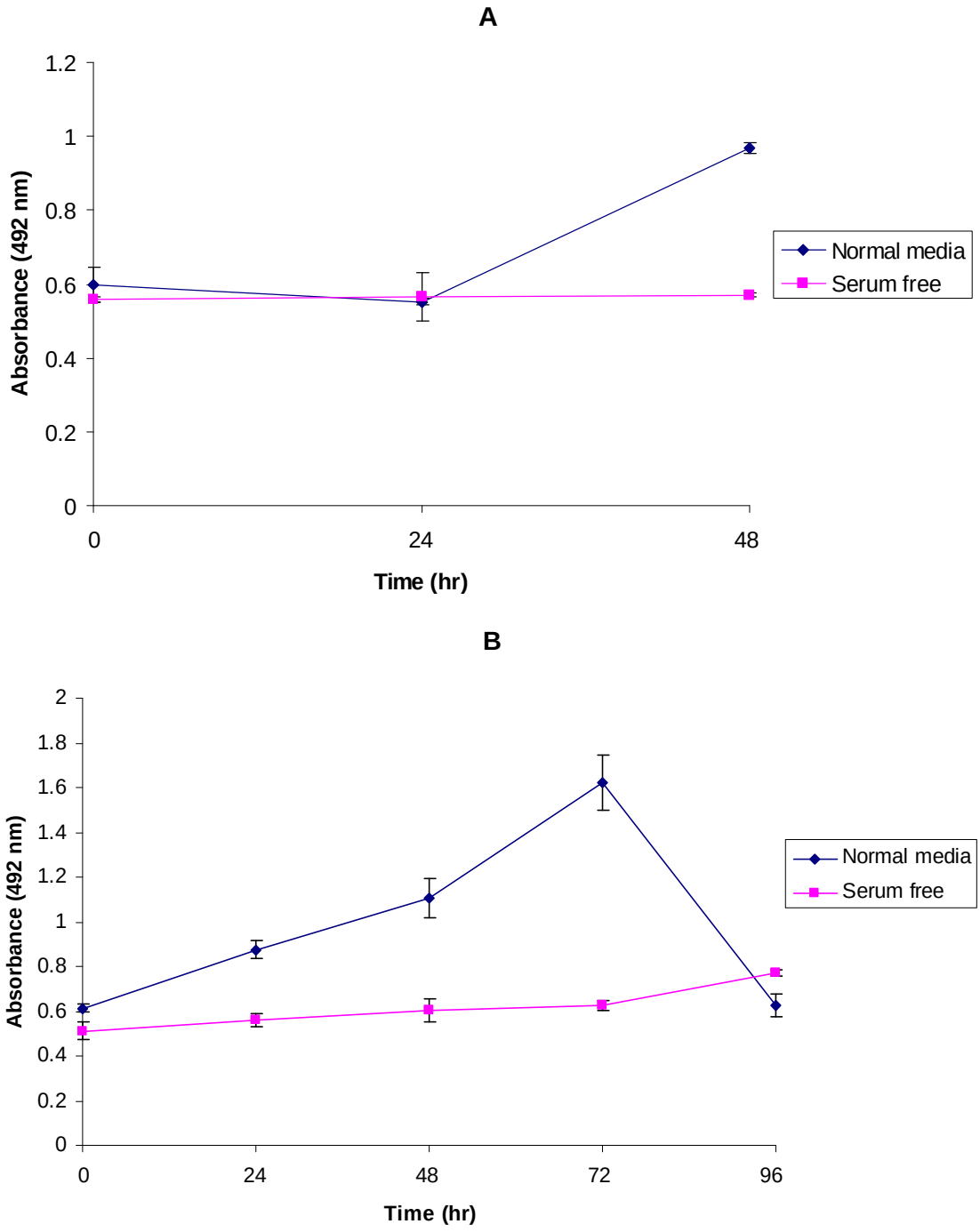

Figure (55). SJSA cell proliferation in normal conditions and with serum deprivation over **A**) 48 hr period **B**) 96 hr period. (Error bars represent triplicates)

This preliminary work showed the MTS assay was a viable model to investigate the proliferative effect of CXCL12.

6.1.1.3 *SJSA proliferation*

Using the parameters established above, SJSA cells with or without serum, were stimulated with CXCL12 (100 & 10 ng/ml) at 0 hr and the growth profile analysed over 96 hrs using the MTS assay (Figure (**56**) (2^{nd} replicate in appendix (A9)). Unfortunately no increase in proliferation was observed with CXCL12 ($p > 0.05$). To mimic the continual concentration of CXCL12 *in vivo*, this assay was performed again with a continual stimulation of CXCL12 (10-100 ng/ml) at every 24 hr interval (Figure (**57**)). Once more there was no significant ($p > 0.0.5$) increase in proliferation of SJSA cells. This suggests SJSA would not be a good model for investigating anti-proliferative effects of blocking CXCL12 signalling, and so other cell lines were investigated.

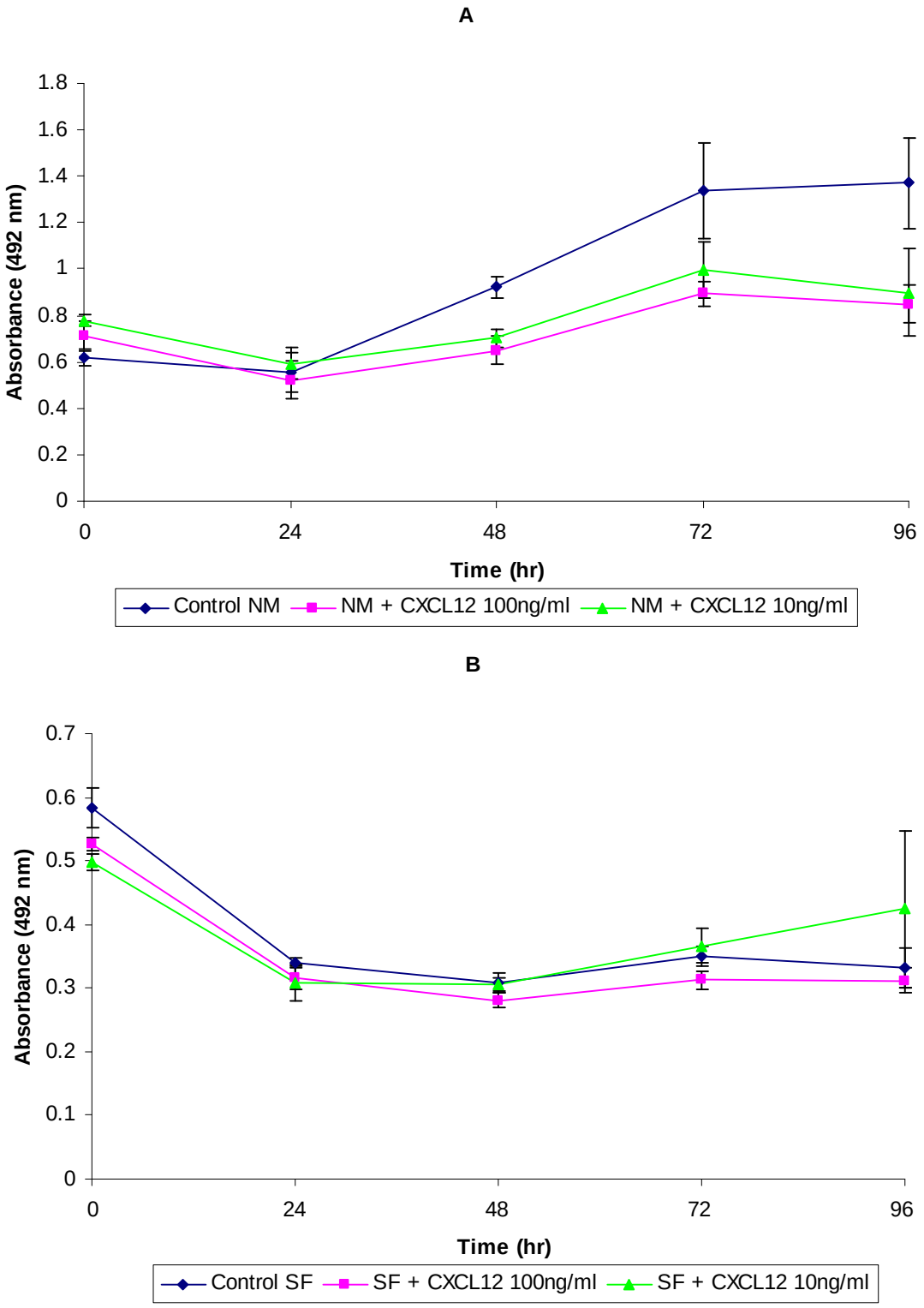

Figure (56). SJSA cell proliferation after CXCL12 stimulation (10-100 ng/ml) in A) Normal media, B) Serum free conditions. (Error bars represent triplicates)

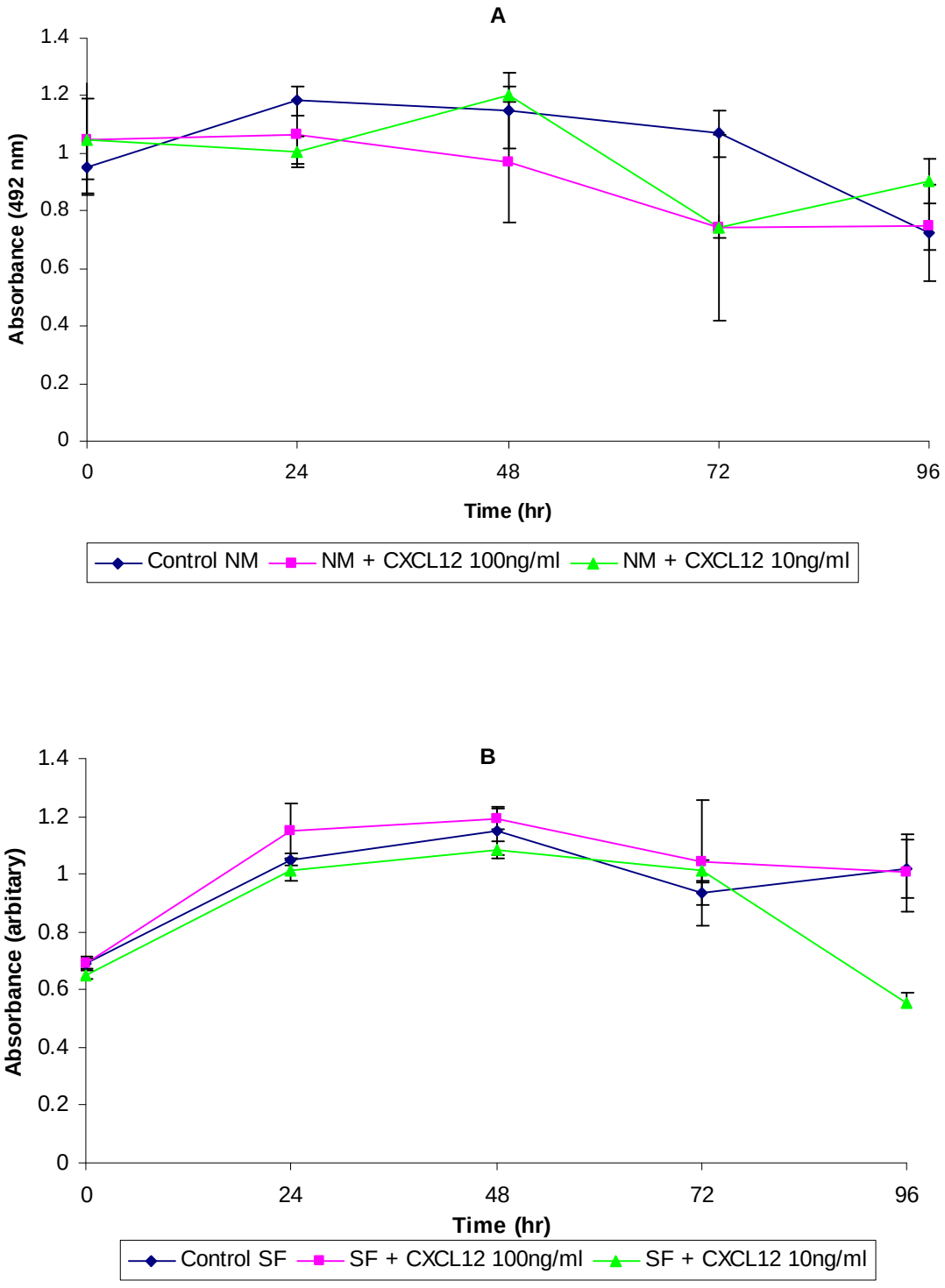

Figure (57). SJSA cell proliferation after CXCL12 stimulation every 24 hrs (10-100 ng/ml) in A) normal conditions, B) serum free conditions. (Error bars represent triplicates)

6.1.1.4 *MDA-MB-231 proliferation*

MDA-MB-231 a breast cancer cell line that has been previously reported to express CXCR4, and therefore this cell line was investigated to establish proliferation activity of CXCL12.[297] Firstly, CXCR4 expression was detected using an anti-CXCR4 mAb (Figure (**58**)).

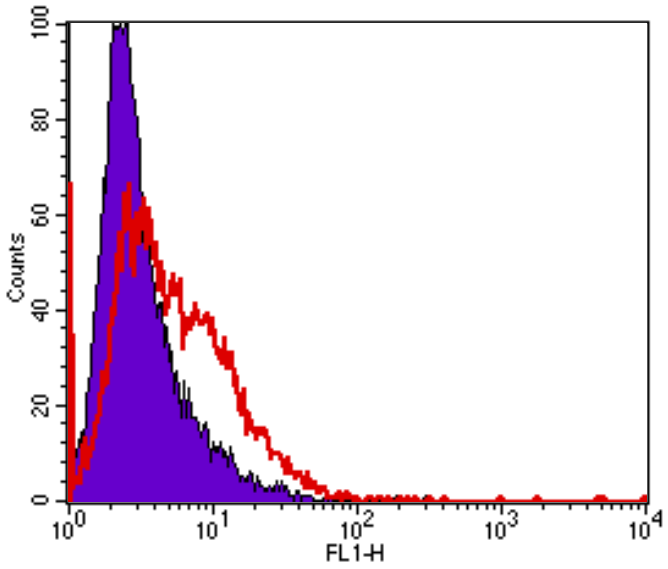

Figure (58). MDA-MB-231 cell surface expression of CXCR4 (red). Background fluorescence is also shown (- control).

The histogram plot revealed a low level of CXCR4 expression on the cell surface, nevertheless this is sufficient to be used in the MTS proliferation assay.

As before a preliminary MTS assay was used to establish the growth profile of MDA-MB-231. MDA-MB-231 cells were grown in normal media and serum free media over a 96 hr period. At each 24 hr interval MTS solution was added and the absorbance recorded (492 nm).

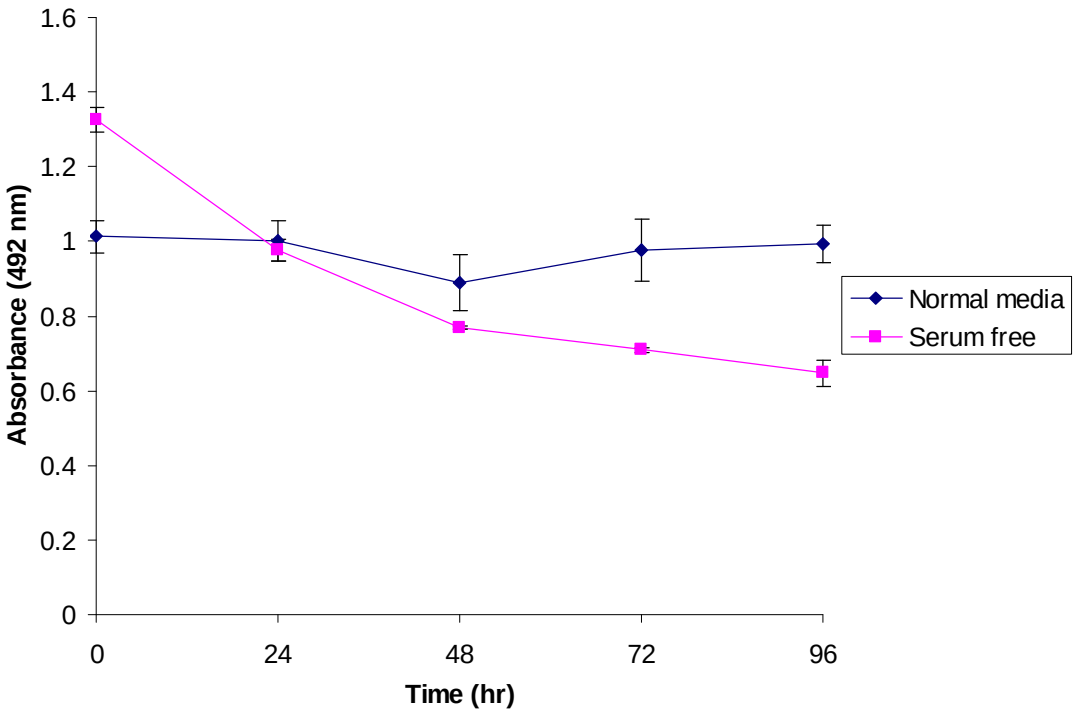

Figure (59). MDA-MB-231 cell proliferation in normal conditions and with serum deprivation over a 96 hr period. (Error bars represent triplicates)

Figure (**59**) shows there is a stagnanation of growth when the cells are in a serum free environment, however more surprisingly there was no significant growth in normal media either. Visual examination of the cell solution under a microscope revealed an increase in the number of cells compared to 0 hr (data not shown).

Although the MTS assay is used as a standard method across the board, this method solely relies on the bioreduction of the MTS solution to give a higher absorbance reading. It is reasonable to suggest that a cell population may have increased in numbers, but may have a lowered metabolic activity and hence may not reduce enough of the MTS product resulting in a higher reading. Thus a different monitoring approach was required which eliminated the need to rely on the metabolic activity of the cells.

6.1.2 CFSE assay

CFSE (carboxyfluorescein diacetate succinimidyl ester) is a fluorescent cell staining-dye. It has commonly been used to detect the movement of cells and proliferation.[298,299] CFSE is highly cell permeable and once inside the cell acetate groups are cleaved by

intracellular esterases to yield a highly fluorescent carboxyfluorescein succinimidyl ester. The succinimidyl ester reacts further with intracellular amines forming fluorescent conjugates and thus this linkage no longer allows the CFSE molecule to diffuse out of the cell. CFSE is retained inside the cell and is not transferred from other cell contacts. In terms of cell proliferation, daughter cells from cell division retain the CFSE cell trace and thus over time as more cell division occurs the fluorescence of the sample population is reduced.

6.1.2.1 *Cancer cell proliferation by CFSE*

To establish the workability of the CFSE assay, some cancer cells were subjected to the CFSE proliferation assay. This preliminary study included the MDA-MB-231 breast cancer cell line and also a further two new cell lines U87-MG (brain) and AsPc-1 (pancreatic). U87-MG and AsPc-1 cells were subjected to CXCR4 screening by a CXCR4 specific mAb and revealed a very low surface expression level of CXCR4 in AsPc-1 cells and no significant expression by U87-MG cells (Figure (**60**)). U87-MG and AsPc-1 have previously been shown to express CXCR4 with a prolilferation increase on CXCL12 stimulation.[137,145]

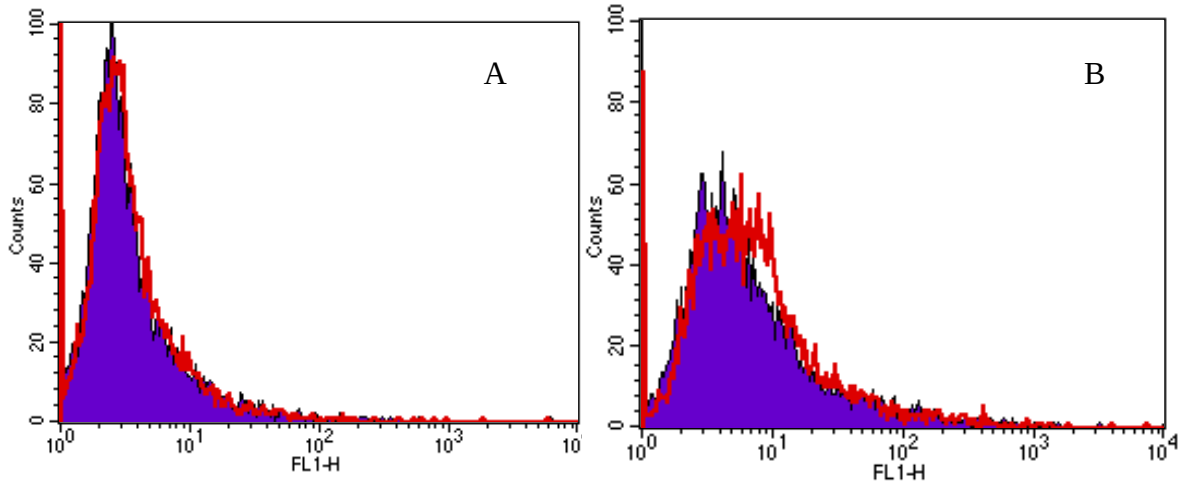

Figure (60). CXCR4 cell surface expression in (A) U87-MG and (B) AsPc-1 cells (red). Background fluorescence is also shown (- control).

All three cell lines were subjected to an initial assay to see whether growth could be detected using CFSE. This was carried out as in the manufacturer's instructions, with the MDA-MB-231, U87-MG and AsPc-1 cells subjected to 12 hrs in a serum free environment. Thereafter, CFSE (5 µM) was added (10 min) and staining quenched by addition of 5 volumes of ice-cold culture media. After centrifugation and extensive washing to remove excess dye, cells where incubated for 3 days to grow. Fluorescence of the cell population was analysed using flow cytometry at day 0 and day 3 (Figure (**61**)).

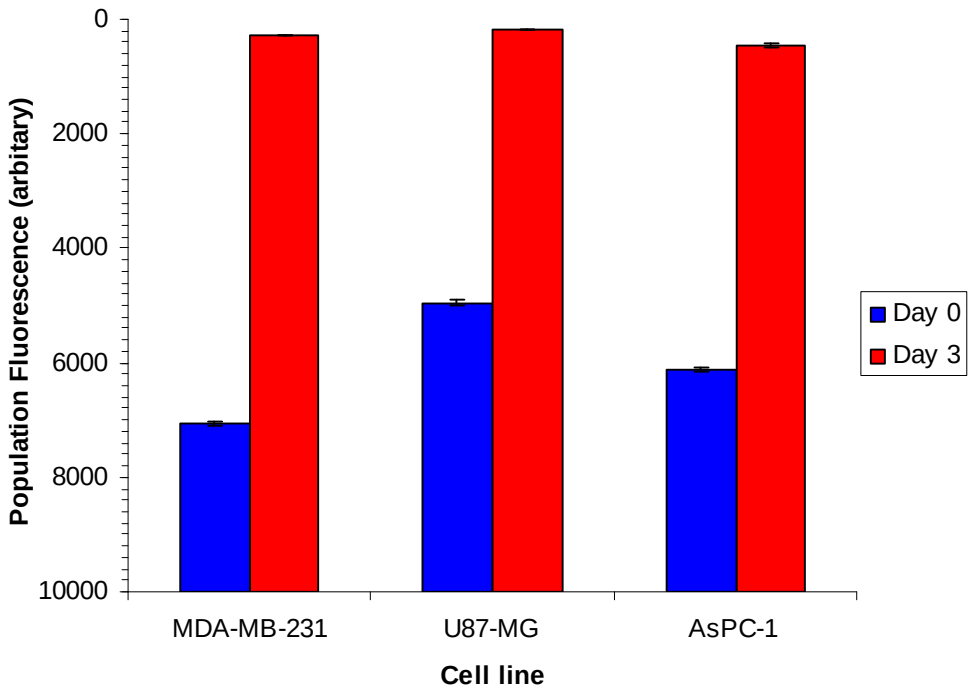

Figure (61). Cell proliferation of MDA-MB-231, U87-MG and AsPc-1 cancer cells over 3 days in normal media. (Data plotted as mean of triplicates)

Analysis of proliferation using the CFSE method was shown to be successful and therefore it was used in further studies.

6.1.2.2 *Effect of CXCL12 on cancer cell proliferation*

All four cancer cell lines, MDA-MB-231, U87-MG, AsPc-1 and SJSA were used to analyse the effect of CXCL12 on their proliferation.

6.1.2.2.1 *CXCL12 stimulation of MDA-MB-231, U87-MG and AsPc-1 cells*

Firstly, three cancer cell lines were subjected to the CFSE proliferation assay as discussed before in section 6.1.2.1, however, with the addition of CXCL12 (100 ng/ml) at day 0 (Figure (**62**))

CXCL12 did not significantly increase proliferation of these cancer cells ($p > 0.05$) (Figure (**62**)). MDA-MB-231 and U87-MG were then subjected to a further study to see if a proliferative effect was initiated with a continual addition of CXCL12 (100 ng/ml) every 24 hrs (Figure (**63**)). However, as can be seen from Figure (**63**) this made no difference to the proliferation rate of these cells ($p > 0.05$).

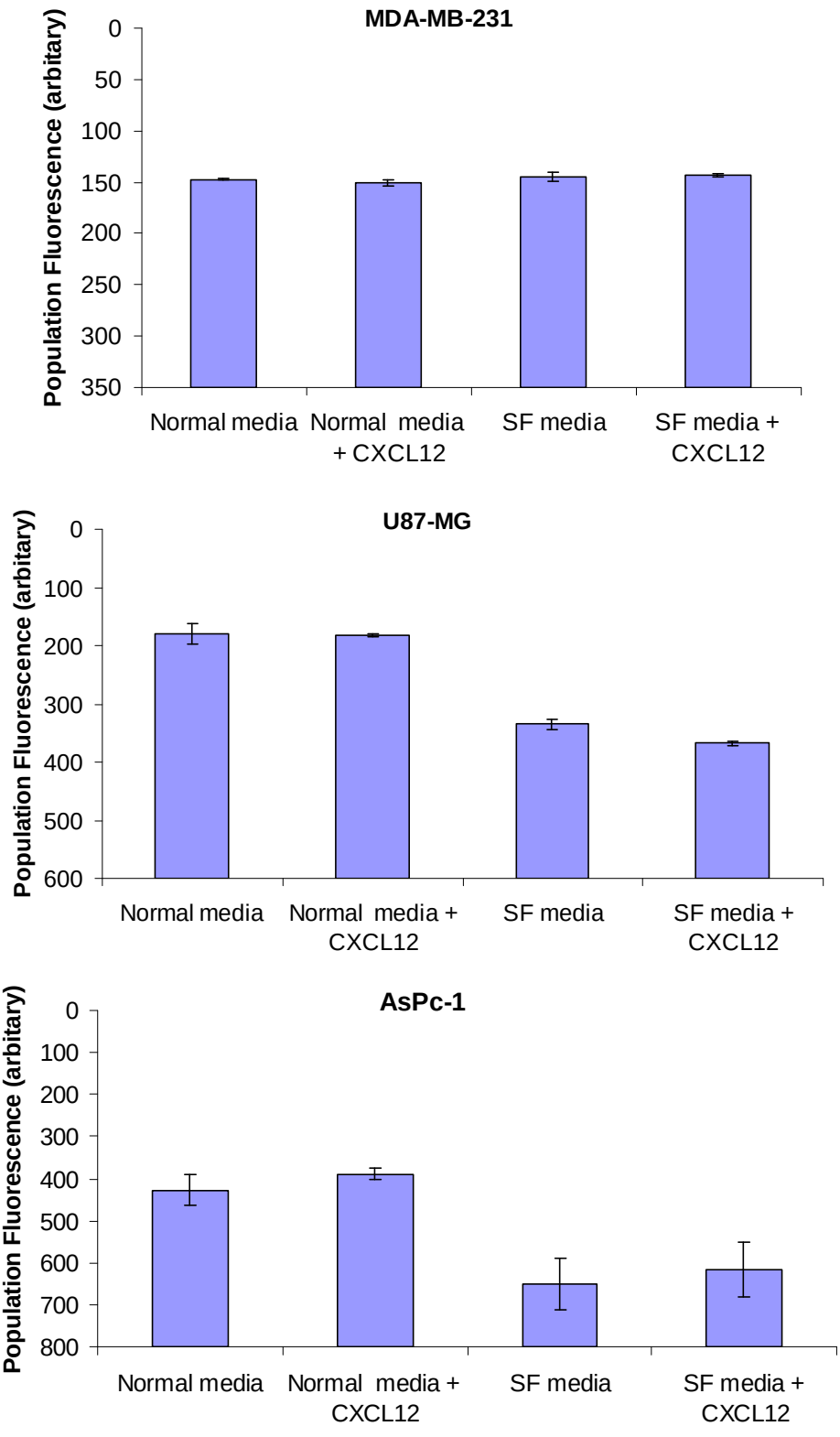

Figure (62). Cell proliferation of MDA-MB-231, U87-MG and AsPc-1 cancer cells after 3 days in normal media and serum free media with CXCL12 stimulation (100 ng/ml). (Data plotted as mean of triplicates)

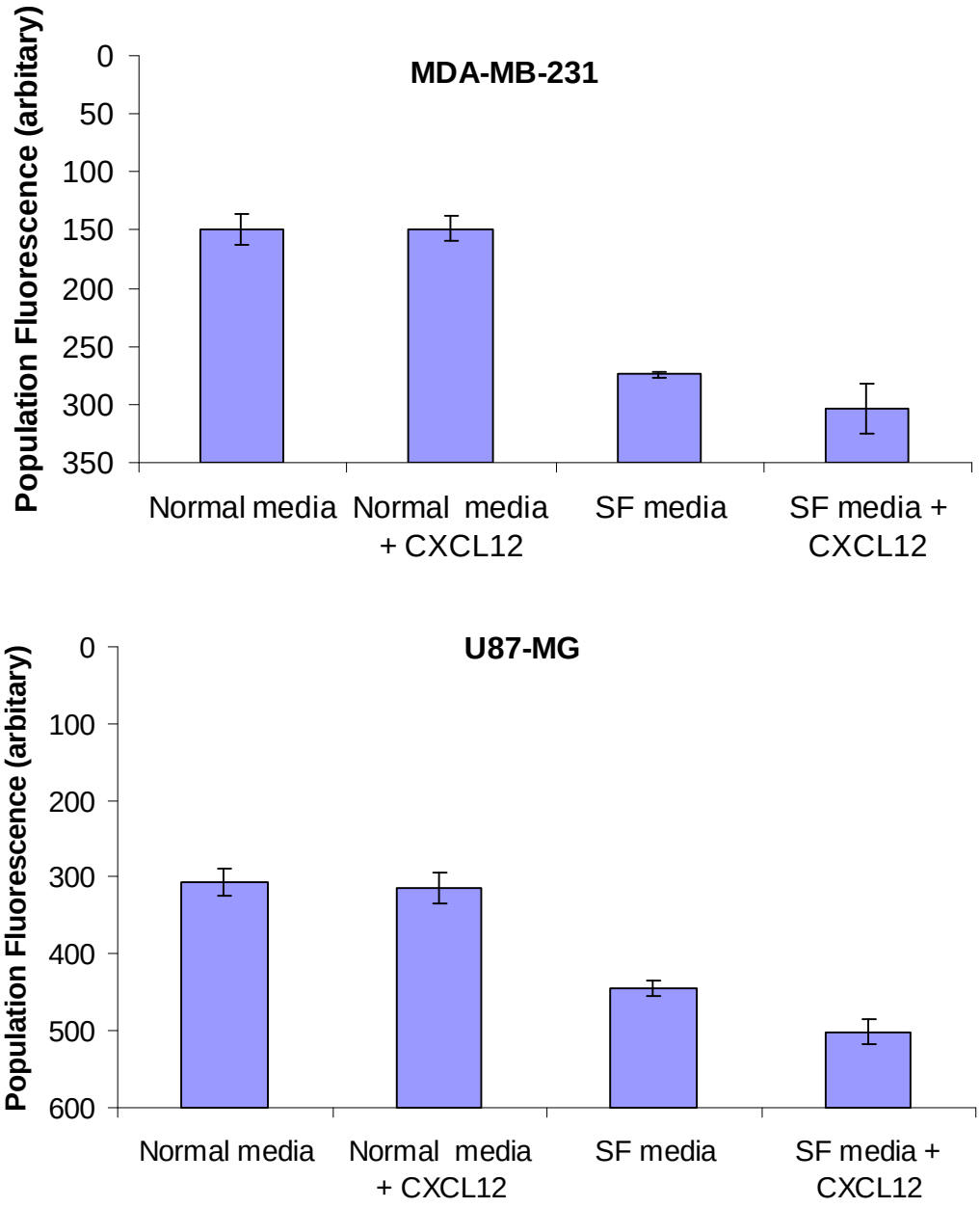

Figure (63). Cell proliferation of MDA-MB-231 and U87-MG cancer cells after 3 days in normal media and serum free media with a continual CXCL12 stimulation every 24 hrs (100 ng/ml). (Data plotted as mean of triplicates)

6.1.2.2.2 *CXCL12 stimulation of SJSA osteosarcoma cells*

In a further study, SJSA cells were also analysed to determine whether CXCL12 could stimulate proliferation using the CFSE proliferation method. As in the case of the other cancer cells, SJSA cells were subjected to an initial stimulation of CXCL12 (100 ng/ml)

at day 0 and also a continual stimulation every 24 hrs over 5 days (Figures (**64**) and (**65**)). Consistent with the other cell lines, CXCL12 did not induce an increase in proliferation in SJSA cells in both sets of experiments ($p > 0.05$).

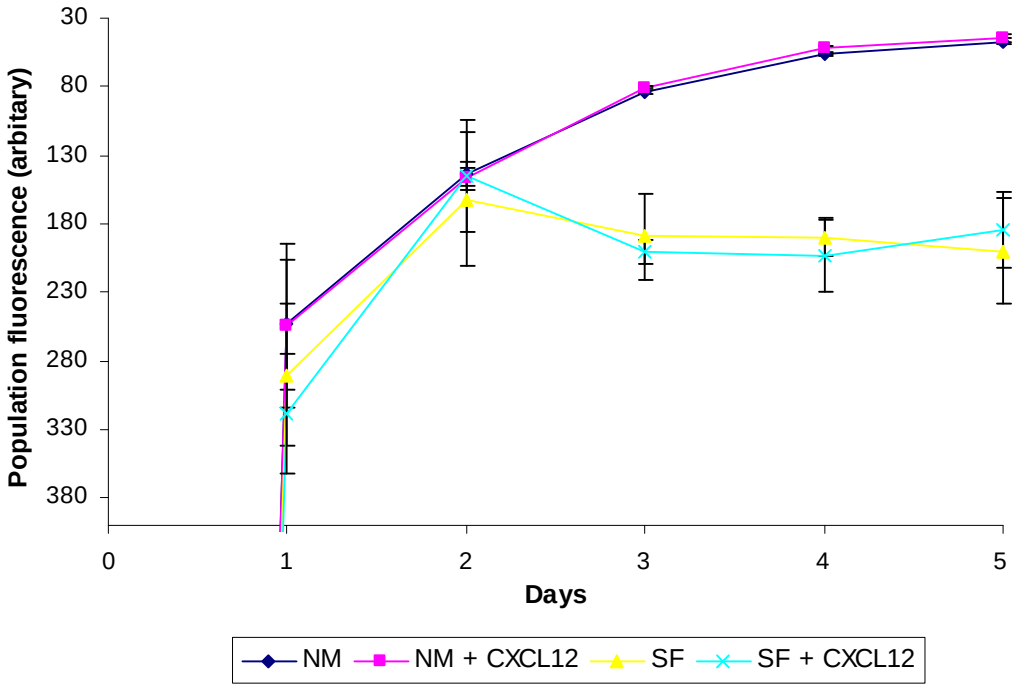

Figure (64). Cell proliferation of SJSA cancer cells over 5 days in normal media and serum free media with CXCL12 stimulation (100 ng/ml). (Each data point plotted as mean of triplicates)

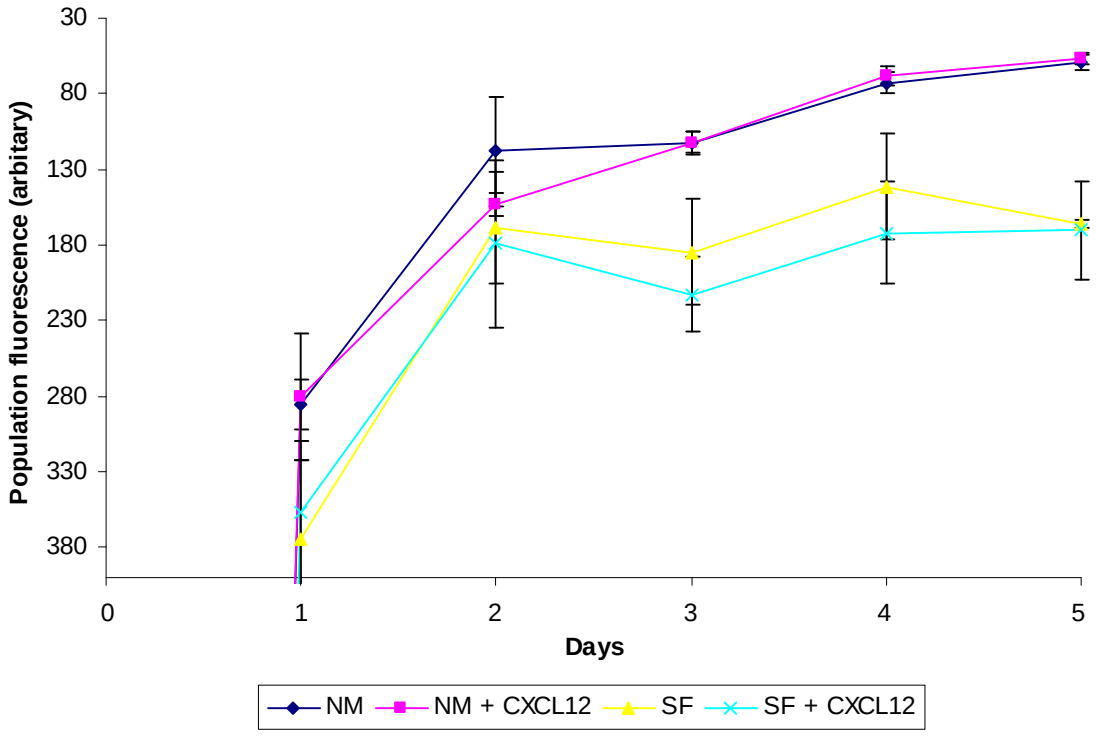

Figure (65). Cell proliferation of SJSA cancer cells over 5 days in normal media and serum free media with a continual CXCL12 stimulation (100 ng/ml) every 24 hrs. (Each data point plotted as mean of triplicates)

In conclusion, an extensive study was conducted using two separate methods investigating the effect of CXCL12 on the proliferation of a number of CXCR4 expressing cancer cells. The CFSE method proved to be a robust, reliable method for analysing cell proliferation. Unfortunately, the investigation revealed low expression of CXCR4 in several cell lines (AsPc-1 and U87-MG) and of the 4 cell lines used, none displayed an increase in proliferation by CXCL12 (section 6.1.2.2). Although some published reports have shown CXCL12 causing an increase in proliferation of these cancer cell lines used here, others have reported CXCL12 causing no effect. CXCL12 (10-200 ng/ml) has been reported to show no effect on MDA-MB-231 proliferation.[297] Furthermore CXCL12 (100 ng/ml) did not effect proliferation of SJSA cells.[295] In addition, the report showing AsPc-1 cell proliferation increase by CXCL12 (100 ng/ml) do not have any error bars on the data shown, and therefore the significance of their data must be put into question (Figure (**66**)).[137]

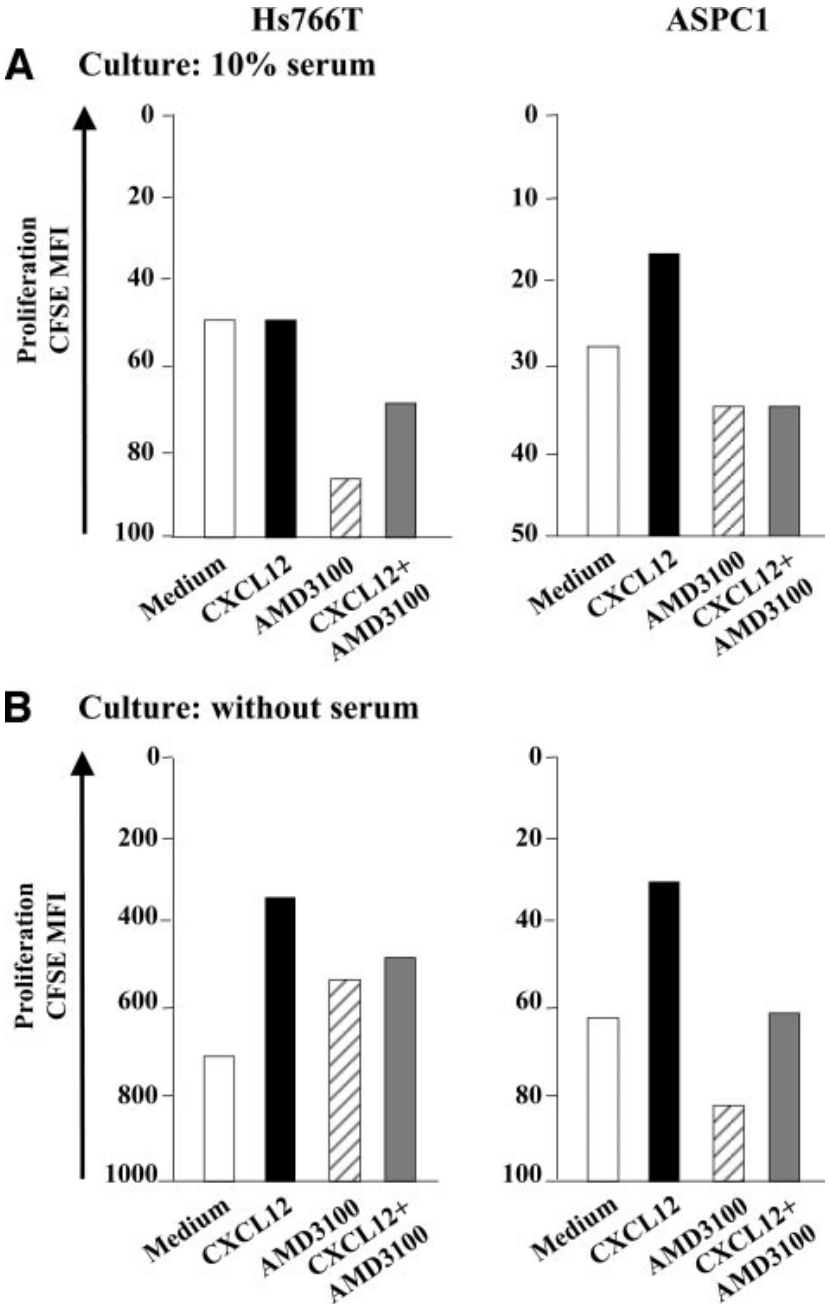

Figure (66). CXCL12 enhances proliferation in Hs766T and AsPC1 cell lines. One representative of three experiments is shown. (*Reproduced from Cancer Research*)[137]

6.1.3 Apoptosis and CXCL12

Apoptosis is a normal cellular event which results in the controlled death of the cell.[300-302] Thus cancer cells can evade or resist apoptosis to prolong their growth. Chemokines have been implicated in assisting cancer cells to resist apoptosis.[24,102,110,118,303] CXCL12 has been reported to have an anti-apoptotic effect in cancer cells, especially when these cells are under stress.[132,137,257] Therefore inhibiting the effect of CXCL12 may assist in a more rapid eradication of the cancer.

6.1.3.1 *Analysing apoptosis*

The appearance of phosphatidylserine (PS) residues (normally hidden within the plasma membrane) on the surface of the cell is a parameter which can be used to detect and measure apoptosis. The presence of PS on the cell surface creates one of the specific signals for recognition and removal of apoptotic cells by macrophages.[300,301] These PS changes can be detected with the anticoagulant, Annexin V, which has a high affinity for binding to PS.[304,305] As the apoptotic process progresses, cell membrane integrity is lost. Using DNA specific viability dyes, such as propidium iodide (PI), it is possible to distinguish between apoptotic and necrotic cells.[306] Here we have used the same method to analyse the apoptotic effect of CXCL12 on SJSA osteosarcoma cancer cells. The ultimate objective is to block any anti-apoptotic effect with our configurationally restricted bicyclam complexes.

6.1.3.2 *Inducing apoptosis*

To analyse any pro- or anti-apoptotic effect by CXCL12, firstly apoptosis was induced using serum deprivation. Analysing for apoptosis or necrosis was carried out using the Annexin-V and PI kit (Serotec, UK) following the manufacturer's instructions. The binding of annexin-V or PI was then analysed by flow cytometry.

To ascertain the correct parameters and settings on the flow cytometer, SJSA cells were taken from a growing culture flask or grown in a 24 well plate cultured for 4 hrs and

22 hrs, followed by addition of annexin-V and PI. Binding of annexin-V or PI was analysed by flow cytomtery. Hydrogen peroxide (100 vol., 30%) (20 µl; 20 min) was added to induce necrosis (Figure (**67**)).

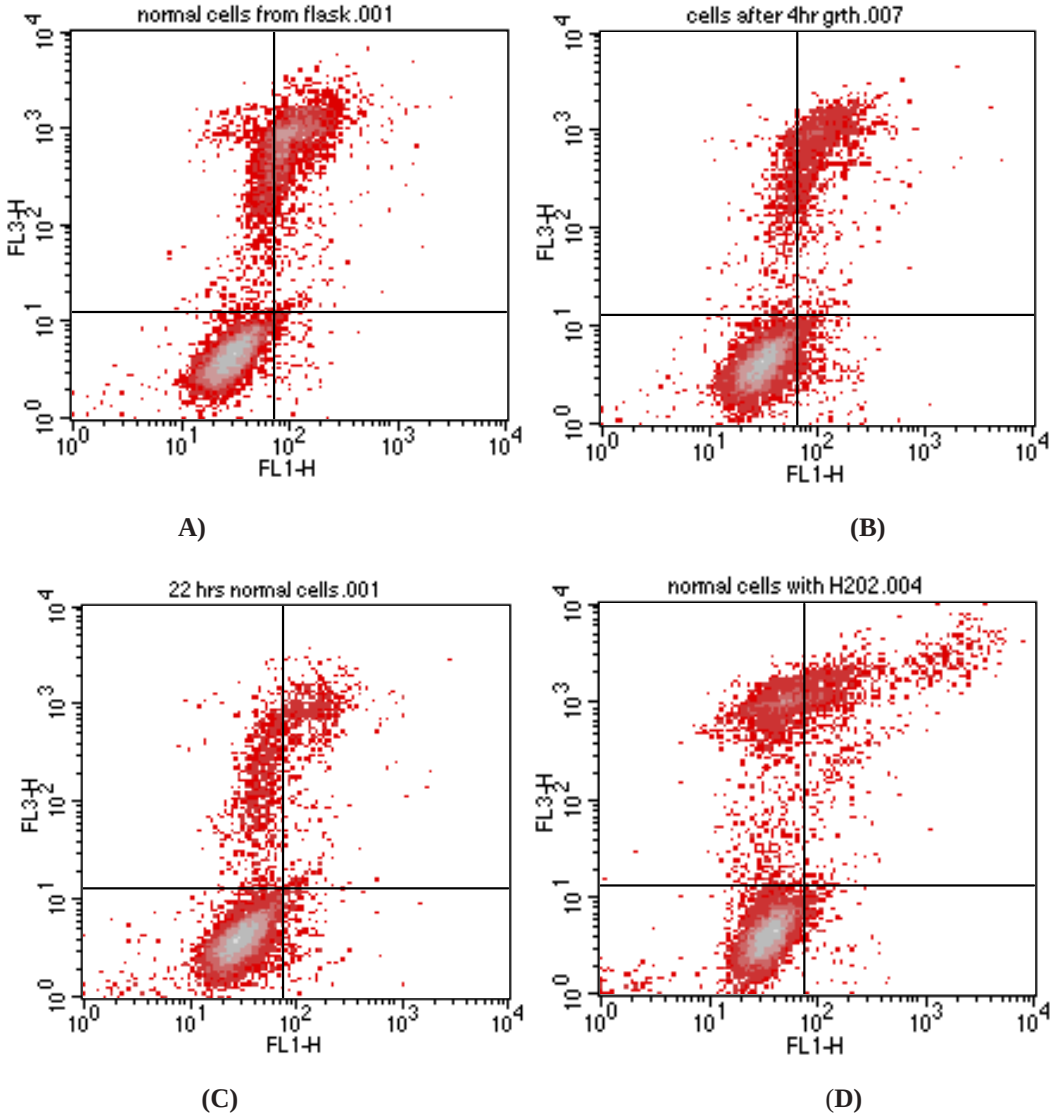

Figure (67). Dot plot of the populations of annexin-V + and PI + SJSA cells under varying growth incubation times (0 (**A**), 4 (**B**) and 22 hr (**C**)) and with hydrogen peroxide (**D**).

Analysis by this method can give three distinct populations. The dot plot can be split into four separate boxes (sections). Lower left box (10^0-10^1) represents viable cells, lower right (>10^1) apoptotic cells (annexin-V) and upper right cells in necrosis.

Here (Figure (**67A,B,C,D**)) we can see only two distinct sets and, although out of alignment, they are a viable and necrotic population. To correctly align the viable population within 10^0-10^1, flow cytometry settings were adjusted.

The results suggested the cells were sufficiently stable growing in a plate (compared with a culture flask). Furthermore, the hydrogen peroxide did not induce sufficient necrosis as there was still a viable cell population (Figure (**67D**)).

Taking into account the information obtained from the above preliminary experiment, SJSA cells were seeded and grown in a 24 well plate for 24 hrs. To induce necrosis, a higher amount of hydrogen peroxide (100 vol., 30%) was added (100 µl) for a longer period of time (30 min). Cells were removed and apoptosis was analysed by flow cytometry (Figure (**68**)).

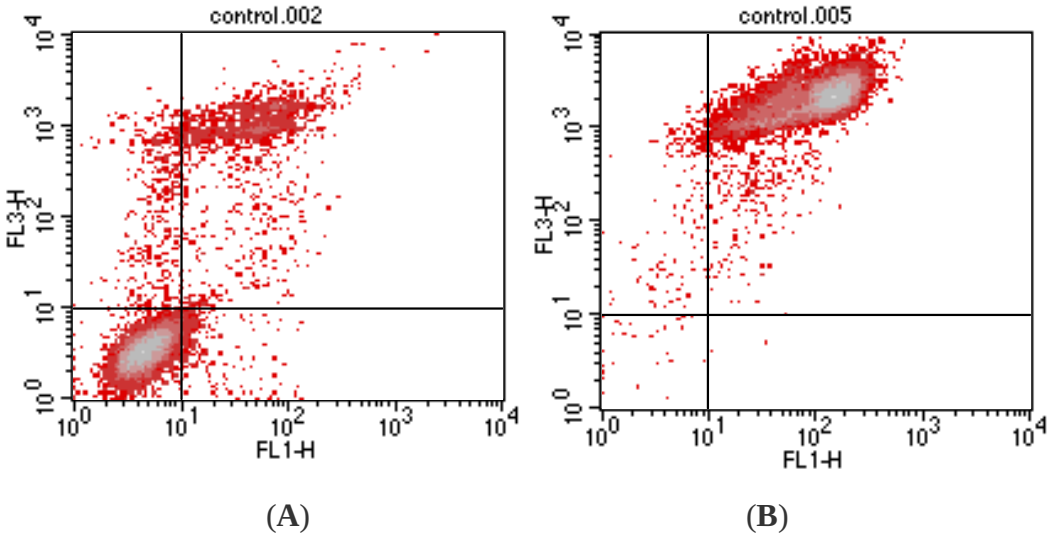

(**A**) (**B**)

Figure (68). Dot plot of the populations of annexin-V + and PI + SJSA cells (**A**) with hydrogen peroxide (**B**)

The results show the flow cytometry settings were correct and the hydrogen peroxide additive was optimised to induce necrosis (Figure. (**68B**)). The average viable and necrotic cell populations were 69.2% (Figure (**68A**)) and 97% (Figure (**68B**)) respectively.

Using this optimised model, apoptosis was induced by serum deprivation. SJSA cells were seeded onto a 24 well plate and cultured for 24 hrs. Media was removed from the cells and then replaced with serum free media and grown for a further 24-72 hrs.

After the relevant incubation time, cells were collected and apoptosis was analysed by flow cytometry (Figure (**69**)).

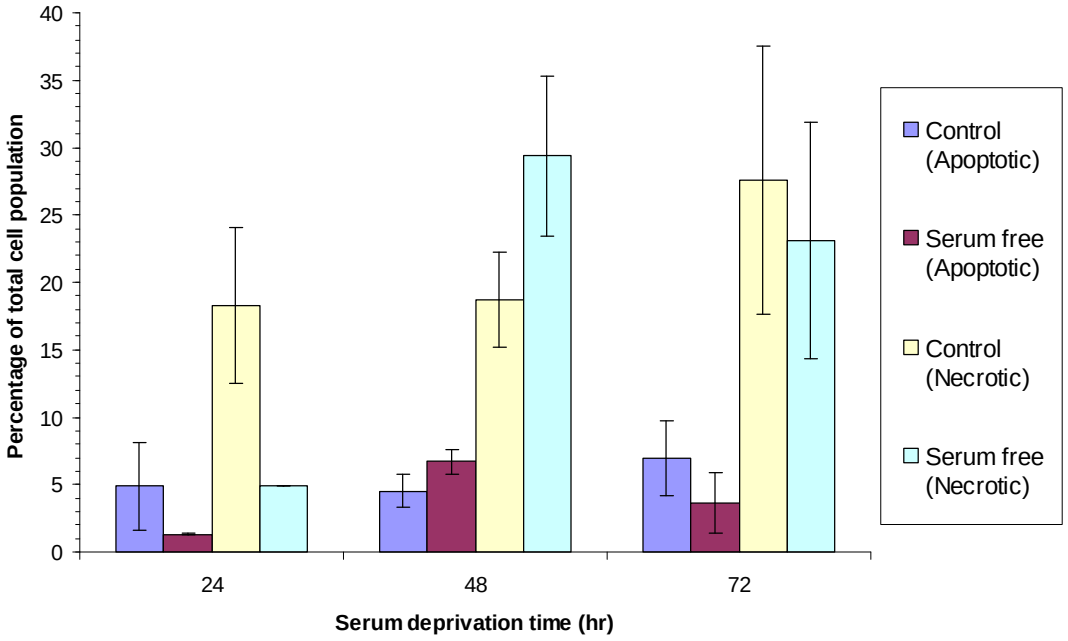

Figure (69). Induction of apoptosis by serum deprivation. (Error bars represent triplicates or duplicates)

Figure (**69**) shows no significant difference (taking into account the error bars) between the cells grown in normal conditions and cells grown without serum over a 72 hr period. At 48 and 72 hr there is an increase in the necrotic population (both control and serum deprived) indicating a rise in dead cells.

To evaluate whether it was possible to induce apoptosis in these SJSA cells, ionomycin was used. Ionomycin is a calcium ionophore and has been previously used to induce apoptosis.[307-309] As before, SJSA cells were seeded and grown in a 24 well plate for 24 hr. The media was replenished, with varying amounts of ionomycin added (4-40 µl; (5 mg/ml)) and further incubated for 24 hr. Cells were collected and apoptosis analysed by flow cytometry (Figure (**70**)). The results show that addition of 4 or 8 µl of ionomycin does not induce apoptosis within a 24 hr period. However, addition of higher amounts of ionomycin (20 & 40 µl) resulted in complete necrosis.

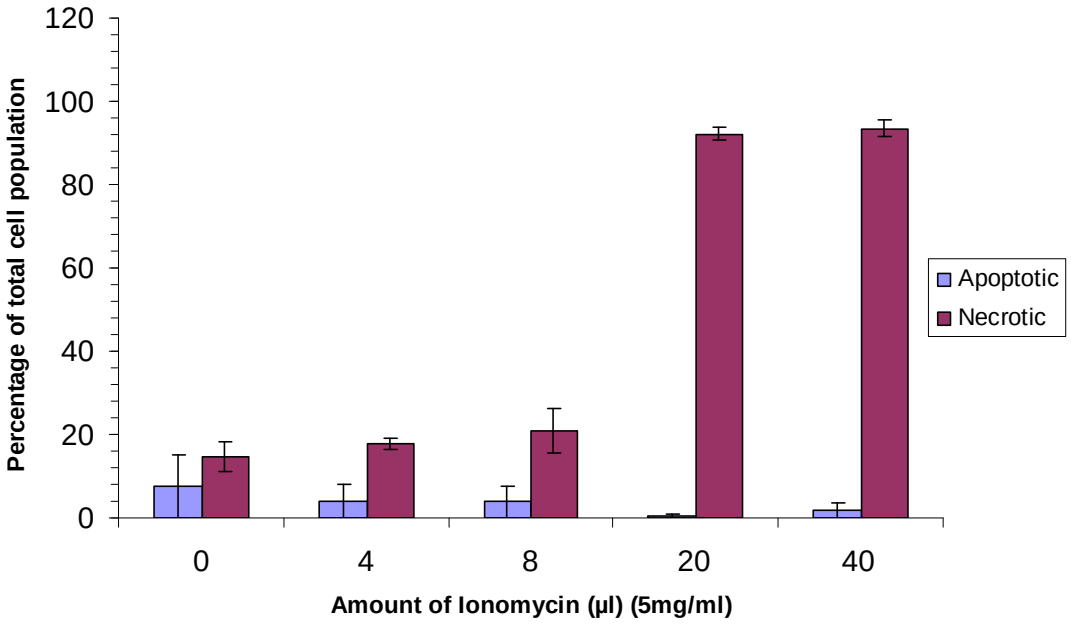

Figure (70). Inducing apoptosis by varying amounts (0-40 µl) of ionomycin (5mg/ml) over a 24 hr period. (Error bars indicate triplicates)

In conclusion, serum deprivation has become a standard method to induce apoptosis, however this was not observed in this study. SJSA cells are an aggressive cancerous cell line and as with most other cancer cells they are able to optimise their growth parameters *in vivo* by evading the normal cell life cycle and inhibiting the process of apoptosis. Furthermore cancer cells are able to resist cell death in extreme environments such as low oxygen (hypoxia) and low availability of essential nutrients. Here we have shown SJSA osteosarcoma cells are able to resist apoptosis in a serum deprived environment.

6.2 CANCER CELL INVASION

The metastatic spread of cancer, which is the growth of cancer cells from a primary site to distant tissues, leads to the uncontrollable growth and spread of cancer. Clinically it is deemed vital to stop this secondary phase in cancer to increase survival.

It has been shown in the previous section (1.2.2.1) chemokine receptors especially CXCR4, are up-regulated in a large number of common cancers to facilitate the growth, survival and metastases of the disease. Binding of CXCL12 to CXCR4 activates key signalling pathways which result in a migratory, proliferative and survival response. Therefore it is not surprising that an array of cancers have been shown to express high levels of CXCR4/CXCL12. Several excellent reviews have discussed in detail the CXCR4/CXCL12 axis in the tumour microenvironment.[110,310]

Many have reported the therapeutic application of neutralising such an interaction in cancer. Mori *et al*. evaluated the growth and invasive potential of human pancreatic cell lines with CXCL12. CXCL12 (100 ng/ml) increased the migratory and invasiveness of these pancreatic cell lines by over 50%. This was inhibited by the use of a peptidic CXCR4 antagonist TN14003 (100 nM).[133]

CXCL12 (3 nM) induced human hepatoma cell invasion into matrigel. The matrigel forms an artificial basement membrane like structure which only invasive cells can penetrate. When pretreated with AMD3100 (12 μM), invasion was inhibited by over 50%.[311] Others report the significance of the CXCR4/CXCL12 interaction in prostate carcinoma. CXCL12 (100 ng/ml) increased the invasion of prostate cancer cells by up to 4-fold and this was inhibited by over 90% on addition of an anti-CXCR4 mAb (1 μg/ml).[135] The treatment of non-small cell lung cancer cell line (A549) with AMD3100 (500 ng/ml) significantly inhibited the increase in invasion by CXCL12 (200 ng/ml) by at least 50%.[312] Furthermore SJSA osteosarcoma cells significantly increased invasiveness through matrigel by addition of CXCL12 (100 ng/ml). This was blocked by pretreating with a CXCR4 mAb (10 μg/ml). *In vivo* analysis revealed coinjection of T134 (CXCR4 inhibitor) with SJSA cells completely prevented lung metastasis formation, both macroscopically and microscopically, in 6 of 6 mice.[295] It is interesting to note many

have attributed the increase in invasion to the up-regulation and production of a number of matrix metalloproteinases following CXCL12/CXCR4 interaction.[135,295,310-312]

Here we describe an investigation into the invasive potential of an osteosarcoma cancerous cell line (SJSA) used previously (section 6.1). Furthermore, the inhibitory effect of our configurationally restricted bicyclam complex on invasion is shown. This was carried out using the standard method of matrigel invasion assay.

6.2.1 Invasion of osteosarcoma cells (SJSA)

6.2.1.1 *SJSA cell invasion with CXCL12*

SJSA cells have been shown previously to express the CXCR4 receptor on their cell membrane (Figure (**52**)). Firstly, an assay was carried out to analyse the invasive potential of this cell line with CXCL12. Following the manufacturer's protocol, SJSA cells (1×10^5) were added to the upper compartment in serum free media with varying concentrations (0-100 nM) of CXCL12 as a chemoattractant in the lower compartment again in serum free media. The cells were allowed to invade for 48 hrs in a 37^oC 5% CO_2 atmosphere. Thereafter cells on the upper compartment were scraped off to leave the cells that have invaded through the matrigel on the lower side of the matrigel filter. Serum (FBS, 10%) was used as a positive control. The filter was then stained with crystal violet (0.5%) and the number of cells per field of view (FOV) at x40 objective was counted. Five different FOV were counted per filter, averaged and plotted as the number of cells invaded per FOV. One FOV was photographed per filter.

Figures (**71**) and (**72**) show the invasion of SJSA cells *in vitro* and the stimulatory effect of CXCL12. SJSA cells invaded in serum free media even without a chemoattractant. CXCL12 caused a significant increase (over 300%) in invasion with the same degree at all concentrations (12.5-100 nM) ($p < 0.01$) (Figure (**71**)).

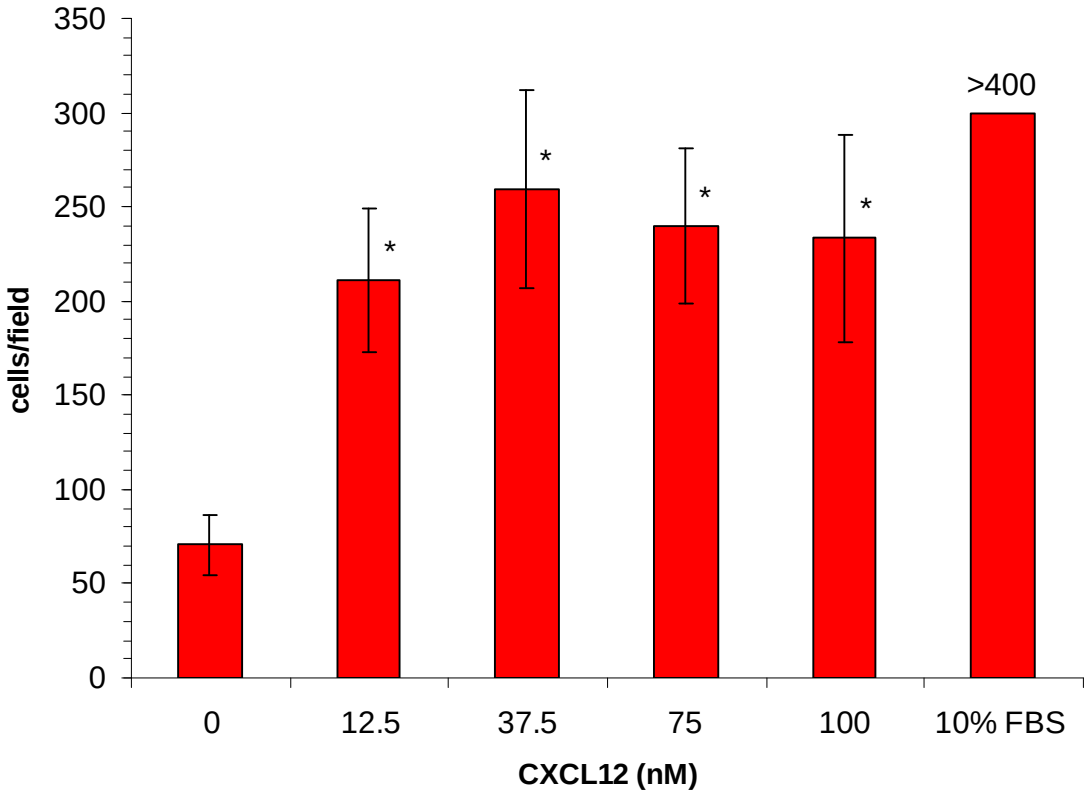

Figure (71). Invasion of SJSA cells in matrigel with CXCL12 (0-100 nM). Cells were counted in five different fields (x40 obj) in duplicates. Mean of the values plotted. Asterisk shows significance ($p < 0.01$) from CXCL12 (0 nM).

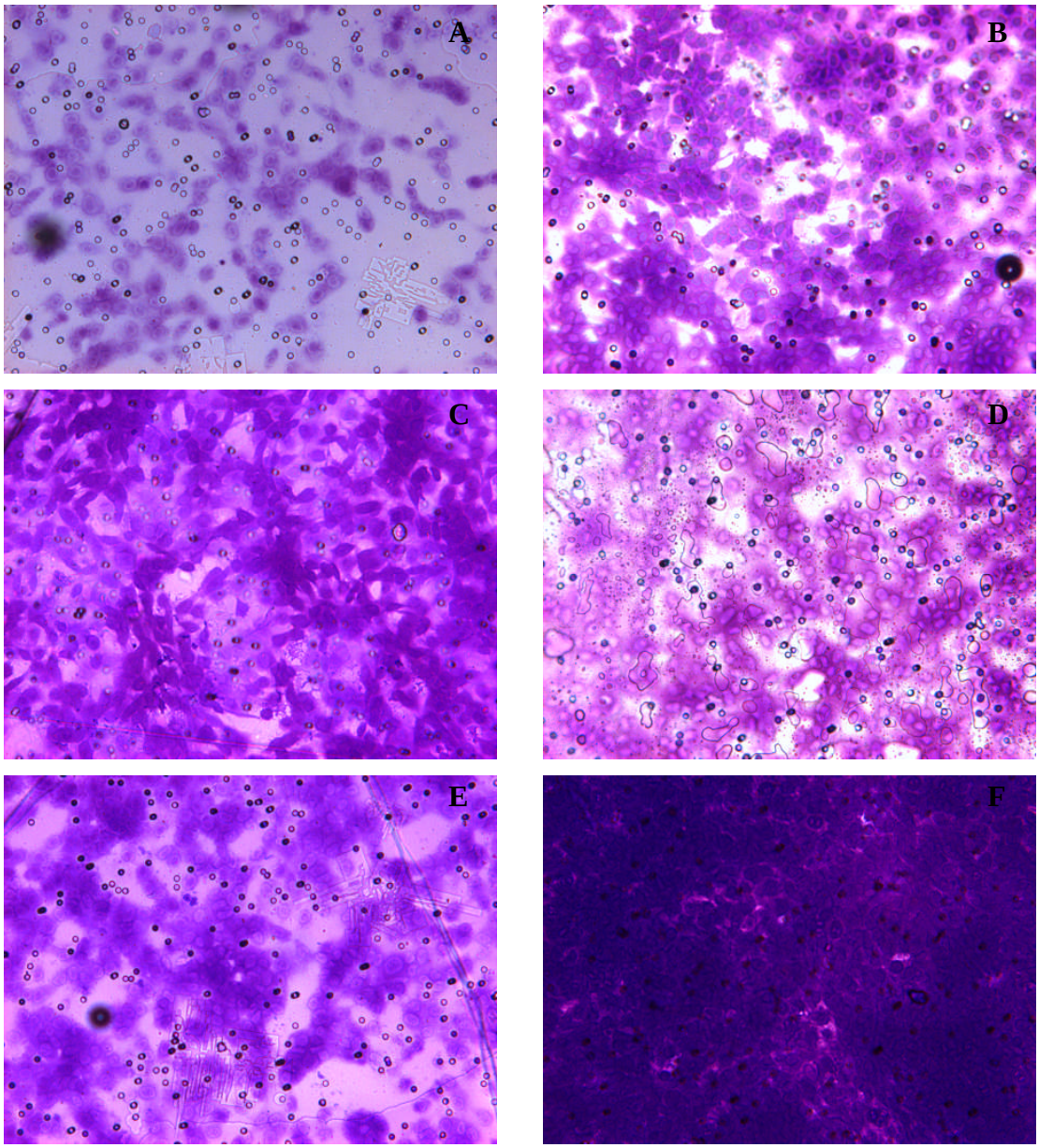

Figure (72). Invasion of SJSA cells with (A) 0 nM, (B) 12.5 nM, (C) 37.5 nM, (D) 75 nM, (E) 100 nM CXCL12 and (F) FBS (10%) across matrigel. Photograph taken of one FOV (x40 obj).

6.2.1.2 *Invasion of SJSA cells with CXCR4 antagonists*

Taking into account the results in Figure (**71**), the assay in section 6.2.1.1 was repeated with CXCL12 (12.5 nM) again used as a chemoattractant. However, one of two CXCR4 antagonists, either AMD3100 ($\mathbf{L}^{11}$) or $[Cu_2\mathbf{L}^{2}Cl_2]^{2+}$ (20 and 200 nM) was added to the upper compartment with the cells. Figures (**73**) and (**74**) show the invasion of SJSA cells in the presence of the CXCR4 antagonists. As expected with CXCL12 (12.5 nM) there

was a significant upsurge in SJSA cell invasion (over 800%). The increase in invasion stimulated by CXCL12 was totally blocked (~ 97%) by $[Cu_2\mathbf{L}^{\mathbf{2}}Cl_2]^{2+}$ at both concentrations (20 and 200 nM) and to a much lesser degree by AMD3100 ($\mathbf{L}^{\mathbf{11}}$) (~ 43%). $[Cu_2\mathbf{L}^{\mathbf{2}}Cl_2]^{2+}$ and AMD3100 ($\mathbf{L}^{\mathbf{11}}$) added in the absence of CXCL12 had no effect on cell invasion (A15).

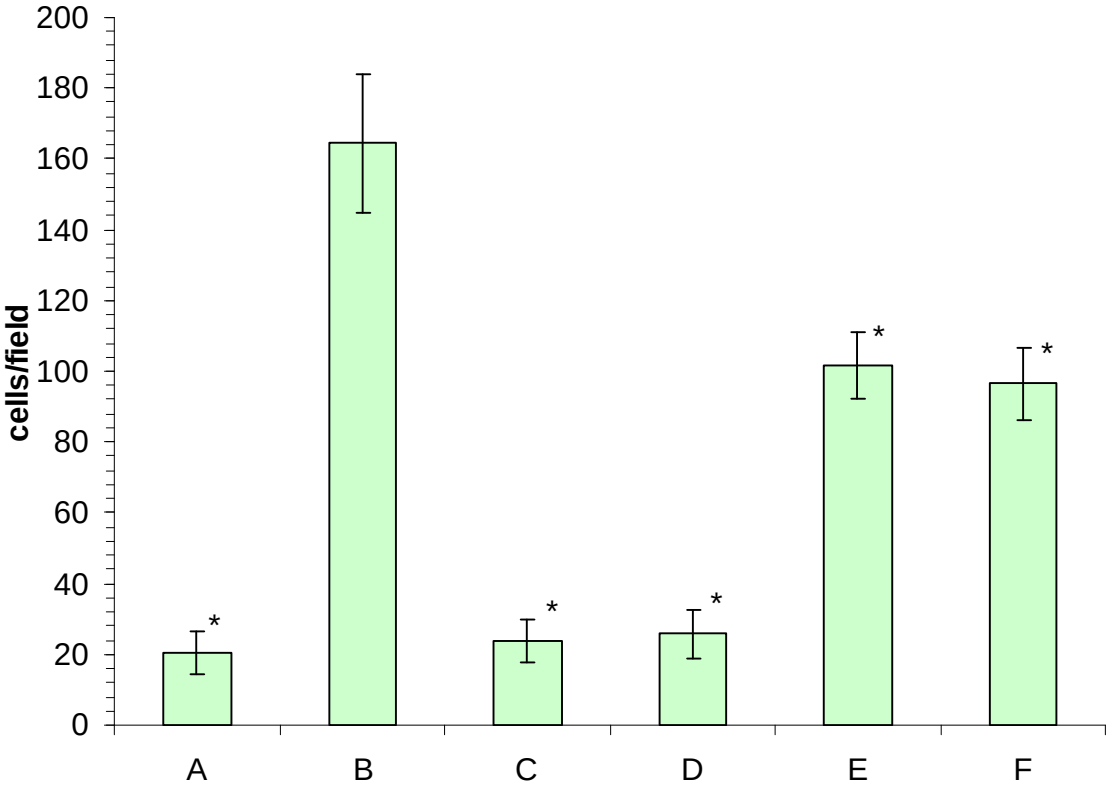

CXCL12 (12.5 nM)	-	+	+	+	+	+
$[Cu_2L^2Cl_2]^{2+}$	-	-	200 nM	20 nM	-	-
AMD3100 (L^{11})	-	-	-	-	200 nM	20 nM
	A	B	C	D	E	F

Figure (73). Invasion of SJSA cells in matrigel with CXCL12 (12.5 nM) and CXCR4 antagonists (20-200 nM). Cells were counted in five different fields (x40 obj) in duplicates. Mean of the values plotted. Asterisk represents significance ($p < 0.01$) from B.

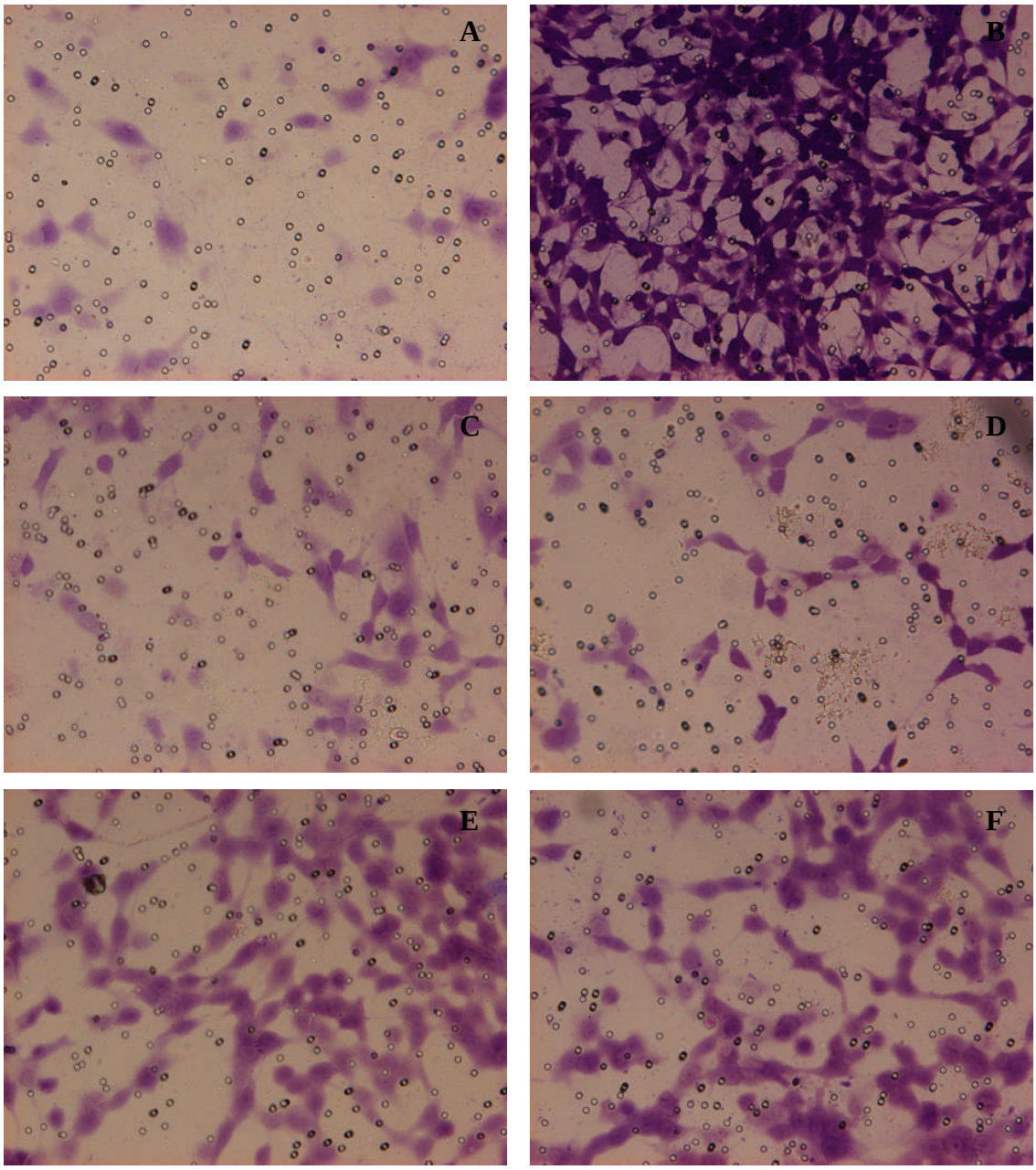

Figure (74). Invasion of SJSA cells in matrigel with CXCL12 (12.5 nM) and CXCR4 antagonists (20-200 nM) across matrigel (for A-E see Figure (**73**)). Photograph taken of one FOV (x40 obj).

6.2.2 CXCR4 truncation and its effect on invasion

Given the established role of CXCR4 in cancer cell migration and invasion (section 6.2), in collaboration with Prof. Tony Ng's group at the Richard Dimbleby Department of Cancer Research, Randall Division of Cell & Molecular Biophysics and Division of

Cancer Studies at Kings College London, the effect of CXCR4 receptor truncations on the invasive behaviour of a rat breast carcinoma cell line (MTLn-3e) was investigated. In particular we were interested in the correlation of the change in downstream trafficking of CXCR4 in the various CXCR4 mutants and the invasive behaviour of these cells. As previously discussed (section 1.2.2.1) receptor regulation is important in understanding the mechanisms by which cancer cells may metastasise.

The C-terminus of CXCR4 has been shown to contain important motifs for the regulation of receptor internalisation, recycling and degradation.[152] A series of mutant CXCR4 receptors expressed on MTLn-3e cells were used to investigate invasion *in vitro* using the matrigel invasion assay.

The following CXCR4 mutant cell lines were used:

WT-CXCR4	–	Human wildtype CXCR4 (as a control)
Δ34-CXCR4	–	Full C-terminal deletion
Δ23-CXCR4	–	Partial C-terminal deletion
AA-CXCR4	–	SS324/325 AA deletion (Part of putative PKC motif in C-terminal)
6A-CXCR4	–	SSILSS324/325/328/329/338/339 AA deletion (Whole PKC-alpha motif)
M-CXCR4	–	Δ34-CXCR4 and WT-CXCR4
C11-CXCR4	–	AA-CXCR4 and WT-CXCR4
A1-CXCR4	–	6A-CXCR4 and WT-CXCR4

6.2.2.1 *CXCR4 mutant cell invasion with CXCL12*

As before (section 6.2.1.1), MTLn-3e cell lines were subjected to the matrigel invasion assay with varying concentrations of CXCL12 (0-100 nM) (Figures (**75**) and (**76**)). Cells expressing WT-CXCR4, M-CXCR4 and A1-CXCR4 showed the lowest invasive potential of all the cells. At all the studied concentrations of CXCL12 the Δ34 truncated mutant showed the highest invasiveness out of all the mutants.

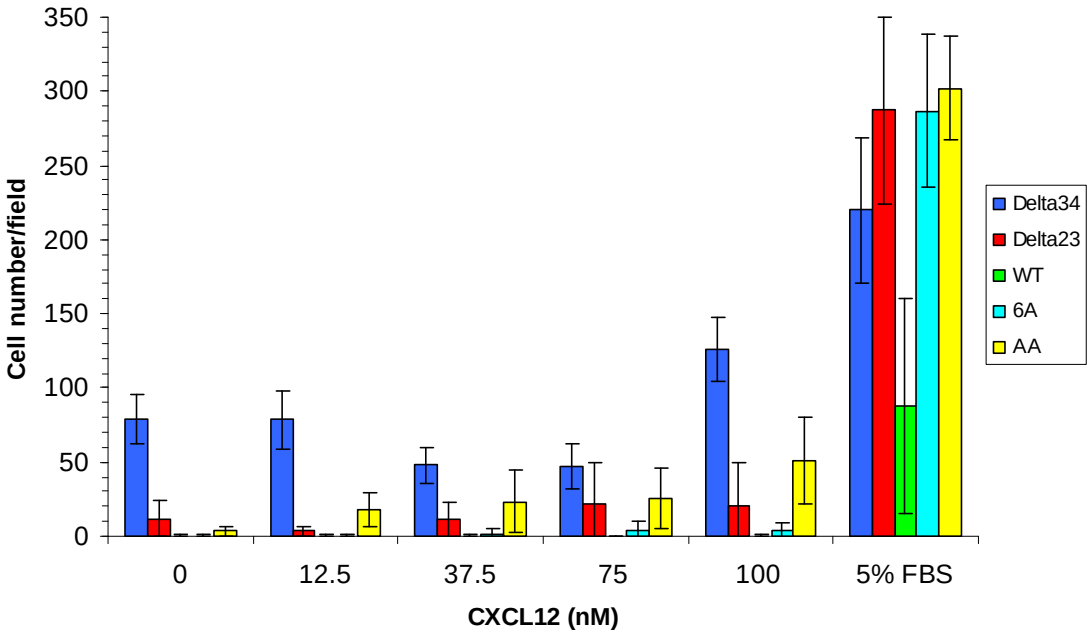

Figure (75). Invasion of CXCR4 mutant MTLn-3e cells in matrigel with CXCL12 (0-100 nM). Cells were counted in five different fields (x40 obj) in duplicates. Mean of the values plotted.

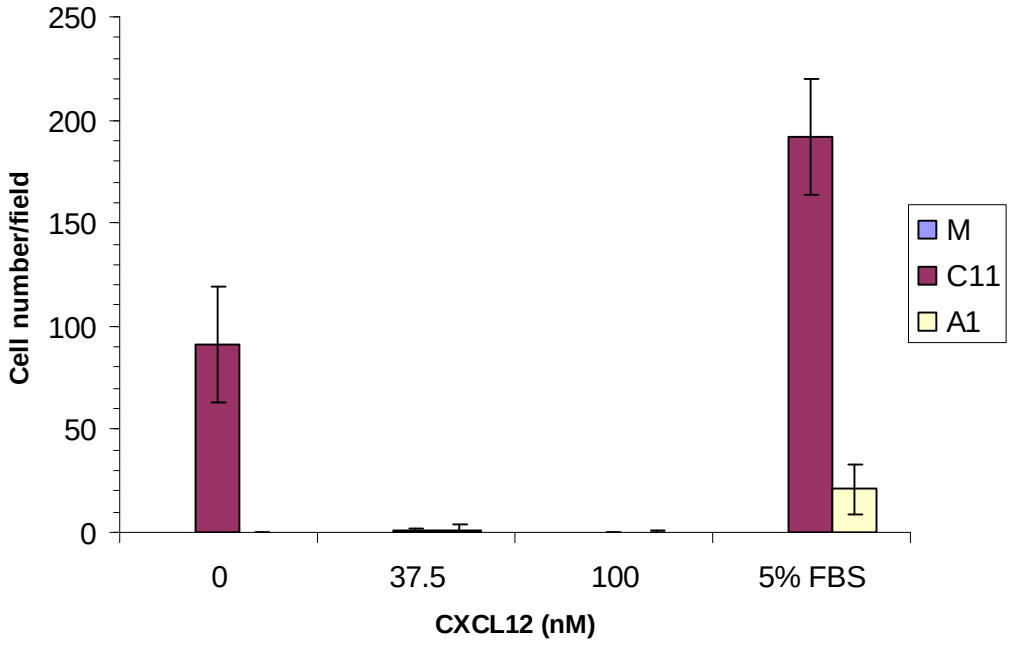

Figure (76). Invasion of CXCR4 double mutant MTLn-3e cells in matrigel with CXCL12 (0-100 nM). Cells were counted in five different fields (x40 obj) in duplicates. Mean of the values plotted.

The cells expressing the AA-CXCR4 mutant showed a ~ 50% reduced invasion at all CXCL12 concentrations as compared to the Δ34 mutant, while the 6A-CXCR4 mutant

did not behave significantly different (~ 5% of Δ34-CXCR4) in comparison to the WT-CXCR4 expressing cells (~ 1% of Δ34-CXCR4). It was interesting to note that the double C11-CXCR4 mutant displayed a reduction in invasion when stimulated by CXCL12 (Figure (**76**)).

6.2.2.2 *Invasion of CXCR4 mutants in the presence of CXCR4 antagonists*

Similar to section 6.2.1.2, the ability of AMD3100 ($\mathbf{L^{11}}$) and $[Cu_2\mathbf{L^2}Cl_2]^{2+}$ (20 and 200 nM) to inhibit the invasion of Δ34-CXCR4 cells was investigated. Δ34-CXCR4 cells were selected as they had been established as the most invasive cell line (Figure (**75**)).

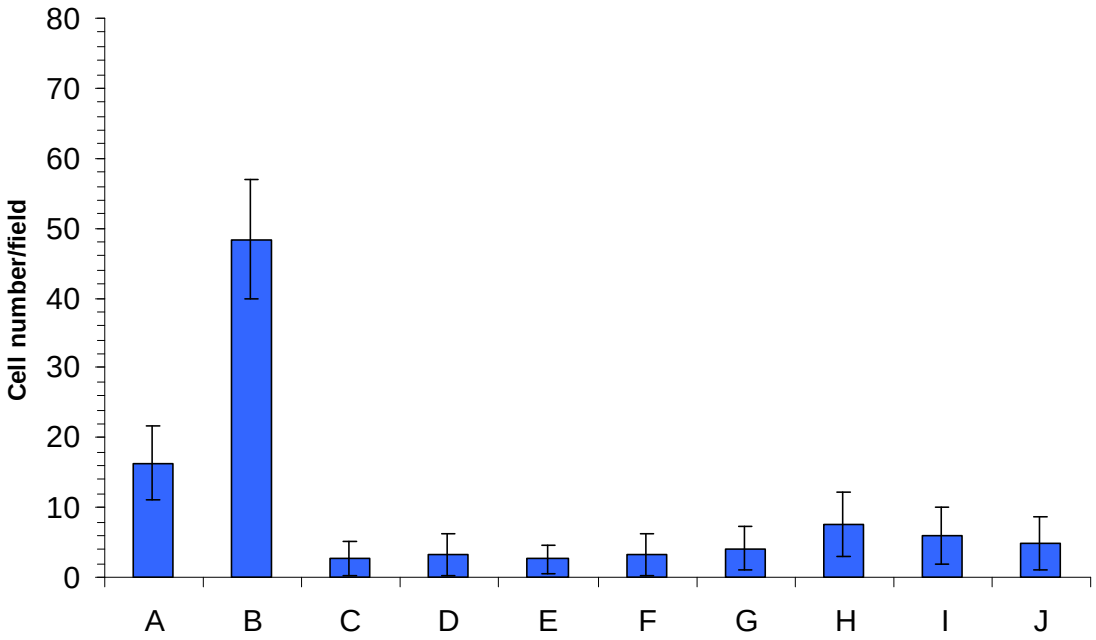

CXCL12 (100nM)	-	+	-	+	-	+	-	+	-	+
$[Cu_2L^2Cl_2]^{2+}$	-	-	200 nM	200 nM	20 nM	20 nM	-	-	-	-
AMD3100 (L^{11})	-	-	-	-	-	-	200 nM	200 nM	20 nM	20 nM
	A	B	C	D	E	F	G	H	I	J

Figure (77). Invasion of Δ34 cells in matrigel with/without CXCL12 (100 nM) and CXCR4 antagonists. Cells were counted in five different fields (x40 obj) in duplicates. Mean of the values plotted.

As can be seen from Figure (**77**), CXCL12 (100 nM) was able to increase invasiveness of the mutant Δ34-CXCR4 cell line and this was totally blocked by both CXCR4 antagonists at very low nanomolar concentrations ($p < 0.01$ (A16)). More interestingly, both AMD3100 ($\mathbf{L^{11}}$) and $[Cu_2\mathbf{L^2}Cl_2]^{2+}$ were able to further inhibit the invasion of these cells below the baseline level in the absence of CXCL12 stimulation ($p < 0.01$ (A16)). To investigate whether this observation was due to a cell killing effect by the antagonists, a cytotoxicity assay was carried out.

6.2.3 Cytotoxicity of AMD3100 ($\mathbf{L^{11}}$) and $[Cu_2\mathbf{L^2}Cl_2]^{2+}$

Similar to section 3.5, AMD3100 ($\mathbf{L^{11}}$) and $[Cu_2\mathbf{L^2}Cl_2]^{2+}$ (20 and 200 nM) were incubated with Δ34-CXCR4 cells for a 48 hr period. Thereafter Δ34-CXCR4 cells were subjected to the tryphan blue exclusion stain and viable cells counted. Figure (**78**) shows that the growth profiles of the cell population with the antagonists follow the growth profile of cells in the absence of antagonists and therefore no cytotoxicity was observed.

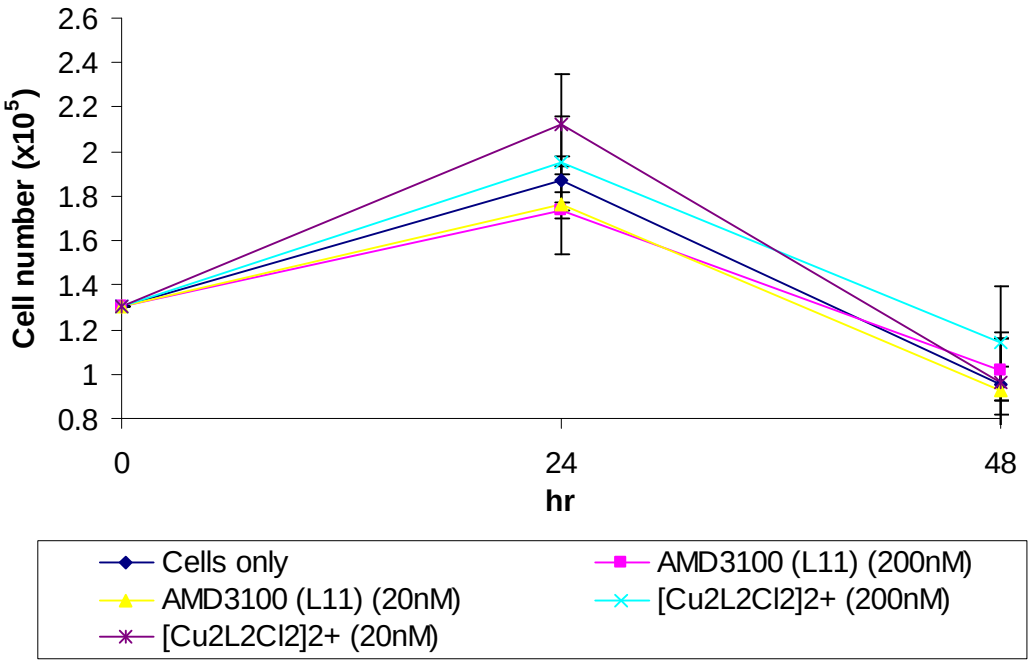

Figure (78). Growth profile of Δ34-CXCR4 cells with CXCR4 antagonists (20-200 nM)

6.2.4 Inhibition of invasion in serum

We investigated further the ability of AMD3100 (**L**[11]) (20-200 nM) and $[Cu_2\mathbf{L}^2Cl_2]^{2+}$ (2-200 nM) to inhibit the invasion of CXCR4 mutant cells in serum. Serum is a rich source of growth factors, hormones, amino acids, sugars, trypsin inhibitors, and lipids and maintains cells in a medium in which they can survive, grow and divide.[313] Addition of serum also provides an *in vivo* like microenvironment. However, the complex nature of serum provides a challenge in isolating the individual cause of effect.

Δ34-CXCR4 cells were chosen with the addition of AA-CXCR4 as a secondary cell line. These cells were allowed to invade in the same fashion as in previous experiments, however with serum (5% FBS) acting as a chemoattractant (Figure (**79**) and (**80**)).

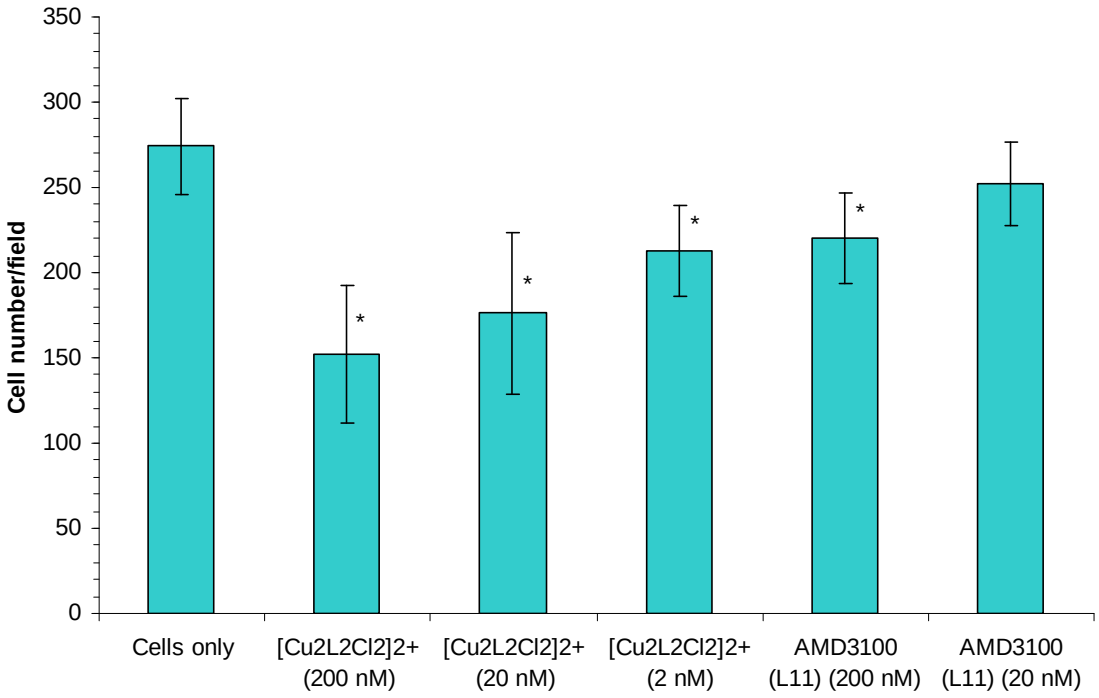

Figure (79). Invasion of Δ34-CXCR4 cells in matrigel with serum (5% FBS) and CXCR4 antagonists. Cells were counted in five different fields (x40 obj) in duplicates. Mean of the values plotted. Asterisk shows significance ($p < 0.01$) from cells only.

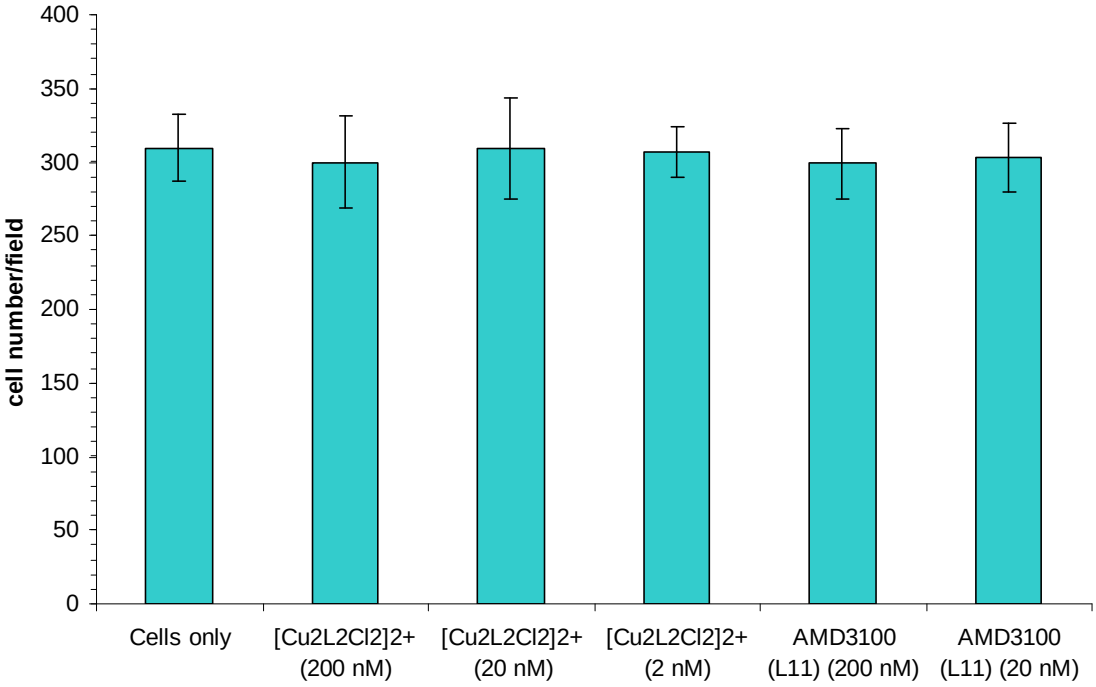

Figure (80). Invasion of AA-CXCR4 cells in matrigel with serum (5% FBS) and CXCR4 antagonists. Cells were counted in five different fields (x40 obj) in duplicates. Mean of the values plotted.

In the Δ34-CXCR4 cell line, $[Cu_2\mathbf{L}^{\mathbf{2}}Cl_2]^{2+}$ was able to inhibit invasion at all concentrations (2-200 nM) ($p < 0.01$) (A17). In contrast, AMD3100 ($\mathbf{L}^{\mathbf{11}}$) was only able to significantly ($p < 0.01$) inhibit the invasion of Δ34 cells at the highest concentration of 200 nM (Figure (**79**)). However in AA-CXCR4 cells, both AMD3100 ($\mathbf{L}^{\mathbf{11}}$) and $[Cu_2\mathbf{L}^{\mathbf{2}}Cl_2]^{2+}$ did not inhibit invasion (Figure (**80**)).

6.2.5 Discussion

AMD3100 ($\mathbf{L}^{\mathbf{11}}$) and $[Cu_2\mathbf{L}^{\mathbf{2}}Cl_2]^{2+}$ are capable of inhibiting the invasion of the human osteosarcoma cell line *in vitro* (Figure (**73**)). However it was interesting to note that AMD3100 ($\mathbf{L}^{\mathbf{11}}$) inhibition was significantly lower (~ 42%) than $[Cu_2\mathbf{L}^{\mathbf{2}}Cl_2]^{2+}$ (~ 97%). I have previously discussed (section 6.3) the difference in binding affinity and residence times of these antagonists. $[Cu_2\mathbf{L}^{\mathbf{2}}Cl_2]^{2+}$ has been shown to have a 5-fold higher residence time and a higher affinity than AMD3100 ($\mathbf{L}^{\mathbf{11}}$) (~ 2 fold).[233,234] The enhanced inhibition of $[Cu_2\mathbf{L}^{\mathbf{2}}Cl_2]^{2+}$ compared to AMD3100 ($\mathbf{L}^{\mathbf{11}}$) was further confirmed in the invasion of Δ34-CXCR4 cells in serum (Figure (**79**)).

These superior binding characteristics of $[Cu_2\mathbf{L^2}Cl_2]^{2+}$ (compared to AMD3100) are likely to correlate to a higher therapeutic activity.

6.2.5.1 *CXCR4 receptor truncation and cancer cell invasion*

Given the established role of CXCR4 in cancer cell invasion, mutant CXCR4 receptors were investigated for any correlation between receptor trafficking and cell invasion. The Δ34-CXCR4 cell line displayed the most significant ligand induced invasion of all the mutants. Recycling of the CXCR4 receptor is dependent on Protein Kinase C (PKC).[314] Truncation of the whole C-terminal (which contains the whole putative PKC motif) in the Δ34-CXCR4 cell line leads to the receptors not being internalised after ligand binding (9.5 ± 6.8%) compared to WT-CXCR4 (68.2 ± 5.4%) (Unpublished). Furthermore, ligand-induced degradation of Δ34-CXCR4 is 85% less than WT-CXCR4.

The AA-CXCR4 mutant also displayed an increase in invasion upon ligand treatment albeit at a reduced level (50%) compared to Δ34-CXCR4. Moreover, the 6A-CXCR4 mutant was found to show a similar invasive potential as the WT-CXCR4 mutant. Receptor internalisation has been shown to be similar for AA-CXCR4 and 6A-CXCR4 however, there was a marked reduction in ligand-induced degradation in the AA-CXCR4 mutant (75% less than WT-CXCR4). AA-CXCR4 does not get degraded efficiently and recycles back to the plasma membrane. Efficient degradation of AA-CXCR4 mutant is said to require additional mutations SS338/339 AA (unpublished). The difference of degradation between 6A-CXCR4 and AA-CXCR4 is due to a sorting defect in the lysosomal degradation pathway via the endosomal sorting complex for transport (ESCRT) machinery. The ESCRT machinery prevents receptor recycling and retrograde trafficking. Receptor mutants defective in degradation via the ESCRT machinery can be efficiently recycled back to the plasma membrane, resulting in an increased receptor availability for ligand binding and downstream signalling processes.

Double-mutant CXCR4 cells were investigated to analyse the effect of CXCR4 dimerisation on invasion. In the case of CXCR4, receptor dimerisation is shown to be ligand-induced and happens at the plasma membrane before receptors become internalised (unpublished). All three of the double mutant CXCR4 cell lines (M, C11,

A1-CXCR4) displayed low invasion comparable to the WT-CXCR4 when stimulated with CXCL12. Similar recycling and degradation analysis revealed that in the M-CXCR4 (Δ34-WT-CXCR4) cell line the receptors became internalized and degraded which is in stark contrast to the single Δ34-CXCR4 mutant. Furthermore, the C11-CXCR4 (AA-WT-CXCR4) cell line showed that the defective degradation process observed in the single AA-CXCR4 mutant was abrogated in the presence of WT-CXCR4 receptors. No changes in receptor degradation were observed for the A1-CXCR4 mutant (6A-WT-CXCR4).

These results clearly show that there is an attenuation of the invasive and metastatic properties of the mutant receptors if paired with WT receptors. They also show that this is due to enhanced degradation of the mutant receptors caused by dimerisation of mutant and WT receptor molecules. An interesting observation was that the C11-CXCR4 mutant displaying a significant reduction in invasion when stimulated with CXCL12 compared to no ligand treatment.

The invasion of Δ34-CXCR4 cells was inhibited by the CXCR4 antagonists AMD3100 ($\mathbf{L^{11}}$) and $[Cu_2\mathbf{L^2}Cl_2]^{2+}$ at low nanomolar concentrations (Figure (**77**)). More interestingly these antagonists caused an inhibition below the baseline level observed in the absence of CXCL12 (Figure (**77**)). This was not observed in the invasion assay carried out using SJSA cells (section 6.2.1.2). Furthermore, in serum $[Cu_2\mathbf{L^2}Cl_2]^{2+}$ was able to block invasion in the Δ34-CXCR4 mutant however this was not observed for the AA-CXCR4 mutant (Figures (**79**) and (**80**)). These results together show the mutations in the mutant CXCR4 cell lines may be responsible for the inconsistent inhibition displayed by the antagonist in this system. Further receptor recycling/degradation/dimerisation analysis with antagonist bound within the receptor may offer an explanation for this result.

6.3 MULTICELLULAR TUMOUR SPHEROID

The study of the complex nature of tumourigenesis has been significantly impaired by the limitations of popular 2D monolayer models. To successfully investigate the biology of cancer, it is necessary to recreate the 3D microenvironment of the tumour tissue.

Although easy and convenient to set up, 2D monolayer models represent many draw backs; (1) The complex cell-cell interactions through adhesion molecules and stimulatory factors such as chemokines, cytokines, and serum proteins cannot be evaluated within single cell suspensions, (2) The effects of the chemokine network on the development of the growth dynamics of the tumour microenvironment cannot be assessed, (3) Growth patterns and expression of receptors have been shown to be different in monolayer cells compared to *in vivo* tumours.[315]

Multicellular tumour spheroids (MTS) are three-dimensional cell cultures and can be regarded as pre-clinical tumours. They resemble avascular solid tumours and can exhibit structural, metabolic, functional and growth patterns similar to those of solid tumours. MTS have been used previously to study tumour growth, tissue organisation, differentiation and invasion.[315,316]

Tumor cell migration and metastasis share many similarities with leukocyte trafficking, which is critically regulated by chemokines and their receptors. Previous reports have highlighted the differential expression of CXCR4 and its regulation of metastasis.[317] One reports how tissue samples of metastasised non-small cell lung cancer cells displayed high expression of CXCR4 in contrast to lower expression of CXCR4 in non metastatic cancer cells.[127] This may provide evidence that the upsurge of CXCR4 expression results in the metastasis of cancer. Furthermore, neuroblastomas have been shown to have differential metastatic behaviour which is coupled to the level of expression of CXCR4 and interaction of CXCL12. Change in the tissue microenvironment of neuroblastomas changes the expression level of CXCR4 and metastatic potential.[318]

Furthermore, the presence of hypoxic areas is a common feature of malignant tumours, including lymphomas. The hypoxic inducible factor -1 (HIF-1) has been identified to activate a number of genes including CXCR4. HIF-1 production is believed to be activated when stress is induced within the tumour microenvironment after initial primary growth. The tumour adapts by initiating angiogenesis and metastasis to oxygen rich areas.[319,320]

More importantly murine breast cancer cell lines displayed 10 times lower expression of CXCR4 than the same cells as a spheroid. Moreover spheroids of these cell

lines displayed up to five times more invasiveness than the cells alone.[321] This report clearly shows the importance of the 3D tumour environment in regulating CXCR4 expression and how the expression level relates to metastatic potential, thus providing the basis of using such 3D models in cancer research.

Several methods exist for producing MTS, dependent on the nature of the cancer cell line, and these include spinner culture, liquid overlay and the hanging drop techniques.[322]

Here we describe a preliminary investigation into MTS formation, using one of our CXCR4 transfected cancer cell lines (Δ34-CXCR4).

6.3.1 Δ34-CXCR4 MTS formation

This was carried out using the liquid overlay technique as described previously.[322-324] This technique relies on the spontaneous aggregation of the cancer cells. Briefly, Δ34-CXCR4 cells in normal media were placed on a non-adhesive layer (agarose gel) to promote cell aggregation and spheroid formation, for 4 days in a 37^{o}C 5% CO_2 atmosphere. After 24 hr and 96 hr periods, cell mass was photographed under a light microscope (x4 obj.).

Figure (**81a**) shows that after a period of 24 hr, the cancer cells have moved to form an irregular cell mass in the middle. After a 96 hr period, the cell mass has formed a more uniform spherical mass with signs of differential layers (see Figure (**81b**)). Furthermore the photos revealed the cell mass had grown significantly in size between 24 hrs and 96 hrs of growth.

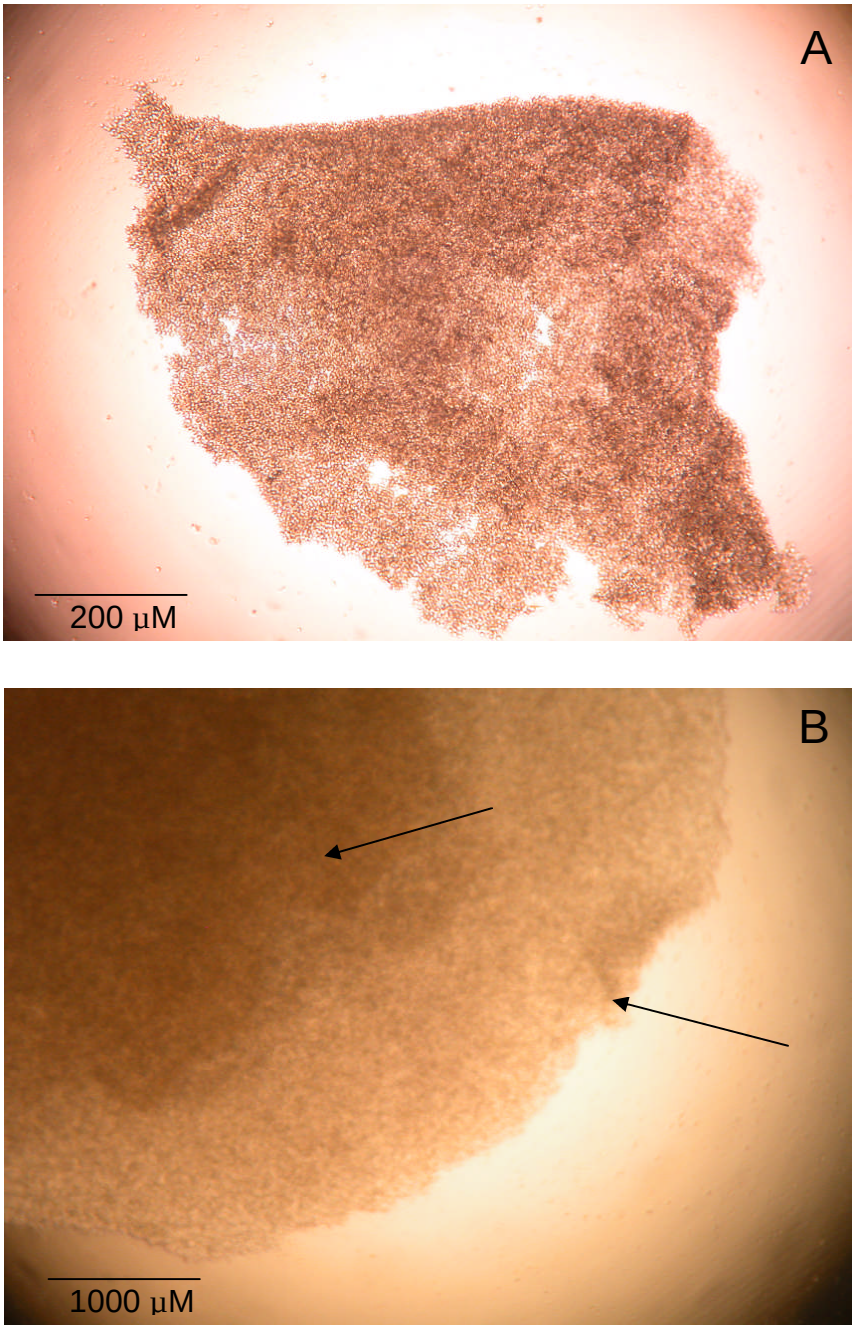

Figure (81). Photographs of Δ34-CXCR4 cells on a non-adhesive agarose layer after (A) 24 hr and (B) 96 hr period of growth. Arrows show outer layer and inner core.

In conclusion, a preliminary study into MTS formation has shown that the Δ34 cancer cell line is able to form spontaneous cell aggregation in line with the characteristic behaviour of an aggressive cancer cell. Furthermore, these cancer cells are then able to

form a spheroid like structure with microscopically visible differential density layers after a short period of time (4 days), reminiscent of a MTS.

Further work is required to establish a MTS model to be used in a CXCR4 study, investigating expression levels and the effect of hypoxia. This will enable a further understanding of how the CXCR4 receptor network is involved in tumour growth, differentiation and invasion close to the true behaviour of an *in vivo* tumour.

6.4 CONCLUSION

CXCL12 stimulation of cancer cells has been shown to increase cell invasion and this is blocked by our configurationally restricted bicyclam antagonist ($[Cu_2\mathbf{L}^{\mathbf{2}}Cl_2]^{2+}$) in a more potent manner than AMD3100 ($\mathbf{L}^{\mathbf{11}}$) in the nanomolar range. This difference may well be attributed to the higher residence time and affinity of $[Cu_2\mathbf{L}^{\mathbf{2}}Cl_2]^{2+}$ compared to AMD3100 ($\mathbf{L}^{\mathbf{11}}$) reported earlier (section 3.6). Moreover, both these antagonists were able to inhibit CXCL12 induced invasion in a human cancer cell line (SJSA) which constitutively expresses CXCR4 and a transfected cell line (MTLn-3e) expressing truncated CXCR4 in the same manner. This further adds to the potential of using $[Cu_2\mathbf{L}^{\mathbf{2}}Cl_2]^{2+}$ as a therapeutic drug in diseases such as cancer.

In addition, CXCR4 C-terminal truncations revealed a correlation between defective degradation and recycling of the CXCR4 receptor and enhanced cell invasion.

Furthermore, Δ34 cells were able to form MTS like structures and thus provide the basis for a possible MTS model to be used in future work investigating the link between CXCR4 and tumour growth in a 3D microenvironment.

Chapter 7

Concluding remarks and future work

7.1 CONCLUDING REMARKS

Synthetic small molecule CXCR4 antagonists exist, including a xylyl bridged bicyclam AMD3100, which has been shown to have a both high binding specificity and an effective inhibitory action against a number of disease states including arthritis, HIV infection and cancer. For this type of molecule binding is thought to occur via stereospecific hydrogen bonding to the carboxylate groups of Asp171 and Asp262 of the CXCR4 receptor. Incorporation of transition metal ions (e.g. zinc(II) to AMD3100) results in an increased binding potency to CXCR4 compared to AMD3100 alone. [207] This is thought to occur via a strong co-ordination interaction between the metal ion and the carboxylate groups of Asp171 and Asp262.

In Hull, we have previously carried out an extensive study into the binding potency of a series of configurationally restricted bicyclam based systems.[233] The strategy of configurational restriction of the cyclam moiety results in an enhanced metal ion co-ordination interaction and potency compared to metal complexes of AMD3100.

The preceding chapters of this thesis describe the binding potency of some new cyclam and cyclen based complexes in competition with an anti-CXCR4 mAb. Furthermore, this has included the investigation of some new tris-cyclam based complexes using the rationale that an additional binding interaction may be possible with CXCR4. I have also described the development of a small CXCR4 monocyclam based antagonist as a potential future CXCR4 fluorescent probe for diagnostic applications.

In further development of these molecules as potential future CXCR4 drug candidates, I have described the relative residence time of the most potent compound to date. This is further supplemented by the investigation into the application of this molecule in inhibiting cancer cell proliferation and invasion. To conclude I investigated the role CXCR4 receptor regulation plays in the progression of cancer using CXCR4 mutant cell lines.

7.2 BINDING OF CONFIGURATIONALLY RESTRICTED CYCLAM AND CYCLEN BASED COMPLEXES

The study of the structure-binding affinity relationships of a range of macrocyclic based complexes has shown and confirmed a number of key structural features that are important in trying to design a high affinity CXCR4 antagonist. In general, reduction in the cavity size of the macrocyclic ring (14 (cyclam) to 12 (cyclen) membered) and changing the substitution pattern to the meta (1,3) positions (on the phenyl ring) reduces the affinity of the complex in binding to the CXCR4 protein. In support of our previous study, the IC_{50} values revealed that inclusion of a metal ion is crucial in increasing the affinity of the complex. Furthermore, the type of metal ion used strongly influences the affinity and this could be attributed to the kinetics and thermodynamics of metal ion coordination (section 2.4).

The data obtained on the tris-cyclam compounds revealed that the ring configuration of the three cyclam moieties shows that a 1,3,5 substitution pattern on a central phenyl ring results in the molecule interacting with CXCR4 in a similar way to the related bicyclam molecules (1,3-disubstutitued phenyl ring) and hence displayed similar binding potencies. However, the linear tris-cyclam complex, with two phenyl rings and a 1,4-disubstituted pattern on each, shows considerable promise as a potential high activity CXCR4 antagonist and warrants further development.

7.3 RESIDENCE TIME OF MACROCYCLIC COMPLEXES

An investigation of the relative residence times was carried out using a selected group of bicyclam-based compounds complexed to the CXCR4 receptor *in vitro.* Binding affinity is an important parameter which can be used to investigate the interaction between a protein and its biological target. However other factors such as the residence time of a macromolecule with its protein target need to be taken into consideration, especially in optimisation of pre-clinical drugs.

Using anti-CXCR4 mAb inhibition as a measure of relative residence time, I have shown that over a 5 day period, different configurationally restricted molecules display

differing relative residence times. Furthermore, the calculated relative (τ) and $t_{1/2}^{diss}$ values revealed the most potent compound ($[Cu_2\mathbf{L}^{\mathbf{2}}Cl_2]^{2+}$) to have a far superior relative residence time in comparison to AMD3100 and its copper(II) complex. Using X-ray crystal structures of similar compounds to rationalise this data, this appears to be the result of a shorter/stronger co-ordination bond formation with aspartate residues for $[Cu_2\mathbf{L}^{\mathbf{2}}Cl_2]^{2+}$.

7.4 FLUORESCENT CYCLAM DERIVATIVES

In further development of the previously reported rhodamine conjugated monocyclam molecule, I investigated the binding and detection of a zinc(II) monocyclam biotin conjugate ($[Zn\mathbf{L}^{\mathbf{12}}]^{2+}$) using the stretavidin-biotin binding model.[235] An attempt to use a Qdot-streptavidin conjugate with $[Zn\mathbf{L}^{\mathbf{12}}]^{2+}$ proved to be unsuccessful, however an anti-CXCR4 mAb competition assay showed that $[Zn\mathbf{L}^{\mathbf{12}}]^{2+}$ was indeed binding to CXCR4. However the dye-streptavidin moiety did not seem to be able to access the biotin molecule, possibly due to steric hinderance. Redesign of the molecule with a longer spacer (linker) between the biotin molecule and the metal cyclam complex would reduce such steric hindrance at the binding site.

7.5 MIF

Migration inhibitory factor has been reported to interact with CXCR4.[290] MIF has been attributed to a number of disease states including arthritis and tumour growth.[291] In this investigation I found MIF did not interact with CXCR4 expressed on Jurkat cells and did not appear to interact with any other cell membrane protein present on these cells. The interaction of MIF with chemokine receptors maybe more complex than first thought and warrants further studies.

7.6 CANCER THERPAEUTICS

The CXCR4/CXCL12 axis has been implicated in the progression of many cancers by way of stimulating the proliferation and/or invasion of cancer cells. The chemokine network has become one of the most important new therapeutic targets for new drugs in anti-cancer therapy. In this research I investigated the effect the CXCR4/CXCL12 axis had on cancer cell proliferation and invasion.

7.6.1 Cancer cell proliferation

Using two alternative methods of detecting cell proliferation, this study showed that CXCL12 had no increase on cell proliferation in the cancer cell lines used whether serum was present or not. Published work shows the proliferation effect of CXCL12 on cancer cells is not uniformly reported. This may relate to the fact that the biological role of CXCL12 in the human body is more of a pro-migratory role than a growth stimulator.

7.6.2 Cancer cell invasion

A plethora of published work exists showing the pro-metastatic effect of CXCL12 interacting with CXCR4 on cancer cells. Neutralising such an interaction by CXCR4 antagonists has proven to be successful *in vitro* and *in vivo*.

In this work, CXCL12 was found to increase the invasion of an osteosarcoma cancer cell line (SJSA) many times over, confirming previous reports. More excitingly, I was able to totally block the increase in invasion by the most potent compound ($[Cu_2\mathbf{L}^{\mathbf{2}}Cl_2]^{2+}$) at very low nanomolar concentrations.

Using a breast carcinoma cell line expressing mutant versions of the CXCR4 receptor revealed the effect of dysregulation of the CXCR4 receptor on invasion. Mutant cell lines that displayed defective CXCR4 degradation and recycling corresponded to an increase in invasive potential by CXCL12 stimulation. Increase in invasion by CXCL12 was totally blocked by $[Cu_2\mathbf{L}^{\mathbf{2}}Cl_2]^{2+}$ in the nanomolar range. In this case the most intriguing result showed that $[Cu_2\mathbf{L}^{\mathbf{2}}Cl_2]^{2+}$ was able to significantly reduce the increase in

invasion stimulated by serum. This supports the idea that $[Cu_2\mathbf{L}^2Cl_2]^{2+}$ may have a considerably higher therapeutic activity than AMD3100.

This work suggest considerable potential for the use of $[Cu_2\mathbf{L}^2Cl_2]^{2+}$ as a therapeutic drug against cancer and supports the progression to *in vivo* testing in the future.

7.6.3 MTS formation

To further test these compounds as drug candidates, a pre-clinical MTS model was successfully developed for future investigation of the effect CXCR4 blocking in a 3D cellular matrix.

7.7 FUTURE WORK

7.7.1 Consideration for future complex design

7.7.1.1 *Tris cyclam compounds*

It would be of interest to design new tris-cyclam linear based complexes containing different metal ions. It has been determined that cross-bridged complexes tend to have higher activity compared to side-bridged complexes, therefore the new tris-cyclam linear complexes could also contain the cyclam rings configurationally restricted in the cross-bridge (*cis*-*V*) fashion. These new complexes could then be used in CXCR4 mAb inhibition assays to determine their respective IC_{50} values and hence affinity.

7.7.1.2 *CXCR4 probes*

Further development is warranted in the potential use of cyclam based derivatives as probes for CXCR4.

1. The use of other fluorescent conjugates such as Fluorescein (FITC), or R-Phcoerythrin (PE) may be more useful in the streptavidin/biotin binding model.
2. Furthermore, a new synthetic strategy could entail direct conjugation of a fluorescent molecule (for example Cy5) to the monocyclam derivative; this may relieve the problem of relying on the interaction of streptavidin and biotin.
3. The use of other probes such as Raman active nanoparticles (surfaced modified gold nanoparticle) could be used to directly conjugate to the monocyclam derivative. Raman active conjugates with large nanoparticles may alleviate cellular uptake problems.
4. Direct conjugation of a Raman active nanoparticle or fluorescent probe to bicyclam-based complexes may provide higher binding activity and hence more efficient detection of the receptor.

7.7.2 Computer modelling

The binding of AMD3100 in CXCR4 has been evaluated using computer modelling studies (section 1.4.7.3). The use of this tool would enable us to carry out binding energy calculations and probe which interactions are possible inside the binding site. This would complement the biological data obtained in this study and further characterise the specific binding interactions of these complexes.

7.7.3 Therapeutic evaluation

AMD3100 has been evaluated in its anti-tumour, anti-HIV and anti-inflammatory effects *in vitro* and *in vivo*. Equivalent anti-inflammatory studies could be performed with the configurationally restricted group of compounds *in vitro*.

In addition, the $[Cu_2\mathbf{L^2}Cl_2]^{2+}$ molecule has a high anti-cancer effect, specifically in cancer invasion (shown in our work). Therefore, this molecule warrants *in-vivo* work to evaluate its therapeutic effect on cancer and tumour progression in animals.

AMD3100 is currently marketed as a stem cell mobiliser (Mozobil®) for stem cell transplantation. It would be interesting to see our $[Cu_2\mathbf{L^2}Cl_2]^{2+}$ antagonist being

evaluated for stem cell mobilisation. It may prove to be a better stem cell mobiliser as it has been shown in our work to have a higher affinity and higher residence time than AMD3100.

Further work is required to establish a MTS model to be used in a CXCR4 study, to investigate expression levels and the effect of hypoxia. This will enable further understanding of how the CXCR4 receptor network is involved in tumour growth, differentiation and invasion in a closer model to an *in vivo* tumour.

Chapter 8

Experimental

8.1 CELL CULTURES

Human leukaemia T cell lymphoblasts (Jurkat), colorectal cancer (HT29, Colo320, CaCo-2), breast carcinoma T47-D and MCF-7, ovarian cancer A2780, lung cancer (Corl105, Corl23), human melanoma (A2058) were obtained from the MRL (University of Hull, Hull, UK). Human osteosarcoma cell (SJSA) was obtained from the Clinical and Medical Research department at the University of Leeds, UK. Breast carcinoma MDA-MB-231, pancreatic carcinoma (AsPc-1) and the brain glioblastoma (U87-MG) cell lines were obtained from ATCC. Colo320, T47-D, MCF-7, A2780, Corl105, Corl23, MDA-MB-231 and SJSA cell lines were cultured in RPMI 1640 medium (PAA, UK) containing 10% (v/v) heat inactivated fetal bovine serum (FBS)(Biowest, France), 1% glutamate (2 mM), 1% (v/v) penicillin and streptomycin (100 units/ml) antibiotics.

HT29, CaCo-2 and A2058 cell lines were cultured in DMEM medium (PAA, UK) containing 10% (v/v) heat inactivated fetal bovine serum (FBS)(Biowest, France), 1% glutamate (2 mM), 1% (v/v) penicillin and streptomycin (100 units/ml) antibiotics.

AsPc-1 was cultured in RPMI 1640 medium (ATCC), containing glucose (4.5 g/l), lower sodium bicarbonate level (1.5 g/l), 10% (v/v) heat inactivated fetal bovine serum (FBS)(Biowest, France), 1% glutamate (2 mM), 1% (v/v) penicillin and streptomycin (100 units/ml) antibiotics.

U87-MG was cultured in MEM-Eagle medium containing Earles balanced salt solution (ATCC), 10% (v/v) heat inactivated fetal bovine serum (FBS)(Biowest, France), 1% glutamate (2 mM), 1% (v/v) penicillin and streptomycin (100 units/ml) antibiotics.

CXCR4 transfected rat breast carcinoma (MTLn-3e) cell lines 4C, Δ34, Δ23, 6A, AA, A1, M, C11, 2K and CL14 were obtained from Prof. Tony Ng at The Richard Dimbleby Department of Cancer Research (King's College London, UK) and were cultured in αMEM (without ribonucleosides) (PAA, UK) containing 5% (v/v) heat inactivated FBS (Biowest, France), 1% glutamate (2 mM), 1% (v/v) penicillin/streptomycin (100 units/ml) and G418 (500 µg/ml) (Sigma-Aldrich, UK).

Additional selective antibiotics were added to the growth media depending on the type of cell line. The growth media used for cell lines 4C, Δ34, Δ23, 6A and AA included puromycin (Sigma-Aldrich, UK) (0.5 µg/ml). Cell lines A1, M, C11 and 2K

were grown in the presence of puromycin (Sigma-Aldrich, UK) (0.25 µg/ml) and hygromycin B (Calbiochem) (200 µg/ml). Cell line CL14 was grown in the presence of hygromycin B (Calbiochem) (400 µg/ml).

The cell cultures were maintained at 37^{o}C in a humidified, CO_2 (5%) controlled atmosphere with subculturing done every 2-3 days as appropriate. Human leukaemia T cell lymphoblasts (Jurkat) were used upto passage number 30 – 40 and where found to show continual stable expression of CXCR4 and viability.

8.2 CXCR4 ANTAGONISTS

L^1-L^{12} and their metal complexes were synthesised in Dr Steve Archibald's laboratory at the University of Hull, UK by Dr Graeme McRobbie and Dr Gary Nicholson.

8.3 ASEPTIC TECHNIQUE

Aseptic techniques were conducted in a Class II microbiological safety cabinet (ICN flow) fitted with a U.V sterilising lamp. All glassware and heat stable solutions were autoclaved prior to use at 121^{o}C for 10 min, disposable equipment and all solutions were of sterile tissue culture grade.

8.4 PROTEINS AND REAGENTS

Unconjugated mouse anti-human CXCR4 mAb clone 44716.111, was purchased from R & D systems Europe, Abingdon, UK. Negative control mouse IgG and the secondary fluorescein isothiocyanate conjugated anti-mouse antibody (IgG-FITC) were purchased from Serotec, UK. Dilutions of mAbs were prepared using PBS supplemented with 0.25% (v/v) BSA and 0.01 M NaN_3. CD8 mAb was purchased from Serotec, UK.

Human CXCL12 (alpha) was purchased from R&D systems (Abington, UK) and was reconstituted as manufacturer's recommendations.

Qdot-streptavidin conjugates were obtained as 1 µM solutions as a kit from Invitrogen, UK. Cy5-streptavidin was obtained from Fisher, UK as a 2 mg/ml solution.

All reagents and antibodies were reconstituted and stored according to the manufacturer's instructions unless otherwise stated.

8.5 CELL COUNTING (TRYPAN BLUE TEST)

The concentration of the cells was determined using a Neubauer hematocytometer. Cells in suspension were diluted 1:1 with 0.2% (w/v) Trypan blue stain. The diluted sample was placed onto a hematocytometer chamber and the cell density was determined using light microscopy by counting the number of cells in a set area. The following equation is used to determine the concentration of cells (Equation (**3**)).

Equation 3:

Cell concentration (cells/ml) = Averaged cell count x 2 (dilution factor) x 10^4 (volume of chamber)

8.6 ANTIBODY BINDING BY FLOW CYTOMETRY (CXCR4 DETECTION)

Cell cultures were centrifuged (180 x g for 3 min), resuspended in 10 ml PBS and centrifuged (180 x g for 3 min) further. The cell pellet was resuspended in 1.0 ml PBS and counted using the Trypan-blue test. Cells at a density of 1 – 2 x 10^5 cells were aliquoted into polypropylene FACS tubes (Falcon 2054 tubes), and then incubated with 10 µl of the appropriate concentration (10 µg/ml) of antibody (44716, 44717 (R&D Systems, UK)) for 1 hr at 4^{o}C. Thereafter cells were washed (centrifuged at 180 x g for 3 min) with 1.0 ml PBS/0.25% BSA/0.01 M NaN_3, and incubated with a secondary fluorescein isothiocyanate conjugated anti-mouse antibody (IgG-FITC) (diluted 1:100 in PBS/0.25% BSA/0.01 M NaN_3) or Northern Lights (R&D Systems, UK) (IgG-NL637) conjugated anti-mouse antibody (10 µl) for 30 min at 4^{o}C. After further washing (centrifuged at 180 x g for 3 min) with 1.0 ml PBS/0.25% BSA/0.01 M NaN_3, the cell samples were fixed in 300 µl of PBS/0.25% BSA/0.01 M NaN_3 and analysed on a FACScan flow cytometer (BD Biosciences Europe, Erembodegem, Belguim). Data were acquired and analysed with CellQuest software (Becton Dickinson). As a negative

control for non specific background staining, the cells were stained in parallel with the negative control mouse IgG (diluted 1:100 in PBS/0.25% BSA/0.01 M NaN_3).

8.6.1 Blocking assay

Prior to adding the antibody, the cell solution was preincubated with 10 µl of the appropriate compound (of varying concentrations), or PBS for the controls, for 30 min at 4^{o}C. The cells were then washed with 1.0 ml PBS (centrifuged at 180 x g for 3 min) to remove excess compound.

8.6.2 Displacement assay

Prior to adding the antibody, the cell solution was preincubated with 10 µl of the appropriate compound (20 µM), or PBS for the controls, for 60 min at 4^{o}C. The cells were then washed with 1.0 ml PBS (centrifuged at 180 x g for 3 min) to remove excess compound.

8.6.3 Concentration dependent assay (competition)

Varying concentrations of compound (~60 – 0.03 µM) were added (10 µl) simultaneously with the antibody.

8.6.4 Residence time assay

Prior to adding the antibody, compound (40 µM or 0.08-16 nM) was added (10 µl) to the cell solution (1 ml media) containing 1 x 10^5 Jurkat lymphoma cells for 1 hr. The cells were then washed with 1.0 ml PBS (centrifuged at 180 x g for 3 min) to remove excess compound. Cells were resuspended in media (1 ml) and incubated at 37^{o}C in a humidified, CO_2 (5%) controlled atmosphere for 96 hrs (or 24 hr only). At every 24 hr period, a cell sample was removed and spun down (centrifuged at 180 x g for 3 min) to

collect cells and remove media. Thereafter the cell sample was subjected to the antibody binding assay as in section 8.6. Appropriate controls were carried out in parallel.

8.6.5 Cytotoxicity

Jurkat lymphoma cells were collected (as in section 8.6) at a density of 1 x 10^5 and incubated with relevant compound (40 µM; 10 µl) for 96 hrs in 1 ml media. Every 24 hr period, a cell sample was removed and the viability of cells was counted using the tryphan blue exclusion test as in section 6.3

8.7 STATISTICAL ANALYSES

IC_{50} values were extrapolated and calculated using non linear regression analysis using the Graphpad prism 4.0 software (San Diego, CA).

Relative (τ) and $t_{1/2}^{diss}$ binding constants were determined using the one phase exponential decay model in Graphpad prism 4.0 software (San Diego, CA).

8.8 MTS PROLIFERATION ASSAY

1 x 10^4 and 2 x 10^4 cells/200 µl were prepared by cell counting and dilution in media (complete or serum free). This 200 µl of cell sample was then transferred to a 96 well plate in triplicates and incubated at 37^{o}C with a 5% CO_2 atmosphere. A separate plate was used for each time interval. CXCL12 (10 or 100 ng/ml) was added at the start or every 24 hr interval as indicated. After each time interval the plate was removed and MTS ((3-(4,5-dimethylthiazol-2-yl)-5-(3-carboxymethoxyphenyl)-2-(4-sulfophenyl)-2H-tetrazolium,salt) (Promega, Madison, WI) was added (10 µL) to each well. The plates were then further incubated for 2 hr (2-4 hr). Absorbance of the MTS was then read in a automated plate reader at a wavelength of 492 nm.

8.9 CFSE PROLIFERATION ASSAY

CFSE (carboxyfluorescein diacetate succinimidyl ester) cell proliferation kits were obtained from Invitrogen, UK. This method follows the protocol recommended by the manufacturer. Normal media was removed from the cell culture flask and the flask washed three times with PBS (sterile) to ensure removal of all media and serum. Thereafter, serum free media was added to the same culture flask and incubated for 12 hrs in the normal environment (37^oC, 5% CO_2).

A 5 mM cell trace CFSE stock solution was prepared by dissolving one vial of CFSE (50 µg) into 18 µl of high grade DMSO (included in kit).

Adherent cells were removed from the culture flask (scraping) and resuspended in PBS/0.25% BSA/0.01 M NaN_3 solution to a final concentration 1 x 10^6 cells/ml. 1 µl of the CFSE stock solution (5 mM) was added to each ml of cells for a final working concentration of 5 µM. The cell solution was then incubated for 10 min (37^oC, 5% CO_2). Staining was quenched with the addition of 5 volumes of ice cold culture media to the cells and incubated for a further 5 min on ice. Excess CFSE dye was removed by centrifuge (180 x g for 3 min) and the pellet was then washed (centrifuge; 180 x g for 3 min) three times in fresh media.

Cells were counted again (tryphan blue exclusion) and 1 x 10^5 cells/ml (in complete or serum free media) were seeded onto a 12 well plate and stimulated with CXCL12 (10 or 100 ng/ml) if required. Plates were then incubated (37^oC, 5% CO_2) for 3-5 days for the cells to proliferate.

After growth period, cells were removed from each well by EDTA-trypsin (1%) (PAA, UK) (100 µl) treatment for 10 min. Cells were then taken off by the addition of PBS (1 ml) and washed (centrifuged; 180 x g for 3 min) to collect cells. The cell pellet was resuspended in PBS (200 µl) and analysed on a FACScan flow cytometer (BD Biosciences Europe, Erembodegem, Belgium). Data were acquired and analysed with CellQuest software (Becton Dickinson).

8.10 APOPTOTIC ASSAY

2 x 10^5 /ml of cells (media) were seeded onto a 24 well plate in triplicates and cultured for various time intervals (usually 24 hr). Normal media was then extracted and replaced with normal media or serum free media (1 ml) and grown further (24-72 hr). The respective media was replenished every 24 hr. Then media was removed and EDTA/Trypsin solution (1%)(100 µl) added to each well to remove the adherent cells (10 min). Once cells were non-adherent, the respective media was added (1 ml) to extract the cells. Apoptosis was then determined using the Annexin-V assay kit (Serotec, UK) as per the manufacturer's instructions. Briefly the cells were counted and 2-5 x 10^5 cells were resuspended in ice cold binding (x1) (1 ml). Hydrogen peroxide (100 µl, 100 vol., 30%) was added at this stage as a positive control for 30 min. Cell samples were washed (centrifuged 180 x g for 3 min) and resuspended in 1 ml binding buffer. Annexin V-FITC (5 µL) was added to each 195 µl of the cell sample prepared above. The sample was mixed and incubated for 10 min in the dark at room temperature. Thereafter the cells were washed (1 ml binding buffer (x1)) by centrifuge (180 x g for 3 min) and resuspended in 190 µl binding buffer (x1) (Falcon tubes). Propidium iodide (PI) (10 µl) was added to each cell sample. The cell sample was then analysed by flow cytometry (FL-1-FL-3 channels)

8.10.1 Apoptosis assay with Ionomycin

Cells were seeded onto a 24 well plate as above and incubated for 24 hr. The media was replenished with varying amounts of the calcium ionophore (ionomycin) (4-40 µl; (5 mg/ml)) and further incubated for 24 hr. Cells were collected and apoptosis analysed by flow cytometry.

8.11 MICROSCOPY STAININGS

Jurkat cells (2 x 10^5) were preincubated with $[Zn\mathbf{L}^{12}]^{2+}$ (77.6 µM) (10 µl) for 1 hr at 4^{o}C. Thereafter cells were washed (centrifuged at 180 x g for 3 min) with 1.0 ml PBS/0.25%

BSA/0.01 M NaN_3 and incubated with Qdot-streptavidin conjugate (1 µL) 30 min at 4°C. The cell samples were then washed again (centrifuged at 180 x g for 3 min) with 1.0 ml PBS and ~200 µl of the sample was placed on a microscope slide with a coverslip for analysis by confocal microscopy.

8.11.1 Image acquisition

Images were obtained using a Bio-Rad Radiance 2100 confocal laser scanning microscope (Bio-Rad Laboratories, Hemel Hempstead, UK) equipped with Ar (488 nm), Green HeNe (563 nm) and Red diode (637 nm) laser lines and connected to a Nikon TE 2000E inverted microscope (Nikon, Japan). Images were collected using Lasersharp2000 software under the following conditions; laser excitation line Ar (488 nm), fluorescence from samples passed through 500 and 560 nm dichroic filters and was collected in photomultiplier tubes (PMT) equipped with the following emission filters, 515/30 and 570 nm long pass. The laser scan speed was set at 166 lines per sec, and the viewable area was between 20 and 200 μm^2 when using a 60x oil objective.

8.12 LABELLING OF JURKAT CELLS USING CD8 MAB

Jurkat cells (2 x 10^5) were incubated with CD8 mAb (10 µl) for 30 min at 4°C. Cells were washed (180 x g for 3 min) (PBS) and then incubated with mouse biotinylated mouse IgG (10 µl) for 30 min at 4°C. Cells were washed again (180 x g for 3 min) (PBS) and finally incubated with Cy5-streptavidin (10 µl) or Qdot-streptavidin conjugates (1 µl) for 30 min at 4°C. Binding was analysed by flow cytometry at FL-3 - FL-4 channels.

8.13 LABELLING OF JURKAT CELLS USING $[ZnL^{12}]^{2+}$ AND CY5

Jurkat cells (2 x 10^5) were incubated with $[Zn\mathbf{L}^{12}]^{2+}$ (77.6 µM, 10 µl) for 1 hr at 4°C. Cells were washed with PBS (180 x g for 3 min) and then incubated with Cy5-streptavidin conjugate (10 µl) for 1 hr at 4°C. Finally cells were washed with PBS (180 x g for 3 min) fixed in 200 µl of PBS and analysed by flow cytometry at FL-3 channel.

8.14 COMPETITIVE BINDING OF $[ZnL^{12}]^{2+}$ WITH MAB 44716

Jurkat cells (2×10^5) were incubated with $[Zn\mathbf{L}^{12}]^{2+}$ (77.6 µM, 10 µl) for 30 min at 4^oC. Cells were washed with PBS (180 x g for 3 min) and then incubated with mAb 44716 (10 µg/ml, 10 µl) for 1 hr. Thereafter cells were washed (centrifuged at 180 x g for 3 min) with 1.0 ml PBS, and incubated with the secondary fluorescein isothiocyanate conjugated anti-mouse antibody (IgG-FITC, diluted 1:100 in PBS) for 30 min at 4^oC. Cells were finally washed with PBS (180 x g for 3 min), fixed in PBS (200 µl) and binding of the mAb analysed by flow cytometry.

8.15 BINDING OF CY5-STREPTAVIDIN CONJUGATE USING ANTI-CXCR4 MAB 44716

This was carried out as in section 8.12 (labelling of CD8 mAb), however anti-CXCR4 mAb 44716 (10 µg/ml, 10 µl) was used instead of the CD8 mAb.

8.16 EMISSION SPECTRA OF QDOT-STREPTAVIDIN CONJUGATES

The emission spectra of the Qdot-streptavidin conjugates 605, 655 and 705 (3.3 nM) were recorded (488-900 nm), with excitation at 488 nm in a fluorescent spectrophotometer set at high sensitivity. Rhodamine B (3.5 nM) was used a positive control and distilled water (dH_2O) as a negative control. Rhodamine B and Qdots were diluted using dH_2O.

8.17 MIF AND CXCR4

Jurkat cells (1×10^5) were incubated (4^oC) with rhMIF (10 µl) (R&D Systems, UK) (10 µg/ml) for 20-60 mins. Thereafter cells were washed with PBS (centrifuged at 180 x g for 3 min), anti-human MIF (IgG goat) (R&D Systems, UK) (10 µg/ml) added (10 µl) and incubated for 30 min at 4^oC. Cells were washed with PBS (centrifuged at 180 x g for 3 min) and incubated for a further 30 min (4^oC) with an anti-goat-IgG FITC conjugate

(1:100) (AbD Serotec, UK). Cells were finally washed with PBS (centrifuged at 180 x g for 3 min) and analysed resuspended in PBS (200 µl) and binding analysed on a FACScan flow cytometer (BD Biosciences Europe, Erembodegem, Belguim). Data were acquired and analysed with CellQuest software (Becton Dickinson) on an Apple Macintosh computer. As a negative control for non specific background staining, the cells were stained in parallel with a negative control goat IgG (R&D Sytsems, UK) (10 µg/ml).

8.18 INTERNALISATION OF CXCR4 AND MIF

Jurkat cells (1 x 10^5) were incubated (4^oC) with rhMIF (R&D Systems, UK) (10 µg/ml, 10 µl) for 10-30 min and 2-4 hr. Cells were then washed with PBS (centrifuged at 180 x g for 3 min) and incubated at 4^oC with an anti-CXCR4 mAb 44716 (R&D Systems, UK) (10 µg/ml, 10 µl)) for 15 min. Thereafter cells were washed (centrifuged at 180 x g for 3 min) with 1.0 ml PBS/0.25% BSA/0.01 M NaN_3, and incubated with the secondary fluorescein isothiocyanate conjugated anti-mouse antibody IgG-FITC, diluted 1:100 in PBS/0.25% BSA/0.01 M NaN_3, for 30 min at 4^oC. After further washing (centrifuged at 180 x g for 3 min) with 1.0 ml PBS/0.25% BSA/0.01 M NaN_3, the cell samples were fixed in 300 µl of PBS/0.25% BSA/0.01 M NaN_3 and analysed on a FACScan flow cytometer (BD Biosciences Europe, Erembodegem, Belgium). Data were acquired and analysed with CellQuest software (Becton Dickinson). As a negative control for non specific background staining, the cells were stained in parallel with a negative control mouse IgG (diluted 1:100 in PBS/0.25% BSA/0.01 M NaN_3).

8.19 INVASION ASSAY

Cell invasion experiments were performed with 8-µm porous chambers coated with matrigel (BD Bioscences) according to the manufacturer's instructions. Matrigel plates were first allowed to thaw for 20 min at room temperature followed by the addition (0.5 ml) of cold serum free culture media in the upper chamber and lower well. These plates

were then incubated for 2 hrs in a 37°C 5% CO_2 humid atmosphere. Thereafter media was removed from both lower and upper compartments and the plate was ready for use.

Cells (2 x 10^5/ml) were added (0.5 ml) to the top compartment in serum free culture media followed by serum free media in the bottom compartment (0.75 ml). CXCL12 (0, 12.5, 37.5, 75, 100 nM) and 5% FBS were used as chemoattractants in the lower compartment. To determine the effect of CXCR4 antagonism, relevant CXCR4 antagonist was added (2-200 nM) in the upper compartment with the cells at the start. Cells were then allowed to invade through the matrigel membrane for 48 h in a 37°C 5% CO_2 humid atmosphere.

Thereafter the upper surface of the filters was scraped twice with cotton swabs (sterile) to remove non-invading cells. The invasive cells underneath were fixed in absolute ethanol (5 min) and stained with crystal violet (0.5 %) (5 min). The experiments were repeated in duplicate wells, and the number of invading cells in five fields of view (FOV) per filter was counted microscopically at x400 magnification. One field per view per filter was photographed using a colour camera (CoolSnap Pro Color (Media Cybernetics Inc, USA) attached to an integrated light microscope (Laborlux S (Leica, Germany)). Photographs were captured using the Image-Pro Plus version 5.1.2 software (Media Cybernetics Inc, USA).

8.20 3D SPHEROID TUMOUR FORMATION

Δ34 cells (5 x 10^4/ml) were placed on an agarose (1.5%) gel layer in a well (24 well plate) containing 1 ml of complete media. The plate was then incubated for 4 days in a 37^oC 5% CO_2 atmosphere. Pictures of the spheroid were taken after 24 hr and 4 days of incubation using a colour camera (CoolSnap Pro Color (Media Cybernetics Inc, USA) attached to an integrated light microscope (Laborlux S (Leica, Germany)). Photographs were captured using the Image-Pro Plus version 5.1.2 software (Media Cybernetics Inc, USA).

8.21 FLOW CYTOMETRY FL DETECTION CHANNELS

Fluorescence was detected using the following FL channels in the FACScan flow cytometer (BD Biosciences Europe, Erembodegem, Belgium):

FL-1 530/30 nm (FITC)
FL-2 575/26 nm (PE/PI)
FL-3 Long Pass 650 nm (PerCp)
FL-4 630/22 nm

References

(1) Laing, K. J.; Secombes, C. J. *Dev. Comp. Immunol.* **2004**, *28*, 443.
(2) http://www.medtrack.com/research/default.asp.(10th November 2009)
(3) Baggiolini, M.; Dewald, B.; Moser, B. *Annu. Rev. Immunol.* **1997**, *15*, 675.
(4) Christopherson, K.; Hromas, R. *Stem Cells* **2001**, *19*, 388.
(5) Hogaboam, C. M.; Carpenter, K. J.; Schuh, J. M.; Proudfoot, A.; Bridger, G.; Buckland, K. F. *Pharmacol. Therapeut.* **2005**, *107*, 314.
(6) Horuk, R. *Cytokine Growth F. R.* **2001**, *12*, 313.
(7) Horn, F.; Bettler, E.; Oliveira, L.; Campagne, F.; Cohen, F. E.; Vriend, G. *Nucleic Acids Res.* **2003**, *31*, 294.
(8) Rot, A.; von Andrian, U. H. *Annu. Rev. Immunol.* **2004**, *22*, 891.
(9) Baggiolini, M. *Nature* **1998**, *392*, 565.
(10) Comerford, I.; Litchfield, W.; Harata-Lee, Y.; Nibbs, R. J. B.; McColl, S. R. *Bioessays* **2007**, *29*, 237.
(11) Bockaert, J.; Pin, J. P. *Embo Journal* **1999**, *18*, 1723.
(12) Murphy, P. M. *Pharmacol. Rev.* **2002**, *54*, 227.
(13) Murphy, P. M.; Baggiolini, M.; Charo, I. F.; Hebert, C. A.; Horuk, R.; Matsushima, K.; Miller, L. H.; Oppenheim, J. J.; Power, C. A. *Pharmacol. Rev.* **2000**, *52*, 145.
(14) Murdoch, C.; Finn, A. *Blood* **2000**, *95*, 3032.
(15) Proudfoot, A. E. I. *Nat. Rev. Immunol.* **2002**, *2*, 106.
(16) Johnson, Z.; Power, C. A.; Weiss, C.; Rintelen, F.; Ji, H.; Ruckle, T.; Camps, M.; Wells, T. N. C.; Schwarz, M. K.; Proudfoot, A. E. I.; Rommel, C. *Biochem. Soc. Trans.* **2004**, *32*, 366.
(17) Palczewski, K.; Kumasaka, T.; Hori, T.; Behnke, C. A.; Motoshima, H.; Fox, B. A.; Le Trong, I.; Teller, D. C.; Okada, T.; Stenkamp, R. E.; Yamamoto, M.; Miyano, M. *Science* **2000**, *289*, 739.
(18) Rasmussen, S. G. F.; Choi, H. J.; Rosenbaum, D. M.; Kobilka, T. S.; Thian, F. S.; Edwards, P. C.; Burghammer, M.; Ratnala, V. R. P.; Sanishvili, R.; Fischetti, R. F.; Schertler, G. F. X.; Weis, W. I.; Kobilka, B. K. *Nature* **2007**, *450*, 383.
(19) Cherezov, V.; Rosenbaum, D. M.; Hanson, M. A.; Rasmussen, S. G. F.; Thian, F. S.; Kobilka, T. S.; Choi, H. J.; Kuhn, P.; Weis, W. I.; Kobilka, B. K.; Stevens, R. C. *Science* **2007**, *318*, 1258.
(20) Olson, T. S.; Ley, K. *Am. J. Physiol-Reg. I.* **2002**, *283*, R7.
(21) Leopoldt, D.; Hanck, T.; Exner, T.; Maier, U.; Wetzker, R.; Nurnberg, B. *J. Biol. Chem.* **1998**, *273*, 7024.
(22) Sallusto, F.; Mackay, C. R.; Lanzavecchia, A. *Annu. Rev. Immunol.* **2000**, *18*, 593.
(23) Li, Z.; Jiang, H. P.; Xie, W.; Zhang, Z. C.; Smrcka, A. V.; Wu, D. Q. *Science* **2000**, *287*, 1046.
(24) Balkwill, F. *Nat. Rev. Cancer* **2004**, *4*, 540.
(25) Balabanian, K.; Lagane, B.; Infantino, S.; Chow, K. Y. C.; Harriague, J.; Moepps, B.; Arenzana-Seisdedos, F.; Thelen, M.; Bachelerie, F. *J. Biol. Chem.* **2005**, *280*, 35760.

(26) Loetscher, M.; Geiser, T.; Oreilly, T.; Zwahlen, R.; Baggiolini, M.; Moser, B. *J. Biol. Chem.* **1994**, *269*, 232.
(27) Bleul, C. C.; Farzan, M.; Choe, H.; Parolin, C.; ClarkLewis, I.; Sodroski, J.; Springer, T. A. *Nature* **1996**, *382*, 829.
(28) Oberlin, E.; Amara, A.; Bachelerie, F.; Bessia, C.; Virelizier, J. L.; ArenzanaSeisdedos, F.; Schwartz, O.; Heard, J. M.; ClarkLewis, I.; Legler, D. F.; Loetscher, M.; Baggiolini, M.; Moser, B. *Nature* **1996**, *382*, 833.
(29) Chabot, D. J.; Zhang, P. F.; Quinnan, G. V.; Broder, C. C. *J. Virol.* **1999**, *73*, 6598.
(30) Zhou, N. M.; Luo, Z. W.; Luo, J. S.; Liut, D. X.; Hall, J. W.; Pomerantz, R. J.; Huang, Z. W. *J. Biol. Chem.* **2001**, *276*, 42826.
(31) Aiuti, A.; Cipponi, A.; Tavian, M.; Arcelloni, C.; Zappone, E.; Ficara, F.; Paroni, R.; Hoxie, J.; Peault, B.; Bordignon, C. *Blood* **1997**, *90*, 1142.
(32) Bleul, C. C.; Wu, L. J.; Hoxie, J. A.; Springer, T. A.; Mackay, C. R. *Proc. Natl. Acad. Sci. U. S. A.* **1997**, *94*, 1925.
(33) Gupta, S. K.; Lysko, P. G.; Pillarisetti, K.; Ohlstein, E.; Stadel, J. M. *J. Biol. Chem.* **1998**, *273*, 4282.
(34) Juremalm, M.; Hjertson, M.; Olsson, N.; Harvima, I.; Nilsson, K.; Nilsson, G. *Eur. J. Immunol.* **2000**, *30*, 3614.
(35) Nakayama, T.; Hieshima, K.; Izawa, D.; Tatsumi, Y.; Kanamaru, A.; Yoshie, O. *J. Immunol.* **2003**, *170*, 1136.
(36) Schecter, A. D.; Berman, A. B.; Taubman, M. B. *Microcirculation* **2003**, *10*, 265.
(37) Zoeteweij, J. P.; Golding, H.; Mostowski, H.; Blauvelt, A. *J. Immunol.* **1998**, *161*, 3219.
(38) Ara, T.; Nakamura, Y.; Egawa, T.; Sugiyama, T.; Abe, K.; Kishimoto, T.; Matsui, Y.; Nagasawa, T. *Proc. Natl. Acad. Sci. U. S. A.* **2003**, *100*, 5319.
(39) Jourdan, P.; Abbal, C.; Nora, N.; Hori, T.; Uchiyama, T.; Vendrell, J. P.; Bousquet, J.; Taylor, N.; Pene, J.; Yssel, H. *J. Immunol.* **1998**, *160*, 4153.
(40) Aiuti, A.; Webb, I. J.; Bleul, C.; Springer, T.; GutierrezRamos, J. C. *J. Exp. Med.* **1997**, *185*, 111.
(41) Broxmeyer, H. E.; Cooper, S.; Kohli, L.; Hangoc, G.; Lee, Y.; Mantel, C.; Clapp, D. W.; Kim, C. H. *J. Immunol.* **2003**, *170*, 421.
(42) Kucia, M.; Jankowski, K.; Reca, R.; Wysoczynski, M.; Bandura, L.; Allendorf, D. J.; Zhang, J.; Ratajczak, J.; Ratajczak, M. Z. *J. Mol. Histol.* **2004**, *35*, 233.
(43) Lataillade, J. J.; Domenech, J.; Le Bousse-Kerdiles, M. C. *Eur. Cytokine Netw.* **2004**, *15*, 177.
(44) Stein, J. V.; Nombela-Arrieta, C. *Immunology* **2005**, *116*, 1.
(45) Levesque, J. P.; Hendy, J.; Takamatsu, Y.; Simmons, P. J.; Bendall, L. J. *J. Clin. Invest.* **2003**, *111*, 187.
(46) Petit, I.; Szyper-Kravitz, M.; Nagler, A.; Lahav, M.; Peled, A.; Habler, L.; Ponomaryov, T.; Taichman, R. S.; Arenzana-Seisdedos, F.; Fujii, N.; Sandbank, J.; Zipori, D.; Lapidot, T. *Nat. Immunol.* **2002**, *3*, 687.

(47) Semerad, C. L.; Christopher, M. J.; Liu, F. L.; Short, B.; Simmons, P. J.; Winkler, I.; Levesque, J. P.; Chappel, J.; Ross, F. P.; Link, D. C. *Blood* **2005**, *106*, 3020.
(48) Kollet, O.; Shivtiel, S.; Chen, Y. Q.; Suriawinata, J.; Thung, S. N.; Dabeva, M. D.; Kahn, J.; Spiegel, A.; Dar, A.; Samira, S.; Goichberg, P.; Kalinkovich, A.; Arenzana-Seisdedos, F.; Nagler, A.; Hardan, Z.; Revel, M.; Shafritz, D. A.; Lapidot, T. *J. Clin. Invest.* **2003**, *112*, 160.
(49) Gerlach, L. O.; Skerlj, R. T.; Bridger, G. J.; Schwartz, T. W. *J. Biol. Chem.* **2001**, *276*, 14153.
(50) Bleul, C. C.; Schultze, J. L.; Springer, T. A. *J. Exp. Med.* **1998**, *187*, 753.
(51) Hauser, A. E.; Debes, G. F.; Arce, S.; Cassese, G.; Hamann, A.; Radbruch, A.; Manz, R. A. *J. Immunol.* **2002**, *169*, 1277.
(52) Ma, Q.; Jones, D.; Borghesani, P. R.; Segal, R. A.; Nagasawa, T.; Kishimoto, T.; Bronson, R. T.; Springer, T. A. *Proc. Natl. Acad. Sci. U. S. A.* **1998**, *95*, 9448.
(53) Nagasawa, T.; Hirota, S.; Tachibana, K.; Takakura, N.; Nishikawa, S.; Kitamura, Y.; Yoshida, N.; Kikutani, H.; Kishimoto, T. *Nature* **1996**, *382*, 635.
(54) Tachibana, K.; Hirota, S.; Iizasa, H.; Yoshida, H.; Kawabata, K.; Kataoka, Y.; Kitamura, Y.; Matsushima, K.; Yoshida, N.; Nishikawa, S.; Kishimoto, T.; Nagasawa, T. *Nature* **1998**, *393*, 591.
(55) Lu, W.; Gersting, J. A.; Maheshwari, A.; Christensen, R. D.; Calhoun, D. A. *Early Hum. Dev.* **2005**, *81*, 489.
(56) Tashiro, K.; Tada, H.; Heilker, R.; Shirozu, M.; Nakano, T.; Honjo, T. *Science* **1993**, *261*, 600.
(57) Hartmann, T. N.; Grabovsky, V.; Pasvolsky, R.; Shulman, Z.; Buss, E. C.; Spiegel, A.; Nagler, A.; Lapidot, T.; Thelen, M.; Alon, R. *J. Leukoc. Biol.* **2008**, *84*, 1130.
(58) Sierro, F.; Biben, C.; Martinez-Munoz, L.; Mellado, M.; Ransohoff, R. M.; Li, M.; Woehl, B.; Leung, H.; Groom, J.; Batten, M.; Harvey, R. P.; Martinez-A, C.; Mackay, C. R.; Mackay, F. *Proc. Natl. Acad. Sci. U. S. A.* **2007**, *104*, 14759.
(59) Shirozu, M.; Nakano, T.; Inazawa, J.; Tashiro, K.; Tada, H.; Shinohara, T.; Honjo, T. *Genomics* **1995**, *28*, 495.
(60) Crump, M. P.; Gong, J. H.; Loetscher, P.; Rajarathnam, K.; Amara, A.; Arenzana-Seisdedos, F.; Virelizier, J. L.; Baggiolini, M.; Sykes, B. D.; Clark-Lewis, I. *Embo Journal* **1997**, *16*, 6996.
(61) Gozansky, E. K.; Louis, J. M.; Caffrey, M. C.; Clore, G. M. *J. Mol. Biol.* **2005**, *345*, 651.
(62) Hesselgesser, J.; Liang, M.; Hoxie, J.; Greenberg, M.; Brass, L. F.; Orsini, M. J.; Taub, D.; Horuk, R. *J. Immunol.* **1998**, *160*, 877.
(63) Nagasawa, T.; Kikutani, H.; Kishimoto, T. *Proc. Natl. Acad. Sci. U. S. A.* **1994**, *91*, 2305.
(64) Bleul, C. C.; Fuhlbrigge, R. C.; Casasnovas, J. M.; Aiuti, A.; Springer, T. A. *J. Exp. Med.* **1996**, *184*, 1101.

(65) Herbein, G.; Mahlknecht, U.; Batliwalla, F.; Gregersen, P.; Pappas, T.; Butler, J.; O'Brien, W. A.; Verdin, E. *Nature* **1998**, *395*, 189.
(66) Aust, G.; Steinert, M.; Kiessling, S.; Kamprad, M.; Simchen, C. *J. Clin. Endocr. Metab.* **2001**, *86*, 3368.
(67) Muller, A.; Homey, B.; Soto, H.; Ge, N. F.; Catron, D.; Buchanan, M. E.; McClanahan, T.; Murphy, E.; Yuan, W.; Wagner, S. N.; Barrera, J. L.; Mohar, A.; Verastegui, E.; Zlotnik, A. *Nature* **2001**, *410*, 50.
(68) Nagasawa, T.; Tachibana, K.; Kishimoto, T. *Semin. Immunol.* **1998**, *10*, 179.
(69) Yun, H. J.; Jo, D. Y. *Journal of Korean Medical Science* **2003**, *18*, 679.
(70) Derdeyn, C. A.; Costello, C.; Kilby, J. M.; Sfakianos, G.; Saag, M. S.; Kaslow, R.; Bucy, R. P. *Aids Res. Hum. Retrovir.* **1999**, *15*, 1063.
(71) Zou, Y. R.; Kottmann, A. H.; Kuroda, M.; Taniuchi, I.; Littman, D. R. *Nature* **1998**, *393*, 595.
(72) McGrath, K. E.; Koniski, A. D.; Maltby, K. M.; McGann, J. K.; Palis, J. *Dev. Biol.* **1999**, *213*, 442.
(73) Andre, F.; Soria, J. C.; Assi, H.; Delaloge, S.; Spielmann, M. *Bull. Cancer* **2004**, *91*, S254.
(74) Carvalho-Pinto, C.; Garcia, M. I.; Gomez, L.; Ballesteros, A.; Zaballos, A.; Flores, J. M.; Mellado, M.; Rodriguez-Frade, J. M.; Balomenos, D.; Martinez, C. *Eur. J. Immunol.* **2004**, *34*, 548.
(75) Luster, A. D. *New Engl. J. Med.* **1998**, *338*, 436.
(76) Matthys, P.; Hatse, S.; Vermeire, K.; Wuyts, A.; Bridger, G.; Henson, G. W.; De Clercq, E.; Billiau, A.; Schols, D. *J. Immunol.* **2001**, *167*, 4686.
(77) Kruizinga, R. C.; Bestebroer, J.; Berghuis, P.; de Haas, C. J. C.; Links, T. P.; de Vries, E. G. E.; Walenkamp, A. M. E. *Curr. Pharm. Design* **2009**, *15*, 3396.
(78) Schroder, J. M.; Noso, N.; Sticherling, M.; Christophers, E. *J. Leukoc. Biol.* **1996**, *59*, 1.
(79) Schulz, B. S.; Michel, G.; Wagner, S.; Suss, R.; Beetz, A.; Peter, R. U.; Kemeny, L.; Ruzicka, T. *J. Immunol.* **1993**, *151*, 4399.
(80) Nelken, N. A.; Coughlin, S. R.; Gordon, D.; Wilcox, J. N. *J. Clin. Invest.* **1991**, *88*, 1121.
(81) Rakesh, K.; Agrawal, D. K. *Int. Immunopharmacol.* **2005**, *5*, 1487.
(82) Hosaka, S.; Akahoshi, T.; Wada, C.; Kondo, H. *Clin. Exp. Immunol.* **1994**, *97*, 451.
(83) Kasama, T.; Strieter, R. M.; Lukacs, N. W.; Lincoln, P. M.; Burdick, M. D.; Kunkel, S. L. *J. Clin. Invest.* **1995**, *95*, 2868.
(84) Strieter, R. M.; Standiford, T. J.; Huffnagle, G. B.; Colletti, L. M.; Lukacs, N. W.; Kunkel, S. L. *J. Immunol.* **1996**, *156*, 3583.
(85) Iwamoto, T.; Okamoto, H.; Toyama, Y.; Momohara, S. *Febs Journal* **2008**, *275*, 4448.
(86) Fife, B. T.; Huffnagle, G. B.; Kuziel, W. A.; Karpus, W. J. *J. Exp. Med.* **2000**, *192*, 899.
(87) Gerard, C.; Rollins, B. J. *Nat. Immunol.* **2001**, *2*, 108.
(88) Ransohoff, R. M.; Bacon, K. B. *Expert Opin. Invest. Drugs* **2000**, *9*, 1079.

(89) Reale, M.; Iarlori, C.; Feliciani, C.; Gambi, D. *J. Alzheimers Dis.* **2008**, *14*, 147.
(90) Baggiolini, M.; Dahinden, C. A. *Immunol. Today* **1994**, *15*, 127.
(91) Gonzalo, J. A.; Lloyd, C. M.; Wen, D. Y.; Albar, J. P.; Wells, T. N. C.; Proudfoot, A.; Martinez, C.; Dorf, M.; Bjerke, T.; Coyle, A. J.; Gutierrez-Ramos, J. C. *J. Exp. Med.* **1998**, *188*, 157.
(92) Keane, M. P.; Strieter, R. M. *Crit. Care. Med.* **2000**, *28*, N13.
(93) Locati, M.; Murphy, P. M. *Annu. Rev. Med.* **1999**, *50*, 425.
(94) Pomerantz, R. J.; Horn, D. L. *Nat. Med.* **2003**, *9*, 867.
(95) Pease, J. E. *Curr. Drug Targets* **2006**, *7*, 3.
(96) Pease, J. E.; Williams, T. J. *J. Allergy Clin. Immunol.* **2006**, *118*, 305.
(97) Palmqvist, C.; Wardlaw, A. J.; Bradding, P. *Br. J. Pharmacol.* **2007**, *151*, 725.
(98) Gosselin, R. D.; Dansereau, M. A.; Pohl, M.; Kitabgi, P.; Beaudet, N.; Sarret, P.; Parsadaniantz, S. M. *Curr. Med. Chem.* **2008**, *15*, 2866.
(99) Savarin-Vuaillat, C.; Ransohof, R. M. *Neurotherapeutics* **2007**, *4*, 590.
(100) Balkwill, F.; Mantovani, A. *Lancet* **2001**, *357*, 539.
(101) Murphy, P. M. *New Engl. J. Med.* **2001**, *345*, 833.
(102) Vicari, A. P.; Caux, C. *Cytokine Growth F. R.* **2002**, *13*, 143.
(103) Azenshtein, E.; Luboshits, G.; Shina, S.; Neumark, E.; Shahbazian, D.; Weil, M.; Wigler, N.; Keydar, I.; Ben-Baruch, A. *Cancer Res.* **2002**, *62*, 1093.
(104) Belperio, J. A.; Keane, M. P.; Arenberg, D. A.; Addison, C. L.; Ehlert, J. E.; Burdick, M. D.; Strieter, R. M. *J. Leukoc. Biol.* **2000**, *68*, 1.
(105) Skinnider, B. F.; Mak, T. W. *Blood* **2002**, *99*, 4283.
(106) Kleeff, J.; Kusama, T.; Rossi, D. L.; Ishiwata, T.; Maruyama, H.; Friess, H.; Buchler, M. W.; Zlotnik, A.; Korc, M. *Int. J. Cancer* **1999**, *81*, 650.
(107) Takamori, H.; Oades, Z. G.; Hoch, R. C.; Burger, M.; Schraufstatter, I. U. *Pancreas* **2000**, *21*, 52.
(108) Panse, J.; Friedrichs, K.; Marx, A.; Hildebrandt, Y.; Luetkens, T.; Bartels, K.; Horn, C.; Stahl, T.; Cao, Y.; Milde-Langosch, K.; Niendorf, A.; Kroger, N.; Wenzel, S.; Leuwer, R.; Bokemeyer, C.; Hegewisch-Becker, S.; Atanackovic, D. *Brit. J. Cancer* **2008**, *99*, 930.
(109) Vandercappellen, J.; Van Damme, J.; Struyf, S. *Cancer Lett.* **2008**, *267*, 226.
(110) Kakinuma, T.; Hwang, S. T. *J. Leukoc. Biol.* **2006**, *79*, 639.
(111) Cameron, M. J.; Arreaza, G. A.; Grattan, M.; Meagher, C.; Sharif, S.; Burdick, M. D.; Strieter, R. M.; Cook, D. N.; Delovitch, T. L. *J. Immunol.* **2000**, *165*, 1102.
(112) Bruck, P.; Bartsch, W.; Penna-Martinez, M.; Kahles, H.; Seidl, C.; Bohme, A.; Badenhoop, K.; Ramos-Lopez, E. *Hum. Immunol.* **2009**, *70*, 552.
(113) Kanbe, K.; Takemura, T.; Takeuchi, K.; Chen, Q.; Takagishi, K.; Inoue, K. *J. Bone Joint Surg. [Br]* **2004**, *86B*, 296.

(114) Terada, R.; Yamamoto, K.; Hakoda, T.; Shimada, N.; Okano, N.; Baba, N.; Ninomiya, Y.; Gershwin, M. E.; Shiratori, Y. *Lab. Invest.* **2003**, *83*, 665.
(115) Ruehr, M. L.; Iqbal, A. S.; Chung, M. K.; Gillinov, A. M.; Van Wagoner, D. R. *Heart Rhythm* **2005**, *2*, S303.
(116) Diaz, G. A. *Immunol. Rev.* **2005**, *203*, 235.
(117) Diaz, G. A.; Gulino, A. V. *Curr. Allergy Asthma Rep.* **2005**, *5*, 350.
(118) Arya, M.; Patel, H. R. H.; Williamson, M. *Curr. Med. Res. Opin.* **2003**, *19*, 557.
(119) Balkwill, F. *Sem. Cancer Biol.* **2004**, *14*, 171.
(120) Burger, J. A.; Kipps, T. J. *Blood* **2006**, *107*, 1761.
(121) Juarez, J.; Bendall, L. *Histol. Histopathol.* **2004**, *19*, 299.
(122) Luker, K. E.; Luker, G. D. *Cancer Lett.* **2006**, *238*, 30.
(123) Murakami, T.; Cardones, A. R.; Hwang, S. T. *J. Dermatol. Sci.* **2004**, *36*, 71.
(124) Payne, A. S.; Cornelius, L. A. *J. Invest. Dermatol.* **2002**, *118*, 915.
(125) Cooper, C. R.; Chay, C. H.; Gendernalik, J. D.; Lee, H. L.; Bhatia, J.; Taichman, R. S.; McCauley, L. K.; Keller, E. T.; Pienta, K. J. *Cancer* **2003**, *97*, 739.
(126) Ben-Baruch, A. *Breast Cancer Res.* **2002**, *5*, 31.
(127) Su, L. P.; Zhang, J. P.; Xu, H. B.; Wang, Y.; Chu, Y. W.; Liu, R. Z.; Xiong, S. D. *Clin. Cancer Res.* **2005**, *11*, 8273.
(128) Hartmann, T. N.; Burger, M.; Burger, J. A. *J. Biol. Reg. Homeos. Ag.* **2004**, *18*, 126.
(129) Majka, M.; Drukala, J.; Lesko, E.; Wysoczynski, M.; Jenson, A. B.; Ratajczak, M. Z. *Folia Histochem. Cyto.* **2006**, *44*, 155.
(130) Kim, J.; Mori, T.; Chen, S. L.; Amersi, F. F.; Martinez, S. R.; Kuo, C.; Turner, R. R.; Ye, X.; Bilchik, A. J.; Morton, D. L.; Hoon, D. S. B. *Ann. Surg.* **2006**, *244*, 113.
(131) Brand, S.; Dambacher, J.; Beigel, F.; Olszak, T.; Diebold, J.; Otte, J. M.; Goke, B.; Eichhorst, S. T. *Exp. Cell Res.* **2005**, *310*, 117.
(132) Koshiba, T.; Hosotani, R.; Miyamoto, Y.; Ida, J.; Tsuji, S.; Nakajima, S.; Kawaguchi, M.; Kobayashi, H.; Doi, R.; Hori, T.; Fujii, N.; Imamura, M. *Clin. Cancer Res.* **2000**, *6*, 3530.
(133) Mori, T.; Doi, R.; Koizumi, M.; Toyoda, E.; Ito, D.; Kami, K.; Masui, T.; Fujimoto, K.; Tamamura, H.; Hiramatsu, K.; Fujii, N.; Imamura, M. *Mol. Cancer Ther.* **2004**, *3*, 29.
(134) Mori, T.; Doi, R.; Masui, T.; Koizumi, M.; Toyoda, E.; Tulachan, S.; Ito, D.; Kami, K.; Tsuji, S.; Namajima, S.; Kawaguchi, M.; Fujimoto, Y.; Imamura, M. *Gastroenterol.* **2002**, *122*, A490.
(135) Singh, S.; Singh, U. P.; Grizzle, W. E.; Lillard, J. W. *Lab. Invest.* **2004**, *84*, 1666.
(136) Lee, H. J.; Kim, S. W.; Kim, H. Y.; Li, S.; Yun, H. J.; Song, K. S.; Kim, S.; Jo, D. Y. *Int. J. Oncol.* **2009**, *34*, 473.
(137) Marchesi, F.; Monti, P.; Leone, B. E.; Zerbi, A.; Vecchi, A.; Piemonti, L.; Mantovani, A.; Allavena, P. *Cancer Res.* **2004**, *64*, 8420.

(138) Li, J. K.; Yu, L.; Shen, Y.; Zhou, L. S.; Wang, Y. C.; Zhang, J. H. *World J. Gastroenterol.* **2008**, *14*, 2308.
(139) Kim, J.; Takeuchi, H.; Lam, S. T.; Turner, R. R.; Wang, H. J.; Kuo, C.; Foshag, L.; Bilchik, A. J.; Hoon, D. S. B. *J. Clin. Oncol.* **2005**, *23*, 2744.
(140) Pantel, K.; Brakenhoff, R. H. *Nat. Rev. Cancer* **2004**, *4*, 448.
(141) Porcile, C.; Bajetto, A.; Barbieri, F.; Barbero, S.; Bonavia, R.; Biglieri, M.; Pirani, P.; Florio, T.; Schettini, G. *Exp. Cell Res.* **2005**, *308*, 241.
(142) Wang, J. H.; Wang, J. C.; Sun, Y. X.; Song, W. Y.; Nor, J. E.; Wang, C. Y.; Taichman, R. S. *Cell. Signal.* **2005**, *17*, 1578.
(143) Ehtesham, M.; Winston, J. A.; Kabos, P.; Thompson, R. C. *Oncogene* **2006**, *25*, 2801.
(144) Hong, X.; Jiang, F.; Kalkanis, S. N.; Zhang, Z. G.; Zhang, X. P.; deCarvalho, A. C.; Katakowski, M.; Bobbitt, K.; Mikkelsen, T.; Chopp, M. *Cancer Lett.* **2006**, *236*, 39.
(145) Rubin, J. B.; Kung, A. L.; Klein, R. S.; Chan, J. A.; Sun, Y. P.; Schmidt, K.; Kieran, M. W.; Luster, A. D.; Segal, R. A. *Proc. Natl. Acad. Sci. U. S. A.* **2003**, *100*, 13513.
(146) Bertolini, F.; Dell'Agnola, C.; Mancuso, P.; Rabascio, C.; Burlini, A.; Monestiroli, S.; Gobbi, A.; Pruneri, G.; Martinelli, G. *Cancer Res.* **2002**, *62*, 3106.
(147) Ierano, C.; Giuliano, P.; D'Alterio, C.; Cioffi, M.; Mettivier, V.; Portella, L.; Napolitano, M.; Barbieri, A.; Arra, C.; Liguori, G.; Franco, R.; Palmieri, G.; Rozzo, C.; Pacelli, R.; Castello, G.; Scala, S. *Cell Cycle* **2009**, *8*, 1228.
(148) Reed, J. C. *J. Clin. Oncol.* **1999**, *17*, 2941.
(149) Chari, N. S.; Pinaire, N. L.; Thorpe, L.; Medeiros, L. J.; Routbort, M. J.; McDonnell, T. J. *Apoptosis* **2009**, *14*, 336.
(150) Sadir, R.; Baleux, F.; Grosdidier, A.; Imberty, A.; Lortat-Jacob, H. *J. Biol. Chem.* **2001**, *276*, 8288.
(151) Netelenbos, T.; Zuijderduijn, S.; van den Born, J.; Kessler, F. L.; Zweegman, S.; Huijgens, P. C.; Drager, A. M. *J. Leukoc. Biol.* **2002**, *72*, 353.
(152) Busillo, J. M.; Benovic, J. L. *Biochim. Biophys. Acta-Biomembr.* **2007**, *1768*, 952.
(153) Rubin, J. B. *Sem. Cancer Biol.* **2009**, *19*, 116.
(154) Weinberg, R. A. *The Biology of Cancer*; Garland Science, 2007.
(155) Vila-Coro, A. J.; Rodriguez-Frade, J. M.; De Ana, A. M.; Moreno-Ortiz, M. C.; Martinez, C.; Mellado, M. *Faseb J.* **1999**, *13*, 1699.
(156) Yang, L. H.; Jackson, E.; Woerner, B. M.; Perry, A.; Piwnica-Worms, D.; Rubin, J. B. *Cancer Res.* **2007**, *67*, 651.
(157) Li, Y. M.; Pan, Y.; Wei, Y. K.; Cheng, X. Y.; Zhou, B. H. P.; Tan, M.; Zhou, X. Y.; Xia, W. Y.; Hortobagyi, G. N.; Yu, D. H.; Hung, M. C. *Cancer Cell* **2004**, *6*, 459.
(158) Leonard, J. T.; Roy, K. *Curr. Med. Chem.* **2006**, *13*, 911.
(159) Briz, V.; Poveda, E.; Soriano, V. *Med. Clin.-Barcelona* **2006**, *126*, 341.
(160) Briz, V.; Poveda, E.; Soriano, V. *J. Antimicrob. Chemoth.* **2006**, *57*, 619.

(161) Endres, M. J.; Clapham, P. R.; Marsh, M.; Ahuja, M.; Turner, J. D.; McKnight, A.; Thomas, J. F.; Stoebenau-Haggarty, B.; Choe, S.; Vance, P. J. *Cell* **1996**, *87*, 745.
(162) Schols, D. *Curr. Top. Med. Chem.* **2004**, *4*, 883.
(163) Ray, N.; Dorns, R. W. In *Chemokines and Viral Infection* 2006; Vol. 303, p 97.
(164) Kwong, P. D.; Wyatt, R.; Robinson, J.; Sweet, R. W.; Sodroski, J.; Hendrickson, W. A. *Nature* **1998**, *393*, 648.
(165) Wyatt, R.; Kwong, P. D.; Desjardins, E.; Sweet, R. W.; Robinson, J.; Hendrickson, W. A.; Sodroski, J. G. *Nature* **1998**, *393*, 705.
(166) Chan, D. C.; Kim, P. S. *Cell* **1998**, *93*, 681.
(167) De Clercq, E. *Nat. Rev. Drug Discov.* **2003**, *2*, 581.
(168) Reeves, J. D.; Lee, F. F.; Miamidian, J. L.; Jabara, C. B.; Juntilla, M. M.; Doms, R. W. *J. Virol.* **2005**, *79*, 4991.
(169) De Clercq, E. *Biochim. Biophys. Acta-Mol. Basis Dis.* **2002**, *1587*, 258.
(170) De Clercq, E. *Med. Chem. Res.* **2004**, *13*, 439.
(171) Lazzarin, A. *Expert Opin. Pharmacother.* **2005**, *6*, 453.
(172) Pomerantz, R. J. *Nature* **2003**, *424*, 136.
(173) Murakami, T.; Nakajima, T.; Koyanagi, N.; Tachibana, K.; Fujii, N.; Tamamura, H.; Yoshida, N.; Waki, M.; Matsumoto, A.; Yoshie, O.; Kishimoto, T.; Yamamoto, N.; Nagasawa, T. *J. Exp. Med.* **1997**, *186*, 1389.
(174) Tamamura, H.; Xu, Y. O.; Hattori, T.; Zhang, X. Y.; Arakaki, R.; Kanbara, K.; Omagari, A.; Otaka, A.; Ibuka, T.; Yamamoto, N.; Nakashima, H.; Fujii, N. *Biochem. Biophys. Res. Commun.* **1998**, *253*, 877.
(175) Tamamura, H.; Hori, A.; Kanzaki, N.; Hiramatsu, K.; Mizumoto, M.; Nakashima, H.; Yamamoto, N.; Otaka, A.; Fujii, N. *FEBS Lett.* **2003**, *550*, 79.
(176) Tamamura, H.; Omagari, A.; Oishi, S.; Kanamoto, T.; Yamamoto, N.; Peiper, S. C.; Nakashima, H.; Otaka, A.; Fujii, N. *Bioorg. Med. Chem. Lett.* **2000**, *10*, 2633.
(177) Tamamura, H.; Tsutsumi, H.; Masuno, H.; Mizokami, S.; Hiramatsu, K.; Wang, Z. X.; Trent, J. O.; Nakashima, H.; Yamamoto, N.; Peiper, S. C.; Fujii, N. *Org. Biomol. Chem.* **2006**, *4*, 2354.
(178) Tamamura, H.; Omagari, A.; Hiramatsu, K.; Gotoh, K.; Kanamoto, T.; Xu, Y. N.; Kodama, E.; Matsuoka, M.; Hattori, T.; Yamamoto, N.; Nakashima, H.; Otaka, A.; Fujii, N. *Bioorg. Med. Chem. Lett.* **2001**, *11*, 1897.
(179) Tamamura, H.; Hiramatsu, K.; Mizumoto, M.; Ueda, S.; Kusano, S.; Terakubo, S.; Akamatsu, M.; Yamamoto, N.; Trent, J. O.; Wang, Z. X.; Peiper, S. C.; Nakashima, H.; Otaka, A.; Fujii, N. *Org. Biomol. Chem.* **2003**, *1*, 3663.
(180) Fujii, N.; Nakashima, H.; Tamamura, H. *Expert Opin. Invest. Drugs* **2003**, *12*, 185.

(181) Tamamura, H.; Fujii, N. *Expert Opinion on Therapeutic Targets* **2005**, *9*, 1267.
(182) Tamamura, H.; Tsutsumi, H.; Fujii, N. *Mini-Rev. Med. Chem.* **2006**, *6*, 989.
(183) Sumnersmith, M.; Zheng, Y.; Zhang, Y. P.; Twist, E. M.; Climie, S. C. *Drugs Exp. Clin. Res.* **1995**, *21*, 1.
(184) Doranz, B. J.; Filion, L. G.; Diaz-Mitoma, F.; Sitar, D. S.; Sahai, J.; Baribaud, F. D.; Orsini, M. J.; Benovic, J. L.; Cameron, W.; Doms, R. W. *Aids Res. Hum. Retrovir.* **2001**, *17*, 475.
(185) Daelemans, D.; Schols, D.; Witvrouw, M.; Pannecouque, C.; Hatse, S.; van Dooren, S.; Hamy, F.; Klimkait, T.; De Clercq, E.; Vandamme, A. M. *Mol. Pharmacol.* **2000**, *57*, 116.
(186) Tamamura, H.; Araki, T.; Ueda, S.; Wang, Z. X.; Oishi, S.; Esaka, A.; Trent, J. O.; Nakashima, H.; Yamamoto, N.; Peiper, S. C.; Otaka, A.; Fujii, N. *J. Med. Chem.* **2005**, *48*, 3280.
(187) Vabeno, J.; Nikiforovich, G. V.; Marshall, G. R. *Chem. Biol. Drug Des.* **2006**, *67*, 346.
(188) Porvasnik, S.; Sakamoto, N.; Kusmartsev, S.; Eruslanov, E.; Kim, W. J.; Cao, W. G.; Urbanek, C.; Wong, D.; Goodison, S.; Rosser, C. J. *Prostate* **2009**, *69*, 1460.
(189) Ichiyama, K.; Yokoyama-Kumakura, S.; Tanaka, Y.; Tanaka, R.; Hirose, K.; Bannai, K.; Edamatsu, T.; Yanaka, M.; Niitani, Y.; Miyano-Kurosaki, N.; Takaku, H.; Koyanagi, Y.; Yamamoto, N. *Proc. Natl. Acad. Sci. U. S. A.* **2003**, *100*, 4185.
(190) Kazmierski, W. M.; Kenakin, T. P.; Gudmundsson, K. S. *Chem. Biol. Drug Des.* **2006**, *67*, 13.
(191) Murakami, T.; Kumakura, S.; Yamazaki, T.; Tanaka, R.; Hamatake, M.; Okuma, K.; Huang, W.; Toma, J.; Komano, J.; Yanaka, M.; Tanaka, Y.; Yamamoto, N. *Antimicrob. Agents Chemother.* **2009**, *53*, 2940.
(192) Schols, D.; Claes, S.; Hatse, S.; Princen, K.; Vermeire, K.; De Clercq, E.; Skerlj, R.; Bridger, G.; Calandra, G. *Antiviral Res.* **2003**, *57*, 2.
(193) Bodart, V.; Anastassov, V.; Darkes, M. C.; Idzan, S. R.; Labrecque, J.; Lau, G.; Mosi, R. M.; Neff, K. S.; Nelson, K. L.; Ruzek, M. C.; Patel, K.; Santucci, Z.; Scarborough, R.; Wong, R. S. Y.; Bridger, G. J.; MacFarland, R. T.; Fricker, S. P. *Biochem. Pharmacol.* **2009**, *78*, 993.
(194) Princen, K.; Hatse, S.; Vermeire, K.; Aquaro, S.; De Clercq, E.; Gerlach, L. O.; Rosenkilde, M.; Schwartz, T. W.; Skerlj, R.; Bridger, G.; Schols, D. *J. Virol.* **2004**, *78*, 12996.
(195) Este, J. A.; DeVreese, K.; Witvrouw, M.; Schmit, J. C.; Vandamme, A. M.; Anne, J.; Desmyter, J.; Henson, G. W.; Bridger, G.; DeClercq, E. *Antiviral Res.* **1996**, *29*, 297.
(196) Baldwin, C. E.; Berkhout, B. *Retrovirology* **2006**, *3*, 84.
(197) Anderson, J.; Akkina, R. *Retrovirology* **2005**, *2*, 53.
(198) De Clercq, E. *Mol. Pharmacol.* **2000**, *57*, 833.
(199) Hatse, S.; Princen, K.; Bridger, G.; Skerlj, R.; Henson, G.; De Clercq, E.; Schols, D. *Antiviral Res.* **2002**, *53*, 5.

(200) Schols, D.; Struyf, S.; VanDamme, J.; Este, J. A.; Henson, G.; DeClercq, E. *J. Exp. Med.* **1997**, *186*, 1383.
(201) De Clercq, E. *Med. Res. Rev.* **2000**, *20*, 323.
(202) Hatse, S.; Princen, K.; De Clercq, E.; Rosenkilde, M. M.; Schwartz, T. W.; Hernandez-Abad, P. E.; Skerlj, R. T.; Bridger, G. J.; Schols, D. *Biochem. Pharmacol.* **2005**, *70*, 752.
(203) Hatse, S.; Princen, K.; Bridger, G.; De Clercq, E.; Schols, D. *FEBS Lett.* **2002**, *527*, 255.
(204) Hatse, S.; Princen, K.; Gerlach, L. O.; Bridger, G.; Henson, G.; De Clercq, E.; Schwartz, T. W.; Schols, D. *Mol. Pharmacol.* **2001**, *60*, 164.
(205) Gupta, S. K.; Pillarisetti, K.; Thomas, R. A.; Aiyar, N. *Immunol. Lett.* **2001**, *78*, 29.
(206) Banisadr, G.; Dicou, E.; Berbar, T.; Rostene, W.; Lombet, A.; Haour, F. *J. Neuroimmunol.* **2000**, *110*, 151.
(207) Gerlach, L. O.; Jakobsen, J. S.; Jensen, K. P.; Rosenkilde, M. R.; Skerlj, R. T.; Ryde, U.; Bridger, G. J.; Schwartz, T. W. *Biochemistry* **2003**, *42*, 710.
(208) Egberink, H. F.; De Clercq, E.; Van Vliet, A. L. W.; Balzarini, J.; Bridger, G. J.; Henson, G.; Horzinek, M. C.; Schols, D. *J. Virol.* **1999**, *73*, 6346.
(209) Adam, K. R.; Antolovich, M.; Atkinson, I. M.; Leong, A. J.; Lindoy, L. F.; McCool, B. J.; Davis, R. L.; Kennard, C. H. L.; Tasker, P. A. *J. Chem. Soc., Chem. Commun.* **1994**, 1539.
(210) Sadler, P. J.; Paisey, S. J. *Chem. Commun.* **2004**, 306.
(211) Bridger, G. J.; Skerlj, R. T.; Thornton, D.; Padmanabhan, S.; Martellucci, S. A.; Henson, G. W.; Abrams, M. J.; Yamamoto, N.; Devreese, K.; Pauwels, R.; Declercq, E. *J. Med. Chem.* **1995**, *38*, 366.
(212) Cabbiness, D. K.; Margerum, D. W. *J. Am. Chem. Soc.* **1970**, *92*, 2151.
(213) DeVos, D. E.; Bein, T. *J. Organomet. Chem.* **1996**, *520*, 195.
(214) Mochizuki, K.; Manaka, S.; Takeda, I.; Kondo, T. *Inorg. Chem.* **1996**, *35*, 5132.
(215) Reichert, D. E.; Lewis, J. S.; Anderson, C. J. *Coord. Chem. Rev.* **1999**, *184*, 3.
(216) Inouye, Y.; Kanamori, T.; Yoshida, T.; Bu, X.; Shionoya, M.; Koike, T.; Kimura, E. *Biol. Pharm. Bull.* **1994**, *17*, 243.
(217) Este, J. A.; Cabrera, C.; De Clercq, E.; Struyf, S.; Van Damme, J.; Bridger, G.; Skerlj, R. T.; Abrams, M. J.; Henson, G.; Gutierrez, A.; Clotet, B.; Schols, D. *Mol. Pharmacol.* **1999**, *55*, 67.
(218) Billo, E. J. *Inorg. Chem.* **1984**, *23*, 236.
(219) Martin, L. Y.; Dehayes, L. J.; Zompa, L. J.; Busch, D. H. *J. Am. Chem. Soc.* **1974**, *96*, 4046.
(220) Liang, X. Y.; Sadler, P. J. *Chem. Soc. Rev.* **2004**, *33*, 246.
(221) Bosnich, B.; Poon, C. K.; Tobe, M. L. *Inorg. Chem.* **1965**, *4*, 1102.
(222) Donnelly, M. A.; Zimmer, M. *Inorg. Chem.* **1999**, *38*, 1650.
(223) Hunter, T. M.; Paisey, S. J.; Park, H. S.; Cleghorn, L.; Parkin, A.; Parsons, S.; Sadler, P. J. *J. Inorg. Biochem.* **2004**, *98*, 713.

(224) Liang, X. Y.; Parkinson, J. A.; Weishaupl, M.; Gould, R. O.; Paisey, S. J.; Park, H. S.; Hunter, T. M.; Blindauer, C. A.; Parsons, S.; Sadler, P. J. *J. Am. Chem. Soc.* **2002**, *124*, 9105.
(225) Liang, X. Y.; Weishaupl, M.; Parkinson, J. A.; Parsons, S.; McGregor, P. A.; Sadler, P. J. *Chem.-Eur. J.* **2003**, *9*, 4709.
(226) Valks, G. C.; McRobbie, G.; Lewis, E. A.; Hubin, T. J.; Hunter, T. M.; Sadler, P. J.; Pannecouque, C.; De Clercq, E.; Archibald, S. J. *J. Med. Chem.* **2006**, *49*, 6162.
(227) De Clercq, E. *Met.-Based Drugs* **1997**, *4*, 173.
(228) Tyson, T. A.; Hodgson, K. O. *Acta Crystallogr.* **1990**, *C46*, 1638.
(229) Rosenkilde, M. M.; Gerlach, L. O.; Jakobsen, J. S.; Skerlj, R. T.; Bridger, G. J.; Schwartz, T. W. *J. Biol. Chem.* **2004**, *279*, 3033.
(230) Brelot, A.; Heveker, N.; Montes, M.; Alizon, M. *J. Biol. Chem.* **2000**, *275*, 23736.
(231) Hunter, T. M.; McNae, I. W.; Liang, X. Y.; Bella, J.; Parsons, S.; Walkinshaw, M. D.; Sadler, P. J. *Proc. Natl. Acad. Sci. U. S. A.* **2005**, *102*, 2288.
(232) Empson, C. J. Ph. D Thesis, University of Hull, Hull, UK, 2006.
(233) Khan, A. M.Sc. Thesis, University of Hull, Hull, UK, 2006.
(234) Khan, A.; Nicholson, G.; Greenman, J.; Madden, L.; McRobbie, G.; Pannecouque, C.; De Clercq, E.; Ullom, R.; Maples, D. L.; Maples, R. D.; Silversides, J. D.; Hubin, T. J.; Archibald, S. J. *J. Am. Chem. Soc.* **2009**, *131*, 3416.
(235) Khan, A.; Silversides, J. D.; Madden, L.; Greenman, J.; Archibald, S. J. *Chem. Commun.* **2007**, 416.
(236) Archibald, S. J.; May, C. M.; Bridgeman, A. J.; Empson, C. J.; Hubin, T. J. *Chem. Commun.* **2004**, 1880.
(237) Boiocchi, M.; Bonizzoni, M.; Fabbrizzi, L.; Foti, F.; Licchelli, M.; Poggi, A.; Taglietti, A.; Zema, M. *Chem.-Eur. J.* **2004**, *10*, 3209.
(238) Weisman, G. R.; Wong, E. H.; Hill, D. C.; Rogers, M. E.; Reed, D. P.; Calabrese, J. C. *Chem. Commun.* **1996**, 947.
(239) Allan, C. C.; Silversides, J. D.; Archibald, S. J. *Dalton Trans.* **2007**, 971.
(240) Niu, W. J.; Wong, E. H.; Weisman, G. R.; Hill, D. C.; Tranchemontagne, D. J.; Lam, K. C.; Sommer, R. D.; Zakharov, L. N.; Rheingold, A. L. *Dalton Trans.* **2004**, 3536.
(241) Hubin, T. J.; McCormick, J. M.; Alcock, N. W.; Busch, D. H. *Inorg. Chem.* **1998**, *37*, 6549.
(242) Hubin, T. J. *Coord. Chem. Rev.* **2003**, *241*, 27.
(243) Hubin, T. J.; McCormick, J. M.; Collinson, S. R.; Alcock, N. W.; Busch, D. H. *Chem. Commun.* **1998**, 1675.
(244) Kowallick, R.; Neuburger, M.; Zehnder, M.; Kaden, T. A. *Helv. Chim. Acta* **1997**, *80*, 948.
(245) Lewis, E. A.; Boyle, R. W.; Archibald, S. J. *Chem. Commun.* **2004**, 2212.
(246) Lewis, E. A.; Hubin, T. J.; Archibald, S. J.; The University of Hull: UK, 2005.

(247) De Clercq, E.; Yamamoto, N.; Pauwels, R.; Baba, M.; Schols, D.; Nakashima, H.; Balzarini, J.; Debyser, Z.; Murrer, B.; Schwartz, D.; Thornton, D.; Bridger, G.; Fricker, S.; Henson, G.; Abrams, M.; Picker, D. *Proc. Natl. Acad. Sci. U. S. A.* **1992**, *89*, 5286.
(248) Glushakova, S.; Yi, Y. J.; Grivel, J. C.; Singh, A.; Schols, D.; De Clercq, E.; Collman, R. G.; Margolis, L. *J. Clin. Invest.* **1999**, *104*, R7.
(249) De Clercq, E. *Rev. Med. Virol.* **2000**, *10*, 255.
(250) Donzella, G. A.; Schols, D.; Lin, S. W.; Este, J. A.; Nagashima, K. A.; Maddon, P. J.; Allaway, G. P.; Sakmar, T. P.; Henson, G.; De Clercq, E.; Moore, J. P. *Nat. Med.* **1998**, *4*, 72.
(251) Schramm, B.; Penn, M. L.; Speck, R. F.; Chan, S. Y.; De Clercq, E.; Schols, D.; Connor, R. I.; Goldsmith, M. A. *J. Virol.* **2000**, *74*, 184.
(252) Blanco, J.; Barretina, J.; Henson, G.; Bridger, G.; De Clercq, E.; Clotet, B.; Este, J. A. *Antimicrob. Agents Chemother.* **2000**, *44*, 51.
(253) Hendrix, C. W.; Flexner, C.; MacFarland, R. T.; Giandomenico, C.; Fuchs, E. J.; Redpath, E.; Bridger, G.; Henson, G. W. *Antimicrob. Agents Chemother.* **2000**, *44*, 1667.
(254) Hendrix, C. W.; Collier, A. C.; Lederman, M. M.; Schols, D.; Pollard, R. B.; Brown, S.; Jackson, J. B.; Coombs, R. W.; Gleshy, M. J.; Flexner, C. W.; Bridger, G. J.; Badel, K.; MacFarland, R. T.; Henson, G. W.; Calandra, G. *Jaids* **2004**, *37*, 1253.
(255) Smith, M. C. P.; Luker, K. E.; Garbow, J. R.; Prior, J. L.; Jackson, E.; Piwnica-Worms, D.; Luker, G. D. *Cancer Res.* **2004**, *64*, 8604.
(256) Scotton, C. J.; Wilson, J. L.; Scott, K.; Stamp, G.; Wilbanks, G. D.; Fricker, S.; Bridger, G.; Balkwill, F. R. *Cancer Res.* **2002**, *62*, 5930.
(257) Burger, M.; Hartmann, T.; Krome, M.; Rawluk, J.; Tamamura, H.; Fujii, N.; Kipps, T. J.; Burger, J. A. *Blood* **2005**, *106*, 1824.
(258) Huang, C. Y.; Lee, C. Y.; Chen, M. Y.; Yang, W. H.; Chen, Y. H.; Chang, C. H.; Hsu, H. C.; Fong, Y. C.; Tang, C. H. *J. Cell. Physiol.* **2009**, *221*, 204.
(259) Huttmann, A.; Duhrsen, U.; Stypmann, J.; Noppeney, R.; Nuckel, H.; Neumann, T.; Gutersohn, A.; Nikol, S.; Erbel, R. *Basic Res. Cardiol.* **2006**, *101*, 78.
(260) Liles, W. C.; Broxmeyer, H. E.; Rodger, E.; Wood, B.; Hubel, K.; Cooper, S.; Hangoc, G.; Bridger, G. J.; Henson, G. W.; Calandra, G.; Dale, D. C. *Blood* **2003**, *102*, 2728.
(261) Korbling, M.; Anderlini, P. *Blood* **2001**, *98*, 2900.
(262) Devine, S. M.; Flomenberg, N.; Vesole, D. H.; Liesveld, J.; Weisdorf, D.; Badel, K.; Calandra, G.; DiPersio, J. F. *J. Clin. Oncol.* **2004**, *22*, 1095.
(263) Liles, W. C.; Rodger, E.; Broxmeyer, H. E.; Dehner, C.; Badel, K.; Calandra, G.; Christensen, J.; Wood, B.; Price, T. H.; Dale, D. C. *Transfusion* **2005**, *45*, 295.
(264) Broxmeyer, H. E.; Orschell, C. M.; Clapp, D. W.; Hangoc, G.; Cooper, S.; Plett, P. A.; Liles, W. C.; Li, X. X.; Graham-Evans, B.; Campbell, T. B.; Calandra, G.; Bridger, G.; Dale, D. C.; Srour, E. F. *J. Exp. Med.* **2005**, *201*, 1307.

(265) Flomenberg, N.; Devine, S. M.; DiPersio, J. F.; Liesveld, J. L.; McCarty, J. M.; Rowley, S. D.; Vesole, D. H.; Badel, K.; Calandra, G. *Blood* **2005**, *106*, 1867.
(266) Goodrich, J. A., Kugel, J.F. *Binding and Kinetics for Molecular Biologists*; Gold Spring Harbor Laboratory Press, 2007.
(267) De Clercq, E.; Schols, D.; Bridger, G.; Henson, G. *Abstr Pap Am Chem Soc* **2001**, *221*, 24.
(268) Hatse, S.; Princen, K.; Vermeire, K.; Gerlach, L. O.; Rosenkilde, M. M.; Schwartz, T. W.; Bridger, G.; De Clercq, E.; Schols, D. *FEBS Lett.* **2003**, *546*, 300.
(269) Di Salvo, J.; Koch, G. E.; Johnson, K. E.; Blake, A. D.; Daugherty, B. L.; DeMartino, J. A.; Sirotina-Meisher, A.; Liu, Y.; Springer, M. S.; Cascieri, M. A.; Sullivan, K. A. *Eur. J. Pharmacol.* **2000**, *409*, 143.
(270) Schols, D.; Este, J. A.; Henson, G.; DeClercq, E. *Antiviral Res.* **1997**, *35*, 147.
(271) Zhou, N. M.; Luo, Z. W.; Luo, J. S.; Fan, X. J.; Cayabyab, M.; Hiraoka, M.; Liu, D. X.; Han, X. B.; Pesavento, J.; Dong, C. Z.; Wang, Y. L.; An, J.; Kaji, H.; Sodroski, J. G.; Huang, Z. W. *J. Biol. Chem.* **2002**, *277*, 17476.
(272) Housecroft, C. E., Sharpe, A.G. *Inorganic Chemistry*; 2nd ed.; Pearson Education Ltd: Essex, 2005.
(273) Tummino, P. J.; Copeland, R. A. *Biochemistry* **2008**, *47*, 5481.
(274) Zhang, R.; Monsma, F. *Curr. Opin. Drug Discov. Dev.* **2009**, *12*, 488.
(275) Copeland, R. A.; Pompliano, D. L.; Meek, T. D. *Nat. Rev. Drug Discov.* **2006**, *5*, 730.
(276) Lee, B.; Sharron, M.; Montaner, L. J.; Weissman, D.; Doms, R. W. *Proc. Natl. Acad. Sci. U. S. A.* **1999**, *96*, 5215.
(277) Manzetti, M.; Macko, L.; NeuburgerZehnder, M.; Kaden, T. A. *Helv. Chim. Acta* **1997**, *80*, 934.
(278) Hubin, T. J.; McCormick, J. M.; Alcock, N. W.; Clase, H. J.; Busch, D. H. *Inorg. Chem.* **1999**, *38*, 4435.
(279) Lin, C. A. J.; Liedl, T.; Sperling, R. A.; Fernandez-Arguelles, M. T.; Costa-Fernandez, J. M.; Pereiro, R.; Sanz-Medel, A.; Chang, W. H.; Parak, W. J. *J. Mater. Chem.* **2007**, *17*, 1343.
(280) Xing, Y.; Rao, J. H. *Cancer Biomark.* **2008**, *4*, 307.
(281) Zheng, J.; Ghazani, A. A.; Song, Q.; Mardyani, S.; Chan, W.; Wang, C. *Lab. Hematol.* **2006**, *12*, 94.
(282) Danussi, C.; Coslovi, A.; Campa, C.; Mucignat, M. T.; Spessotto, P.; Uggeri, F.; Paoletti, S.; Colombatti, A. *Glycobiology* **2009**, *19*, 1056.
(283) Green, N. M. *Methods Enzymol.* **1990**, *184*, 51.
(284) Bayer, E. A.; Benhur, H.; Hiller, Y.; Wilchek, M. *Biochem. J.* **1989**, *259*, 369.
(285) Bayer, E. A.; Benhur, H.; Wilchek, M. *Methods Enzymol.* **1990**, *184*, 217.
(286) Wilchek, M.; Bayer, E. A. *Anal. Biochem.* **1988**, *171*, 1.
(287) Dahan, M.; Levi, S.; Luccardini, C.; Rostaing, P.; Riveau, B.; Triller, A. *Science* **2003**, *302*, 442.

(288) Young, S. H.; Rozengurt, E. *Am. J. Physiol.-Cell Physiol.* **2006**, *290*, C728.
(289) Lue, H. Q.; Kleemann, R.; Calandra, T.; Roger, T.; Bernhagen, J. *Microbes Infect.* **2002**, *4*, 449.
(290) Bernhagen, J.; Krohn, R.; Lue, H.; Gregory, J. L.; Zernecke, A.; Koenen, R. R.; Dewor, M.; Georgiev, I.; Schober, A.; Leng, L.; Kooistra, T.; Fingerle-Rowson, G.; Ghezzi, P.; Kleemann, R.; McColl, S. R.; Bucala, R.; Hickey, M. J.; Weber, C. *Nat. Med.* **2007**, *13*, 587.
(291) Mitchell, R. A.; Bucala, R. *Sem. Cancer Biol.* **2000**, *10*, 359.
(292) Heilker, R. In *GPCRs: From Deorphanization to Lead Structure Identification*; Springer-Verlag Berlin: Berlin, 2007; Vol. 2, p 229.
(293) Smith, J. M.; Johanesen, P. A.; Wendt, M. K.; Binion, D. G.; Dwinell, M. B. *Am J Physiol-Gastrointest Liver Physiol* **2005**, *288*, G316.
(294) Grundler, R.; Thiede, C.; Miething, C.; Steudel, C.; Peschel, C.; Duyster, J. *Blood* **2003**, *102*, 646.
(295) Perissinotto, E.; Cavalloni, G.; Leone, F.; Fonsato, V.; Mitola, S.; Grignani, G.; Surrenti, N.; Sangiolo, D.; Bussolino, F.; Piacibello, W.; Aglietta, M. *Clin Cancer Res* **2005**, *11*, 490.
(296) Galli, G.; Fratelli, M. *Exp. Cell Res.* **1993**, *204*, 54.
(297) Lee, B. C.; Lee, T. H.; Avraham, S.; Avraham, H. K. *Mol. Cancer Res.* **2004**, *2*, 327.
(298) Gil, L.; Alonso, R.; Lopez, C.; Blanco, A.; Romero, Y.; Guillen, G.; Hermida, L. *Acta Virol.* **2009**, *53*, 147.
(299) Labadi, A.; Balogh, P. *Int. Immunol.* **2009**, *21*, 1047.
(300) Martin, S. J.; Reutelingsperger, C. P. M.; McGahon, A. J.; Rader, J. A.; Vanschie, R.; Laface, D. M.; Green, D. R. *J. Exp. Med.* **1995**, *182*, 1545.
(301) Fadok, V. A.; Voelker, D. R.; Campbell, P. A.; Cohen, J. J.; Bratton, D. L.; Henson, P. M. *J. Immunol.* **1992**, *148*, 2207.
(302) Kerr, J. F. R.; Wyllie, A. H.; Currie, A. R. *Brit. J. Cancer* **1972**, *26*, 239.
(303) Gangur, V.; Birmingham, N. P.; Thanesvorakul, S. *Vet. Immunol. Immunopathol.* **2002**, *86*, 127.
(304) Vermes, I.; Haanen, C.; Reutelingsperger, C. *Clin. Chem.* **1995**, *41*, S91.
(305) Vermes, I.; Haanen, C.; Steffensnakken, H.; Reutelingsperger, C. *J. Immunol. Methods* **1995**, *184*, 39.
(306) Darzynkiewicz, Z.; Bruno, S.; Delbino, G.; Gorczyca, W.; Hotz, M. A.; Lassota, P.; Traganos, F. *Cytometry* **1992**, *13*, 795.
(307) Chatila, T.; Silverman, L.; Miller, R.; Geha, R. *J. Immunol.* **1989**, *143*, 1283.
(308) Takei, N.; Endo, Y. *Brain Res.* **1994**, *652*, 65.
(309) Aagaardtillery, K. M.; Jelinek, D. F. *J. Immunol.* **1995**, *155*, 3297.
(310) Kryczek, I.; Wei, S.; Keller, E.; Liu, R.; Zou, W. P. *Am. J. Physiol.-Cell Physiol.* **2007**, *292*, C987.
(311) Sutton, A.; Friand, V.; Brule-Donneger, S.; Chaigneau, T.; Ziol, M.; Sainte-Catherine, O.; Poire, A.; Saffar, L.; Kraemer, M.; Vassy, J.; Nahon, P.; Salzmann, J. L.; Gattegno, L.; Charnaux, N. *Mol. Cancer Res.* **2007**, *5*, 21.

(312) Tang, C. H.; Tan, T. W.; Fu, W. M.; Yang, R. S. *Carcinogenesis* **2008**, *29*, 35.
(313) Bjare, U. *Pharmacol. Therapeut.* **1992**, *53*, 355.
(314) Peter, M.; Ameer-Beg, S. M.; Hughes, M. K. Y.; Keppler, M. D.; Prag, S.; Marsh, M.; Vojnovic, B.; Ng, T. *Biophys. J.* **2005**, *88*, 1224.
(315) Kunz-Schughart, L. A. *Cell Biol. Int.* **1999**, *23*, 157.
(316) de Ridder, L.; Cornelissen, M.; de Ridder, D. *Crit. Rev. Oncol./Hematol.* **2000**, *36*, 107.
(317) Rubie, C.; Kollmar, O.; Frick, V. O.; Wagner, M.; Brittner, B.; Graber, S.; Schilling, M. K. *Scand. J. Immunol.* **2008**, *68*, 635.
(318) Zhang, L. B.; Yegery, H.; Das, B.; Irwin, M. S.; Baruchel, S. *Neoplasia* **2007**, *9*, 36.
(319) Piovan, E.; Tosello, V.; Indraccolo, S.; Masiero, M.; Persano, L.; Esposito, G.; Zamarchi, R.; Ponzoni, M.; Chieco-Bianchi, L.; Dalla-Favera, R.; Amadori, A. *Cancer Res.* **2007**, *67*, 8605.
(320) Schioppa, T.; Uranchimeg, B.; Saccani, A.; Biswas, S. K.; Doni, A.; Rapisarda, A.; Bernasconi, S.; Saccani, S.; Nebuloni, M.; Vago, L.; Mantovani, A.; Melillo, G.; Sica, A. *J. Exp. Med.* **2003**, *198*, 1391.
(321) Krohn, A.; Song, Y. H.; Muehlberg, F.; Droll, L.; Beckmann, C.; Alt, E. *Cancer Lett.* **2009**, *280*, 65.
(322) Kim, J. B. *Sem. Cancer Biol.* **2005**, *15*, 365.
(323) Burleson, K. M.; Hansen, L. K.; Skubitz, A. P. N. *Clin. Exp. Metastasis* **2004**, *21*, 685.
(324) Yuhas, J. M.; Li, A. P.; Martinez, A. O.; Ladman, A. J. *Cancer Res.* **1977**, *37*, 3639.

Appendices

A1

Flow cytometric plots of $\mathbf{L}^{\mathbf{3a\text{-}d}}$ anti-CXCR4 mAb competition (blocking) assay (2nd replicate).

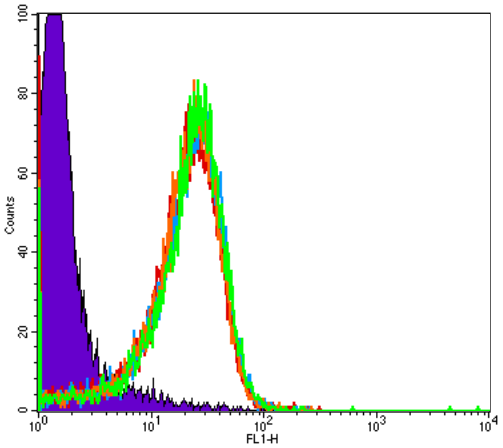

Flow cytometric plots of the inhibition of CXCR4 mAb 44716 by varying concentrations of $\mathbf{L}^{\mathbf{3a}}$ (85.695, 8.5695, 0.85695 µM). (-) control (purple) and (+) control (green) are shown.

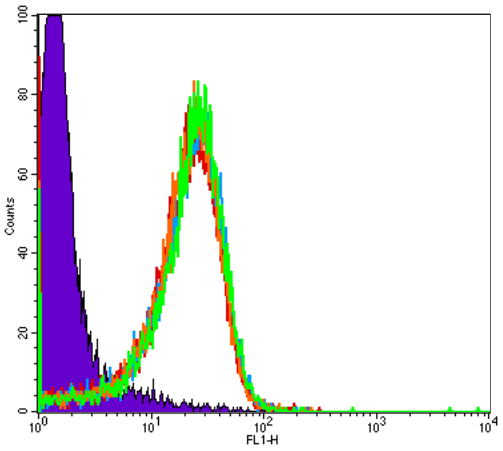

Flow cytometric plots of the inhibition of CXCR4 mAb 44716 by varying concentrations of $\mathbf{L}^{\mathbf{3b}}$ (86.03, 8.603, 0.8603 µM). (-) control (purple) and (+) control (green) are shown.

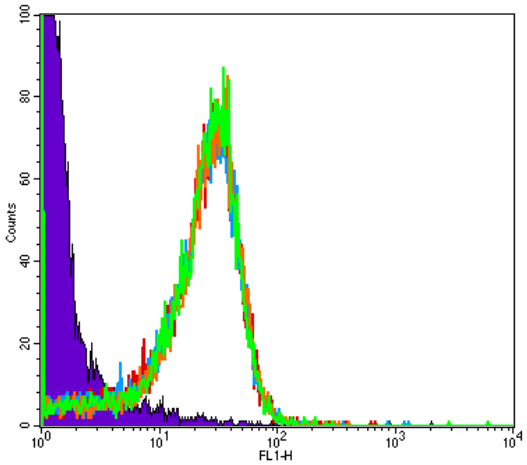

Flow cytometric plots of the inhibition of CXCR4 mAb 44716 by varying concentrations of **L**^{3c} (53.8, 5.38, 0.538 µM). (-) control (purple) and (+) control (green) are shown.

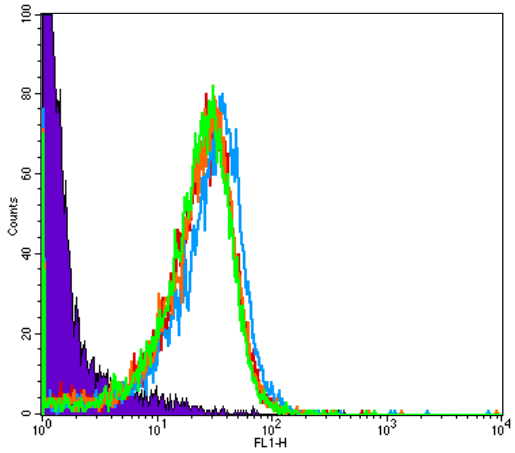

Flow cytometric plots of the inhibition of CXCR4 mAb 44716 by varying concentrations of **L**^{3d} (80.95, 8.95, 0.895 µM). (-) control (purple) and (+) control (green) are shown.

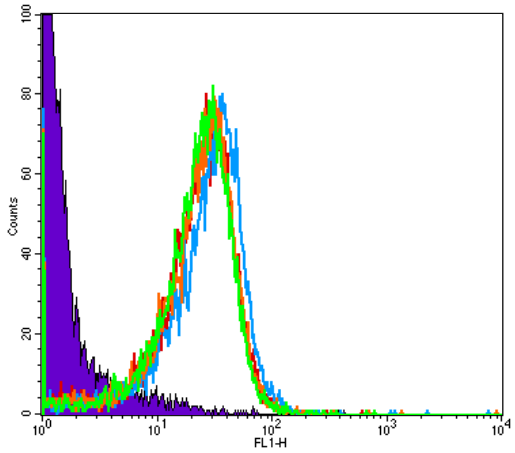

Flow cytometric plots of the inhibition of CXCR4 mAb 44716 by varying concentrations of **L**^{3} (78.43, 7.843, 0.7843 µM). (-) control (purple) and (+) control (green) are shown.

A2 Binding of L^{6-7} (table (7))

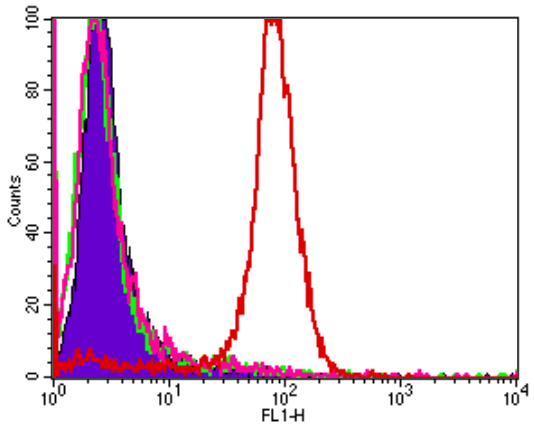

Flow cytometric plot of the inhibition of the binding of CXCR4 mAb 44716 by $[Zn_2\mathbf{L}^{6}(OAc)_2](PF_6)_2$ (green and pink represent duplicates) (20 µM). (-) control (purple) and (+) control (red) are shown.

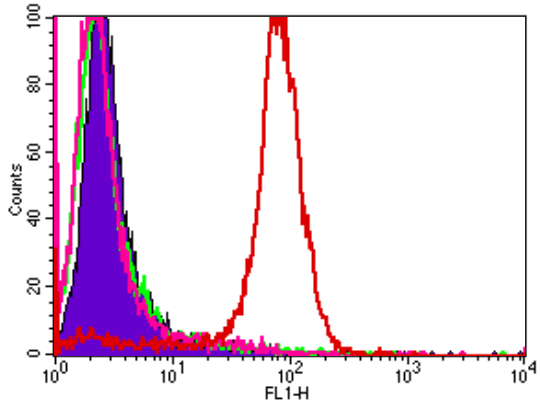

Flow cytometric plot of the inhibition of the binding of CXCR4 mAb 44716 by $[Cu_2\mathbf{L}^{6}(OAc)_2](PF_6)_2$ (green and pink represent duplicates) (20 µM). (-) control (purple) and (+) control (red) are shown.

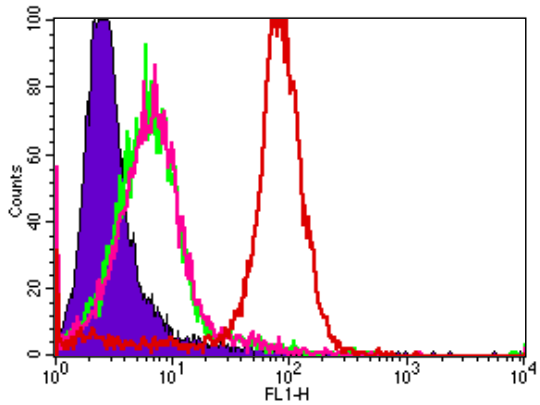

Flow cytometric plot of the inhibition of the binding of CXCR4 mAb 44716 by $[Cu_2\mathbf{L}^{7}(OAc)_2](PF_6)_2$ (green and pink represent duplicates) (20 µM). (-) control (purple) and (+) control (red) are shown.

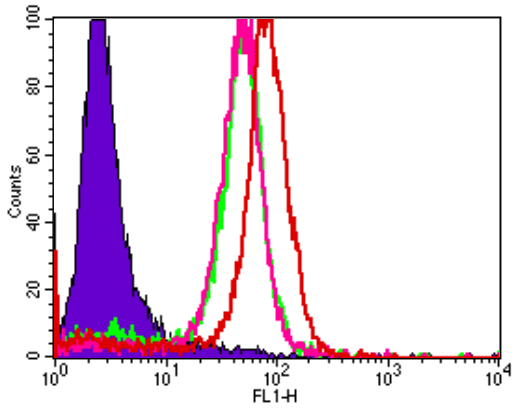

Flow cytometric plot of the inhibition of the binding of CXCR4 mAb 44716 by $[Zn_2\mathbf{L}^7(OAc)_2](PF_6)_2$ (green and pink represent duplicate) (20 µM). (-) control (purple) and (+) control (red) are shown.

A.3 Concentration dependent assay

A.3.1 Flow cytometric plots of metal complexes of L^4 and L^5

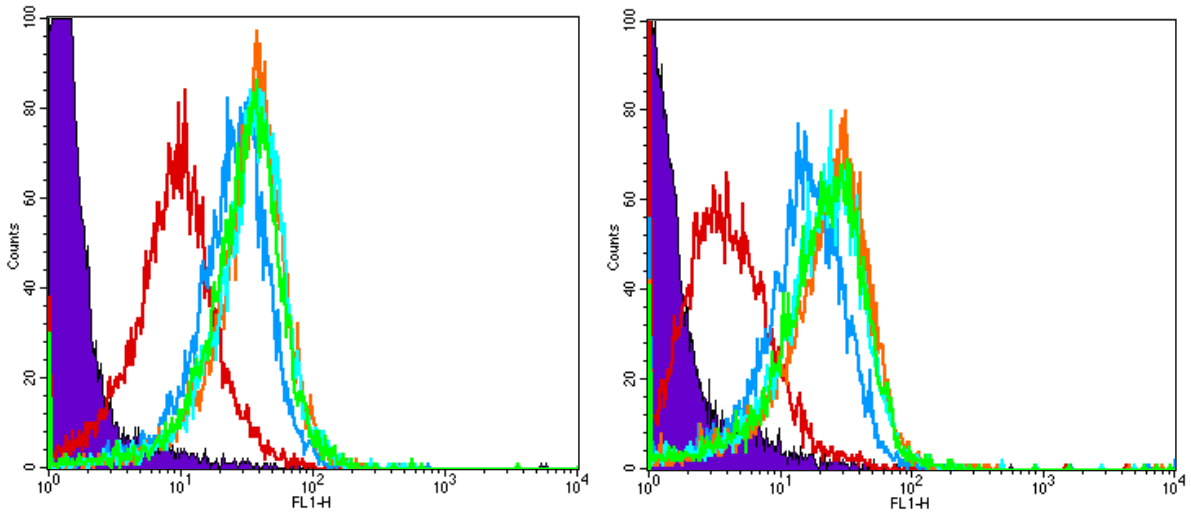

Flow cytometric plots of the inhibition of CXCR4 mAb 44716 by varying concentrations of $[Zn_2\mathbf{L}^4(OAc)_2](PF6)_2$ (35.66, 3.566, 0.3566, 0.03566 µM). (-) control (purple) and (+) control (green) are shown. Both plots represent replicates.

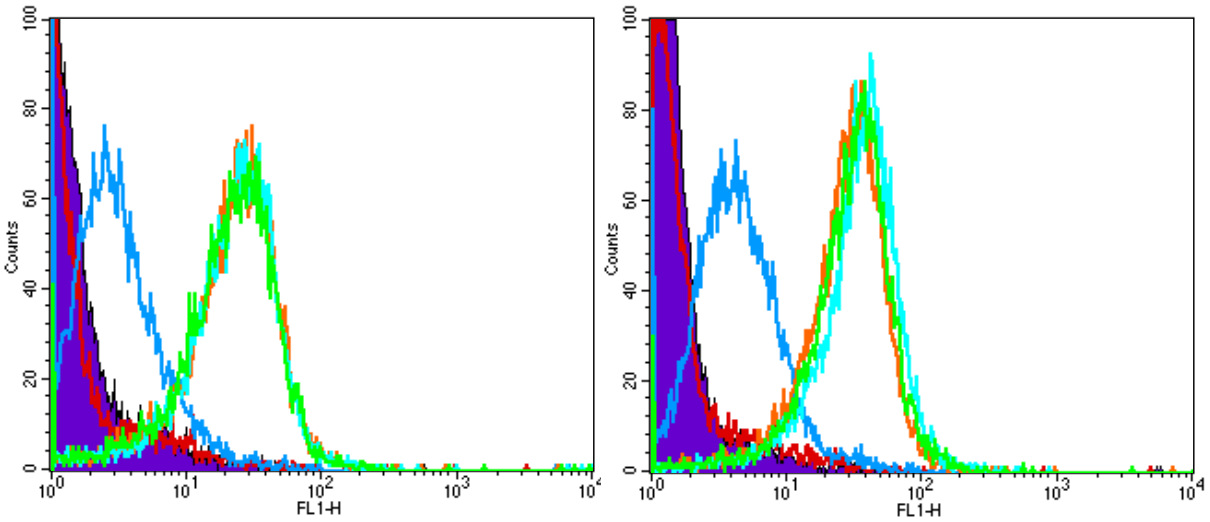

Flow cytometric plots of the inhibition of CXCR4 mAb 44716 by varying concentrations of $[Cu_2\mathbf{L}^4(OAc)_2](PF6)_2$ (35.66, 3.566, 0.3566, 0.03566 µM). (-) control (purple) and (+) control (green) are shown. Both plots represent replicates.

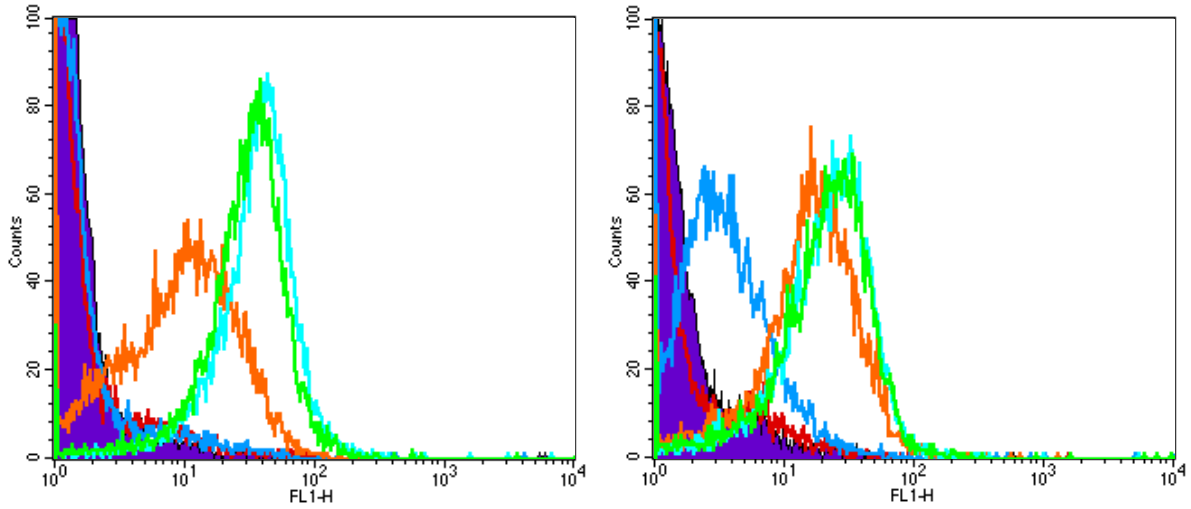

Flow cytometric plots of the inhibition of CXCR4 mAb 44716 by varying concentrations of $[Zn_2\mathbf{L}^5(OAc)_2](PF6)_2$ (56.31, 5.631, 0.5631, 0.05631 µM). (-) control (purple) and (+) control (green) are shown. Both plots represent replicates.

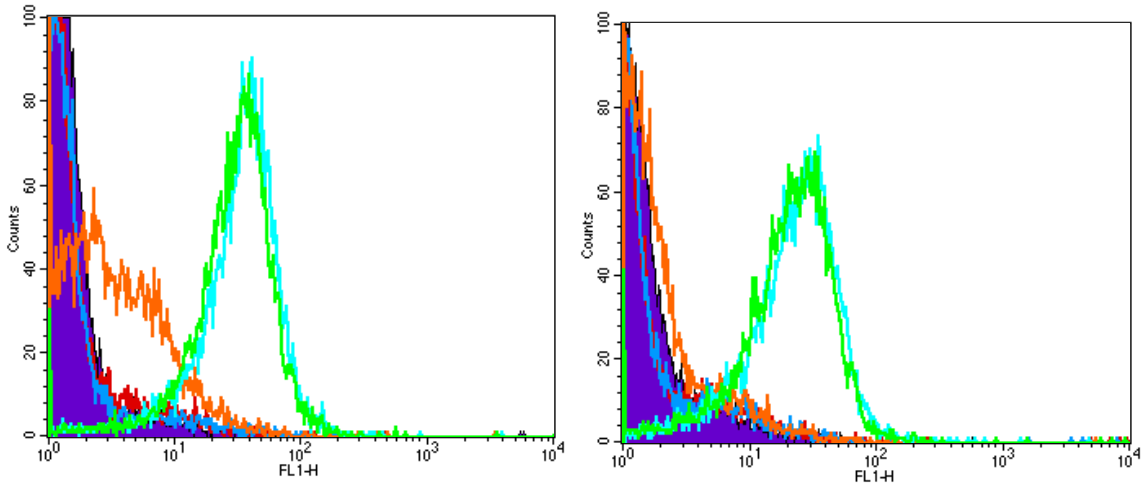

Flow cytometric plots of the inhibition of CXCR4 mAb 44716 by varying concentrations of $[Cu_2\mathbf{L}^5(OAc)_2](PF6)_2$ (45.20, 4.520, 0.4520, 0.04520 µM). (-) control (purple) and (+) control (green) are shown. Both plots represent replicates.

A4 Binding of L^{8-10} (table (9))

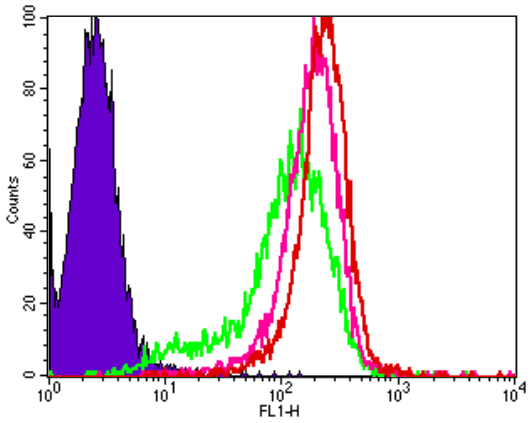

Flow cytometric plot of the inhibition of the binding of CXCR4 mAb 44716 by $\mathbf{L}^{8}$ (green and pink represent duplicates) (20 µM). (-) control (purple) and (+) control (red) are shown.

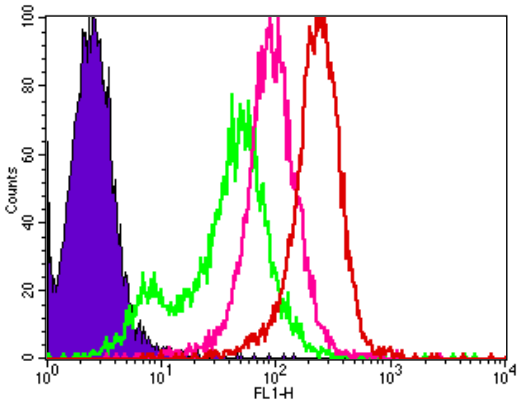

Flow cytometric plot of the inhibition of the binding of CXCR4 mAb 44716 by $[Cu_3\mathbf{L}^{8}(OAc)_3](OAc)_3$ (green and pink represent duplicates) (20 µM). (-) control (purple) and (+) control (red) are shown.

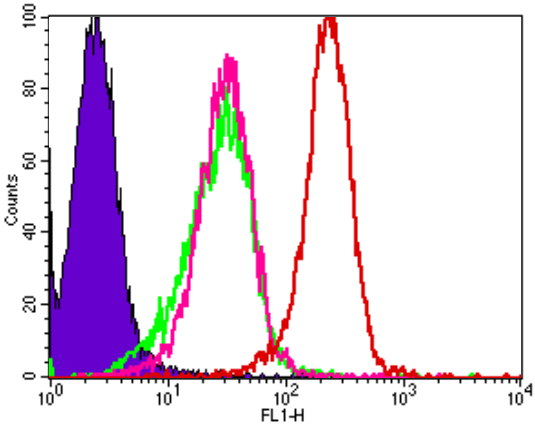

Flow cytometric plot of the inhibition of the binding of CXCR4 mAb 44716 by $[Zn_3\mathbf{L}^{8}(Cl)_3](PF_6)$ (green and pink represent duplicates) (20 µM). (-) control (purple) and (+) control (red) are shown.

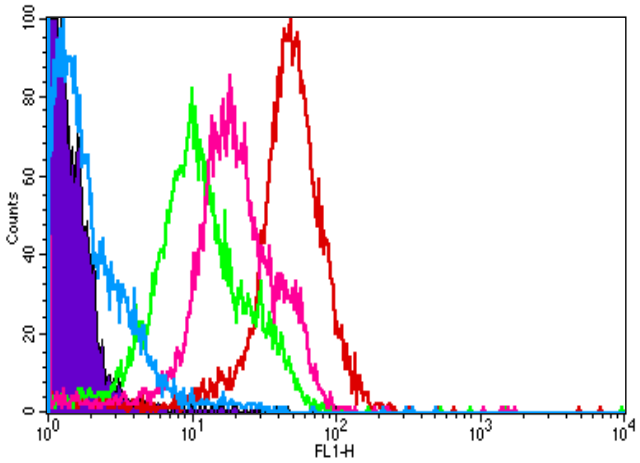

Flow cytometric plot of the inhibition of the binding of CXCR4 mAb 44716 by $[Ni_3\mathbf{L}^{8}](ClO_4)_6$, $[Cu_3\mathbf{L}^{9}(OAc)_3](OAc)_3$, $[Cu_3\mathbf{L}^{10}(Cl)_3](Cl)_3$ (20 μM). (-) control (purple) and (+) control (red) are shown.

A5 Residence time of macrocyclic based complexes (calculations)

1. No of compound molecules in solution:

40 µM of compound added (10 µl) to 990 µl of cell solution (total volume 1 ml)

(40/1000) x 10 = 0.4 µM or 4×10^{-7} M (final concentration)

No of moles = 4×10^{-7} M x 0.001 l (1 ml)

= 4×10^{-10} moles

No of molecules = 4×10^{-10} moles x 6.23×10^{23} mol^{-1} (Avogadro constant)

= 2.492×10^{14} molecules of compound in solution

2. No of CXCR4 receptors in solution:

140000 (no of receptors per cell) x 100000 (cells in sample)

= 1.4×10^{10} receptors in sample

3. No of compound molecules per receptor:

2.492×10^{14} / 1.4×10^{10} = **17800 molecules per receptor**

1. **No of compound molecules in solution:**

16 nM of compound added (10 µl) to 990 µl of cell solution (total volume 1 ml)

(16/1000) x 10 = 0.16 nM or 1.6×10^{-10} M (final concentration)

No of moles = 1.6×10^{-10} M x 0.001 l (1 ml)

= 1.6×10^{-13} moles

No of molecules = 1.6×10^{-13} moles x 6.23×10^{23} mol^{-1} (Avogadro constant)

= 9.968×10^{10} molecules of compound in solution

2. **No of CXCR4 receptors in solution:**

140000 (no of receptors per cell) x 100000 (cells in sample)

= 1.4×10^{10} receptors in sample

3. **No of compound molecules per receptor:**

9.968×10^{10} / 1.4×10^{10} = **7.1 molecules per receptor**

1. **No of compound molecules in solution:**

32 nM of compound added (10 µl) to 990 µl of cell solution (total volume 1 ml)

(32/1000) x 10 = 0.32 nM or 3.2×10^{-10} M (final concentration)

No of moles = 3.2×10^{-10} M x 0.001 l (1 ml)

= 3.2×10^{-13} moles

No of molecules = 3.2×10^{-13} moles x 6.23×10^{23} mol^{-1} (Avogadro constant)

= 1.9936×10^{11} molecules of compound in solution

2. **No of CXCR4 receptors in solution:**

140000 (no of receptors per cell) x 100000 (cells in sample)

= 1.4×10^{10} receptors in sample

3. **No of compound molecules per receptor:**

1.9936×10^{11} / 1.4×10^{10} = **14.2 molecules per receptor**

A6 Relative half-life and k_{off} constants calculated using the one phase exponential decay model (Graphpad Prism 4.0)

	16 nM		
One phase exponential decay	**AMD3100 (L^{11})**	**$[Cu_2L^{11}Cl_2]^{2+}$**	**$[Cu_2L^{2}Cl_2]^{2+}$**
Best-fit values			
SPAN	105.9	54.5	102.9
k_{off}	0.103	0.04252	0.02042
PLATEAU	0	0	0
HalfLife	6.729	16.3	33.94
Std. Error			
SPAN	5.555	6.2	10.97
k_{off}	0.02118	0.01036	0.0042
95% Confidence Intervals			
SPAN	88.24 to 123.6	34.77 to 74.23	67.98 to 137.8
k_{off}	0.03563 to 0.1704	0.009549 to 0.07548	0.007057 to 0.03379
HalfLife	4.068 to 19.46	9.183 to 72.59	20.51 to 98.21
Goodness of Fit			
Degrees of Freedom	3	3	3
R^2	0.9914	0.9519	0.9239
Absolute Sum of Squares	58.08	100.5	377.2
Sy.x	4.4	5.787	11.21
Constraints			
k_{off}	K > 0.0	K > 0.0	K > 0.0
PLATEAU	PLATEAU = 0.0	PLATEAU = 0.0	PLATEAU = 0.0
Data			
Number of X values	5	5	5
Number of Y replicates	1	1	1
Total number of values	5	5	5
Number of missing values	0	0	0

A6 Relative halflife and k_{off} constants calculated using the one phase exponential decay model (Graphpad Prism 4.0)

	32 nM		
One phase exponential decay	**AMD3100 (L^{11})**	**$[Cu_2L^{11}Cl_2]^{2+}$**	**$[Cu_2L^{2}Cl_2]^{2+}$**
Best-fit values			
SPAN	103.8	77.82	110.1
k_{off}	0.07585	0.04238	0.02046
PLATEAU	0	0	0
HalfLife	9.139	16.35	33.88
Std. Error			
SPAN	1.938	8.901	11.13
k_{off}	0.004183	0.01038	0.003988
95% Confidence Intervals			
SPAN	97.62 to 110.0	49.50 to 106.1	74.66 to 145.5
k_{off}	0.06254 to 0.08916	0.009369 to 0.07540	0.007769 to 0.03315
HalfLife	7.775 to 11.08	9.194 to 73.98	20.91 to 89.22
Goodness of Fit			
Degrees of Freedom	3	3	3
R^2	0.9988	0.9485	0.9404
Absolute Sum of Squares	8.503	207.1	387.7
Sy.x	1.684	8.309	11.37
Constraints			
k_{off}	K > 0.0	K > 0.0	K > 0.0
PLATEAU	PLATEAU = 0.0	PLATEAU = 0.0	PLATEAU = 0.0
Data			
Number of X values	5	5	5
Number of Y replicates	1	1	1
Total number of values	5	5	5
Number of missing values	0	0	0

A7 Surface expression of CXCR4 receptor in Jurkat lymphoma cells

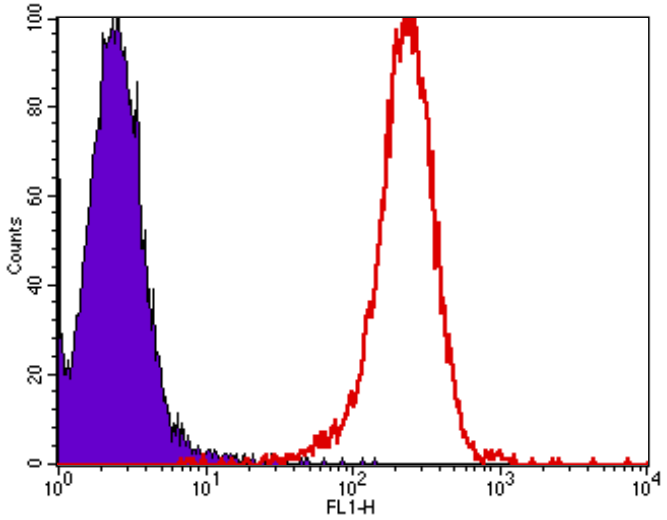

Flow cytometric plot of the binding of anti-CXCR4 mAb (44716) in Jurkat cells. (-) control is also shown.

A8 MIF and CXCR4

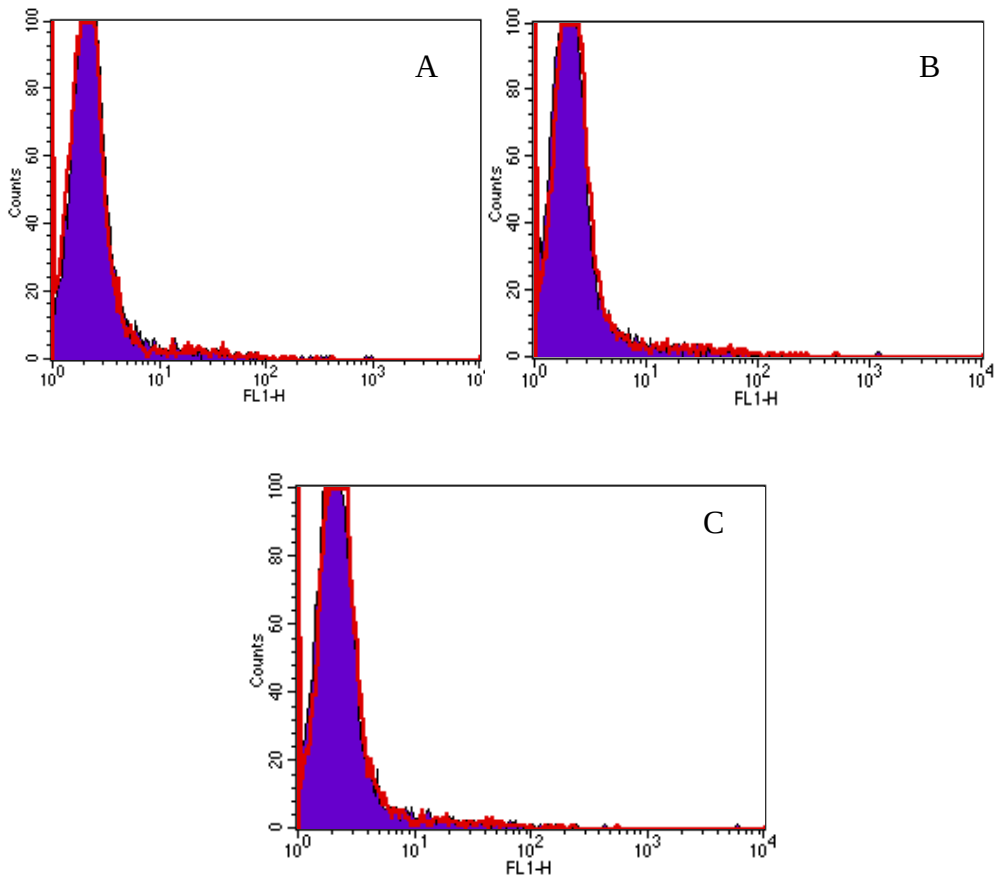

Flow cytometric plots of the binding of rhMIF in Jurkat cells. A) 20 min, B) 40 min, C) 60 min incubation period with rhMIF. (-) control (purple) (cells only) and rhMIF and cells (red) are shown. Plots represent second replicate.

A8.1 Internalisation of CXCR4 with MIF

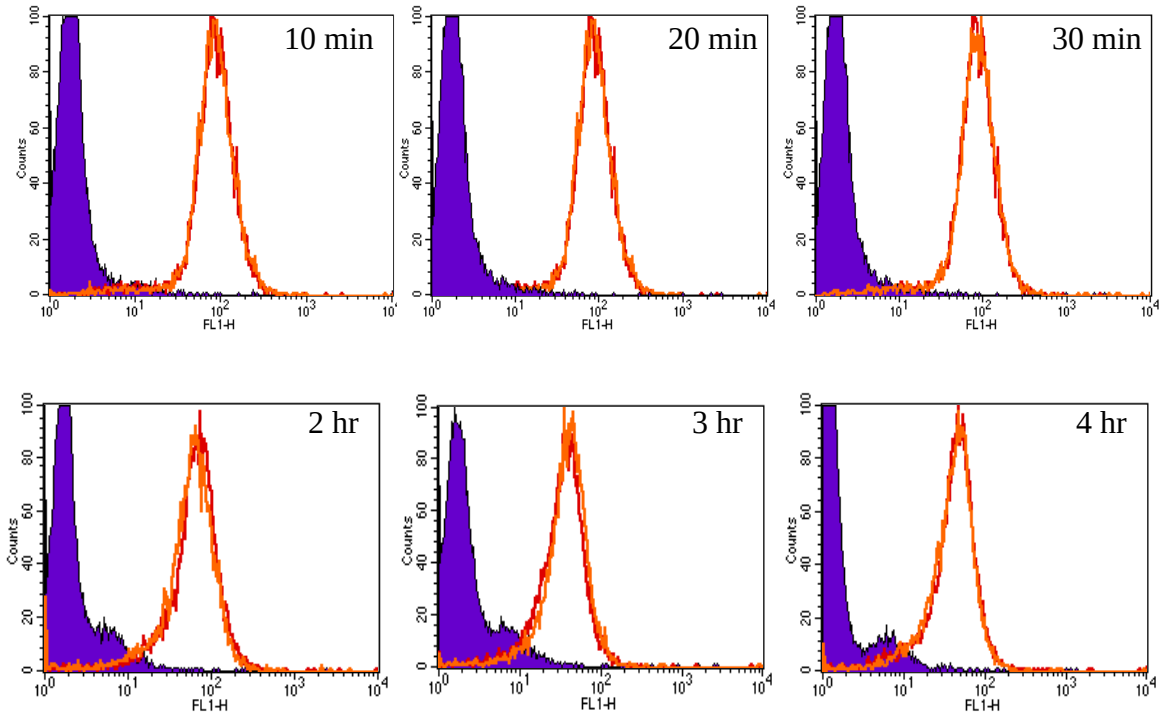

Flow cytometric plots of the binding of CXCR4 mAb (44717) in Jurkat cells after incubation with rhMIF (10-30 min, 2-4 hr). (-) control (purple) (cells only), CXCR4 mAb after rhMIF interval(red) and (+) control (orange) (CXCR4 mAb only) are shown. Plots represent second replicate.

A9 SJSA cell proliferation (MTS assay)

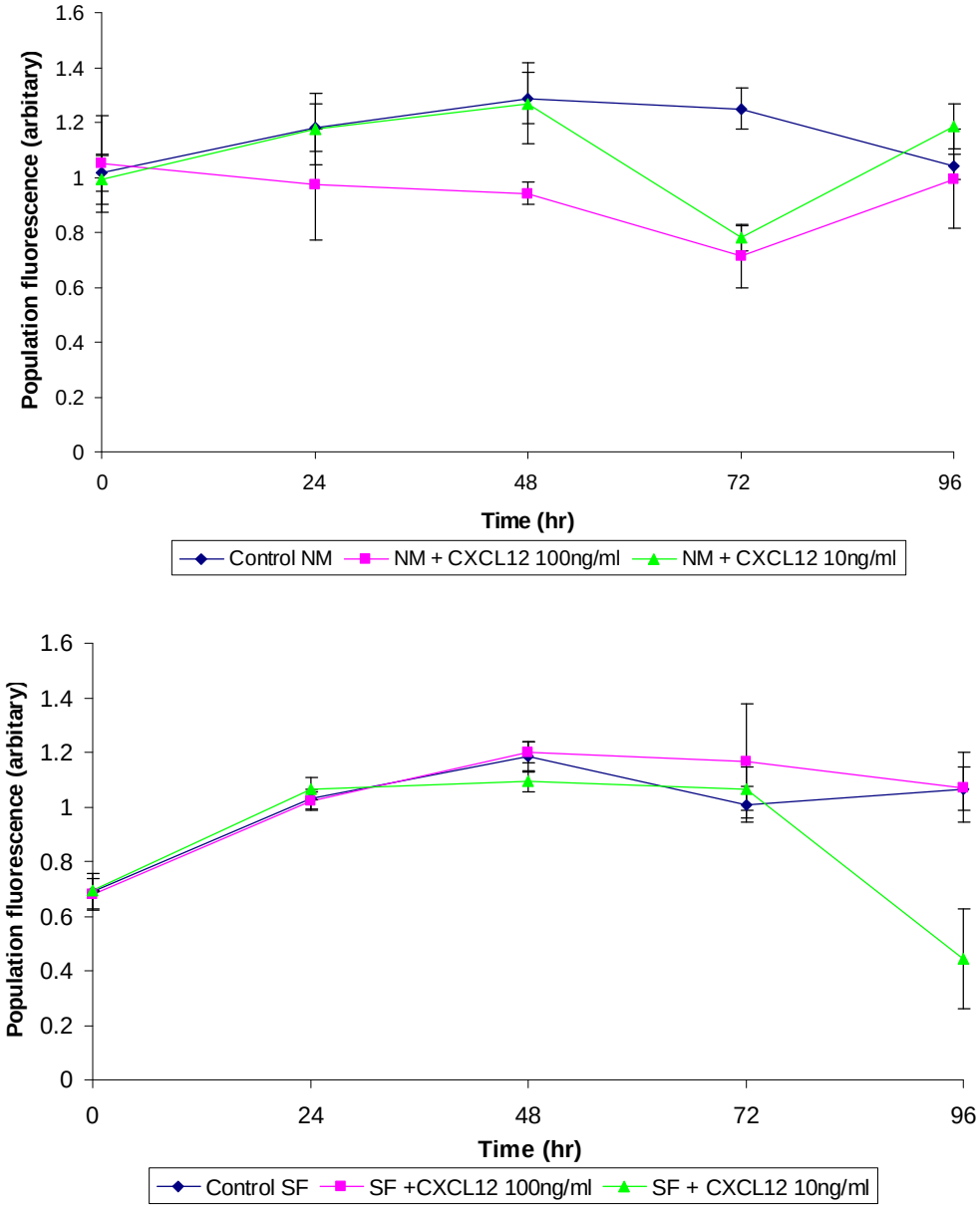

SJSA cell proliferation after CXCL12 stimulation (10-100 ng/ml) in A) Normal media, B) Serum free conditions. (Error bars represent triplicates)

A10 Statistical analyses of SJSA proliferation with CXCL12 in normal media (NM) and serum free media (SF)

t-Test: Two-Sample Assuming Unequal Variances

CXCL12 stimulation only at 0 hr

Normal media

	0 hr		24 hr		48 hr	
	control	CXCL12 (100 ng/ml)	control	CXCL12 (100 ng/ml)	control	CXCL12 (100 ng/ml)
Mean	0.616	0.713666667	0.552333	0.521	0.922667	0.65
Variance	0.000873	0.003514333	0.007401	0.006841	0.002074	0.003559
Observations	3	3	3	3	3	3
Hypothesized Mean Difference	0		0		0	
df	3		4		4	
t Stat	-2.55392		0.454754		6.292308	
P(T<=t) one-tail	0.041828		0.336436		0.00163	
t Critical one-tail	2.353363		2.131846		2.131846	
P(T<=t) two-tail	0.083657		0.672873		0.003259	
t Critical two-tail	3.182449		2.776451		2.776451	

	72 hr		96 hr	
	control	CXCL12 (100 ng/ml)	control	CXCL12 (100 ng/ml)
Mean	1.337667	0.893	1.369667	0.849666667
Variance	0.041349	0.002847	0.03721	0.007169333
Observations	3	3	3	3
Hypothesized Mean Difference	0		0	
df	2		3	
t Stat	3.66355		4.275353	
P(T<=t) one-tail	0.033548		0.011748	
t Critical one-tail	2.919987		2.353363	
P(T<=t) two-tail	0.067095		0.023497	
t Critical two-tail	4.302656		3.182449	

CXCL12 stimulation only at 0 hr

Normal media

	0 hr		24 hr		48 hr	
	control	CXCL12 (10 ng/ml)	control	CXCL12 (10 ng/ml)	control	CXCL12 (10 ng/ml)
Mean	0.616	0.776666667	0.552333	0.593	0.922667	0.701
Variance	0.000873	0.000610333	0.007401	0.004423	0.002074	0.001348
Observations	3	3	3	3	3	3
Hypothesized Mean Difference	0		0		0	
df	4		4		4	
t Stat	-7.22549		-0.64776		6.562962	
P(T<=t) one-tail	0.000973		0.276223		0.001394	
t Critical one-tail	2.131846		2.131846		2.131846	
P(T<=t) two-tail	0.001946		0.552446		0.002788	
t Critical two-tail	2.776451		2.776451		2.776451	

	72 hr		96 hr	
	control	CXCL12 (10 ng/ml)	control	CXCL12 (10 ng/ml)
Mean	1.337667	0.997333333	1.369667	0.9
Variance	0.041349	0.014766333	0.03721	0.035557
Observations	3	3	3	3
Hypothesized Mean Difference	0		0	
df	3		4	
t Stat	2.488416		3.015658	
P(T<=t) one-tail	0.044304		0.019665	
t Critical one-tail	2.353363		2.131846	
P(T<=t) two-tail	0.088608		0.039331	
t Critical two-tail	3.182449		2.776451	

CXCL12 stimulation only at 0 hr

Serum free media

	0 hr		24 hr		48 hr	
	control	CXCL12 (100 ng/ml)	control	CXCL12 (100 ng/ml)	control	CXCL12 (100 ng/ml)
Mean	0.582667	0.526	0.338667	0.317333333	0.309667	0.280666667
Variance	0.00095	9.10E-05	5.73E-05	0.000394333	0.000197	0.000134333
Observations	3	3	3	3	3	3
Hypothesized Mean Difference	0		0		0	
df	2		3		4	
t Stat	3.041539		1.738643		2.758085	
P(T<=t) one-tail	0.046613		0.090242		0.025475	
t Critical one-tail	2.919987		2.353363		2.131846	
P(T<=t) two-tail	0.093227		0.180483		0.05095	
t Critical two-tail	4.302656		3.182449		2.776451	

	72 hr		96 hr	
	control	CXCL12 (100 ng/ml)	control	CXCL12 (100 ng/ml)
Mean	0.350333	0.312666667	0.332333	0.312333333
Variance	0.000264	0.000217333	0.000921	0.000424333
Observations	3	3	3	3
Hypothesized Mean Difference	0		0	
df	4		4	
t Stat	2.972655		0.944326	
P(T<=t) one-tail	0.020518		0.199237	
t Critical one-tail	2.131846		2.131846	
P(T<=t) two-tail	0.041036		0.398473	
t Critical two-tail	2.776451		2.776451	

CXCL12 stimulation only at 0 hr

Serum free media

	0 hr		24 hr		48 hr	
	control	CXCL12 (10 ng/ml)	control	CXCL12 (10 ng/ml)	control	CXCL12 (10 ng/ml)
Mean	0.582667	0.497666667	0.338667	0.307333333	0.309667	0.305333333
Variance	0.00095	0.000158333	5.73E-05	0.000801333	0.000197	0.000134333
Observations	3	3	3	3	3	3
Hypothesized Mean Difference	0		0		0	
df	3		2		4	
t Stat	4.421596		1.852059		0.412128	
P(T<=t) one-tail	0.01074		0.102607		0.350688	
t Critical one-tail	2.353363		2.919987		2.131846	
P(T<=t) two-tail	0.02148		0.205214		0.701375	
t Critical two-tail	3.182449		4.302656		2.776451	

	72 hr		96 hr	
	control	CXCL12 (10 ng/ml)	control	CXCL12 (10 ng/ml)
Mean	0.350333	0.366666667	0.332333	0.424
Variance	0.000264	0.000752333	0.000921	0.015151
Observations	3	3	3	3
Hypothesized Mean Difference	0		0	
df	3		2	
t Stat	-0.88725		-1.25237	
P(T<=t) one-tail	0.220148		0.168515	
t Critical one-tail	2.353363		2.919987	
P(T<=t) two-tail	0.440297		0.33703	
t Critical two-tail	3.182449		4.302656	

A10.1 SJSA cell prolifertaion with CXCL12 in normal media (NM) and serum free media (SF)

t-Test: Two-Sample Assuming Unequal Variances

CXCL12 stimulation every 24 hr						
Normal media						
	0 hr		**24 hr**		**48 hr**	
	control	*CXCL12 (100 ng/ml)*	*control*	*CXCL12 (100 ng/ml)*	*control*	*CXCL12 (100 ng/ml)*
Mean	0.951667	1.048	1.182	1.065	1.146667	0.970666667
Variance	0.00858	0.037852	0.002833	0.010647	0.01748	0.043932333
Observations	3	3	3	3	3	3
Hypothesized Mean Difference	0		0		0	
df	3		3		3	
t Stat	-0.77433		1.745426		1.230111	
P(T<=t) one-tail	0.24758		0.089625		0.15316	
t Critical one-tail	2.353363		2.353363		2.353363	
P(T<=t) two-tail	0.495161		0.179251		0.30632	
t Critical two-tail	3.182449		3.182449		3.182449	

	72 hr		**96 hr**	
	control	*CXCL12 (100 ng/ml)*	*control*	*CXCL12 (100 ng/ml)*
Mean	1.069667	0.743666667	0.725333	0.749666667
Variance	0.006604	0.001566333	0.028344	0.007560333
Observations	3	3	3	3
Hypothesized Mean Difference	0		0	
df	3		3	
t Stat	6.246683		-0.22243	
P(T<=t) one-tail	0.004138		0.419132	
t Critical one-tail	2.353363		2.353363	
P(T<=t) two-tail	0.008276		0.838264	
t Critical two-tail	3.182449		3.182449	

CXCL12 stimulation every 24 hr						
Normal media						
	0 hr		**24 hr**		**48 hr**	
	control	*CXCL12 (10 ng/ml)*	*control*	*CXCL12 (10 ng/ml)*	*control*	*CXCL12 (10 ng/ml)*
Mean	0.951667	1.049666667	1.182	1.005333333	1.146667	1.203333333
Variance	0.00858	0.020177333	0.002833	0.003090333	0.01748	0.000745333
Observations	3	3	3	3	3	3
Hypothesized Mean Difference	0		0		0	
df	3		4		2	
t Stat	-1.00094		3.97587		-0.72702	
P(T<=t) one-tail	0.195306		0.008229		0.271398	
t Critical one-tail	2.353363		2.131846		2.919987	
P(T<=t) two-tail	0.390612		0.016458		0.542796	
t Critical two-tail	3.182449		2.776451		4.302656	

	72 hr		**96 hr**	
	control	*CXCL12 (10 ng/ml)*	*control*	*CXCL12 (10 ng/ml)*
Mean	1.069667	0.742333333	0.725333	0.904
Variance	0.006604	0.104842333	0.028344	0.005833
Observations	3	3	3	3
Hypothesized Mean Difference	0		0	
df	2		3	
t Stat	1.698311		-1.67392	
P(T<=t) one-tail	0.115773		0.09637	
t Critical one-tail	2.919987		2.353363	
P(T<=t) two-tail	0.231546		0.19274	
t Critical two-tail	4.302656		3.182449	

CXCL12 stimulation every 24 hr
Serum free media

	0 hr		**24 hr**		**48 hr**	
	control	*CXCL12 (100 ng/ml)*	*control*	*CXCL12 (100 ng/ml)*	*control*	*CXCL12 (100 ng/ml)*
Mean	0.690333	0.691	1.051	1.149	1.148667	1.192333333
Variance	0.000508	0.000333	0.0004	0.008983	0.00714	0.001290333
Observations	3	3	3	3	3	3
Hypothesized Mean Difference	0		0		0	
df	4		2		3	
t Stat	-0.03981		-1.75233		-0.82372	
P(T<=t) one-tail	0.485076		0.110907		0.235239	
t Critical one-tail	2.131846		2.919987		2.353363	
P(T<=t) two-tail	0.970153		0.221814		0.470478	
t Critical two-tail	2.776451		4.302656		3.182449	

	72 hr		**96 hr**	
	control	*CXCL12 (100 ng/ml)*	*control*	*CXCL12 (100 ng/ml)*
Mean	0.935667	1.039666667	1.0196	1.005666667
Variance	0.00157	0.047097333	0.010053	0.017989333
Observations	3	3	3	3
Hypothesized Mean Difference	0		0	
df	2		4	
t Stat	-0.81653		0.144116	
P(T<=t) one-tail	0.249992		0.446189	
t Critical one-tail	2.919987		2.131846	
P(T<=t) two-tail	0.499983		0.892378	
t Critical two-tail	4.302656		2.776451	

CXCL12 stimulation every 24 hr
Serum free media

	0 hr		**24 hr**		**48 hr**	
	control	*CXCL12 (10 ng/ml)*	*control*	*CXCL12 (10 ng/ml)*	*control*	*CXCL12 (10 ng/ml)*
Mean	0.690333	0.652333333	1.051	1.015333333	1.148667	1.085
Variance	0.000508	0.000264333	0.0004	0.001429333	0.00714	0.000925
Observations	3	3	3	3	3	3
Hypothesized Mean Difference	0		0		0	
df	4		3		3	
t Stat	2.367817		1.444364		1.227896	
P(T<=t) one-tail	0.038502		0.122186		0.15352	
t Critical one-tail	2.131846		2.353363		2.353363	
P(T<=t) two-tail	0.077004		0.244371		0.30704	
t Critical two-tail	2.776451		3.182449		3.182449	

	72 hr		**96 hr**	
	control	*CXCL12 (10 ng/ml)*	*control*	*CXCL12 (10 ng/ml)*
Mean	0.935667	1.011333333	1.0196	0.553
Variance	0.00157	0.001564333	0.010053	0.001213
Observations	3	3	3	3
Hypothesized Mean Difference	0		0	
df	4		2	
t Stat	-2.34083		7.614242	
P(T<=t) one-tail	0.039653		0.008407	
t Critical one-tail	2.131846		2.919987	
P(T<=t) two-tail	0.079306		0.016815	
t Critical two-tail	2.776451		4.302656	

A11 Statistical analysis of cell proliferation with CXCL12 in normal media and serum free media (CFSE assay)

t-Test: Two-Sample Assuming Unequal Variances

Primary CXCL12 stimulation only

MDA-MB-231

Normal media	*control*	*CXCL12 (100 ng/ml)*
Mean	147.0533	150.97
Variance	0.047633	9.5823
Observations	3	3
Hypothesized Mean Difference	0	
df	2	
t Stat	-2.18608	
P(T<=t) one-tail	0.080188	
t Critical one-tail	2.919987	
P(T<=t) two-tail	0.160376	
t Critical two-tail	4.302656	

Serum free media	*control*	*CXCL12 (100 ng/ml)*
Mean	145.1233	143.14
Variance	17.33503	3.9351
Observations	3	3
Hypothesized Mean Difference	0	
df	3	
t Stat	0.744854	
P(T<=t) one-tail	0.255201	
t Critical one-tail	2.353363	
P(T<=t) two-tail	0.510403	
t Critical two-tail	3.182449	

U87-MG

Normal media	*control*	*CXCL12 (100 ng/ml)*
Mean	180.0367	182.09
Variance	299.4249	3.1483
Observations	3	3
Hypothesized Mean Difference	0	
df	2	
t Stat	-0.20446	
P(T<=t) one-tail	0.428457	
t Critical one-tail	2.919987	
P(T<=t) two-tail	0.856914	
t Critical two-tail	4.302656	

Serum free media	*control*	*CXCL12 (100 ng/ml)*
Mean	335.3167	368.3
Variance	67.59263	16.7203
Observations	3	3
Hypothesized Mean Difference	0	
df	3	
t Stat	-6.22169	
P(T<=t) one-tail	0.004185	
t Critical one-tail	2.353363	
P(T<=t) two-tail	0.008371	
t Critical two-tail	3.182449	

Primary CXCL12 stimulation only

AsPc-1

Normal media	*control*	*CXCL12 (100 ng/ml)*
Mean	427.1733	389.3333333
Variance	1216.234	169.3852333
Observations	3	3
Hypothesized Mean Difference	0	
df	3	
t Stat	1.760718	
P(T<=t) one-tail	0.088254	
t Critical one-tail	2.353363	
P(T<=t) two-tail	0.176508	
t Critical two-tail	3.182449	

Serum free media	*control*	*CXCL12 (100 ng/ml)*
Mean	650.17	616.5
Variance	3839.294	4180.9348
Observations	3	3
Hypothesized Mean Difference	0	
df	4	
t Stat	0.651194	
P(T<=t) one-tail	0.275219	
t Critical one-tail	2.131846	
P(T<=t) two-tail	0.550439	
t Critical two-tail	2.776451	

Continuous CXCL12 stimulation every 24 hr

MDA-MB-231

Normal media	*control*	*CXCL12 (100 ng/ml)*
Mean	149.66	149.12
Variance	168.8229	118.4079
Observations	3	3
Hypothesized Mean Difference	0	
df	4	
t Stat	0.055187	
P(T<=t) one-tail	0.479318	
t Critical one-tail	2.131846	
P(T<=t) two-tail	0.958636	
t Critical two-tail	2.776451	

Serum free media	*control*	*CXCL12 (100 ng/ml)*
Mean	274.2533	303.4633333
Variance	4.427033	459.5016333
Observations	3	3
Hypothesized Mean Difference	0	
df	2	
t Stat	-2.34891	
P(T<=t) one-tail	0.071646	
t Critical one-tail	2.919987	
P(T<=t) two-tail	0.143291	
t Critical two-tail	4.302656	

Continuous CXCL12 stimulation every 24 hr

U87-MG

Normal media	*control*	*CXCL12 (100 ng/ml)*
Mean	305.9533	313.57
Variance	342.1317	386.3137
Observations	3	3
Hypothesized Mean Difference	0	
df	4	
t Stat	-0.4888	
P(T<=t) one-tail	0.325288	
t Critical one-tail	2.131846	
P(T<=t) two-tail	0.650575	
t Critical two-tail	2.776451	

Serum free media	*control*	*CXCL12 (100 ng/ml)*
Mean	445.0967	501.0033333
Variance	109.4966	268.9234333
Observations	3	3
Hypothesized Mean Difference	0	
df	3	
t Stat	-4.9778	
P(T<=t) one-tail	0.007791	
t Critical one-tail	2.353363	
P(T<=t) two-tail	0.015581	
t Critical two-tail	3.182449	

A12 Statistical analysis of SJSA cell proliferation with CXCL12 in normal media and serum free media (CFSE assay)

t-Test: Two-Sample Assuming Unequal Variances

CXCL12 added at day 0 only

Normal media

Days	1		2		3	
	control	*CXCL12 (100 ng/ml)*	*control*	*CXCL12 (100 ng/ml)*	*control*	*CXCL12 (100 ng/ml)*
Mean	253.5733	254.3066667	143.2767	146.9766667	83.48667	80.87666667
Variance	2197.876	3509.466233	72.82603	71.14243333	5.078633	1.795433333
Observations	3	3	3	3	3	3
Hypothesized Mean Difference	0		0		0	
df	4		4		3	
t Stat	-0.01681		-0.53411		1.724226	
P(T<=t) one-tail	0.493695		0.310785		0.091567	
t Critical one-tail	2.131846		2.131846		2.353363	
P(T<=t) two-tail	0.987391		0.62157		0.183135	
t Critical two-tail	2.776451		2.776451		3.182449	

Days	4		5	
	control	*CXCL12 (100 ng/ml)*	*control*	*CXCL12 (100 ng/ml)*
Mean	56.86	52.52	47.09	44.11333333
Variance	1.3351	6.4137	3.4167	7.193733333
Observations	3	3	3	3
Hypothesized Mean Difference	0		0	
df	3		4	
t Stat	2.700431		1.582794	
P(T<=t) one-tail	0.03688		0.094318	
t Critical one-tail	2.353363		2.131846	
P(T<=t) two-tail	0.073759		0.188635	
t Critical two-tail	3.182449		2.776451	

CXCL12 added at day 0 only						
Serum free media						
Days	1		2		3	
	control	*CXCL12 (100 ng/ml)*	*control*	*CXCL12 (100 ng/ml)*	*control*	*CXCL12 (100 ng/ml)*
Mean	290.1467	318.7633333	161.9433	145.3366667	188.9533	200.74
Variance	2672.785	1890.300933	2358.739	1625.748633	976.0865	73.7167
Observations	3	3	3	3	3	3
Hypothesized Mean Difference	0		0		0	
df	4		4		2	
t Stat	-0.73375		0.455677		-0.63008	
P(T<=t) one-tail	0.251894		0.336132		0.296515	
t Critical one-tail	2.131846		2.131846		2.919987	
P(T<=t) two-tail	0.503787		0.672263		0.593029	
t Critical two-tail	2.776451		2.776451		4.302656	

Days	4		5	
	control	*CXCL12 (100 ng/ml)*	*control*	*CXCL12 (100 ng/ml)*
Mean	190.07	184.44	199.73	203.0933333
Variance	193.2519	692.9011	1510.388	778.3752333
Observations	3	3	3	3
Hypothesized Mean Difference	0		0	
df	3		4	
t Stat	0.327578		-0.12177	
P(T<=t) one-tail	0.38238		0.454478	
t Critical one-tail	2.353363		2.131846	
P(T<=t) two-tail	0.764759		0.908956	
t Critical two-tail	3.182449		2.776451	

A12.1 Statistical analysis of SJSA cell proliferation with CXCL12 in normal media and serum free media (CFSE assay)

t-Test: Two-Sample Assuming Unequal Variances						
CXCL12 added every 24 hr						
Normal media						
Day	1		2		3	
	control	*CXCL12 (100 ng/ml)*	*control*	*CXCL12 (100 ng/ml)*	*control*	*CXCL12 (100 ng/ml)*
Mean	285.98	280.68	118.33	153.0566667	112.2733	112.4133333
Variance	266.9437	1730.5501	1348.908	56.15093333	57.92103	47.06613333
Observations	3	3	3	3	3	3
Hypothesized Mean Difference	0		0		0	
df	3		2		4	
t Stat	0.205397		-1.60464		-0.02367	
P(T<=t) one-tail	0.425205		0.124891		0.491126	
t Critical one-tail	2.353363		2.919987		2.131846	
P(T<=t) two-tail	0.85041		0.249781		0.982253	
t Critical two-tail	3.182449		4.302656		2.776451	

Day	4		5	
	control	*CXCL12 (100 ng/ml)*	*control*	*CXCL12 (100 ng/ml)*
Mean	72.95667	68.20666667	59.31	56.65
Variance	47.72763	38.65423333	28.1041	17.6527
Observations	3	3	3	3
Hypothesized Mean Difference	0		0	
df	4		4	
t Stat	0.885203		0.681106	
P(T<=t) one-tail	0.213026		0.266597	
t Critical one-tail	2.131846		2.131846	
P(T<=t) two-tail	0.426053		0.533193	
t Critical two-tail	2.776451		2.776451	

CXCL12 added every 24 hr						
Serum free media						
Day	1		2		3	
	control	*CXCL12 (100 ng/ml)*	*control*	*CXCL12 (100 ng/ml)*	*control*	*CXCL12 (100 ng/ml)*
Mean	374.5867	357.17	168.77	179.34	184.63	212.8533333
Variance	2754.763	2274.2425	1383.787	3004.6575	1228.795	614.1642333
Observations	3	3	3	3	3	3
Hypothesized Mean Difference	0		0		0	
df	4		4		4	
t Stat	0.425387		-0.27636		-1.1387	
P(T<=t) one-tail	0.346221		0.39798		0.159197	
t Critical one-tail	2.131846		2.131846		2.131846	
P(T<=t) two-tail	0.692442		0.795961		0.318395	
t Critical two-tail	2.776451		2.776451		2.776451	

Day	4		5	
	control	*CXCL12 (100 ng/ml)*	*control*	*CXCL12 (100 ng/ml)*
Mean	141.2867	170.41	166.2233	172.0533333
Variance	1228.819	1113.6541	8.113733	1026.872133
Observations	3	3	3	3
Hypothesized Mean Difference	0		0	
df	4		2	
t Stat	-1.04223		-0.31388	
P(T<=t) one-tail	0.178075		0.391663	
t Critical one-tail	2.131846		2.919987	
P(T<=t) two-tail	0.35615		0.783327	
t Critical two-tail	2.776451		4.302656	

A13 Statistical analysis of SJSA cell invasion in matrigel with CXCL12

t-Test: Two-Sample Assuming Unequal Variances

	CXCL12							
	0 nM	*12.5 nM*	*0 nM*	*37.5 nM*	*0 nM*	*75 nM*	*0 nM*	*100 nM*
Mean	70.7	211.1	70.7	259.5	70.7	239.8	70.7	228.555556
Variance	247.7888889	1460.32222	247.7888889	2798.5	247.7888889	1705.95556	247.7888889	3191.27778
Observations	10	10	10	10	10	10	10	9
Hypothesized Mean Difference	0		0		0		0	
df	12		11		12		9	
t Stat	-10.74259119		-10.81723953		-12.09789273		-8.104590273	
P(T<=t) one-tail	8.21469E-08		1.67703E-07		2.20857E-08		9.97499E-06	
t Critical one-tail	1.782286745		1.795883691		1.782286745		1.833113856	
P(T<=t) two-tail	1.64294E-07		3.35406E-07		4.41715E-08		1.995E-05	
t Critical two-tail	2.178812792		2.200986273		2.178812792		2.262158887	

A14 Statistical analysis of SJSA cell invasion in matrigel with CXCL12 and CXCR4 antagonists

t-Test: Two-Sample Assuming Unequal Variances				
	CXCL12 (12.5 nM only)	$[Cu_2\mathbf{L}^2Cl_2]^{2+}$ (200 nM)	*CXCL12 (12.5 nM)*	$[Cu_2\mathbf{L}^2Cl_2]^{2+}$ (20 nM)
Mean	164.4	23.9	164.4	25.7
Variance	389.6	36.76666667	389.6	44.9
Observations	10	10	10	10
Hypothesized Mean Difference	0		0	
df	11		11	
t Stat	21.51714776		21.04173616	
P(T<=t) one-tail	1.21788E-10		1.54883E-10	
t Critical one-tail	1.795883691		1.795883691	
P(T<=t) two-tail	2.43577E-10		3.09765E-10	
t Critical two-tail	2.200986273		2.200986273	
	CXCL12 (12.5 nM)	AMD3100 ($\mathbf{L}^{11}$) (200 nM)	*CXCL12 (12.5 nM)*	AMD3100 ($\mathbf{L}^{11}$) (20 nM)
Mean	164.4	101.6	164.4	96.5
Variance	389.6	91.37777778	389.6	104.0555556
Observations	10	10	10	10
Hypothesized Mean Difference	0		0	
df	13		13	
t Stat	9.055181049		9.66401866	
P(T<=t) one-tail	2.80931E-07		1.33546E-07	
t Critical one-tail	1.770931704		1.770931704	
P(T<=t) two-tail	5.61861E-07		2.67092E-07	
t Critical two-tail	2.16036824		2.16036824	

	Cells only	*CXCL12 (12.5 nM)*
Mean	20.4	164.4
Variance	38.48888889	389.6
Observations	10	10
Hypothesized Mean Difference	0	
df	11	
t Stat	-22.00875694	
P(T<=t) one-tail	9.54881E-11	
t Critical one-tail	1.795883691	
P(T<=t) two-tail	1.90976E-10	
t Critical two-tail	2.200986273	

A15 Invasion of SJSA cells in matrigel with CXCL12 and CXCR4 antagonists

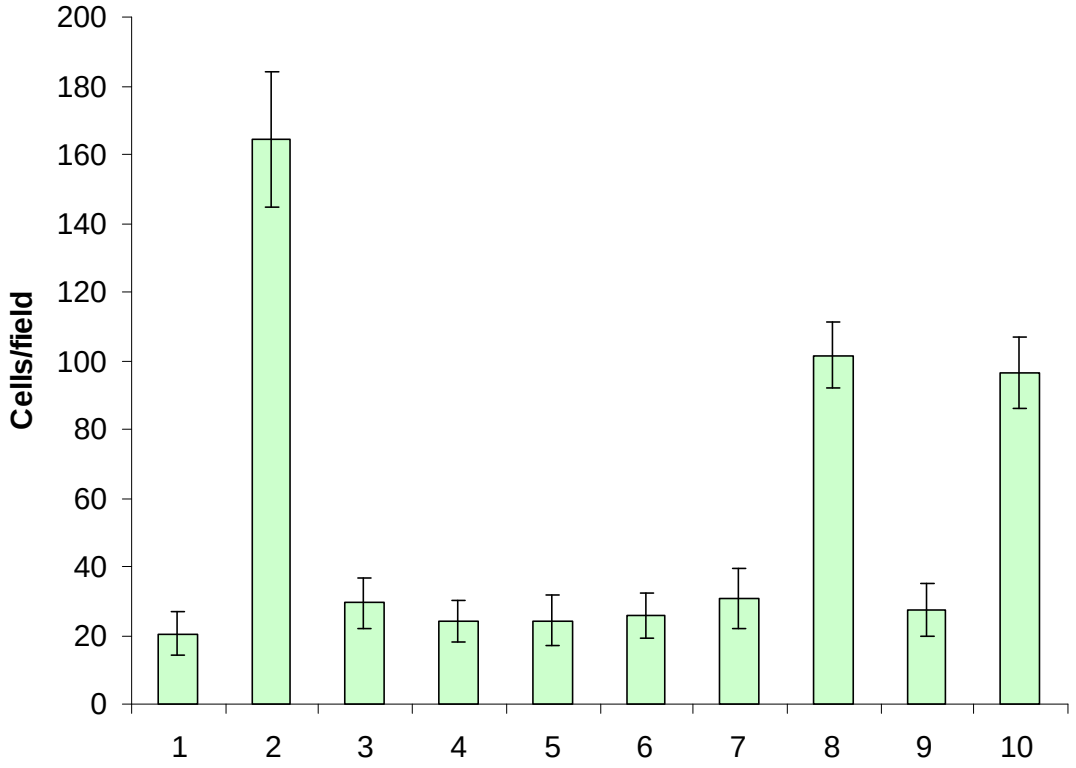

CXCL12 (12.5 nM)	-	+	-	+	-	+	-	+	-	+
$[Cu_2L^2Cl_2]^{2+}$	-	-	200 nM	200 nM	20 nM	20 nM	-	-	-	-
AMD3100 (L^{11})	-	-	-	-	-	-	200 nM	200 nM	20 nM	20 nM
	1	2	3	4	5	6	7	8	9	10

Invasion of SJSA cells in matrigel with CXCL12 (12.5 nM) and CXCR4 antagonists (20-200 nM). Cells were counted in five different fields (x40 obj) in duplicates. Mean of the values plotted.

A16 Statistical analysis of Δ34-CXCR4 cell invasion in matrigel with CXCL12 and CXCR4 antagonists

t-Test: Two-Sample Assuming Unequal Varia

CXCL12 (100nM)	-	+	-	+	-	+	-	+	-	+
$[Cu_2L^2Cl_2]^{2+}$	-	-	200 nM	200 nM	20 nM	20 nM	-	-	-	-
AMD3100 (L^{11})	-	-	-	-	-	-	200 nM	200 nM	20 nM	20 nM
	A	B	C	D	E	F	G	H	I	J

	A	*C*	*A*	*D*	*A*	*E*	*A*	*F*	*A*	*G*
Mean	16.4	2.8	16.4	3.2	16.4	2.6	16.4	3.3	16.4	4.2
Variance	26.71111111	5.955555556	26.71111111	9.288888889	26.71111111	4.044444444	26.71111111	8.455555556	26.71111111	10.4
Observations	10	10	10	10	10	10	10	10	10	10
Hypothesized Mean Difference	0		0		0		0		0	
df	13		15		12		14		15	
t Stat	7.524653358		6.957010852		7.868959285		6.985631835		6.332976143	
P(T<=t) one-tail	2.1721E-06		2.29957E-06		2.22536E-06		3.19587E-06		6.71665E-06	
t Critical one-tail	1.770931704		1.753051038		1.782286745		1.76130925		1.753051038	
P(T<=t) two-tail	4.3442E-06		4.59913E-06		4.45073E-06		6.39174E-06		1.34333E-05	
t Critical two-tail	2.16036824		2.131450856		2.178812792		2.144788596		2.131450856	

	A	*H*	*A*	*I*	*A*	*J*
Mean	16.4	7.6	16.4	6	16.4	4.9
Variance	26.71111111	21.15555556	26.71111111	15.77777778	26.71111111	13.87777778
Observations	10	10	10	10	10	10
Hypothesized Mean Difference	0		0		0	
df	18		17		16	
t Stat	4.022222393		5.045400573		5.708135304	
P(T<=t) one-tail	0.000399639		4.98296E-05		1.617E-05	
t Critical one-tail	1.734063062		1.739606432		1.745884219	
P(T<=t) two-tail	0.000799279		9.96591E-05		3.234E-05	
t Critical two-tail	2.100923666		2.109818524		2.119904821	

	B	*A*	*B*	*C*	*B*	*D*	*B*	*E*	*B*	*F*
Mean	48.4	16.4	48.4	2.8	48.4	3.2	48.4	2.6	48.4	3.3
Variance	73.6	26.71111111	73.6	5.955555556	73.6	9.288888889	73.6	4.044444444	73.6	8.455555556
Observations	10	10	10	10	10	10	10	10	10	10
Hypothesized Mean Difference	0		0		0		0		0	
df	15		10		11		10		11	
t Stat	10.10358403		16.16700551		15.69966103		16.43653559		15.74427065	
P(T<=t) one-tail	2.18129E-08		8.49224E-09		3.52317E-09		7.23775E-09		3.4191E-09	
t Critical one-tail	1.753051038		1.812461505		1.795883691		1.812461505		1.795883691	
P(T<=t) two-tail	4.36258E-08		1.69845E-08		7.04635E-09		1.44755E-08		6.83821E-09	
t Critical two-tail	2.131450856		2.228139238		2.200986273		2.228139238		2.200986273	

	B	*G*	*B*	*H*	*B*	*I*	*B*	*J*
Mean	48.4	4.2	48.4	7.6	48.4	6	48.4	4.9
Variance	73.6	10.4	73.6	21.15555556	73.6	15.77777778	73.6	13.87777778
Observations	10	10	10	10	10	10	10	10
Hypothesized Mean Difference	0		0		0		0	
df	11		14		13		12	
t Stat	15.25044886		13.2543313		14.1824441		14.70755178	
P(T<=t) one-tail	4.78621E-09		1.2924E-09		1.37535E-09		2.4334E-09	
t Critical one-tail	1.795883691		1.76130925		1.770931704		1.782286745	
P(T<=t) two-tail	9.57242E-09		2.58479E-09		2.7507E-09		4.8668E-09	
t Critical two-tail	2.200986273		2.144788596		2.16036824		2.178812792	

A17 Statistical analysis of the invasion of Δ34-CXCR4 cells in matrigel with serum (5 % FBS)

t-Test: Two-Sample Assuming Unequal Variances

	Cells only	$[Cu_2\mathbf{L}^2Cl_2]^{2+}$ (200 nM)	*Cells only*	$[Cu_2\mathbf{L}^2Cl_2]^{2+}$ (20 nM)	*Cell only*	$[Cu_2\mathbf{L}^2Cl_2]^{2+}$ (2 nM)
Mean	274.2	152	274.2	176.3	274.2	212.7
Variance	794.4	1631.333333	794.4	2231.566667	794.4	724.6777778
Observations	10	10	10	10	10	10
Hypothesized Mean Difference	0		0		0	
df	16		15		18	
t Stat	7.8460248		5.6279551		4.989822655	
P(T<=t) one-tail	3.565E-07		2.404E-05		4.74548E-05	
t Critical one-tail	1.7458842		1.753051		1.734063062	
P(T<=t) two-tail	7.129E-07		4.809E-05		9.49095E-05	
t Critical two-tail	2.1199048		2.1314509		2.100923666	

	Cells only	AMD3100 ($\mathbf{L}^{11}$) (200 nM)	*Cells only*	AMD3100 ($\mathbf{L}^{11}$) (20 nM)
Mean	274.2	220.4	274.2	251.8
Variance	794.4	703.8222222	794.4	604.4
Observations	10	10	10	10
Hypothesized Mean Difference	0		0	
df	18		18	
t Stat	4.395357		1.8939574	
P(T<=t) one-tail	0.0001745		0.0372081	
t Critical one-tail	1.7340631		1.7340631	
P(T<=t) two-tail	0.000349		0.0744162	
t Critical two-tail	2.1009237		2.1009237	